Variation in water quality of Chilika lake (Odisha) with special reference to phosphorus and its sequestration using novel adsorbent

काशी हिन्दू विश्वविद्यालय BANARAS HINDU UNIVERSITY

THESIS SUBMITED IN PARTIAL FULFILMENT OF
THE REQUIREMENTS FOR THE DEGREE OF

Doctor of Philosophy

in

Soil Science and Agricultural Chemistry

Supervisor
Prof. A. K. Gosh

Submitted by
Satya Narayana Pradhan

DEPARTMENT OF SOIL SCIENCE & AGRICULTURAL CHEMISTRY
INSTITUTE OF AGRICULTURAL SCIENCES
BANARAS HINDU UNIVERSITY
VARANASI – 221 005
INDIA

ID. No. PS-17062 **2022** **Enrolment No.379862**

Variation in water quality of Chilika lake (Odisha) with special reference to phosphorus and its sequestration using novel adsorbent

Satya Narayana Pradhan

2022

Dedicated to

My Beloved Parents

UNDERTAKING FROM THE CANDIDATE

I, Satya Narayana Pradhan, hereby declare that the experimental work and its interpretation in the thesis entitled **"VARIATION IN WATER QUALITY OF CHILIKA LAKE (ODISHA) WITH SPECIAL REFERENECE TO PHOSPHORUS AND ITS SEQUESTRATION USING NOVEL ADSORBENT"** being submitted by me for the degree of Doctor of Philosophy is a record of first-hand research work done by me during the period of study. I avail myself to responsibility such as an act will be taken on behalf of me, mistakes, errors of fact and misinterpretations are of course entirely my own.

Date: …….

Place: B.H.U., Varanasi

(Satya Narayana Pradhan)

ID. No. PS-17062

Enroll. No. 379862

ANNEXURE – E

[See clause XIII.2 (b) (iii)]

CANDIDATE'S DECLARATION

I, **Satya Narayana Pradhan, ID. No. PS-17062, Enrolment No. 379862** certify that the work embodied in this Ph.D. thesis is my own bonafide work carried out by me under the supervision of **Prof. A.K. Ghosh** for a period from October, 2017 to September, 2022 at Banaras Hindu University, **Department of Soil Science and Agricultural Chemistry, Institute of Agricultural Sciences.** The matter embodied in this Ph.D. thesis has not been submitted for the award of any other degree/ diploma.

I declare that I have faithfully acknowledged, given credit to, and referred to the research workers wherever their works have been cited in the text and the body of the thesis. I further certify that I have not willfully lifted some other's work, para, text, data, results, etc. reported in the journals, books, magazines, reports, dissertations, thesis, etc. or available at web-sites and included them in this Ph.D. thesis and cited as my own work.

Date : ……..

Place: BHU, Varanasi **(Satya Narayana Pradhan)**

(Signature of the candidate)

CERTIFICATE FROM THE SUPERVISOR/ CO-SUPERVISOR

This is to certify that the above statement made by the candidate is correct to the best of my/our knowledge.

(Dr. A.K. Ghosh)
Professor
Supervisor's Signature

(Signature of the HOD/Coordinator of the School with seal)

ANNEXURE – F

[See clause XIII. I (c) and XIII.2 (b) (iv)]

COURSE WORK COMPLETION CERTIFICATE

This is to certify that **Mr. Satya Narayana Pradhan, ID. No. PS-17062, Enrolment No. 379862** a bonafide research scholar of Department of Soil, Science & Agricultural Chemistry, Institute of Agricultural Sciences, has successfully completed the course work requirement which is the part of his Ph.D. programme.

Date:…….

Place: B.H.U., Varanasi **(Signature of the Head of the Department)**

ANNEXURE – F

[See clause XIII. I (c) and XIII.2 (b) (iv)]

COMPREHENSIVE WRITTEN EXAMINATION AS WELL AS COMPREHENSIVE ORAL COMPLETION CERTIFICATE

This is to certify that **Mr. Satya Narayana Pradhan, ID. No. PS-17062, Enrolment No. 379862** a bonafide research scholar of Department of Soil, Science & Agricultural Chemistry, Institute of Agricultural Sciences, has successfully completed the comprehensive written examination as well as comprehensive oral examination requirement which is the part of his Ph.D. programme.

Date:…….

Place: B.H.U., Varanasi **(Signature of the Head of the Department)**

ANNEXURE – F

[See clause XIII. I (c) AND XIII.2 (b) (iv)]

PRE-SUBMISSION SEMINAR COMPLETION CERTIFICATE

This is to certify that Mr. **Satya Narayana Pradhan, ID. No. PS-17062, Enrolment No. 379862** a bonafide research scholar of this department, has successfully completed the pre-submission seminar on (topic) **"VARIATION IN WATER QUALITY OF CHILIKA LAKE (ODISHA) WITH SPECIAL REFERENECE TO PHOSPHORUS AND ITS SEQUESTRATION USING NOVEL ADSORBENT"** dated 27.08.2022 requirement which is a part of his Ph.D. programme.

Date: …….

Place: B.H.U., Varanasi **(Signature of the Head of the Department)**

ANNEXURE – G

[See clause XIII. 2 (b) (v)]

COPYRIGHT TRANSFER CERTIFICATE

Title of the thesis: **"VARIATION IN WATER QUALITY OF CHILIKA LAKE (ODISHA) WITH SPECIAL REFERENECE TO PHOSPHORUS AND ITS SEQUESTRATION USING NOVEL ADSORBENT"**

Candidate's Name : **Satya Narayana Pradhan**

Copyright Transfer

The undersigned hereby assigns to the Banaras Hindu University all rights under copyright that may exist in and for the above thesis submitted for the award of the Ph.D. degree.

(Satya Narayana Pradhan)
Signature of the candidate
ID. No. PS-17062
Enroll. No. 379862

Note: However, the author may reproduce or authorize others to reproduce material extracted verbatim from the thesis or derivative of the thesis for author's personal use provided that the source and the University's copyright notice are indicated.

"VARIATION IN WATER QUALITY OF CHILIKA LAKE (ODISHA) WITH SPECIAL REFERENECE TO PHOSPHORUS AND ITS SEQUESTRATION USING NOVEL ADSORBENT"

By

Satya Narayana Pradhan

Thesis Supplicated to
Department of Soil Science & Agricultural Chemistry, Institute of Agricultural Sciences, Banaras Hindu University, Varanasi - 221005, in partial fulfilment of the requirements for the degree of Doctor of Philosophy in Soil Science & Agricultural Chemistry

2022

Approved by Research Programme Committee

Supervisor	:	**Dr. A. K. Ghosh, Professor** Department of Soil Science & Agril. Chemistry, I.Ag.Sc., BHU, Varanasi
Members		
DRC Nominee	:	**Dr. R. Meena, Assistant Professor** Department of Soil Science & Agril. Chemistry, I.Ag.Sc., BHU, Varanasi
Internal Subject expert	:	**Dr. P. Raha, Professor** Department of Soil Science & Agril. Chemistry, I.Ag.Sc., BHU, Varanasi
External Subject experts-I	:	**Dr. M. K. Singh, Professor** Department of Agronomy, I.Ag.Sc., BHU, Varanasi
External Subject experts-II	:	**Dr. Praveen Prakash, Professor** Department of Plant Physiology, I.Ag.Sc., BHU, Varanasi
External Examiner	:	

ACKNOWLEDGEMENT

*With limitless humility, I bow my head towards almighty, merciful, compassionate and supreme power **"GOD"** whoshowed his mercy on me and blessed me to complete my Ph.D. successfully hitherto and present the piece of work for which I am eternally indebted.*

*Indeed, with knee down, I bow my head and offer flowers of reverence to **Bharat Ratna Mahamana Pandit Madan Mohan Malaviyaji,** the founder of the Banaras Hindu University, for his lifetime sacrifice and efforts in establishing such a great temple of learning for the cause of millions of students like me.*

*I bow my head in great reverence to the omnipotent and omnipresent **Lord Kashi VishwanathJi, Shri SankatMochan Hanuman Ji, Lord Ganesha, Kal Bhairwa ji and Goddess Saraswati** for their kindness and true blessings towards me and to every creature resending on this wonderful planet. In addition, I am highly obliged to this holy city Varanasi which is situated at bank of **Maa Ganga**.*

*I feel immense pleasure to express my deepest sense of gratitude to **my Supervisor Dr. A. K. Ghosh**, Professor, for his inspiring & ingenious guidance, disciplined attitude, enthusiastic interest, constructive criticism, innovative suggestions, unending zeal & constant encouragement during the entire course of investigation and preparation of manuscript. His noble guidance & untiring efforts helped me greatly during the course. I feel myself wordless to express my thanks to him for providing all kind of help in completion of manuscript. I will always remain deeply indebted to him for his affection and generosity bestowed upon me.*

*I am highly thankful to Members of my **Research Programme Committee, Dr. R. Meena**, Professor, Department of Soil Science & agricultural Chemistry, **Dr. P. Raha,** Professor, Department of Soil Science & agricultural Chemistry, **Dr. M. K. Singh,** Professor, Department of Agronomy, and **Dr. Praveen Prakash,** Professor, Department of Plant Physiology, for their valuable guidance and thoughtful suggestions in the need of time during this research work.*

*I extend my indebtedness to **Prof. A. P. Singh, Prof. S. Singh, Prof. B.R. Maurya, Prof. Janardan Yadav, Dr. P.K. Sharma, Dr. A. Rakshit, Dr. Y. V. Singh** and I am thankful to all staff members of Department of Soil Science and Agricultural Chemistry, Institute of Agricultural Sciences, Banaras Hindu University for all kinds of help and cooperation to me during my study period.*

*I am also extremely thankful to **Prof. N. De**, Head, Department of Soil Science & agricultural Chemistry, Institute of Agricultural Sciences, B.H.U. for providing all the necessary facilities and suggestions during investigation.*

*I wish to place on record my appreciation and sincere thanks to **Mr. Shishir Bhaiya, Agraj Bhaiya, H.N. Bhaiya, Anil Sharma, Murti Ji, K.K.***

Bhaiya, Amrinder bhaiya and Abishek *non-teaching Staff members of Department of Soil Science and Agricultural Chemistry for extending their kind cooperation and motivation during the entire course of this study.*

I also thank to my laboratory staff of carbon sequestration and soil technology Laboratory, ***Mr. Sanjay Bhaiya*** *for his timely help during my study.*

With profound regards in a more personal sense, I owe deepest debts to my revered parents ***Shri Bijaya Pradhan*** *and* ***Smt. Sumita Pradhan****, who taught me the value of wisdom based on erudition but without being enslaved by it and their persistent inspiration, selfless sacrifice, continuous encouragement, and blessing gave untiring help and have enabled me to be what I am, today. I will also like to acknowledge my affection towards my Brother* ***Mr. Subodha Pradhan****, who were always with me during my ups and downs. I thank them once again for their kind cooperation.*

I feel great and thankful for the contributions rendered by my seniors, ***Priti mam, Seema mam, Priyanka mam, Surinder sir, Ashish sir*** *I am also thankful to my classmates* ***Abhik, Rishi, Babu sir, Aditi, Mukta, Saroj, Shiva, Jaya, Pratibha mam.***

I feel great and thankful for the contributions rendered by my ever-loving PhD odia team ***Sudipta and Sauranshu, Jhumishree, Monalisha, Bandana,*** *during this eventful journey at Banaras Hindu University.*

I record my special thanks to my dear junior friends, Tusar, ***Abhisek, Kanhu, Gourishankar, Dibyajyoti, Chandini and Prachi.***

I am also expressing my sincere thanks to ***University Grants Commission*** *for providing financial assistance during my study.*

It is more likely that I have missed many names in these acknowledgements and hope that those concerned although unnamed, will accept my grateful thanks. I still solicit their benediction to proceed at every step of a perfect destined life.

Date: ***(Satya Narayana Pradhan)***
Place: B.H.U.,Varanasi

CONTENTS

ABBREVIATIONS

%	:	Per cent
km	:	Kilometer
ug/l	:	Microgram per liter
µ	:	Micron
cm	:	Centimeter
m	:	meter
mL	:	Milliliter
et al.	:	et alia (and associates)
nm	:	Nanometer
mg	:	Milligram
L	:	Liter
i.e.	:	(ed est.) that is
g	:	gram
Kg	:	Kilogram
m^2	:	Square meter
rpm	:	Revolutions per minute
^oC	:	Degree Celsius
Min	:	Minute
M	:	Molar
NTU	:	Nephelometric Turbidity Unit
PSU	:	Practical salinity unit
ppm	:	Parts per million
meq	:	Milli equivalent
mol	:	mole
θ	:	Theta
^{0}	:	degree
β	:	beta
λ	:	lambda
A^o	:	Armstrong
cc	:	Cubic meter
eV	:	Electron volt

LIST OF TABLES

LIST OF FIGURES

PREFACE

The present investigation is written for the award of doctoral degree in Soil Science & Agricultural Chemistry under the supervision of **Prof. A. K. Ghosh.** The Chilika lake was on the verge of eutrophication due to both external and internal loading of phosphorus. The present study entitled "Variation in water quality of Chilika lake (Odisha) with special reference to phosphorus and its sequestration using novel adsorbent" was conducted to analyze the water quality variables of lake and distribution of forms of phosphorus in the lake and river sediment and soils of catchment area and synthesize a novel adsorbent to effectively remove phosphate from aqueous solution. The research work was conducted at Soil technology and carbon sequestration laboratory, department of Soil Science and Agricultural Chemistry, Chilika lake, Chilika development authority, from 2017 to 2022. The chapter wise presentation of the thesis is as follows

Chapter I includes the introduction which provides a general background. This chapter justifies the purpose for choosing this research topic and objectives pertaining to this thesis work.

Chapter II includes review of literature which elaborates the available literatures covering various aspects under the scope of the present study.

Chapter III includes the materials and methodology employed for carrying the research work and the details of methods. The statistical analysis used in the present study has also been mentioned in this chapter.

In *Chapter IV* the experimental findings are presented. The analysis revealed by this study will be valuable in furthering the knowledge in this field. The results obtained have been discussed and interpreted in light of research work done.

In *Chapter V* a brief description of the achievements obtained in the present investigation has been given and a conclusion is drawn from this study with the hope that it will provide scope for further research and their application in management.

Lastly, references include the list of references in alphabetical order which has been consulted during the course of investigation and cited in the text.

Chapter I

INTRODUCTION

Water is one of the most vital natural resources for all life on Earth. Water contains many nutrients and minerals essential for human life. Access to safe water is essential for human health, social and economic development. Surface water is most vulnerable to pollution due to its easy access for disposal of pollutant and waste water (Manjare *et al.*, 2010). Water quality is important in every aspect of the ecosystem and wellbeing of human beings (UN Water, 2010). The river and lake ecosystem directly or indirectly influence human health and aquatic life (Kar, 2013). Lake water quality is influenced by anthropogenic activities surrounding the lake such as agriculture, waste dumping etc. (Mahananda et al., 2010). Meeting the water quality of rivers and lakes are also a major issue as these are the source for supplying water to various domestic, industrial and agricultural uses. The surface water bodies such as lakes and rivers are the important source of fresh water. High spatial variability in the physical, chemical, and biological parameter makes coastal lakes a highly unstable ecosystem.

Coastal lakes like Chilika, with estuarine characteristics are regions of high primary productivity. Water quality of coastal lakes, like Chilika, is influenced by fresh water flow, ocean exchange and river runoff. This results in change in salinity, increase in organic matter content, algal bloom, and alteration in bottom sediment properties, which makes ecology of lakes highly dynamic. The growth of plankton and productivity of lagoon ecosystems can be significantly impacted by the stoichiometric properties of nutrients (Ganguly *et al.,* 2015). Nitrogen and phosphorus have been limiting nutrients responsible for primary productivity of coastal lagoons. Nutrients enter the lake ecosystem through the river from the agricultural

waste and human excreta. As water enters the lake through the catchment area, it adds various soluble and insoluble substances depending on the land use type, altering properties of water. Transformation of nutrients occur in the catchment area as physico-chemical properties of soil varies in different land use type which also influence nutrient stoichiometry. Therefore, quantitative assessment of water quality is important for efficient water management (Banerjee and Srivastava, 2009).

The problem associated with monitoring of water quality is associated with measurement of large number of variables and the high variability caused due to anthropogenic and natural in origin (Boyacioglu, 2007). Extensive research in this area leads to development of a number of methods and models for analysis and interpretation of the measured variables. For water quality assessment various international and regional standard for different parameters were established however they do not provide picture of the complete scenario (Ali *et al*., 2014). There is an immediate need to know the pollution status of a lake at a given time so that necessary conservation activities may be undertaken to regain/improve the health of the water body. This can be done by measuring the trophic state index (TSI) to know the trophic state of the lake. Classifying water bodies according to their trophic states enables comparisons between ecosystems within and between different ecoregions and provides an understanding of the degree of cultural eutrophication that a system has experienced. Consequently, such a classification can be utilised as a crucial management tool for determining the state of the ecosystem under investigation. In addition to TSI, water quality index serves as an indicator for assessment of water quality as proposed for the first time by Horton (1965). Water quality index summarizes various water quality parameters into a simple index. It helps to interpret water quality as a means of single numerical value. Several Water Quality Indices (WQI) have been developed globally in order to monitor water quality for direct human consumption and other uses (Sun *et al.*, 2016).

External nutrient loadings alter the food chain and renders the lake eutrophic. Change in trophic status of lake due to external nutrient loading results in emergence of new species and algal bloom. After the death of algal population, the large biomass sinks to the bottom of the lake and its decay results in hypoxic conditions in the ecosystem resulting in death of fish and crab population. Mostly, increase in P content in the oligotrophic lake leads to rapid growth of algal population.

Phosphorus enters the lake by deposition, surface run-off, and from the drainage area via ditches and brooks. The phosphorus loading of the lake depends on the form of land use (especially agriculture) and the rock types on the soil of the drainage area. Annual phosphorus loading can be estimated by taking samples and measuring the discharge in the ditches and brooks leading to the lake. (Helminen *et al*., 1995). External nutrient loading can be divided as point source loading and nonpoint source loading. Point source loading originates from a specific source, such as a factory, fish farm or urban community, which can be easily measured and controlled. Non-point source loading originates from wide, unspecific areas (loadings from cultivated area, forest area, fallow land), making the controlling of it more difficult than point source loading.

Non-point source pollution from agriculture has been identified as a major cause of degradation of water bodies (USEPA, 2002). Excess P application beyond a crop requirement would result in its loss from soil to adjacent water bodies via the surface and subsurface, accelerating the process of eutrophication. This has become a common and growing problem in rivers, lakes, estuaries, and oceanic coasts. P is deposited as particulate matter and buried into marine sediments as organic compounds, detrital and amorphous minerals, adsorbed P, and incorporated into skeletal debris as biogenic calcium carbonate (Paytan and McLaughlin, 2007). P content in overlaying water is controlled by release of P from the sediment. P speciation, pH, redox condition and concentration of Fe, Al, and Ca can influence the P

exchange between water column and sediment. P fractionation is one such tool to extract different forms of P sequentially. Five different fractions can be extracted using P fractionation, namely; water soluble P (WSP), loosely bound P (L-P), Al & Fe bound P, calcium bound P (Ca-P), and residual P (R-P). Fe-P is the redox sensitive fraction, which can reduce into iron (II) phosphate and release phosphate into overlaying water column which can be consumed by phytoplankton (Bastami *et al*., 2018). Among various forms of P, WSP, L-P, Al & Fe-P, and R-P are considered as biologically active form as they can release phosphate into overlaying water (Zhuang *et al.*, 2014). As increase in P concentration increase algal bloom, study of P in lake ecosystem is of great importance. Effect of P on lake ecosystem is depend on its chemical composition and its form in the sediment.

Loss of P from soil or sediment primarily depend on 1) initial soil P concentration and 2) P sorption capacity of soil. Soil P concentration can be measure as Melhich-3 P (Mehlich, 1984), Olsen P (Olsen *et al.*, 1954), Bray (Bray and Kurtz, 1954), etc. Since the loss of soluble P through runoff from a particular soil is related to its strength with which the P is adsorbed to the soil solid phase, a good understanding of P sorption characteristics is needed to access its environmental impact. P sorption capacity can be estimated by using adsorption isotherms which is widely used to calculate maximum adsorption capacity. Sediments can both act as source or sink of P. Sediments are often regarded as source of P to water, but may also adsorb P from the overlaying water. Sharpley (1981) reported decrease in P loss to water due to increase in sediment content in run-off as it acts as sink for P. It is important to study the desorption behavior of soil or sediment in order to determine whether the soil or sediment is source or sink of P.

Removal of P from the wastewater or reduction in P level in the lake system is necessary to prevent eutrophication of lake. P removed from the wastewater can be used as a raw material for fertilizer production in agriculture. Successful and economical recovery of P would change

the current thinking of P as a pollutant to P as a resource. There are numerous methods to recover P from wastewater or lake, particularly capping of P with a P-fixative, chemical precipitation with iron salt, alum, lime is popular option. However, variation of pH and redox state of shallow lake, like Chilika, may cause the release of the P from this metal oxide-based material. Furthermore, precipitation method is less effective when the P concentration is relatively low, which is the case with lake ecosystems. Therefore, sorption process is considered as most effective procedure to remove P because of its ease of operation, simplicity of design, economy compared to chemical treatment and biological processes (Bhatnagar and Sillanp¨a¨a, 2011). In recent years, use of P adsorbent to remove P from eutrophic water bodies such as rivers and lakes is increasing (Ding *et al*., 2018; Yang *et al*., 2014; Yin *et al*., 2016). Furthermore, use of lanthanum-based adsorbent as P-sorbent to control release of P from sediment has gained attention due to strong affinity of lanthanum towards phosphate (Copetti *et al*., 2016; Fang *et al*., 2018; Wang *et al*., 2018). Lanthanum-based bentonite (phoslock) was first invented to sequester P from sediment. Later, several La-based adsorbents were synthesized for P removal from lake ecosystems (Xie et al., 2015; Wang et al., 2017). Despite advantages of using La-based material, its use is limited due to high consumption of La resource. Magnetizing the La nanoparticle with Fe_3O_4 is the best solution to separate, recover and reuse the adsorbent. P recovery from lake sediments and overlaying water using La based magnetite is an alternative to restore eutrophic lakes and simultaneously avoid excess consumption of La resource.

Chilika lake is habitant to several endangered species listed in International Union for Conservation of Nature (IUCN) Red List of threatened species. Given the ecological importance of Chilika lake, various national and international bodies has been conducting research related to water quality, phytoplankton growth, hydrodynamics etc. However, studies related to P speciation and release of P from sediment is limited. Considering the ecological

importance of lake and its associated environmental risk due to pollution from the catchment area, a study entitled "Variation in water quality of Chilika lake (Odisha) with special reference to phosphorus and its sequestration using novel adsorbent" was undertaken with the following objectives:

(1) To determine seasonal water quality of Chilika lake

(2) To estimate the external nutrient loading of lake Chilika

(3) To study the P fractions in sediments of lake Chilika

(4) To synthesize and characterize a magnetic based novel adsorbent

(5) To study the phosphorus removal efficiency of synthesized novel adsorbent

Chapter III

Review of literature

External and internal loading of phosphorus affect the lake water quality and extent of eutrophication. Studies on distribution of forms of P and its distribution is important to have a insight into effect of P on lake ecosystem health. Therefore, P needs to be sequestered to remove excess P from the lake water reduce lake eutrophication. This chapter provides some reviews relating to the research work entitled “Variation in water quality of Chilika lake (Odisha0 with special reference to phosphorus and its sequestration using novel adsorbent”. The reviews have been categorized in following order;

2.1 Eutrophication

2.1.1 classification of eutrophicated water bodies

2.1.2 factors responsible for eutrophication

2.1.3 Manifestation of eutrophication

2.2 Transfer of P along the land-lake continuum

2.3 P fertilizer in agriculture

2.4 Sources of eutrophication in lake

2.4.1 Natural eutrophication

2.4.2 Cultural eutrophication

2.5 Water quality assessment

2.5.1 Trophic state index

2.1 Eutrophication

One of the most challenging environmental issues that surface water bodies are currently dealing with is eutrophication (Li-Kun *et al*., 2017). Eutrophication refers to the increased production of organic material/ phytoplankton due to the enrichment of water bodies with nutrients, particularly nitrogen and phosphorus. It is like an aging process where the lake gets continuously enriched with nutrients increasing photosynthesis of the aquatic ecosystem.

2.1.1 Classification of eutrophicated water bodies

Eutrophication is used to describe the condition of aquatic habitats. This uses the 'trophic status of the waterbody as a description of the waterbody. Typically, the phrases oligotrophic, mesotrophic, eutrophic, and hypertrophic are used to describe the nutrient status of a waterbody. Oligotrophic refers to the condition of having low nutrient concentration and ineffective aquatic animal and plant life. These lakes are ideal for drinking purposes and produce very little algae. Mesotrophic is a level of nutrients in between, reasonably productive in terms of aquatic plant and animal life and beginning to exhibit indicators of water quality issues. The eutrophic state of water bodies represents a very high concentration of nutrients, is

very productive in terms of aquatic animal and plant life, and is beginning to show indicators of poor water quality. Transparency of water bodies is reduced due to high algal bloom. In a hypertrophic state, high nutrient concentrations predominate and physical variables may affect plant development. There are substantial and almost constant issues with water quality. At lower depths, dissolved oxygen content decreases, causing the water to become less clear and aquatic life to end.

2.1.2 Factors responsible for eutrophication

Eutrophication is an imbalance in the functioning of aquatic bodies triggered by a change in the relative quantity of nitrogen and phosphorus. The response of the aquatic body to the changing nutrient concentration is an environmental factor depending on the process. Residence time, temperature, and light affect the response of water bodies to nutrient enrichment. Increased biomass/phytoplankton production from nitrogen/phosphorus enrichment in the lake reduces light penetration. The aquatic body shifted from a nutrient-limit ecosystem to nutrient saturated system where light penetration is the limiting factor.

2.1.3 Manifestation of eutrophication

New plant species replace the original species present in the lake due to changes in environmental conditions due to eutrophication. A rapid increase in new plant species changes the structure and function of the lake. The main sign of eutrophication is a rapid rise in the algae population. The distribution of algal growth can provide information about a lake's water quality. 25^{o}C is the ideal temperature for algae development. Chilika Lake's alkaline pH and average water temperature are favorable for phytoplankton growth. Large amounts of biomass are produced by the algal bloom, and when bacteria break that down, it causes anoxia or hypoxia in the deeper parts of the water body and can even release toxins (CO_2, H_2S, and CH_4). Disturbances in the lake functioning are first detected at the individual level, later

morphological and community level. Some of the repercussions of eutrophication include algal bloom, hypoxic or anoxic conditions, and the mortality of aquatic organisms. The growth of water fern as Azolla sp. can create a hypoxic or anoxic condition in the river and lake ecosystem. Cyanobacteria is dominant in the lake ecosystem due to eutrophication capable of producing toxins. They fall under the genera *Oscillatoria, Lyngbya, Nodularia, Microcystis, Planktothrix, and Dolichospermum*. Eutrophication also leads to severe health hazards to humans and animals. It has an impact on aesthetic views and the economy.

2.2 Transfer of phosphorus along the land-lake continuum

Risk related to eutrophication depends on nutrient flow from the catchment area to the aquatic ecosystem/ lake via river or water pathways. Nutrient input comes from a hundred and thousand kilometers away from the lake. Along the land-lake continuum, the nutrient gets adsorbed by soil and sediment. The adsorbed P gets mobilized under specific environmental conditions. P cycle in the soil/sediment-water interface occurs in solid and liquid forms. Different biogeochemical processes controlling the transfer of P along the land-lake continuum result in changes in the stoichiometry of nutrients from catchment to lake. This explains the difficulty in the assessment of P retentions of sediments. There is a difference in water flow from catchment to lake ecosystem, therefore it is difficult to establish a clear relation between landscape and water quality of river and lake.

2.3 Phosphorus fertilizer in agriculture

P is considered a critical nutrient for crop growth and production. Historically soil available P and organic manure are the major source of P in the field of agriculture. With growing food demand due to population explosion, mineral fertilizer has taken over as the major source of P input in agriculture. Common P fertilizers used in agriculture, such as mono- and di-ammonium phosphate, are often water-soluble, rapidly dissolve in soil solutions, and

immediately available for plant uptake. These highly mobile soluble phosphates in soil are released into surface water bodies by runoff and leaching, enriching the aquatic ecology (Maghsoodi *et al*., 2020). 25 percent of the 250 million metric tonnes of phosphorus mined since 1950, according to Rosemarin (2004), ended up in water bodies.As a result, P poses a danger of damage to water bodies that could result in environmental issues such as eutrophication, groundwater pollution, and the rapid growth of hazardous algae. 14 Mt of phosphorus per year, as opposed to the proposed limit of 6.2 Mt P per year, is lost from fertilizer to waterbodies through soil erosion (Steffen *et al*., 2015). In their study of P intake in 100 lakes around the globe between 2005 and 2010, Fink *et al*. (2018) found that P loading has increased overall by 17–82 percent in Latin America, North America, and Africa. Malago *et al*. (2019)'s study of P input to the Mediterranean Sea identified agricultural, urban trash, and soil erosion as the sources of P. According to the Water Research Commission, eutrophication poses a risk to 54 percent, 53 percent, 46 percent, and 28 percent of the lakes in Asia, Europe, North America, and Africa, respectively. (Nyenje *et al*., 2010). The natural transition of the lake from oligotrophic to eutrophic is a slow process, however, with the intervention of a human, this process is accelerated. Therefore, evaluating the lake's water quality and determining the cause of lake pollution is the scientific community's top priority to develop a solution to environmental management (Huo *et al*., 2018).

Although the concentration of P in agricultural runoff is lower than that of P in domestic or industrial waste, excess P from cropland nonetheless serves as a primary source of P diffusion into aquatic ecosystems (Mockler *et al.,* 2017). Various global agency has recommended a critical level of P in natural waterbodies to prevent eutrophication of aquatic bodies including lake and river. P levels of 0.01 mg P L^{-1} for standing water and 0.2 mg P L^{-1} for flowing water were recommended by the European Environmental Agency. For standing water, the US Environmental Protection Agency recommended a level of.05 mg P L^{-1}, while

0.1 mg P L^{-1} was advised for flowing water. For a long time, wetlands have been regarded as efficient nutrient sinks (Ji *et al*., 2020; Ma *et al*., 2016; Vymazal and Bˇrezinov´a, 2018). Permanent burial and sorption by clay and metal particles remove P from the wetland. P is removed from water columns and organic material is incorporated into the sediments during burial. However, when the sediments of wetland exceeded the capacities of retention, wetland soon become the source of bioavailable P for algal and microphyte populations (Audet *et al*., 2020; Bakhshoodeh *et al*., 2020). Additionally, anaerobic condition facilitates the release of P from sediment (Bakhshoodeh *et al*., 2020).

2.4 Sources of eutrophication in lakes

Eutrophication has a variety of ecological, social, and other economic causes that are quite complicated. Eutrophication-causing variables can be divided into two categories: natural factors and human intervention factors (David *et al*., 2020; Lin *et al*., 2020). The use of phosphatic fertilizer in agriculture, the use of pesticides and herbicides, industrial waste from nearby factories, and other human interventions are the main sources (Wang *et al*., 2017).

2.4.1 Natural eutrophication

The natural eutrophication process takes place very slowly with geological time. Climate change's increase in daily mean water temperature gives algae a favorable habitat for growth (Nalley *et al*., 2018). Water released into the lake during rainfall events carries nutrients from land to the lake which is sufficient for the eutrophication process (He *et al*., 2018; Zhang *et a*l., 2020). Additionally, under certain environmental conditions, nutrients from sediments might be released into water columns (Lei et al., 2018). Debris decomposition increases the lake's nutrient concentration. Eutrophication is brought on by both dry and wet deposition, which increases the nutrient concentration (He et al., 2018). The wet deposition of nutrients takes the form of rainfall events (Zhang *et al*., 2020).

2.4.2 Cultural eutrophication

Eutrophication triggered by human interventions is called cultural eutrophication (David *et al*., 2020). Population growth, various types of environmental pollution, intensified land use, the use of nutrients as agricultural fertilizers in developed countries starting in the 1940s, and the use of phosphate compounds in laundry detergents starting in the 1950s (Kroes, 1980) have all contributed to the global eutrophication of water bodies. Fertilizers used in the agricultural field in the catchment area are transported to the lake which carries a substantial amount of nutrients (nitrogen and phosphorus) (Ortiz-Reyes and Anex, 2018). Farmland, forests, and grasslands thus serve as the lake's main non-point sources of nutrient loss (Xue *et al*., 2017). As a result of increased soil erosion brought on by deforestation, agricultural and forest soil are lost, and eventually, nutrients are carried to the lake. Eutrophication is caused by domestic water from the washing machine, toilet, and detergent (Huang *et al.*, 2017). Industrial wastewater from the nearby factories is a point source of phosphorus and nitrogen (Rajasulochana and Preethy, 2016). Domestic and commercial wastewater was discharged into the lake via leaching or surface runoff (Khan and Jhariya, 2017). Nearby fisheries and animal breeding operations, such as poultry farms, contribute to the lake's nutrient pollution.

According to Zhang *et al*. (2019), urban, forest, and agricultural areas account for 61%, 21%, and 18%, respectively, of the total P (TP) load in the lake. Additionally, he noted a 50% increase in TP load when 15% of the basin's area is used for agriculture. Additionally, he attributed a 2–9% TP load from the river system to the lake. Human efforts caused TP load to the lake to increase quickly. Increased non-point source of input into the lake is mostly caused by extensive farming and a lack of proper environmental management techniques. (Zhang *et al*., 2019).

2.5 Water quality assessment

This section discusses the different indices used to determine the eutrophication status and water quality of the lake.

2.5.1 Trophic state index

There is no ideal or set of evaluative criteria for determining the trophic status of a waterbody. However, the common metrics used to evaluate the trophic stage or eutrophication were total nutrient content (N and P), algal chlorophyll, water transparency, etc. Carlson proposed Carlson's trophic state index (1977). Sechi disc depth in meters (SD), total phosphorus (TP) in mg L^{-1}, and chlorophyll (Chl-a) in mg L^{-1} were the three variables that Carlson used to measure TSI. Sechi disc depth is a measurement of the lake's water transparency and a crucial eutrophication indicator (Zou *et al*. 2020). Secchi disc depth is a direct indicator of the lake's primary productivity. The limiting ingredient for phytoplankton growth in the lake is phosphorus. (An *et al*., 2019). The types and distribution of phosphorus have an impact on the lake's algae growth. Most of the phytoplankton in the lake are made up of photosynthesis-capable algae. The regional and temporal distribution of Chl-a in the water column is used to assess TSI since it is a key indicator of algal development in the lake. (Cao *et al*., 2018). Table 2.1 summarizes general guidelines for the nutrient concentrations indicating various trophic statuses of a waterbody.

Table 2.1. N and P status of water bodies with the different trophic states.

Trophic status	**Total phosphorus (µg/L)**	**Total nitrogen (µg/L)**
Oligotrophic	5–10	250–600
Mesotrophic	10–30	500–1100
Eutrophic	30–100	1000–2000
Hypertrophic	>100	>2000

2.5.2 Water quality index

To evaluate the lake's eutrophication level and water quality, a water quality index was utilized. It considers the lake or river system's biological, chemical, and nutritional components (Yan *et al*., 2016). Several researchers have proposed WQI as a depiction of lake overall water quality. It is expressed as a single number that combines the values of various parameters to reflect the level of pollution or water quality. The concept of WQI was originally developed by Horton (1965), a German scientist. However, the WQI evaluation method undergoes various changes with time and different methods have been formulated by various researchers (Boyacioglu, 2007; Reza *et al.*, 2013; Silvert, 2000). The WQI can be used to derive necessary information like, comparison of water quality of different sources, to plan related to policy, to identify the difference between water quality after and before implementation of a regulatory policy etc. generally, there are four steps in calculating WQI, namely;

- parameter selection
- assigning sub-index value to parameter
- assigning weight to different parameter corresponding to their relative importance
- index aggregation of weighted sub-index values

The WQI was proposed by the National Sanitation Foundation (NSF) by adopting a Delphi technique, and its equation is listed in Equations;

(i) $\mathrm{RW} = \frac{AWI}{\sum AWI}$,

Where RW = relative weight, AW = assigned weight of each parameter,

(ii) Rating of each parameter is calculated by dividing its concentration in lake water by respective standard according to World Health guidelines.

$$Qi = \frac{Ci}{Si} \times 100,$$

While the rating of pH and DO was calculated from the following equations,

$$Q = \frac{Ci - Vi}{Si - Vi} \times 100,$$

Where, Qi = the quality rating, Ci = value of water quality parameter from laboratory analysis, Si = standard value of water quality according to WHO and BIS standard.

(iii) $SI_i = W_r \times Q_i$

(iv) $WQI = \sum SI_i$

The development of water quality management tool technologies has utilized a variety of strategies over past few decades including mathematical techniques (artificial intelligence, neural networks), optimization techniques (fuzzy programming) etc. (Basatnia *et al.*, 2018). Various physical, chemical, and biological parameter influence the water quality of aquatic bodies and its frequent monitoring produces a large set of data which is challenging to understand. Therefore, use of multivariate analysis like principal component analysis (PCA), cluster analysis helps to comprehend the result in a better way (Esdras *et al.*, 2017). Various research has used PCA tool to assess the water quality of river and lake (Basatnia *et al.*, 2018; Dutta *et al.*, 2018; Tripathi *et al.*, 2019). PCA has been used to reduce the number of datasets to capture maximum variance with minimum number of parameters. In the next step of assigning weightage to different parameter, some researcher used subjective or objective methods. Finally, the sub-indices are aggregated to get the WQI. Barakat *et al.* (2016) used PCA and CA to assess the spatial variation in water quality of Oum Er Riba River and EI Abid River. These tools are essential to identify the source of pollution and group sampling stations with similar characteristics.

2.6 Mechanism and transfer of phosphorus

Frequent algal bloom causes degradation of the ecological function of the lake. Human intervention leads to the transfer of excess nutrients (particularly nitrogen and phosphorus) from agricultural and other point sources to the lake. Algal growth destroys the ecological balance of the lake. Therefore, it is urgent to better understand the mechanism of eutrophication to adopt mitigating measures to prevent eutrophication. In this section, we are discussing the mechanism and transfer of phosphorus.

2.6.1 Nutrient deposition

The accumulation of too many nutrients in the lake ecosystem is the main cause of eutrophication. The lake can absorb nutrients in several ways. First, both dry and wet deposition can deposit nutrients (nitrogen and phosphorus) in the lake. A frequent method of wet nutrient deposition in lakes is precipitation (Zhang *et al.*, 2020). In both dry and wet deposition, nutrients are deposited as particles and eventually dissolved. These dissolved nutrients are accessible to phytoplankton and other aquatic plants for absorption (Yang *et al*., 2016). Second, outside sources such as home and industrial wastewater as well as freshwater flow from rivers and their tributaries significantly contribute nutrients to the lake. Thirdly, nutrients are transferred between the water column and particulate particles (Li *et al.*, 2014). Fourth, nutrients can be transferred between the water column and sediment (Yan *et al*., 2018). Decomposition of organic materials and nutrient transformation is made possible by photocatalytic degradation (nitrogen and phosphorus). When this process is interfered with, nutrients build up and algae in the lake proliferate.

2.6.2 Nutrient transformation

Nutrient in the lake is exchanged between the primary producer (phytoplankton, algae), the consumer (zooplankton, fish), and micro-organism. Primarily, algae use nitrate nitrogen, ammonium nitrogen, and orthophosphate as the source of the nutrient. The rate of transformation of nitrogen and phosphorus is key to the eutrophication process. Particulate matter is the carrier for nitrogen and phosphorus in the lake.

2.6.3 Transformation mechanism associated with water column

The main sources of nutritious particulate matter come from outside sources such as freshwater influx, plant debris, and lake bottom sediments (Li *et al*., 2018). The enormous surface area of sediment allows it to both absorb and desorb nutrients into the water column. Under specific physical, chemical, and biological conditions, nutrients from particulate matter can be released into the water column (Yang *et al*., 2016). Under the influence of microorganisms, dissolved organic nitrogen, dissolved organic phosphorus, and organic molecules (-COOH, -OH) can be converted into inorganic nutrients that can be used as a source of nutrients by algae, phytoplankton, fish, and other organisms (Li *et al*., 2019). Consumers consider primary producers to be their food sources (Zooplankton and fish). Additionally, consumers release pollutants that microorganisms can use. An essential factor in the phosphorus and nitrogen cycle is the rate of matter transformation in this process (Guo *et al*., 2020).

The three main forms of nitrogen in the water column are nitrate, NH_4-N, and NO_2-N. In phytoplankton and suspended form in sediment, organic nitrogen is stored (Xia *et al*., 2018). Ammonification, nitrification, denitrification, and assimilation are the processes that determine how different types of nitrogen are transformed (Han *et al*., 2016). Ammonification is the term for the aerobic decomposition of nitrogenous organic compounds. Denitrifying bacteria convert NO_3-N to N_2 in a reduction environment. Algae and phytoplankton decompose inorganic forms of nitrogen to produce organic versions (Xia *et al*., 2018). P is present in the

water column in both dissolved and particle forms (Liu *et al*., 2016). There are two types of dissolved P: dissolved inorganic and dissolved organic. Soluble P is utilized by the aquatic organism to form organic P.

As the amount of nutrients (nitrogen and phosphorus) in the water column rises, algae take up more nutrients, which causes the number of nutrients in the water column to fall (Zhang *et al*., 2019). These cause the sediment to release nitrogen and phosphorus into the water column. Additionally, as, and when the algae and other debris decompose, the nutrients flow into the water column. The mechanism for nutrient transformation is determined by the type of microbial organism (aerobic or anaerobic) (Li *et al*., 2019). Organic matter partially or completely decomposes due to anaerobic bacteria, producing nitrogen (Li *et al*., 2019). Nitrogen, nitrate, and ammonia are released into the water column as a result of the incomplete aerobic breakdown of organic waste, encouraging the growth of phytoplankton (Zhang *et al*., 2018).

Lakes can be categorized as shallow lakes, transitional lakes, or deep lakes. Increased denitrification and decreased phosphorus deposition brought on by hydrodynamic disturbances in the shallow lake result in a greater N/P ratio and more phosphorus in the water column (Grantz and Haggard, 2014). This kind of lake is thought to be nitrogen-limited. Deep lake processes, however, differ from shallow lake processes. The distribution of TN, TP, and Chl-a along with maximum lake water depth globally demonstrates that the concentration of TN, TP, and Chl-a rises as lake water depth declines (Qin *et al*., 2020). This suggests that eutrophication issues and algal bloom are more common in shallow lakes. Lakes with water depth < 20m are susceptible to eutrophication. Chilika lake is a shallow lake with a mean water depth of 2 m, suggesting concern regarding algal bloom and eutrophication. Therefore, lake management strategies considering the lake water depth and water column features should be formulated.

2.6.4 Transformation mechanism associated with sediment

Sediment on the lake bottom act as a sink for nutrients. Different forms of nutrients imported from the exogenous source are utilized by aquatic organisms. The remaining nutrient gets adsorbed and deposited into the bottom sediment. Under varied concentration gradients, nutrients that enter the pore water of the sediment are exchanged with the water column (Gong *et al*., 2019). The exchange rate of DOP is facilitated by a high water-sediment water contact. DOP gradient at the water-sediment contact was 80%. (Kim *et al*., 2018). P is present as mineral P, DIP, and DOP (Liu *et al*., 2016). Mineral P is absorbed into iron and manganese hydroxide preventing its mobility (Ji *et al*., 2016). When certain conditions, such as a lowered pH, a redox state, or microbial decomposition, are met, adsorbed P can be released into the water that is overlying it (Xie *et al*., 2019). Fish, zooplankton, and phytoplankton are all buried in silt and make up organic P. DIP and organic P can be transferred through the pore water of sediment, assimilation, dissolution, and release into the water column (Liu *et al*., 2016). Inorganic P included aluminum P (Al-P, iron P (Fe-P, calcium P (Ca-P), and occluded P (Oc-P). When certain conditions are met at the water-sediment interface, organic P can be transformed into dissolved organic P and particulate organic P. P transformation in the sediment is influenced by a variety of physio-chemical processes and lake environmental factors.

2.7 Eutrophication management

2.71 Release of P from sediment

Sediment plays an important role in the dynamics of nutrients in the shallow lake. Due to differences in sediment characteristics and physical, chemical, and biological processes operating in the overlaying water column, the factor controlling the release of P from sediment also differs from place to place and season to season. The P settled as part of the organic subject to mineralization and regeneration. The P that has been regenerated may be recovered by

incorporation in newly produced minerals or by adsorption to ferric oxyhydroxides (Katsev, 2016). Under specific conditions, some of the soluble P may diffuse upward and finally migrate into the water column. Diffusion or sediment disturbance can supply the redox-released P in the pore water to the overlying water column (Tammeorg *et al.*, 2020).Additionally, the release of P may be caused both directly and indirectly by the mineralization of organic matter, which does so by lowering the redox potential at sediment surfaces. Shallow lakes that show an increase in the concentration of P in the water column during the summer, when most external inputs stop, are particularly susceptible to sediment P release (Nurnberg, 2020).A short-lived thermal stratification and an anoxic situation may develop in the bottom waters after an extended period of weak circulation during warm seasons, which can accelerate the diffusive migration of soluble P across the sediment-water interface (Giles *et al.*, 2016). Alternately, during stormy occasions, sediments in large shallow lakes like Lake Chilika are prone to vigorous resuspension. When the oxic microlayer is disrupted, it can also quickly raise water turbidity, water TP concentrations, and the contact between P-bearing particles and algae. This will also accelerate diffusive P movement across the sediment-water interface (Chao *et al.*, 2017).

Over the past few decades, phosphorus accumulation in lake sediments has drawn a lot of interest as a potential source of lake eutrophication. Sequential P fraction has been widely used to assess the P transformation and dynamics. Numerous studies have used sediment P fractionation to assess the dangers associated with P release into the lake water and possible P availability (Kangur *et al.*, 2013; Cavalcante *et al.*, 2018). Different forms of P fractions have varied abilities to release P back to lake water. Characterization of sedimentary P fractions is necessary for a better comprehension of the primary P release mechanisms. Because organic and loosely-bound fractions and redox-sensitive Fe-bound fractions are more and less susceptible to changes in redox conditions, respectively. The assessment of sedimentary P

fractions can help shed light on important mechanisms governing the release of P from sediments. Chemical sequential assessment of surface sediment will help to reveal the spatiotemporal variation in P fractions and provide the trophic condition of Chilika lake and the time lag for recovery even after the reduction in external loading. It was intended that the outcomes of this research would be helpful to water quality modelers and decision-makers in defining the optimum management approaches for Lake Chilika.

2.8 Need for P fractionation of lake sediment

Most P is retained particulate P and deposited into sediments after entering the lake from point and non-point sources; from these sediments, P can be released into the water column to promote algal biomass (Zhang *et al.*, 2020; Zhang *et al.*, 2023). Due to the limited physical distance between sediments and surface water, where energy may be quickly transmitted to the lake bottom, shallow lakes have highly active P cycles compared to deep lakes (Qin *et al*., 2020; Zou *et al*., 2020). If the external P load is significantly reduced, the improvement of the water quality and management of cyanobacterial harmful algal blooms in shallow lakes depends more on the lowering of sediment P pools (Xu *et al*., 2021). As a result, guidelines for sediment P concentrations must be created to help regulate water quality and reduce pollution (Rydin and Carey, 2011). In comparison to other harmful compounds, the standards for sediment P concentration are still lacking currently. Currently, the P release flux used to calculate the contribution of sediments is largely connected to sediment P management (Fan *et al*., 2020). Estimates of sediment P release potential, however, are based on a variety of experimental procedures that are site-specific and influenced by a variety of variables, such as estimate methods, sediment characteristics, and environmental circumstances (temperature, oxygen, pH, resuspension, etc.). It is required to establish criteria for sediment P content that link sediment characteristics and algal growth. P release from sediment is the most important factor determining the P concentration of overlaying water. However, not all P fractions release

P to the water column and render to lake eutrophication. It is well established that Fe/Al (hydr)oxides are related to the P bioavailability of sediments. Through pore water, iron reduction in underlying sediments causes P release and diffusion into the water column (Ding *et al*., 2018a; Zhang *et al*., 2020). More crucially, during the growth of algae in shallow lakes, Fe/Al (hydr)oxide-adsorbed P would directly desorb with an increase in pH, creating a phenomenon known as "P-pumping suction" from sediments to algae (Zhang *et al*., 2020; Deng *et al*., 2022). This suggests that the criterion for sediment P concentration may be attainable in shallow lakes where a direct relationship between algal biomass and sediment P pools can be established. Bioavailable sediment P pools are mostly evaluated using chemical or biological extraction procedures. Algal growth potential (AGP) bioassays, which have been used extensively around the world, may measure the quantity of P that is directly available to algae. The chemical approach has gained popularity since it is less complicated and time-consuming than bioassays, although it can be challenging to identify exactly which proportion and how much P is available to algae. To create the standards for sediment P concentrations in shallow lakes, a quantitative link between algal accessible P and chemical components of sediments is essential. The most crucial variables that reflect P pollution level, bioavailability, and possible mobility/immobilization under various environmental circumstances are sediment P content and its fractional composition. Fe (hydr)oxide-bound P (Fe-bound P), Al (hydr)oxide-bound P (Al-bound P), Ca compound-bound P (Ca-bound P), and organic P are the four main fractions of sediment P. Al-bound P is susceptible to alkaline settings, Fe-bound P tends to release under anoxia, and Ca-bound P is stable in circumneutral or alkaline lakes. In this study, we concentrated on the relationship between sources, sediment fractions, and algal availability of P in sediments to help create the criteria for sediment P concentrations to reduce cyanoHABs in shallow lakes.

Understanding the biogeochemical cycle of P is necessary for both future conservation efforts and the control of P loads to the environment, which calls for analytical tools for the precise speciation and measurement of P and its different forms and species.

2.9 P fractionation of lake sediment

The role of P in lake eutrophication can be more effectively evaluated by measuring the contents of different P fractions instead of total P. Typically, P forms are chemically bound in minerals, physically adsorbed onto sediment surfaces, and physiologically assimilated in cells and detritus derived from the sediment infauna. These processes are assessed by several sequential extraction procedures called P fractionations. A key indicator of approaching internal loading and the release to the water column is the amount of mobile or bioavailable P in the sediments (Rydin, 2000). Identification of the levels of various P types, as well as the total amount of P present in the sediments, is necessary for this context. P in the sediment is mainly adsorbed by clay, metal (Fe, Mn, Al) oxides, and hydroxides. In addition to the inorganic constituent, P is also settled onto organic matter, and biologically by some micro-origamis as polyphosphate (Amirbahman *et al*., 2013). P is found in different forms in sediment and can be separated by fractionation procedure.

2.10 P adsorption-desorption

Sorption experiments are usually carried out to estimate the mobility of sediment P. Adsorption and desorption of P to lake sediment influence the dynamic equilibrium between sediment interface and water. The adsorption-desorption equilibrium affects the biogeochemical cycles of P in the lake sediment. These reactions at the sediment-water interface results in release of P from the sediment to overlaying water and contribute to lake eutrophication. Adsorption isotherm, kinetics was usually used to evaluate the P release potential of sediment to lake water. P adsorption and desorption plays a key role in determining the P bioavailability and its

concentration in the lake. Sediment texture, pH, salinity, organic matter, CEC, Al & Fe oxide influence the P adsorption capacities of sediment. Finer particle with high organic matter and Al & Fe oxide, and large specific surface area hold high amount of P. Sediment with different physico-chemical properties vary in their P adsorption capacities. Increase in acidity (pH <7) or alkalinity (pH > 8) increase the P adsorption, with lowest P adsorption observed in the pH range of 6-7. Ligand exchange between HPO_4^{2-} and $H_2PO_4^-$ in the aqueous solution and OH- of sediment surface increase P adsorption (Du *et al*., 2016). P adsorption decreased with increase in salinity, as anions present in saline condition compete with phosphate for same adsorption site. Similarly, Al & Fe oxide decrease P adsorption at alkaline pH as OH^- compete with phosphate for same binding site (Fink *et al*., 2016b). Increase in organic matter also decrease P adsorption, as organic anion competes for same adsorption site as phosphate (Fink *et al*., 2016a). Hydrological condition like submergence of sediment could alter the oxidation and reduction state of sediment, thereby influencing adsorption process. Repeated redox condition could result in release of P from sediment (Scalenghe *et al*., 2014). Gilbert *et al*. (2014) demonstrate that rewetting of dried sediment ca release high P. Equilibrium P adsorption process of sediment is usually described by Langmuir and Freundlich equation.

2.11 Removal of P from lake

P from the lake or wastewater can be captured by various methods;

1. Enhanced biological P removal: P accumulating organisms trap the P present in the wastewater as microbial biomass-rich polyphosphate.
2. Precipitation as sparingly soluble compound: Ca and Mg are used to precipitate the phosphate as calcium or magnesium phosphate.
3. Adsorption of dissolved P using suitable adsorbent: Various adsorbents are used to sequester P from streams

4. Thermochemical combustion coupled with wet extraction is used to separate P from solid waste and then extract P from ash using mineral acid.

2.11.1 Enhanced biological P removal

To achieve biological P removal in municipal wastewater treatment systems, several biological suspended growth process designs have been put into place over the past 30 years. Enhancing bioprocess P removal (EBPR), also known as biological P removal, includes accumulating polyphosphate (polyP) from influent wastewater into microbial biomass before removing the biomass. In this process, fermentation of biodegradable C is carried out by PAO using polyp as an energy source releasing soluble phosphate ions and magnesium, calcium, and potassium ion (Zach-Maor *et al*., 2011). Then this undergoes an aerobic process where PAOS takes up soluble P and stores it as polyp using carbon as an energy source. This EBPR system is designed for the municipal system where P concentration in the effluent is relatively low (<25 mg L^{-1}).

2.11.2 Precipitation

In this process, P was removed from the stream as precipitate by adding different salts of Al, Fe, Ca, and Mg. The use of Al and Fe phosphate is limited in the field of industrial and agricultural applications. Generally, salts of Ca and Mg are used to recover P as a precipitate from the stream (Rittmann *et al*., 2011).

2.11.3 Recovery of phosphorus as magnesium ammonium phosphate (struvite)

P can be removed as a precipitate of magnesium ammonium phosphate. P recovery using magnesium is the most common technology as it removes N and P simultaneously. Struvite precipitates as the solubility of magnesium, ammonia, and phosphate exceeds the solubility of struvite.

$Mg_2^{+} + NH_4^{+} + PO_4^{3-} + 6H_2O \rightarrow MgNH_4PO_4.6H_2O$

The pH and molar ratio of Mg: NH4: PO_4 controls the precipitation of struvite. Struvite precipitation occurs at alkaline pH (optimum at pH 8.5-9) and with a suitable molar ratio of Mg: NH_4: PO_4:: 1:1:1 (Celen and Turker, 2001).

Bowers and Westerman (2005) designed a struvite crystallizer and tested it for P removal from lagoon water by adding ammonia. They observed an increase in struvite formation by raising pH from 7.7 to 8.2 and 8.7 and P increase in soluble P removal from 13% to 82%. Recovery of P from dairy effluent requires the elimination of Ca interference by pre-treatment with hydrochloric acid (Zhang *et al*., 2010).

2.11.4 Recovery of P as calcium phosphate

P was removed as a precipitate of the various compound of calcium with the most common being hydroxyapatite.

$$10Ca^{2+} + 6PO_4^{3+} + 2OH^- \rightarrow 2Ca_5(PO_4)_3\,OH$$

Production of thermodynamic supersaturation is a prerequisite for calcium phosphate precipitation. Precipitation of P starts with the nucleation process induced by the addition of artificial nucleic material (sand, calcite, etc). pH, P concentration, and presence of carbonate affect the calcium P precipitation as the formation of calcium carbonate reduce P precipitation. The efficiency of P removal by this method is 75-80%. Alkaline pH is necessary for the formation of calcium phosphate.

2.11.5 Adsorption and ion exchange

Different low-cost industrial by-products and naturally occurring materials are used as adsorbents to remove P from wastewater (Loganathan *et al*., 2013). However, high operation cost and removal efficiency limit its wider application. P removal from this method depends on the nature of the adsorbent, pH, surface area, and contact time. Ion exchange helps to remove

P in the form of precipitation by the addition of Ca, Fe, and Al solutes (Kuzawa *et al.*, 2006). In the case of ion exchange, the adsorbent can be regenerated and reused.

2.12 Strategies to control eutrophication

To control the eutrophication of the lake, control of point and non-point sources of nutrient import to water bodies is important. The non-point source is difficult to manage as they have multiple sources of pollution. Some of the steps to manage eutrophication are as follows;

(1) Source retention: Avoiding excess use of chemical fertilizer in agricultural field

(2) Process retention: retention of P before they enter river or lake

(3) Nutrient reuse: Recycling and reuse of trapped nutrient

(4) Ecological restoration: ecological measures

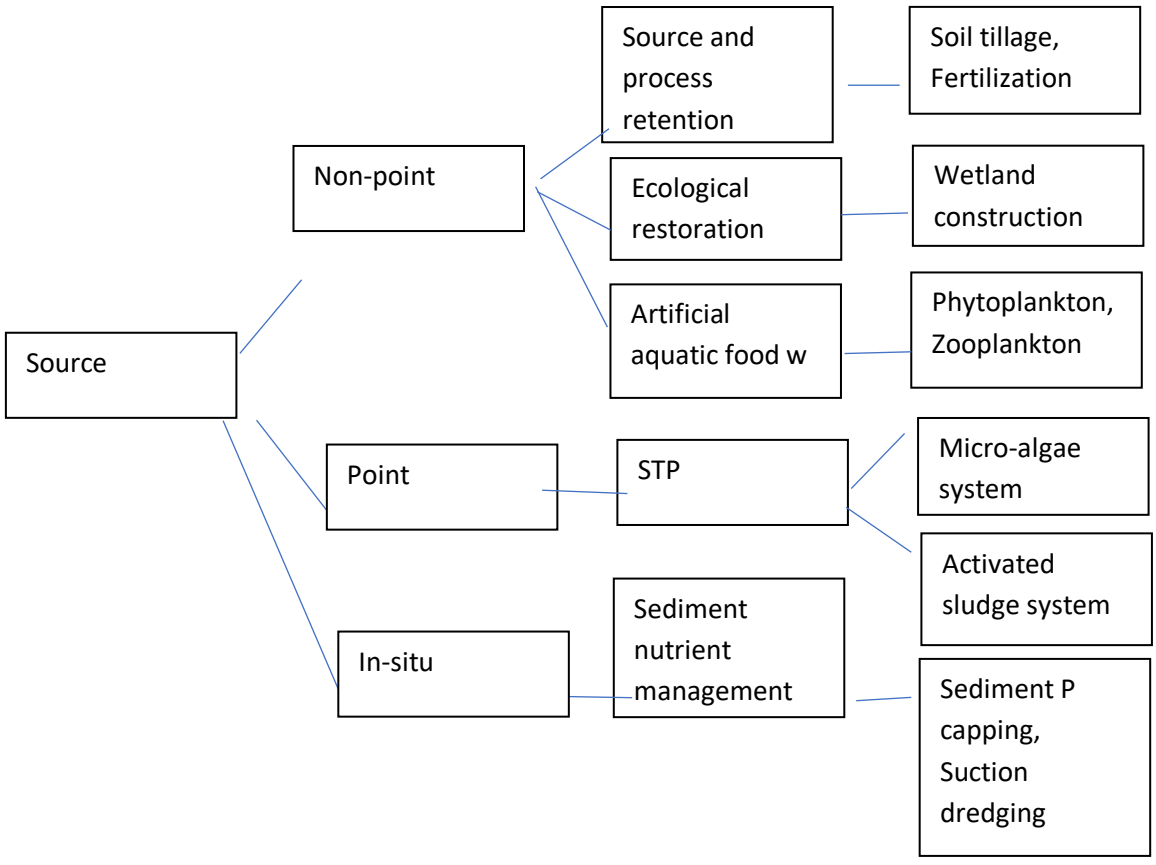

Fig 2.1. Flow chart showing management of point and non-point sources of pollution. STP; sewage treatment plant

Source pollution can be managed by soil tillage and fertilizer management that improves soil fertility and reduces surface run-off. Process retention removes P from the run-off with the help of an ecological ditches system (EDS). EDS consists of the use of periphyton that removes the nutrient from runoff through adsorption. Wetland construction can help for ecological restoration by reducing nutrient load and pathogen load from landscape to streams and lakes (Xia *et al*., 2020). In the wetland, slow flow and high contact time between wastewater and surface soil help sediment to settle down and transform the organic and inorganic substances. Wang *et al*. (2021) reported wetland construction effectively removed 42% t and 35% TN and 72% particulate P. construction of an artificial food web system consisting of phytoplankton and zooplankton helps to remove agricultural non-point sources of pollution in eutrophic Jiyu River. This system reduced 47% TP and cyanobacteria from 44% to 2.36% using *Scenedesmus obliquus* and *Daphnia pulex* (Guo *et al*., 2016). Suction dredging and sediment P capping are used to control P release from SRP/ PO_4^{3-} (Gibbs and Hicky, 2018). The method involves the use of capping material like calcium peroxide to precipitate dissolved and particulate P and lowers P release from sediment to the water column (Zhou *et al*., 2020). Microalgae like *Chlorella* and *Scenedesmus* species are used for biotransformation of pollutants which removes N and P along with organic and inorganic matter responsible for eutrophication.

2.13 Use of nanomaterials for phosphate removal

The above-discussed techniques such as sediment dredging, sediment capping metal salt (e.g., aluminum and calcium), and the addition of AL and Fe have been widely applied for P sequestration by effectively precipitating phosphate in the sediment (Funes *et al*., 2016). However, the capped sediment in the sediment may be rereleased to overlaying water due to the aging of the material and under the environmental condition of the lake such as redox potential and pH (Egemose *et al*., 2009).

In recent years, nanoparticles have drawn an increasing amount of attention in the environmental remediation field. Excellent biocompatibility, effective antibacterial agent, surface area to volume ratio, and stable optical properties make metal nanomaterial very effective against phosphate removal from water (Fu *et al.*, 2019). Due to its effective antibacterial agent eco-friendly composition, and affordable rare earth element the rare earth metal lanthanum (La) is regarded as one of the most effective metal nanoparticles for removing phosphate from water and wastewater (He *et al*., 2016; Qiu *et al*., 2017). Meanwhile, La^{3+} ions can draw oxygen-donor atoms from phosphate via the anion-ligand exchange mechanism since La has a significant natural affinity for phosphate. La could form a complex with phosphate ($LaPO_4$) even at a very low concentration of phosphate, which gives it added advantage when considering an adsorbent for phosphate removal (Makita *et al*., 2020). Lanthanum-based bentonite (phoslock) was first invented to sequester phosphate from water owing to its strong affinity for phosphate (Douglas *et al*.,1999, 2016; Copetti *et al*., 2016). It can be applied at a wide range of pH to recover phosphate from the eutrophication lake. However, it can release toxic La^{3+} which could be detrimental to the health of the aquatic organism. Therefore, various adsorbents using lanthanum oxide and hydroxide are synthesized instead of La^{3+}. La carbonate has been also used to synthesize adsorbents due to its low toxicity for human and aquatic organisms (Yang *et al*., 2020).

Later, various La-based adsorbent was synthesized for phosphate removals such as La-modified alumina, and zeolite/ hydroxide (Xie *et al*., 2014, wang *et al*., 2017). The stability of La-based adsorbent in the sediment and negligible effect on aquatic organisms makes its use eco-friendly (Copetti *et al*., 2016). Despite the advantages of using La-based adsorbent, its use is limited owing to its non-recyclable La-based material and high chemical consumption of La. Further, high surface energy and Van der force interaction make La nanoparticle susceptible to

aggregation. This makes it difficult to separate and reuse it. Therefore, embedding La nanomaterial with different carrier materials is gaining attention to overcome this problem.

To enable separation, recovery, and reuse of the nanoparticles, it may be practical to magnetize them through hybridization with biocompatible Fe_3O_4 nanoparticles. This approach has recently been widely employed to create magnetic sorbents and catalysts (Lai *et al*. 2016; Wang *et al*., 2016; Fang *et al*., 2017). Magnetite-based La appears to be the practical solution for recovery of eutrophic lake and reuse of La resources. However, research regarding the use of magnetite-based adsorbents is very limited. Some of the methods followed by different scientists are very tedious, therefore a simpler method for synthesis of magnetite-based La is needed. This work focuses on the synthesis of magnetic-based adsorbent and evaluating its sequestration capacity for phosphate so that it can be used for phosphate removal from the lake.

Various literature shows that the shape and size of La-based nanomaterial affect the adsorption efficiency of phosphate. Co-precipitation and hydrothermal process are the widely used protocols for the synthesis of La nanomaterial owing to their simpler, low cost, and high efficiency. Various La-based nanomaterials such as lanthanum oxide and hydroxide, lanthanum chitosan nanocomposite, magnetic tetrahydric nanocomposite, lanthanum incorporated zeolite, etc. are synthesized using the co-precipitation method (He *et al*., 2017; Fu *et al*., 2018; Xie *et al*., 2015). Various La-based nanomaterials such as zeolite-coated lanthanum hydroxide nanocomposite, magnetic Fe3O4 core-shell lanthanum, and 3D rice-like lanthanum-doped nanocomposites have been synthesized using a thermal process. However, the high cost of autoclaves and safety issues related to this protocol are some of the disadvantages associated with this protocol.

2.14 Phosphate removal mechanism of La-based adsorbents

La^{3+} ion, lanthanum hydroxide, and lanthanum carbonate are the common species used for P adsorption. La 3+ ion can attract oxygen donor atom in P through the anion-ligand exchange as shown in the following equation;

$$La^{3+} + PO_4^{3-} \rightarrow LaPO_4$$

P adsorption associated with lanthanum hydroxide is governed by ligand exchange and electrostatic attraction. When solution pH was lower than ZPC of adsorbent, positive surface charge develops due to protonation, thus attracting P anions through electrostatic attraction to from outer sphere complexation. La hydroxide also can combine with P through ligand exchange and form monodentate or bidentate inner sphere complex by replacing the hydroxyl group. P adsorption mechanism can be illustrated by the following equations;

$$LaOH + H^+ \rightarrow LaOH_2^+$$

$$LaOH_2^+ + H_2PO_4^- \rightarrow (LaOH_2^+)(H_2PO_4^-)$$

$$LaOH_2^+ + HPO_4^{2-} \rightarrow (LaOH_2^+)(HPO_4^{2-})$$

$$La - OH + H_2PO_4^- \rightarrow La - H_2PO_4 + OH +$$

$$2\,La = OH + HPO_4^{2-} \rightarrow La_2 - HPO_4 + 2\,OH^-$$

the P adsorption between La carbonate and P is due to ligand exchange and the mechanism is described by the following equations;

$$La_2(CO_3)_3 + 2\,H_2PO^{4-} \rightarrow LaPO_4 + 2\,HCO_3^- + H_2CO_3$$

$$La\,2(CO_3)_3 + 3\,HPO_4^{2-} \rightarrow La_2(HPO_4)_3 + 3CO_3^{2-}$$

$$La\,2(CO_3)_3 + 2\,H_2PO_4^- \rightarrow 2(LaH_2PO_4)^{2+} + 3CO_3^{2-}$$

$$La\,2(CO_3)_3 + 2\,PO_4^{3-} \rightarrow 2LaPO_4 + 2\,CO_3^{2-}$$

2.15 Classification of La-based adsorbents

La-based adsorbents can be categorized into three groups depending on their structures: single La compounds, La-metal composites, and "La-carrier" adsorbents. A type of La material that is not combined with other metals is known as a single La compound. On the other hand, La-metal composites are created by combining La with other metals, a process that may result in the formation of novel hybrid structures. By combining host materials and La, a "La-carrier" adsorbent is created, with the host materials serving as the foundation for La loading.

2.15.1 Single La compound

These are nano-rod-shaped materials capable of adsorbing P. high surface energy and susceptibility to aggregation decrease its P adsorption efficiency. Further, the separation of nano-rod-shaped material from the solution after adsorption limits the use of single La compounds (Xie *et al*., 2014).

2.15.2 La metal composites

La-metal composites combine La and other metals by establishing atomically close contact with one another. It ensures adsorbents' ecological safety owing to less dissolution of metal due because of the firmly combined different cations in the heterogeneous composite. Yu *et al*. (2019) investigated the effect of Fe insertion on La (oxy) hydroxide and the outcomes demonstrate that the oxygen p orbital could be shifted to an unoccupied state by the hybridization of La/Fe metal orbitals, allowing P adsorption.Chen *et al*. (2020) demonstrates that many inter-particle nanopores produced by the needle-like Mg-La bimetal oxide nanocomposite (PC@La) could make it easier for anions to enter the interior region, interact with active groups there, and so encourage P.

2.15.3 La-carrier adsorbent

To increase P adsorption effectiveness, materials with robust mechanical qualities, large porous structures, and inexpensive costs are frequently employed as La carriers. Magnetic (Fe3O4) (Fu *et al*., 2018), hydrogel (Dong *et al*., 2017), chitosan (Liu *et al*., 2020), biochar (Qiu *et al*., 2017), silica materials (Jing *et al*., 2019) have been used as La carriers. For example, biochar is used due to its low cost of preparation, and low environmental risk, and magnetite is used due to its easy separation and reusability.

2.16 Characterization of La-based nanomaterial

Surface characterization and analysis of surface properties are essential tools to confirm the doping of La on-carrier material. Scanning electron microscope (SEM) and Brunner-Emmett-Teller (BET) could achieve the surface characterization (surface area, morphology, size) of La-nanomaterial. X-ray diffraction (XRD), Fourier transform IR spectroscopy (FTIR), and X-ray Photoelectron Spectroscopy (XPS) could determine the crystal structure, presence of La on-carrier material, and mechanism for phosphate removal.

2.17 P removal using La-based Adsorbent

Lai *et al*. (2016) observes a maximum adsorption capacity of 27.8 mg/g for Fe-Si-La by loading 1 mmol lanthanum per gram of magnetite. Additionally, he observed 95% phosphate removal from the effluent of wastewater and favored the pH range of 5.0 - 9.0. Adsorbed P was completely desorbed with the use of NaOH. Luo *et al.* (2021) synthesized lanthanum molybdate/magnetite (M-La_2 $(MoO_4)_3$) with various $LaCl_3$ / Fe_3O_4 mass ratios and selected M-La_2 $(MoO_4)_3$ (2:1) for adsorption of P. Fitting of adsorption data to Langmuir adsorption isotherm suggest heterogeneous multilayer sorption was dominant during phosphate sorption process. A further pseudo-first-order kinetics model was used to describe the phosphate sorption process. Li *et al.* (2020) found a maxim adsorption capacity of 93.91 mgg^{-1} for lanthanum-modified biochar with the highest P adsorption in the pH range of 3.0 to 6.0. FTIR

and XPS of the sample after P adsorption suggest electrostatic attraction and inner-sphere complexation as the mechanism of P adsorption. Song *et al*. (2020) synthesized magnetic/lanthanum hydroxide composite and investigated the effect on P removal. They observed a P sorption capacity of 19.34 mg P g^{-1} and attributed P removal to electrostatic attraction and the formation of an inner-sphere complex. Wu *et al*. (2017) investigated the effect of magnetic La (OH)/ Fe3O4 with varied La to Fe mass ration on phosphate removal and chose La (OH)/ Fe_3O_4 composite with La to Fe mass ration of 4:1 for further P sorption experiment. They reported a maximum P adsorption capacity of 83.5 mg P g^{-1} with the highest sorption capacities observed between the pH range of 4.0 to 6.0. They attributed P removal to the mechanism of ligand exchange and formation of the inner-sphere complex due to electrostatic attraction. Fu *et al*. (2018) investigated the effect of La decorated magnetite (Mag@Fh-La) on P removal and observed a maximum P sorption capacity of 44.8 mg P g-1 which can be applied at a wide range of pH (3.2-10.7). The analysis of FTIR and XPS revealed ligand exchange and electrostatic attraction as a mechanism of P adsorption. Wang *et al*. (2020) used lanthanum-doped carbon films as adsorbents to sequestrate phosphate for eutrophication management. He reported that the adsorbent achieves maxim P adsorption capacity between pH of 3.0 and 7.0. Further observed Langmuir equation and pseudo-second order model fitted well to the sorption isotherm and sorption kinetics. Yang *et al*. (2013) investigated the effect of La-EDTA coated magnetite on phosphate removal from wastewater and observed maximum adsorption capacities were achieved at a pH of 6.0-7.0. Zhong *et al*. (2020) investigated the effect of magnetic La-impregnated bentonite granule on P sequestration. They observed the maximum P sorption capacity to be 48.4 mg g^{-1} and can be applied for P sequestration between the pH range of 3.0-9.0. The electrostatic attraction facilitates ligand exchange and accelerated chemical precipitation via the formation of the $LaPO_4$ complex.

MATERIALS AND METHODS

To address the effect of external and internal P loading on water quality of lake a study entitled "Variation in water quality of Chilika lake (Odisha) with special reference to phosphorus and its sequestration using novel adsorbent" was undertaken in 2017-2022 in the water and sediment samples of lake Chilika at the Department of Soil Science and Agricultural Chemistry, Institute of Agriculture Sciences, B.H.U. In the present study, water and sediment samples were collected during post-monsoon, pre-monsoon, and monsoon seasons to study the effect of forms and distribution of P on water quality of lake. Further, a novel adsorbent was synthesized to sequester phosphate from the aqueous solution of P.

3.1. Study area

The present study was carried out at the largest brackish water lagoon in Asia, Chilika (19^0 28′ –$19^0$54′ N: $85^0$60′–85^0 35′E), which is located on the east coast of India. The semi-enclosed, shallow lacustrine water body presents a unique gathering of marine, brackish and freshwater ecosystems with estuarine characters with a mean depth of 2 m (Mukherjee, Muduli, Barik, & Kumar, 2019). The lagoon has been designated as a Ramsar site on the Ramsar Convention of Wetlands in 1981. The lagoon is 65 km in length, spreading from northeast to southwest parallel to the coastline with a variable breadth reaching 20.1 km. The lagoon is spread over an area of 950 km^2 during summer, which swells up to 1165 km^2 during monsoon (Siddiqui and Rao, 1995). The lagoon is connected with the Bay of Bengal near Satapara (Sipakuda) by means of an artificial opening made in September 2000.

The catchment area of the lagoon is about 4406 km^2; 68% of this is constituted by the western catchment and 32% by the Mahanadi Delta in the northeast. The total in flow of

freshwater has been estimated at 14,331 M m^3. The areas draining to Mahanadi and its tributaries, Daya, Bhargavi and Nuna make up the north and north east watershed contributing to 55% of water inflow (Annon, 2003) while the streams flowing in to Rushikulya make up the south watershed. Besides the area of lagoon, the drainage basin includes 54% of agricultural land, 12.2 % of forest, 4.4 % permanent vegetation,1.6 % of swamp and wetland and 2 % of grassy mud flats (Kadekodi *et al*., 2005). Influx of nutrient through runoff and lack of catchment area management possess a threat of eutrophication and loss of biodiversity in the lagoon.

3.2 Lake water collection

Based on ecological characteristics, physiographic setting and various dynamic processes controlling the circulation and exchange of water, the lagoon can be divided into four different sectors: viz. southern (SS), central (CS), northern sectors (NS) and outer channel (OC). SS has comparatively higher salinity than NS and CS due to sea water intrusion through Palur canal. In contrast, NS has least salinity as it receives huge freshwater inflow from Mahanadi and its tributaries. CS represents the portion of the lagoon, where mixing of fresh water and sea water occurs. OC has highest salinity as it is directly connected to Bay of Bengal.

For the present study, sampling was performed during pre-monsoon season, monsoon, and post monsoon season during the year 2018-2019 covering the entire lagoon from 33 different locations. Surface water samples were collected at each location in a 500 mL wide mouth bottle and were bought back to laboratory on ice and preserved in 4^0 C for further analysis.

3.3 Lake water quality measurement

The water quality parameter such as pH, electrical conductivity, salinity was measure in-situ using water quality Sonde (6 Series; DATA-BUOY; YSI, USA/ YSI Model no. 6600 V2). Water transparency was measured using a Secchi disc (KC Denmark). Nitrate, nitrite and phosphate were measured using a nutrient autoanalyzer (SKALAR SANplus). Dissolved oxygen (DO) was analysed using the method of modified Winkler (Grasshoff *et al.*, 1999). Biological oxygen demand (BOD) was analysed by the titrimetric method of Young (1973).

3.4 Trophic state index

Numerous methods have been used to evaluate trophic state index of lake. Carlson's Trophic State Index was most common method used to determine trophic state of lake. The following equation was used to calculate TSI;

TSI - P = 14.42 * ln [TP] + 4.15 (in ug/l)

TSI - C = 30.6 + 9.81 ln [Chlor-a] (in ug/l)

TSI - S = 60 - 14.41 * ln [SD] (in meters)

Average TSI = [TSI (P) + TSI (CHL a) + TSI (SD)] /3

Where, TP is total phosphorus, Chl a is chlorophyll a, SD is the Sechi depth.

The lake was divided into different trophic level based on TSI value;

Table 3.1 TSI values and its status of trophic level

TSI	State
< 30	Oligotrophic
30-50	Mesotrophic
50-70	Eutrophic
>70	Hypertrophic

3.5 Water quality Index

Principal component analysis (PCA) was used to calculate WQI. PCA was used to create a minimum data set to reduce indicator load on the model. The PCs with high Eigen values represented the maximum variation in the dataset. PCs with Eigen value greater than 1 were selected. Under a given PC, each variable had corresponding Eigen vector weight value or factor loading. Only the 'highly weighted' variables were retained to include in the MDS. The 'highly weighted' variables were defined as the highest weighted variable under a certain PC and absolute factor loading value within 10% of the highest values under the same PC. Variables under each PC were used for Pearson's correlation analysis. Variables showing insignificant correlation were selected for WQI calculation. If any two variables were correlated then variable with highest factor loading was selected for WQI calculation. The parameter showing high correlation within the first component or can be simply calculated from the other parameters were not considered for further analysis. Whereas some parameters showed high correlation were still included as these were highly important for calculation of water quality index.

Each PC explained a certain percentage of the variation in the total data set. This percentage, divided by the total percentage of variation explained by all the previously selected PCs, gave the weighted factor (W) for attributes selected under a given PC. Weight of each PCs were calculated from the following formula

$$\text{Weight } (W_i) = \frac{Variance}{Total\ variance}$$

W_i is the weighting factor derived from the PCA.

Indicators were categorized based on whether a higher value was considered "good" or "bad" in terms of soil function. For "more is better" indicators, each observation was divided

by the highest observed value so that the highest observed value received a score of 1 while all others received a score of <1. For “less is better” indicators, the lowest observed value was divided by each observation such that the lowest observed value received a score of 1 while all others received a score of <1. For “optimum is better” indicators, observations were scored as “more is better” up to a threshold value and then scored as “less is better” above that threshold level.

Score for each variable were calculated from the following formula

$$\text{Score } (S_i) = \frac{obsrved\ value}{highest\ observed\ value}$$

Where Si is the score for variable i

WQI was calculated using the formula

$$WQI = \sum W_i \times S_i$$

By taking highest value of WQI as unity, WQI for all the station were calculated. Based on the value of WQI, the lake water was classified in to 4 classes namely very poor, poor, moderate and good.

3.7 Estimation of external nutrient loading to lake Chilika

3.7.1 Catchment area delineation and land use land cover map

Catchment area of the lake was demarcated using ArcGIS software and land use and land cover map were prepared using ERDAS. CARTOSAT-1 was used to prepare the digital elevation model (DEM) at 24-m resolution. The remote sensing data was received from linear imaging and self-scanning sensor (LISS) which operates in three spectral bands in VNIR and SWIR with 24-meter spatial resolution and a swath of 141 km. The ortho corrected satellite imagery was captured by LISS-III sensor of Resourcesat-2 satellite of ISRO, NRSC, India.

Land use/land cover map was prepared using remote sensing data of LISS-III. In the present study, the unsupervised classification method was used for preparation of the LULC map. The study area was classified into different classes viz. Agriculture area, Forest area, water bodies, Residential, fallow land.

3.7.2 Catchment area sampling

Thirteen river/ streams were chosen as the major inlet channel contributing water and sediment flow into lake Chilika. Thirteen monitoring sites in the stream or river were chosen as the sampling point; one from each stream or river. The streams that run through the catchment area of lake Chilika were listed with their UTM coordinate number and presented in the Table 3.2. Bed sediment were collected from the upper 10 cm of stream or river bottom in the stream channel. The land surrounding these streams were under different land use such as agriculture, forestry, fallow, establishment etc. Soil samples were also collected from different land use surrounding the river monitoring sites. Total number of soil samples collected from the river or stream was 13 and the total number of samples collected from the different land use of catchment area was 22. The number of samples with their nearby stream or river monitoring sites are listed in the Table 3.2. All the soil and sediment samples were collected in the post monsoon season from October 2019 to October 2019. The samples were collected in the plastic bag and transported to the laboratory for further analysis. The samples were air-dried and passed through a 2mm sieve and stored in a plastic bag.

3.7.3 River water sampling:

Water samples were collected from the 13 monitoring stations of the streams / rivers in a wide mouth bottle. The samples were transported to the laboratory and stored at 4^0 C until further analysis. The samples were filtered immediately through a 0.45-µm, and the P in the samples were determined by the colorimetric method (Murphey and Riley, 1962).

Table 3.2 Location of river water and catchment area sampling site

Sample ID	River name	Latitude	Longitude	Agriculture	Forest	Fallow
1	Bhargavi	19.86	85.66	1	-	1
2	Luna	19.95	85.67	2	-	
3	Daya	19.97	85.62	-	-	1
4	Makara	19.97	85.62	-	-	1
5	Mangalajodi	19.92	85.42	2	-	1
6	Tarimi	19.91	85.40	2	-	1
7	Kusumi	19.90	85.38	-	1	-
8	Badanai	19.81	85.27	1	-	1
9	Kansari	19.78	85.23	1	1	-
10	Janjira	19.73	85.20	2	-	1
11	Langaleswar	19.66	85.15	2	-	-
12	Palur canal	19.47	85.14	2	-	-

The measurements of water velocity were conducted using a CURRENT MASTER current meter with a propeller diameter of 5 cm. River water samples were collected during the monsoon season (July, August, September, October) to calculate the external nutrient loading as water flow was negligible during months other than monsoon season. Water flow rate of rivers were measured daily during this 4-month period and water samples of rivers were collected twice a month and analysed for nutrient concentration using Autoanalyzer.

Flow rate determination: Flow Rate, Q (m^3s^{-1}) was determined using the following equation:

$Q = A \times V$

Where, A = Area of measurement (m^2), Q = flow rate (m^3s^{-1}) and V = velocity of water course (ms^{-1})

Transport of nitrate (moles day^{-1}) = Q x N

Where, N= nitrate concentration (µ mol L^{-1})

Similarly, phosphate, silicate, nitrite, and ammonia loading were calculated using the above equation, substituting the values for their respective concentrations.

3.8 Lake sediment sample collection

The lake sediment samples were collected during from the upper 10 cm of the sediment surface of the lagoon by usingVan-Veen grab sampler (KC Denmark) with a surface area of 250 cm^2 and the coordinate position of sampling points were simultaneously recorded. The wet sediment samples were air dried for two weeks and the visible plant litter, root material and stones were removed.

3.8.1 Physico-chemical analysis:

For physico-chemical characterization, sediments were air-dried, passed through 0.5 mm sieve, and analyzed for pH, EC, organic carbon (OC), cation exchange capacity (CEC), $CaCO_3$, and texture. pH was measured in1:2.5 sediment-water suspensions (m/v) using a pH meter. The pH meter was standardized with pH buffers 4, 7, and 9.2 prior to use. Texture was determined using the hydrometer method (Bouyoucous, 1927). Organic carbon content was determined by the potassium dichromate sulfuric acid oxidation method (Nelson and Sommers, 1982). $CaCO_3$ of sediments were determined using the rapid titration method given by Puri (1930). CEC was measured by the method described by Hesse (1971). Available P was extracted using 0.5 M sodium bicarbonate ($NaHCO_3$) (Olsen *et al*., 1954) and determined colorimetrically.

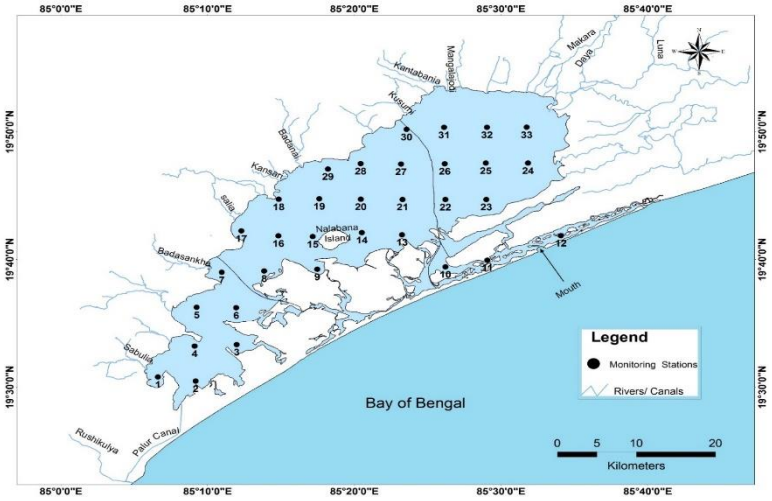

Fig. 3.1 Samplings points of lake sediment

3.8. 2 P fractionation:

The P fractionation was carried out using wet sediment by using the method described by vanEck (1982) as modified by Moore and Reddy (1994). Wet sediments were transferred to a centrifuge tube of known weight and centrifuged to extract the pore water. The pore water was immediately filtered using a 0.45µ membrane filter and acidified to avoid precipitation of soluble iron as iron P. The acidified, filtered sample was analysed by the Murphy-Riley method (Murphy and Riley, 1962) and referred to as water-soluble or soluble reactive P. Then the remaining sample was shaken with 1 *M* KCl, 0.1 *M* NaOH, and 0.5 *M* HCl for 2, 17, and 24 hrs respectively to extract loosely sorbed P (L-P), aluminum and iron-bound P (Al & Fe-P) and calcium-bound P (Ca-P) respectively. The extract after shaking was centrifuged and filtered using a 0.45µ membrane filter. Few drops of 4-nitrophenol were added to the filtrate and then neutralized using 2 M HCl or NaOH to adjust the pH. Then inorganic phosphate in the extract was determined using blue colour method Murphy and Riley, (1962). The remaining sample was analysed for residual P (R-P) following digestion with perchloric - hydrofluoric acid (HF) mixture. Total P of the dry sediments were analysed colorimetrically following digestion with $HClO_4$- HF and analysed colorimetrically (Murphey and Riley, 1962).

3.8.3 Phosphorus sorption isotherm

Sorption isotherm experiment was conducted by using dry sediment samples of (NS, CS, and SS) the lake in triplicate. Two samples from each sector were chosen for sorption isotherm as representative samples. Approximately 0.5 g sediment sample was weighed into a 50 mL centrifuge tube with 10 mL of phosphate standard solution with various concentration of 1, 2, 4, 6, 10, 20, and 40 mg L^{-1} respectively. The tubes were shaken for 24 hrs in an end-to-end mechanical shaker till equilibrium. Then, the tubes were centrifuged at 5000 rpm for 20 min and the supernatant was filtered to collect the filtrate. The P concentration in the aliquot was analyzed spectrophotometrically at 660 nm using the methods of Murphey and Riley (1962). The amount of P adsorbed by the sediment was calculated by the difference in added and equilibrium P concentration measured in the aliquot as given by the expression;

$$Q = (Co- Ce) \times V/ W$$

Where, Q is the net amount of P adsorbed by the sediment (mg kg^{-1}); Co is the added P concentration (mg L^{-1}); Ce is the amount of equilibrium P Concentration (mg L^{-1}); W is the weight of the sediment sample (g); and V is the volume of P solution added (mL).

The data obtained from the above experiment were fitted into Langmuir and Freundlich sorption isotherm to explain P sorption in the sediment. The equation of the Langmuir equation can be expressed as follows;

$$\frac{Ce}{x/m} = \frac{1}{kb} + \frac{Ce}{b}$$

where x/m = Amount of P adsorbed per gram of soil (µg/g)

Ce= Equilibrium P concentration (µg P mL^{-1})

b= the Langmuir adsorption maximum (µg/g)

k = Langmuir bonding energy constant

A plot of Ce/x/m versus Ce gives a straight line. The constants k and b were obtained from the intercept and slope, respectively.

Freundlich equation:

The Freundlich equation can be represented as;

$\frac{x}{m} = K \times C_e^{1/n}$

The linear form of the equation is

$\text{Log } x/m = \log k + 1/n \log C_e$

Where;

x/m= The amount of phosphorus adsorbed per unit mass of adsorbent.

C_e = The equilibrium solution in the solution (µg P/mL)

A plot of log x/m vs. log Ce gives a straight line where 1/n is the slope and log K is the intercept.

Phosphorus Sorption Index (PSI) was derived from single point adsorption isotherm to estimate P sorption capacities of sediment sample. A single point adsorption experiment was conducted by taking 0.5 g sediment sample and equilibrating it with 10 mL of 40 mg P L^{-1} solution in a polypropylene plastic tube. The sample tubes were shaken for 2 hr and at the end of equilibration, the suspension was centrifuged at 2000 rpm for 20 min and then filtered through Whatman no.1 filter paper and the filtrate were stored in a plastic container to estimate the equilibrium P concentration. The P concentration in the filtrate was determined by the colorimetric method (Murphey and Riley, 1962). PSI was calculated from the following equation;

PSI = XV/S

Where PSI is the P sorption index (mg kg^{-1}),

V is the solution volume(L),

S is the sediment weight (kg), and

X = initial-final solution P concentration (mg L^{-1}).

3.8.4 Desorption experiment

After the adsorption experiment, the remaining sediment sample after the sorption experiment were subjected to desorption experiment. For this 10 mL of 0.01 N KCl was added to the sample tube to extract clear aliquot and shaken in an end-to-end shaker. Samples were drawn at 6 hr, 12 hr, 18 hr, 24 hr, 42 hr of shaking and then centrifuged to extract the aliquot. Then, the suspension was centrifuged at 2000 rpm for 20 min and filtrate was collected in a plastic container for further analysis by filtering through a Whatman no. 1 filter paper. Desorption experiment were performed in triplicate.

3.9 Synthesis of magnetite based novel adsorbent

Magnetic adsorbent was prepared in a reactor vessel under N_2 environment by chemical co-precipitation method (Fang *et al*., 2018). A ferric chloride ($FeCl_3$) solution was freshly prepared by adding1.8 g $FeCl_3$ (110.97 mmol) into 130 ml of distilled water and a ferrous sulphate ($FeSO_4.7H_2O$) solution was prepared by adding 3.6 g of $FeSO_4.7H_2O$ into 15 mL of distilled water. The $FeSO_4.7H_2O$ solution was poured into $FeCl_3$ solution and the resulting mixture was placed on magnetic stirrer and stirred at 60-70^0 C for 5 Min at 200 rpm. Nitrogen gas was supplied to eliminate oxygen from the water. Then a pre calculated amount of $LaCl_3$ was added to the above combined solution under stirring. The amount of $LaCl_3$ was calculated

based on the mass ratio of La $(OH)_3$/$(LaOH)_3$ + Fe_3O_4) to achieve a final mass ration of 5, 25, 50, and 75%. Afterwards, 2 M NaOH was added dropwise (over 1 hr) using a burette to the above solution until a pH of 10-11 was attained. Dark brown precipitate was observed at pH 6 and then black precipitate at pH 10. Then the resultant La-magnetite based adsorbent was centrifuged, filtered and washed with distilled water. Then the precipitate was placed on a porcelain dish and dried at 50^0 C in hot air oven and finally ground to pass through 100 mesh sieve. The resultant adsorbent was stored in air tight plastic container until its use. The synthesis of adsorbent was carried out under nitrogen environment by supping nitrogen gas externally to the reaction vessel.

3.9.1 Characterization of magnetic adsorbent:

The crystal structure of the magnetic adsorbent was studied using X-ray diffraction technology. The morphological structure of the sorbents was analysed by scanning electron microscopy (SEM). Functional groups were determined using a Fourier Transform Infrared Spectrophotometer (FT-IR). Prior to the FT-IR analysis, the samples were prepared by mixing with KBr at a ratio of 1:100(w/w) and pressed in to a film. Specific surface area was measured from adsorption branch of isotherm using Brunauer-Emmett-Teller (BET) method. The changes in chemical composition and functional group of the magnetic adsorbent after and before adsorption were determined using X-ray photoelectron spectroscopy (XPS).

3.9.2 Adsorption experiments:

A preliminary experiment showed that adsorption of phosphate to the polypropylene plastic tube was negligible. Kinetics experiment was conducted to determine optimum time required for sorption equilibrium of the sorbent (M-La $(OH)_3$). The experiment was conducted by taking 0.025 g of sorbent with 40 mL of 30.0 mg P/L solutions in a polypropylene plastic tube. The pH of the suspension was maintained at 7.0. The sample tubes were then shaken for varying

time (5, 10, 20, 30, 60, 120, 180 min.) in a mechanical shaker at 300 rpm. At each reaction time, samples were centrifuged at 2000 rpm for 20 min, and then the filtrate was collected in the plastic container. The amount of P in the aliquot was analysed using Murphey and Riley blue colour method. The amount of P adsorbed (Qt, mg/g) by the M-La $(OH)_3$ at different time was estimated by the following equation;

$$Qt = (Ci-Ct)\ V/M$$

Where, Ct is the amount of adsorbed phosphate at time t, and Ci is the initial phosphate concentration. V is the solution volume and M is the mass of the adsorbent. The kinetics data were fitted using the pseudo-first-order model and pseudo-second order model.

Adsorption-desorption cycles were conducted to investigate the reusability of M-La $(OH)_3$. Adsorption experiment were carried out in 50 mL centrifuge tube, which were fixed on a water bath oscillator with a constant temperature at 25^0 C. Sorption isotherm experiment was conducted by taking 0.025 g of M-La $(OH)_3$ and equilibrating it with variable concentration of P solution in a polypropylene plastic tube at 25^0 C. The concentration of solutions was 0, 10, 20, 30, 40, 50, 75, and 100 mg P L^{-1}. The pH of the solution containing varying concentration of P were maintained at 7.5. The sample tubes were shaken for 2 hr and at the end of equilibration, the aliquot was obtained through centrifugation, filtration of the suspension and the filtrate were stored in a plastic container to estimate the equilibrium P concentration.

Thereafter, desorption experiments were carried out using the remaining sorbent from the sorption isotherm experiment by adding 40 mL of 0.1 N NaOH and samples were drawn at 2 hr, 4 hr, 6 hr, 8 hr, 10 hr of shaking. Then, filtrate was collected and stored for further analysis. The phosphate desorption efficiency was calculated as a ratio of desorbed to the initially adsorbed phosphate. The effect of initial solution pH on sorption of P by the sorbent was also investigated by taking 0.025 g of sorbent with an initial P concentration of 30 mg-P/L at 25^0 C

in a pH range of 3-11 (3.5, 4.5, 5.5, 6.5, 7, 7.5, 8, 8.5, 9, 9.5 10, 11) by adjusting the pH by 0.1 M NaOH or 0.1 M HCl. pH was measured using pH meter after the solution has been stable for 2 min. The sample tubes were shaken in an end-to-end shaker for 3 hr and then centrifuged at 2000 rpm for 20 min and filtered to collect the aliquot. The filtrate was stored in a plastic container for further analysis. The percentage of P removal by the adsorbent was calculated to determine the optimum pH at which maximum P is removed by the adsorbent.

Percentage of P removal (R%) = $\frac{concentrationof\ P\ removed}{concentration\ of\ initial\ P\ added} \times 100$

In addition, effect of temperature on the sorption of P by the sorbent was also carried out by taking 0.025 g of sorbent with an initial P concentration of 30 mg P/L at 25^0, 35^0, and 45^0 C. All the experiments were run in triplicate along with blank. The P concentration in the filtrate was analysed using Murphey and Riley blue colour method using a spectrophotometer at the wavelength of 660 nm (Murphey and Riley, 1962). The amount of P adsorbed was analysed by difference between initial and final concentration of P in the solution using relationship explained earlier in the section 3.8.3. The sorption data were fitted to Langmuir and Freundlich equation by the methods described in the section 3.8.3.

3.10 Statistical analysis:

All the experimental data were expressed as average values of three replicates. Pearson correlation was performed to investigate the relationship among P sorption parameter and the selected soil physico-chemical properties. One-way analysis of variance was used to compare the difference among the sorption/ soil physico-chemical properties among the sampling stations. All the statistical analysis including principal component analysis and cluster analysis were performed using SPSS 20.0 software package.

Chapter IV

RESULT AND DISCUSSION

4.1 Water quality characteristics

Based on ecological characteristics and various dynamic processes controlling the circulation of water, the lake can be divided into four different sectors; southern (SS), central sector (CS), northern sector (NS) and outer channel (OC). For water quality analysis, water samples were collected during pre-monsoon, monsoon, and post-monsoon season from 33 different locations representing entire area of lagoon. Water quality parameter differed significantly for the three sectors of the lagoon. The average seasonal and spatial values for different water quality parameter of lagoon was presented in the Table 4.1. Water quality parameters of the lagoon for Pre-monsoon (PRM), Monsoon (MON), and Post-monsoon (PSM) are presented in the Table 4.2, 4.3,4.4. The correlation matrix between the physicochemical properties is depicted in Table 4.5. Spatial variability map for Pre-monsoon (PRM), Monsoon (MON), and Post-monsoon (PSM) are presented in the Fig. 4.1.

4.1.1. Water Temperature (WT)

One-way ANOVA revealed significant seasonal variation in WT in the lagoon (p<0.001). From the perusal of Table 4.1., it was observed that water temperature (WT) of the lagoon varied from 29-32.7°C, 27.5-33°C, and 20.4-29.2°C during PRM, MON, and PSM respectively. Mean value of WT was observed to be 31.7 °C, 30.3°C, 31.3°C, and 30.8°C for SS, OC, CS, and NS respectively for PRM season. Similarly, sectoral mean WT for MON were 28.7°C, 29.1°C, 29.7°C, 29.9°C respectively and for PSM the mean value was 21.7°C, 23.6°C, 23°C, 24.2°C. Water temperature of the lagoon, varied among the sectors, with NS recording

highest water temperature (28.33±3.69°C) and SS (27.37±4.39°C) showing lowest water temperature. However, variation in WT of the lagoon for different sectors are non-significant for all the

Table 4.1 Spatiotemporal variation in water quality of Chilika Lake.

Parameters	Seasons			Sectors			
	Pre monsoon	Monsoon	Post monsoon	SS	NS	CS	OC
WT	31.18±0.95^{a}	29.48±1.37^{b}	23.04±2.35^{c}	27.37±4.39	28.33±3.69	28±3.92	27.44±3.5
Transparency(cm)	43.27±28.6^{a}	95.06±67.77^{b}	62.5±37.32^{a}	105.87±50.74^{A}	28.33±26.26^{B}	78.54±47.92^{A}	21.11±15.84^{B}
Depth(cm)	146.48±60.98^{a}	207.12±62.82^{b}	143.11±51.66^{a}	210.96±86.51^{A}	130.96±39.52^{B}	153.48±47.42^{B}	212.44±64.62^{A}
Conductivity (mS cm^{-1})	25.52±13.95^{a}	4.26±4.2^{b}	9.47±8.1^{b}	16.23±5.63^{A}	3.52±6.33^{B}	14.38±12.92^{A}	24.73±23.44^{C}
Salinity (PSU)	13.48±7.99^{a}	2.42±2.37^{b}	5.54±4.97^{b}	8.86±2.65^{AB}	1.77±3.15^{A}	7.76±6.91^{AB}	14.41±13.44^{B}
pH	7.99±0.36^{a}	7.97±0.49^{a}	8.61±0.4^{b}	8.28±0.37^{AB}	7.91±0.68^{A}	8.36±0.42^{B}	7.89±0.28^{A}
Turbidity (NTU)	66.02±111.83^{a}	27.86±45.13^{b}	46.49±82.7^{c}	13.71±21.52^{A}	127.11±139.24^{B}	17.74±22.45^{A}	55.03±42.61^{B}
Chl a	0.73±0.99^{a}	0.42±0.41^{b}	0.7±1.2^{c}	0.17±0.13^{A}	1.12±0.97^{C}	0.57±1.1^{AB}	0.5±0.32^{BC}
DO (ppm)	7.18±1.45^{a}	7.97±1.47^{a}	10.35±1.95^{b}	7.65±1.92	8.9±2.46	8.63±2.11^{A}	8.77±0.94
BOD (ppm)	2.56±1.08^{a}	2.64±1.2^{a}	2.91±2.16^{b}	2.11±0.86	2.73±1.82	2.95±1.69^{A}	2.8±1
Alkalinity (meq L^{-1})	125.27±20.4^{a}	115.7±22.81^{a}	138.52±20.08^{b}	142.57±12.52^{A}	106.54±17.55^{B}	131.93±21.59^{A}	115±20.34^{B}
Nitrite(µmol/l)	0.42±0.53^{a}	0.33±0.33^{a}	0.7±0.91^{b}	0.33±0.27^{A}	0.69±1.08^{A}	0.36±0.42	0.91±0.44^{B}
Nitrate(µmol/l)	5.12±3.63^{a}	4.93±3.37^{b}	5.6±5.24^{a}	2.95±1.5^{A}	8.18±5.69^{B}	4.17±2.47	7.84±4.79^{B}
Silicate(µmol/l)	81.24±37.88^{a}	85.29±34.43^{a}	129.06±41.96^{c}	74.48±28.48	128.89±57.67	96.09±32.42	85.84±38.2
Phosphate(µmol/l)	0.2±0.04^{a}	0.1±0.03^{b}	0.15±0.13^{c}	0.16±0.16	0.14±0.06	0.15±0.07	0.17±0.05
Ammonia(µmol/l)	2.17±0.89^{a}	1.65±1.1^{b}	2.5±1.22^{a}	1.69±0.49	2.55±1.54	2.08±1.07	2.04±0.9

WT, Water temperature; DO, Dissolved oxygen; BOD, Biological oxygen demand.

Mean value followed by lower and upper case later in a row are significantly different.

Table 4.2 Water quality parameter of lake during Pre-Monsoon season.

Sector	Station no.	WT (°C)	Trans(cm)	Depth(cm)	Conductivity (PSU)	Salinity (mS cm^{-1})	pH	Turbidity (NTU)	Chl a(µg/lit)	DO (ppm)	BOD (ppm)	Alkalinity (meq L^{-1})	NO_2^- (µmol/l)	NO_3^- (µmol/l)	Silicate(µmol/l)	PO_4^{3-} (µmol/l)	NH_4^+(µmol/l)
SS	1	32	47	178	22.5	11.39	8.08	19.9	0.06	5.83	1.52	144	0.11	2.44	73.19	0.19	2.36
	2	31.5	111	111	24.16	12.36	8.39	3.72	0.01	8.19	1.04	170	0.17	3.85	83.12	0.19	1.86
	3	31.5	62	62	23.21	12.12	8.85	7.67	0.03	9.18	2.78	137	0.24	4.47	80.25	0.2	2.69
	4	32	30	221	21.92	11.03	7.96	77.6	0.06	6.22	2.62	156	0.05	3.19	73.37	0.21	2.19
	5	32.0	40	240	23.24	11.64	7.95	28.2	0.08	5.52	2.08	132	0.01	3.97	65.25	0.18	1.73
	6	31	84	233	23.57	12.35	8.11	14.62	0.04	4.61	2.12	132	0.12	2.17	68.59	0.18	1.73
	7	32	34	236	23.83	12.11	7.64	72.6	0.06	5.12	1.76	121	0.11	4.11	57.19	0.19	2.11
	Min	31.0	30.00	62.00	21.92	11.03	7.64	3.72	0.01	4.61	1.04	121.00	0.01	2.17	57.19	0.18	1.73
	Max	32.0	111.00	240.00	24.16	12.36	8.85	77.60	0.08	9.18	2.78	170.00	0.24	4.47	83.12	0.21	2.69
	Mean	31.7	58.29	183.00	23.20	11.86	8.14	32.04	0.05	6.38	1.99	141.71	0.12	3.46	71.57	0.19	2.10
	Std	0.40	29.74	70.54	0.77	0.51	0.38	30.50	0.02	1.68	0.61	16.58	0.08	0.88	8.85	0.01	0.35
CS	8	30.5	47	139	22.85	12.02	8.81	27.3	0.03	4.14	1.69	136	0.12	3.26	90.04	0.25	2.11
	9	31.5	54	54	27.34	13.91	8.11	6.54	0.10	7.17	2.63	157	0.32	4.38	92.13	0.18	4.4

13	30.5	65	137	50.17	28.71	7.82	13.39	0.70	6.62	2.79	142	0.49	5.92	72.34	0.2	1.8
14	32	66	66	36.59	19.43	8.04	4.64	0.05	8.33	2.8	143	0.58	2.7	71.37	0.19	3.69
15	30	83	133	28.13	15.09	8.21	8.33	0.16	7.64	2.9	135	0.02	4.87	68.61	0.19	1.42
16	31	51	200	26.45	13.82	8.06	16.53	0.33	8.86	4.83	128	0.25	1.9	69.33	0.19	1.41
17	32.5	84	182	17.7	8.614	8.50	3.09	0.02	9.53	2.82	102	0.14	3.49	70.05	0.19	1.54
18	30.5	115	159	21.81	11.25	8.40	3.92	0.39	7.58	2.72	136	0.18	3.74	100.14	0.19	1.44
19	31.5	40	175	43.57	23.45	7.89	26	0.28	6.64	2.93	158	0.24	2.92	53.11	0.2	1.6
20	31.5	34	156	38.06	19.86	8.00	18.9	0.47	7.13	2.82	116	0.27	3.44	58.35	0.19	1.6
21	32	50	138	29.97	15.08	7.99	21.2	1.00	7.37	3.54	93	0.4	6.78	72.16	0.19	1.78
27	31	25	125	31.29	16.6	7.83	111	0.60	4.85	2.95	117	0.47	4.93	62.31	0.43	4.56
28	31.5	33	120	36.36	19.25	8.00	26.4	0.22	5.57	3.43	116	0.21	2.06	56.78	0.2	1.67
29	31	61	129	26.58	13.81	7.98	14.48	0.83	7.15	4.3	122	0.18	2.3	76.04	0.19	1.77
30	32.7	18	97	13.89	6.893	7.50	64.6	3.62	9	0.75	108	0.32	3.62	129	0.24	3.41
Min	30.0	18.00	54.00	13.89	6.89	7.50	3.09	0.02	4.14	0.75	93.00	0.02	1.90	53.11	0.18	1.41
Max	32.7	115.00	200.00	50.17	28.71	8.81	111.00	3.62	9.53	4.83	158.00	0.58	6.78	129.00	0.43	4.56
Mean	31.3	55.07	134.00	30.05	15.85	8.08	24.42	0.59	7.17	2.93	127.27	0.28	3.75	76.12	0.21	2.28

	Std	0.78	25.36	39.82	9.66	5.64	0.31	28.40	0.89	1.49	0.95	19.04	0.15	1.40	19.69	0.06	1.13
NS	22	29.5	18	135	17.04	8.448	7.56	38.7	1.64	5.91	1.01	149	0.17	2.89	56.65	0.19	1.36
	23	29.5	29	123	19.63	9.95	8.05	20.6	0.65	8.7	2.78	105	0.15	4.75	74.14	0.19	1.61
	24	29	11	116	0.733	0.361	7.71	574	0.44	7.17	1.84	90	0.9	13.8	121.61	0.19	1.64
	25	31.5	24	124	6.805	3.105	8.18	34.7	0.85	9.31	2.64	103	0.97	9.02	82.41	0.19	1.21
	26	31	13	126	19.4	9.719	8.01	233	1.20	6.34	5.11	110	0.03	3.71	53.26	0.19	1.9
	31	32.4	8	84	10.45	5.099	7.70	134	3.77	8.13	0.23	100	0.14	3.79	92.62	0.19	3.38
	32	32.7	8	90	2.505	1.164	7.60	298	3.11	8.35	1.12	105	1.76	11.9	180.16	0.19	3.37
	33	30.5	38	83	0.5304	0.271	6.94	60.2	0.71	6.64	3	112	2.37	17.5	229.58	0.21	1.42
	Min	29.0	8.00	83.00	0.53	0.27	6.94	20.60	0.44	5.91	0.23	90.00	0.03	2.89	53.26	0.19	1.21
	Max	32.7	38.00	135.00	19.63	9.95	8.18	574.00	3.77	9.31	5.11	149.00	2.37	17.5	229.58	0.21	3.38
	Mean	30.8	18.63	110.13	9.64	4.76	7.72	174.15	1.55	7.57	2.22	109.25	0.81	8.43	111.30	0.19	1.99
	Std	1.38	10.88	21.00	8.21	4.15	0.39	190.73	1.24	1.23	1.52	17.40	0.87	5.51	62.97	0.01	0.88
OC	10	30.5	7	158	42.33	23.38	7.91	90.2	0.65	7.58	2.76	129	0.39	3.46	68.06	0.2	3.15
	11	30.5	17	350	48.33	26.83	7.93	60.1	1.28	8.23	2.74	104	0.66	6.12	53.47	0.19	2.05
	12	30	21	154	61.3	35.62	7.89	44.4	0.50	8.43	3.53	126	1.48	11.3	26.11	0.2	1.8

	Min	30.0	7.00	154.00	42.33	23.38	7.89	44.40	0.50	7.58	2.74	104.00	0.39	3.46	26.11	0.19	1.80
	Max	30.5	21.00	350.00	61.30	35.62	7.93	90.20	1.28	8.43	3.53	129.00	1.48	11.3	68.06	0.20	3.15
	Mean	30.3	15.00	220.67	50.65	28.61	7.91	64.90	0.81	8.08	3.01	119.67	0.84	6.97	49.21	0.20	2.33
	Std	0.29	7.21	112.02	9.70	6.31	0.02	23.27	0.41	0.44	0.45	13.65	0.57	4.00	21.30	0.01	0.72
Lake	Min	29.0	7.00	54.00	0.53	0.27	6.94	3.09	0.01	4.14	0.23	90.00	0.01	1.90	26.11	0.18	1.21
	Max	32.7	115.00	350.00	61.30	35.62	8.85	574.00	3.77	9.53	5.11	170.00	2.37	17.5	229.58	0.43	4.56
	Mean	31.1	43.27	146.48	25.52	13.48	7.99	66.02	0.73	7.18	2.56	125.27	0.42	5.12	81.24	0.20	2.17
	Std	0.95	28.60	60.98	13.95	7.99	0.36	111.83	0.99	1.45	1.08	20.40	0.53	3.63	37.88	0.04	0.89

SS, Southern sector; CS, Central sector; NS, Northern sector; OC, Outer channel; WT, Water temperature; Trans, Transparency; DO, Dissolved oxygen; BOD, Biological oxygen demand.

Table 4.3 Water quality parameters of lake during Monsoon season

Sector	Station no.	WT (°C)	Trans(cm)	Depth(cm)	Conductivity (mS cm^{-1})	Salinity (PSU)	pH	Turbidity (NTU)	Chl a(µg/lit)	DO (ppm)	BOD (ppm)	Alkalinity (meq L^{-1})	NO_2^- (µmol/l)	NO_3^- (µmol/l)	Silicate(µmol/l)	PO_4^{3-} (µmol/l)	NH_4^+(µmol/l)
SS	1	29.5	184	271	8.36	4.72	8.09	2.4	0.38	7.87	2.94	138	0.2	3.71	73.98	0.12	1.37
	2	28	124	124	11.05	6.33	7.84	2.48	0.11	5.79	2.11	158	0.17	4.49	35.91	0.12	1.55
	3	29	127	127	11.42	6.55	8.06	0.66	0.08	6.85	0.69	146	0.22	3.85	29.09	0.1	1.82
	4	29	208	308	10.41	5.93	8.16	1.73	0.17	7.87	2.39	139	0.23	2.77	46.12	0.1	1.07
	5	29.5	182	328	9.85	5.59	8.16	2.73	0.22	7.05	2.78	128	0.17	3.27	45.6	0.1	0.93
	6	27.5	149	317	10.12	5.76	8.12	3.32	0.19	8.46	2.66	141	0.17	1.27	46.82	0.1	1.08
	7	28.5	149	374	8.78	4.97	8.16	3.04	0.17	7.99	2.82	124	0.1	3.12	54.57	0.1	0.7
	Min	27.5	124.00	124.00	8.36	4.72	7.84	0.66	0.08	5.79	0.69	124.00	0.10	1.27	29.09	0.10	0.70
	Max	29.5	208.00	374.00	11.42	6.55	8.16	3.32	0.38	8.46	2.94	158.00	0.23	4.49	73.98	0.12	1.82
	Mean	28.7	160.43	264.14	10.00	5.69	8.08	2.34	0.19	7.41	2.34	139.14	0.18	3.21	47.44	0.11	1.22
	Std	0.76	31.60	99.46	1.12	0.67	0.12	0.90	0.10	0.91	0.78	11.26	0.04	1.02	14.32	0.01	0.38

	8	27.5	196	196	9.48	5.37	8.16	2.35	0.13	8.97	1.56	150	0.07	2.15	40.66	0.12	0.98
	9	29.5	136	136	9.32	5.27	8.52	1.21	0.10	6.93	3.02	121	0.24	6.45	84.05	0.13	1.06
	13	28.5	50	208	2.20	1.17	8.36	14.47	0.34	8.11	2.03	114	0.34	4.97	107.38	0.11	0.65
	14	29.5	100	142	4.09	1.93	8.50	1.43	0.32	7.95	2.51	112	0.22	6.24	72.29	0.12	0.94
	15	28.1	206	206	7.86	4.40	8.69	1.98	0.07	10.3	2.34	143	0.1	1.3	31.03	0.1	0.86
	16	28	105	291	9.29	5.26	8.18	4.552	0.27	7.05	2.27	113	0.13	3.09	82.95	0.11	0.66
	17	27.5	172	168	4.73	2.58	8.57	1.72	0.20	9.41	1.59	117	0.03	2.73	72.12	0.11	1.15
CS	18	30	172	207	4.08	2.20	8.41	3.82	0.21	9.13	3.1	139	0.14	3.3	69.46	0.1	2.4
	19	32	152	214	6.53	3.62	8.34	3.83	0.12	6.38	2.63	134	0.25	4.17	95.43	0.1	2.35
	20	31.3	89	229	4.53	2.47	8.12	5.23	0.16	7.08	4.24	125	0.18	2.92	83.8	0.1	1.22
	21	31.2	32	218	1.86	1.00	7.98	12.25	0.39	11.3	4.15	106	0.58	6.91	106.37	0.09	1.2
	27	31.5	19	162	0.52	0.30	7.61	79.9	0.41	8.07	0.92	110	0.45	7.35	110.43	0.11	4.86
	28	30.5	106	162	1.20	0.65	8.57	13.7	0.15	9.21	3.93	118	0.14	4.51	82.25	0.1	2.25
	29	30.5	96	165	1.26	0.68	8.43	8.69	0.29	8.86	5.11	139	0.19	4.62	131.47	0.11	5.24

	30	29.2	40	166	0.32	0.20	7.87	26.5	0.82	5.20	1.76	80	0.22	4.48	135.65	0.05	1.49
	Min	27.5	19.00	136.00	0.32	0.20	7.61	1.21	0.07	5.20	0.92	80.00	0.03	1.30	31.03	0.05	0.65
	Max	32.0	206.00	291.00	9.48	5.37	8.69	79.90	0.82	11.3	5.11	150.00	0.58	7.35	135.65	0.13	5.24
	Mean	29.7	111.40	191.33	4.48	2.47	8.29	12.11	0.26	8.26	2.74	121.40	0.22	4.35	87.02	0.10	1.82
	Std	1.50	59.97	40.03	3.31	1.88	0.30	20.01	0.19	1.58	1.18	17.73	0.15	1.80	29.08	0.02	1.43
	22	28.2	10	214	0.17	0.13	8.12	117	1.45	8.46	5.23	83	0.7	10.0	127.8	0.08	1.18
	23	28.8	12	202	0.16	0.13	7.38	78	1.23	6.42	0.65	88	0.58	6.16	107.37	0.07	1.23
	24	29	20	185	0.15	0.13	7.03	40.4	1.02	8.30	2.31	91	0.25	5.17	131.15	0.05	1.48
	25	31.5	29	194	0.14	0.12	7.72	26.7	1.73	10.5	3.16	75	0.11	0.17	122.87	0.07	1.53
NS	26	33	25	166	0.26	0.18	7.68	183	0.67	7.91	2.47	124	0.44	5.99	128.42	0.11	3.5
	31	30	50	156	0.39	0.24	7.47	14.66	0.81	6.73	1.6	96	0.03	0.78	51.21	0.04	1.46
	32	29	123	155	0.27	0.18	7.23	3.39	0.32	5.63	1.36	89	0.1	2.19	48.53	0.03	3.02
	33	30.1	51	131	0.15	0.12	6.59	19.3	0.31	6.18	5.46	96	0.61	7.68	139.6	0.04	2.02
	Min	28.2	10.00	131.00	0.14	0.12	6.59	3.39	0.31	5.63	0.65	75.0	0.03	0.17	48.53	0.03	1.18

	Max	33.0	123.00	214.00	0.39	0.24	8.12	183.00	1.73	10.5	5.46	124.0	0.70	10.0	139.60	0.11	3.50
	Mean	29.9	40.00	175.38	0.21	0.15	7.40	60.31	0.94	7.51	2.78	92.75	0.35	4.77	107.12	0.06	1.93
	Std	1.60	36.92	28.00	0.09	0.04	0.47	62.23	0.51	1.58	1.76	14.38	0.26	3.45	36.49	0.03	0.87
	10	28.7	7	250	0.52	0.30	7.82	130	0.31	8.62	2.14	98	1.71	17.2	120.18	0.13	1.07
	11	29	7	205	0.84	0.46	7.40	98.7	0.27	10.3	3.17	89	0.9	10.9	98.35	0.12	1.58
	12	29.7	9	258	0.31	0.81	7.55	10.1	0.58	7.99	2.15	94	0.76	8.76	101.53	0.1	0.58
OC	Min	28.	7.00	205.00	0.31	0.30	7.40	10.10	0.27	7.99	2.14	89.00	0.76	8.76	98.35	0.10	0.58
	Max	29.7	9.00	258.00	0.84	0.81	7.82	130.00	0.58	10.3	3.17	98.00	1.71	17.2	120.18	0.13	1.58
	Mean	29.1	7.67	237.67	0.55	0.52	7.59	79.60	0.39	8.99	2.49	93.67	1.12	12.3	106.69	0.12	1.08
	Std	0.51	1.15	28.57	0.27	0.26	0.21	62.19	0.17	1.22	0.59	4.51	0.51	4.39	11.79	0.02	0.50
	Min	27.5	7.00	124.00	0.14	0.12	6.59	0.66	0.07	5.20	0.65	75.00	0.03	0.17	29.09	0.03	0.58
	Max	33.0	208	374.00	11.42	6.55	8.69	183.00	1.73	11.3	5.46	158.00	1.71	17.2	139.60	0.13	5.24
Lake	Mean	29.5	95.06	207.12	4.26	2.42	7.97	27.86	0.42	7.97	2.64	115.70	0.33	4.93	85.29	0.10	1.65
	Std	1.35	66.74	61.86	4.14	2.33	0.48	44.45	0.40	1.44	1.19	22.47	0.33	3.31	33.90	0.03	1.08

Table 4.4 Water quality parameter of lake during Post Monsoon season

Sector	Station	WT (°C)	Trans(cm)	Depth(cm)	Conductivity (mS cm^{-1})	Salinity (PSU)	pH	Turbidity (NTU)	Chl a(µg/L)	DO (ppm)	BOD (ppm)	Alkalinity (meq L^{-1})	NO_2^- (µmol/l)	NO_3^- (µmol/l)	Silicate(µmol/l)	PO_4^{3-} (µmol/l)	NH_4^+(µmol/l)
SS	1	21.4	75.44	181.94	17.10	10.05	8.53	12.14	0.41	9.9	1.69	139	0.7	1.74	94.36	0.42	2.25
	2	21.5	62.13	62.13	16.27	9.52	9.09	2.06	0.10	10.1	2.98	151	0.78	2.77	63.25	0.07	1.74
	3	20.4	115.38	115.38	15.32	8.91	9.05	2.51	0.16	10.6	2.44	146	0.68	1.45	98.6	0.02	1.65
	4	22	115.38	221.88	16.42	9.61	8.40	7.49	0.44	7.38	0.78	140	0.67	0.98	108.09	0.03	1.51
	5	24.3	124.25	257.38	15.02	8.74	8.40	7.36	0.35	7.9	1.34	138	0.75	6.76	122.04	0.02	1.68
	6	21	106.50	230.75	14.47	8.38	8.42	8.15	0.30	11.8	3.91	150	0.61	0.86	111.01	0.74	1.88
	7	21.2	93.19	230.75	13.91	8.09	8.33	7.43	0.18	6.2	0.79	164	0.69	0.71	133.77	0.04	1.69
	Min	20.4	62.13	62.13	13.91	8.09	8.33	2.06	0.10	6.20	0.78	138	0.61	0.71	63.25	0.02	1.51
	Max	24.3	124.25	257.38	17.10	10.05	9.09	12.14	0.44	11.8	3.91	164	0.78	6.76	133.77	0.74	2.25
	Mean	21.7	98.89	185.74	15.50	9.04	8.60	6.73	0.28	9.15	1.99	146.86	0.70	2.18	104.45	0.19	1.77
	Std	1.25	23.02	71.57	1.14	0.71	0.33	3.47	0.13	2.02	1.18	9.21	0.06	2.14	22.58	0.28	0.24
CS	8	20.7	133.13	150.88	13.02	7.54	8.58	3.74	0.06	9.41	2.26	169	0.63	1.17	87.18	0.18	1.72
	9	22.2	56.00	56	7.83	4.35	9.16	3.95	0.52	10.2	1.63	194	0.35	4.16	115.02	0.15	2.23
	13	21.9	38.00	123	2.72	1.45	8.31	30.00	0.15	9.41	1.63	138	0.25	5.34	164.17	0.13	2.63
	14	22.5	78.00	78	9.75	5.61	8.99	4.06	0.04	8.47	1.20	141	0.41	3.50	100.99	0.16	2.15
	15	21.0	55.00	135	12.02	6.89	8.23	15.22	0.26	15.6	5.56	130	0.49	2.23	127.78	0.12	2.40

	16	21.2	65.00	208	13.42	7.76	8.27	10.60	0.43	10.2	2.93	168	0.49	2.09	128.28	0.13	2.39
	17	21.4	102.06	178	13.57	7.89	8.36	6.99	0.26	9.02	0.81	137	0.63	0.88	87.83	0.02	1.85
	18	22.5	58.00	171	8.98	5.95	8.62	13.11	0.78	9.79	4.85	135	2.88	15.3	148.23	0.11	1.89
	19	23.1	42.00	172	11.97	6.80	8.52	17.86	0.26	9.31	1.57	147	0.40	1.85	133.60	0.11	2.30
	20	23.8	130.00	154	8.41	4.63	9.12	4.43	0.17	11.9	4.27	133	0.31	3.83	90.62	0.11	2.16
	21	23.3	41.00	133	3.22	1.73	9.41	21.10	1.08	12.4	2.49	117	0.14	5.89	153.84	0.17	2.94
	27	24.6	24	119	3.95	2.14	9.11	44.70	6.78	11.4	11.0	153	0.38	7.66	162.60	0.11	1.82
	28	24.1	84	126	10.79	6.14	8.89	5.30	0.66	10.7	3.17	147	0.46	2.34	125.00	0.09	1.66
	29	24.2	94	128	8.51	4.75	8.81	6.54	0.60	9.14	2.58	167	0.50	2.46	129.16	0.09	1.48
	30	29	37	95	1.07	0.57	8.26	62.70	0.67	9.61	1.79	131	0.20	7.48	122.63	0.19	2.65
	Min	20.7	24.00	56.00	1.07	0.57	8.23	3.74	0.04	8.47	0.81	117	0.14	0.88	87.18	0.02	20.70
	Max	29.0	133.13	208.00	13.57	7.89	9.41	62.70	6.78	15.6	11.0	194	2.88	15.3	164.17	0.19	29.00
	Mean	23.0	69.15	135.09	8.61	4.95	8.71	16.69	0.85	10.4	3.19	147.13	0.57	4.41	125.13	0.12	23.03
	Std	2.06	33.68	39.67	4.13	2.44	0.39	17.15	1.67	1.81	2.56	19.95	0.65	3.70	25.50	0.04	2.06
	22	21.0	14.00	137	0.94	0.51	8.22	268.00	0.86	9.45	1.47	128	0.26	16.7	211.24	0.23	7.81
	23	21.4	10.00	126	0.69	0.37	8.14	329.00	0.66	9.33	1.35	95	0.18	10.2	222.94	0.21	2.48
NS	24	20.6	22.00	93	0.64	0.34	8.58	73.90	0.32	10.6	2.75	119	0.09	6.99	165.69	0.14	2.34
	25	24.0	6.00	121	0.50	0.28	8.73	267.00	3.24	13.1	3.20	117	0.49	9.11	208.88	0.20	2.10
	26	25.7	16.00	127	1.18	0.62	8.31	133.00	0.49	13.6	8.31	114	0.80	16.1	154.50	0.10	5.32

	31	29.0	32	94	1.08	0.58	8.39	71.90	0.13	11.2	3.80	122	0.36	6.21	132.89	0.13	3.19
	32	29.2	34	84	0.21	0.06	8.88	16.12	0.70	11.7	2.27	134	0.04	3.44	57.57	0.12	2.61
	33	23.4	77	77	0.54	0.29	9.66	16.10	0.59	13.8	2.39	112	5.01	21.9	192.20	0.16	3.97
	Min	20.6	6.00	77.00	0.21	0.06	8.14	16.10	0.13	9.33	1.35	95.00	0.04	3.44	57.57	0.10	2.10
	Max	29.2	77.00	137.00	1.18	0.62	9.66	329.00	3.24	13.8	8.31	134.00	5.01	21.9	222.94	0.23	7.81
	Mean	24.2	26.38	107.38	0.72	0.38	8.61	146.88	0.87	11.6	3.19	117.63	0.90	11.3	168.24	0.16	3.73
	Std	3.42	22.73	22.83	0.32	0.18	0.49	123.99	0.98	1.78	2.22	11.67	1.68	6.29	54.46	0.05	1.96
OC	10	22.4	34	169	9.595	5.511	8.04	26	0.33	9.57	1.79	128	0.47	6.81	142.52	0.24	3.23
	11	22.6	40	207	20.74	12.43	8.22	19.2	0.30	9.86	4.96	151	0.76	4.08	112.07	0.15	2.26
	12	23.6	48	161	38.61	24.32	8.27	16.58	0.27	8.27	1.95	116	1.09	1.83	50.31	0.21	2.66
	Min	22.4	34.00	161.00	9.60	5.51	8.05	16.58	0.27	8.27	1.79	116	0.47	1.83	50.31	0.15	2.26
	Max	23.6	48.00	207.00	38.61	24.32	8.27	26.00	0.33	9.86	4.96	151	1.09	6.81	142.52	0.24	3.23
	Mean	22.9	40.67	179.00	22.98	14.09	8.18	20.59	0.30	9.23	2.90	131.67	0.77	4.24	101.63	0.20	2.72
	Std	0.64	7.02	24.58	14.64	9.51	0.12	4.86	0.03	0.85	1.79	17.79	0.31	2.49	46.98	0.05	0.49
Lake	Min	20.4	6	56	0.208	0.062	8.05	2.06	0.04	6.2	0.78	95	0.04	0.71	50.31	0.02	1.48
	Max	29.2	133.12	257.38	38.61	24.32	9.66	329	6.78	15.6	11.0	194	5.01	21.9	222.94	0.74	7.81
	Mean	23.0	62.5	143.1	9.5	5.5	8.6	46.5	0.7	10.3	2.9	138.5	0.7	5.6	129.1	0.2	2.5
	Std	2.4	37.3	51.7	8.1	5.0	0.4	82.7	1.2	1.9	2.2	20.1	0.9	5.2	42.0	0.1	1.2

SS, Southern sector; CS, Central sector; NS, Northern sector; OC, Outer channel; WT, Water temperature; Trans, Transparency; DO, Dissolved oxygen; BOD, Biological oxygen demand.

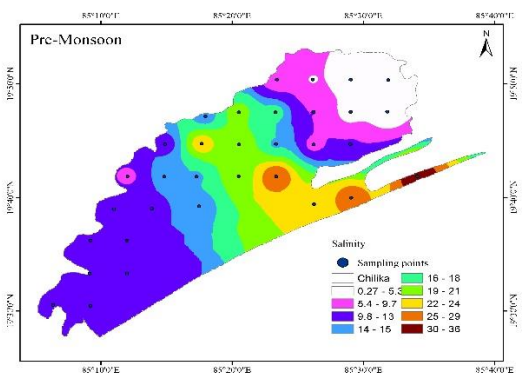
Pre-Monsoon
Salinity
Sampling points
Chilika
0.27 - 5.3
5.4 - 9.7
9.8 - 13
14 - 15
16 - 18
19 - 21
22 - 24
25 - 29
30 - 36

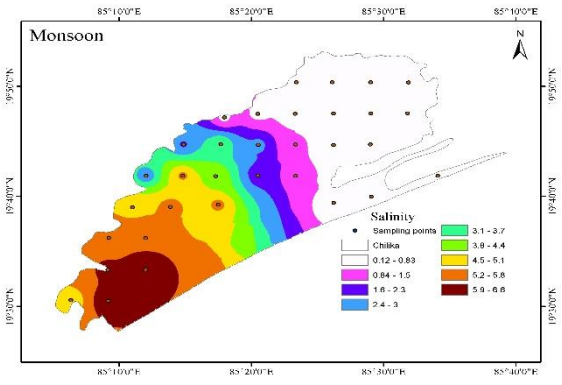
Monsoon
Salinity
Sampling points
Chilika
0.12 - 0.83
0.84 - 1.5
1.6 - 2.3
2.4 - 3
3.1 - 3.7
3.8 - 4.4
4.5 - 5.1
5.2 - 5.8
5.9 - 6.6

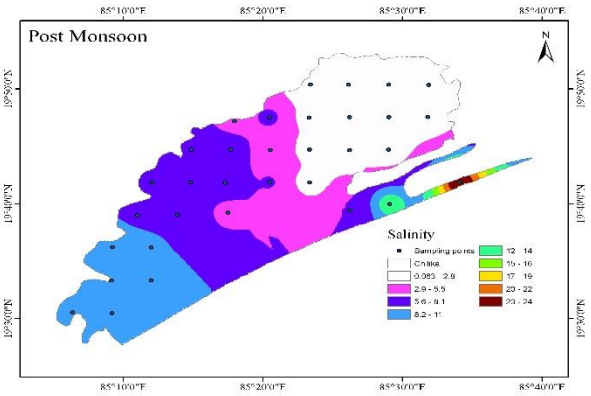
Post Monsoon
Salinity
Sampling points
Chilika
0.085 - 2.9
2.9 - 5.5
5.6 - 8.1
8.2 - 11
12 - 14
15 - 16
17 - 19
20 - 22
23 - 24

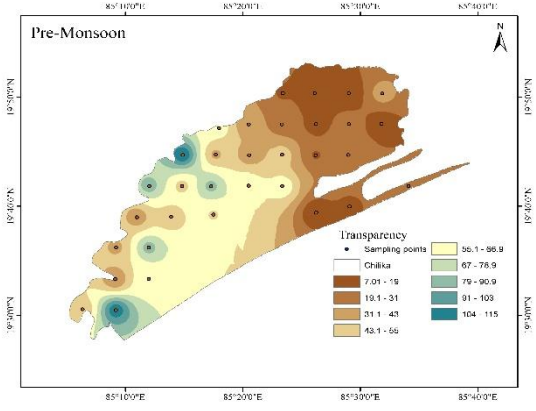
Pre-Monsoon
Transparency
Sampling points
Chilika
7.01 - 19
19.1 - 31
31.1 - 43
43.1 - 55
55.1 - 66.9
67 - 78.9
79 - 90.9
91 - 103
104 - 115

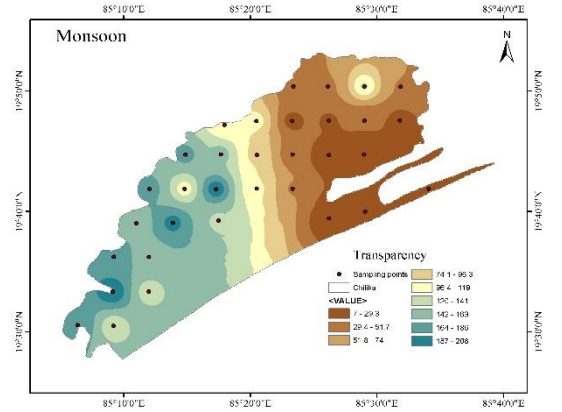
Monsoon
Transparency
Sampling points
Chilika
74.1 - 95.3
96.4 - 119
142 - 163
164 - 185
187 - 208

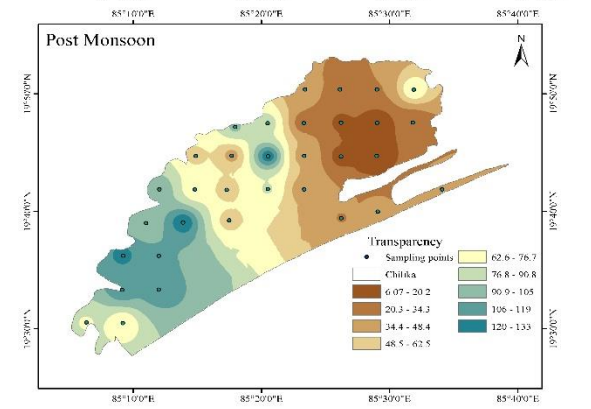
Post Monsoon
Transparency
Sampling points
Chilika
6.07 - 20.2
20.3 - 34.3
34.4 - 48.4
48.5 - 62.5
62.6 - 76.7
76.8 - 90.8
90.9 - 105
106 - 119
120 - 133

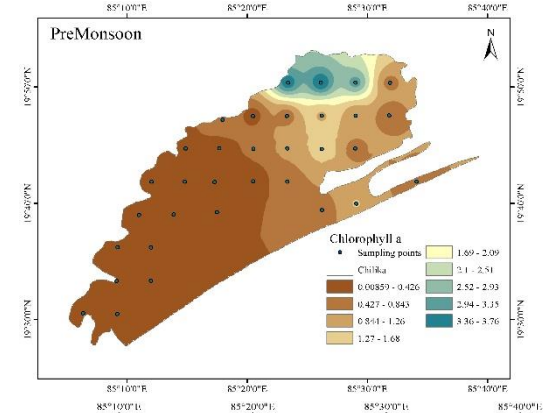
PreMonsoon
Chlorophyll a
Sampling points
Chilika
0.00859 - 0.426
0.427 - 0.843
0.844 - 1.26
1.27 - 1.68
1.69 - 2.09
2.1 - 2.51
2.52 - 2.93
2.94 - 3.35
3.36 - 3.76

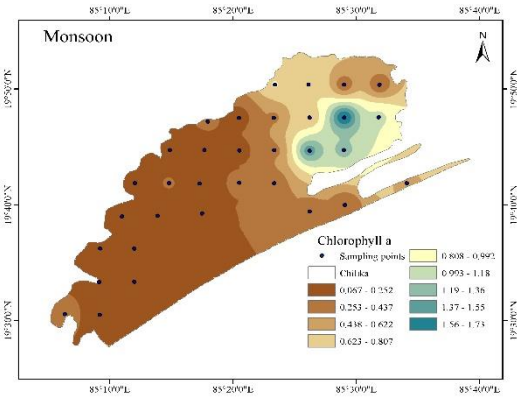
Monsoon
Chlorophyll a
Sampling points
Chilika
0.067 - 0.252
0.253 - 0.437
0.438 - 0.622
0.623 - 0.807
0.808 - 0.992
0.993 - 1.18
1.19 - 1.36
1.37 - 1.55
1.56 - 1.73

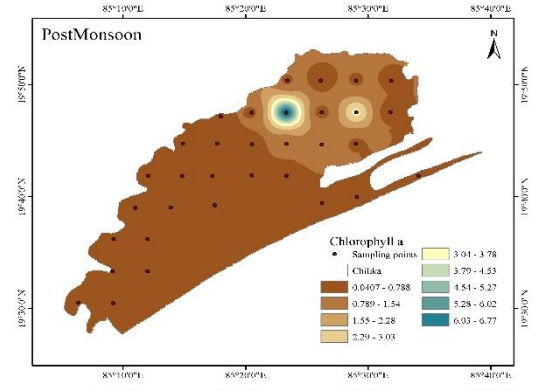
PostMonsoon
Chlorophyll a
Sampling points
Chilika
0.0407 - 0.788
0.789 - 1.54
1.55 - 2.28
2.29 - 3.03
3.04 - 3.78
3.79 - 4.53
4.54 - 5.27
5.28 - 6.02
6.03 - 6.77

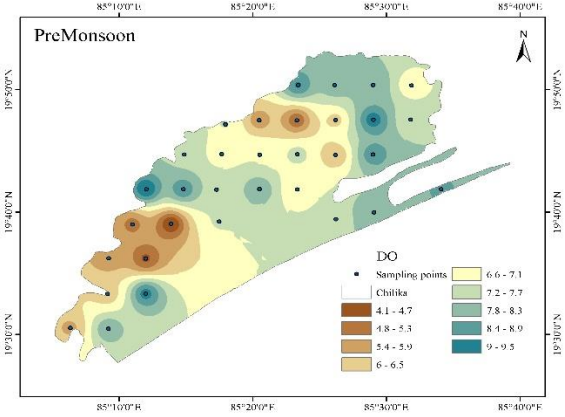
PreMonsoon
DO
Sampling points
Chilika
4.1 - 4.7
4.8 - 5.3
5.4 - 5.9
6 - 6.5
6.6 - 7.1
7.2 - 7.7
7.8 - 8.3
8.4 - 8.9
9 - 9.5

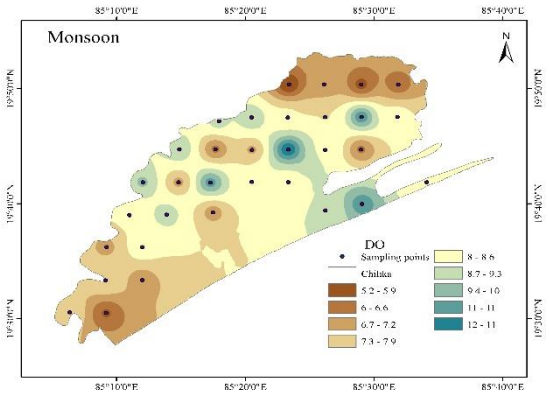
Monsoon
DO
Sampling points
Chilika
5.2 - 5.9
6 - 6.6
6.7 - 7.2
7.3 - 7.9
8 - 8.6
8.7 - 9.3
9.4 - 10
11 - 11
12 - 11

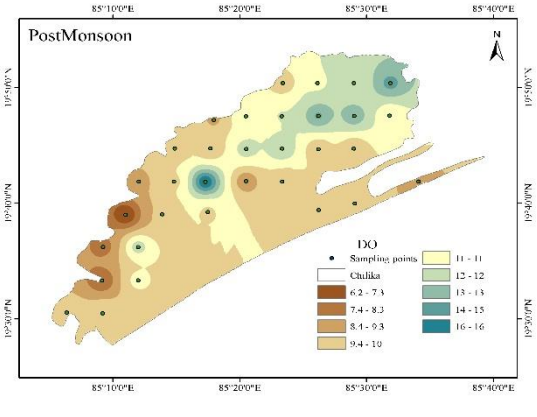
PostMonsoon
DO
Sampling points
Chilika
6.2 - 7.3
7.4 - 8.3
8.4 - 9.3
9.4 - 10
11 - 11
12 - 12
13 - 13
14 - 15
16 - 16

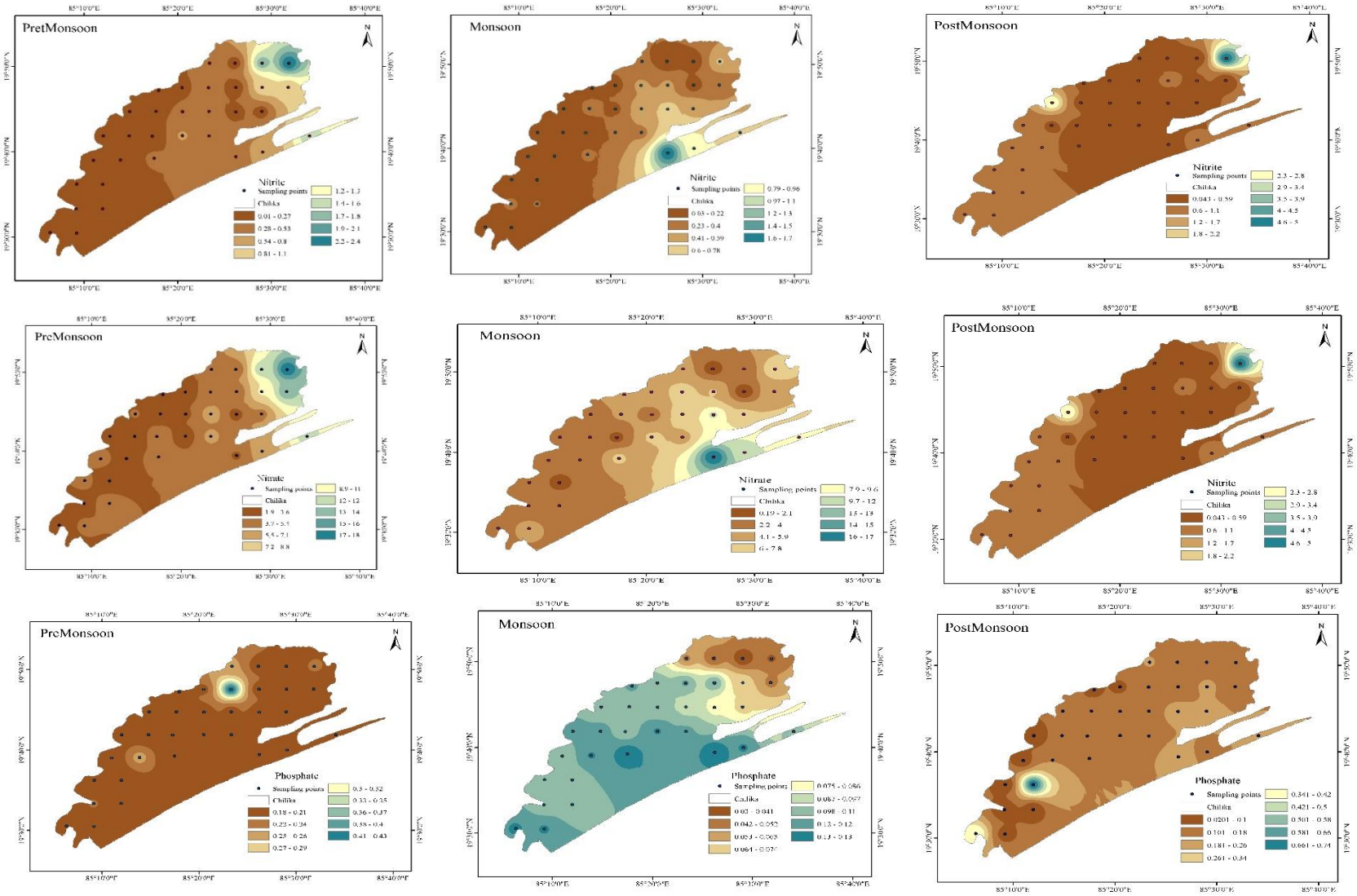
PretMonsoon
Nitrite
Sampling points
Chilika
0.01 - 0.27
0.28 - 0.53
0.54 - 0.8
0.81 - 1.1
1.2 - 1.3
1.4 - 1.6
1.7 - 1.8
1.9 - 2.1
2.2 - 2.4
Monsoon
Nitrite
Sampling points
Chilika
0.03 - 0.22
0.23 - 0.4
0.41 - 0.59
0.6 - 0.78
0.79 - 0.96
0.97 - 1.1
1.2 - 1.3
1.4 - 1.5
1.6 - 1.7
PostMonsoon
Nitrite
Sampling points
Chilika
0.043 - 0.59
0.6 - 1.1
1.2 - 1.7
1.8 - 2.2
2.3 - 2.8
2.9 - 3.4
3.5 - 3.9
4 - 4.5
4.6 - 5
PreMonsoon
Nitrate
Sampling points
Chilika
1.9 - 3.6
3.7 - 5.5
5.5 - 7.1
7.2 - 8.8
8.9 - 11
12 - 12
13 - 14
15 - 16
17 - 18
Monsoon
Nitrate
Sampling points
Chilika
0.19 - 2.1
2.2 - 4
4.1 - 5.9
6 - 7.8
7.9 - 9.6
9.7 - 12
13 - 13
14 - 15
16 - 17
PostMonsoon
Nitrite
Sampling points
Chilika
0.043 - 0.59
0.6 - 1.1
1.2 - 1.7
1.8 - 2.2
2.3 - 2.8
2.9 - 3.4
3.5 - 3.9
4 - 4.5
4.6 - 5
PreMonsoon
Phosphate
Sampling points
Chilika
0.18 - 0.21
0.22 - 0.24
0.25 - 0.26
0.27 - 0.29
0.3 - 0.32
0.33 - 0.35
0.36 - 0.37
0.38 - 0.4
0.41 - 0.43
Monsoon
Phosphate
Sampling points
Chilika
0.03 - 0.041
0.042 - 0.052
0.053 - 0.063
0.064 - 0.077
0.078 - 0.086
0.087 - 0.097
0.098 - 0.11
0.12 - 0.12
0.13 - 0.13
PostMonsoon
Phosphate
Sampling points
Chilika
0.0201 - 0.1
0.101 - 0.18
0.181 - 0.26
0.261 - 0.34
0.341 - 0.42
0.421 - 0.5
0.501 - 0.58
0.581 - 0.66
0.661 - 0.74

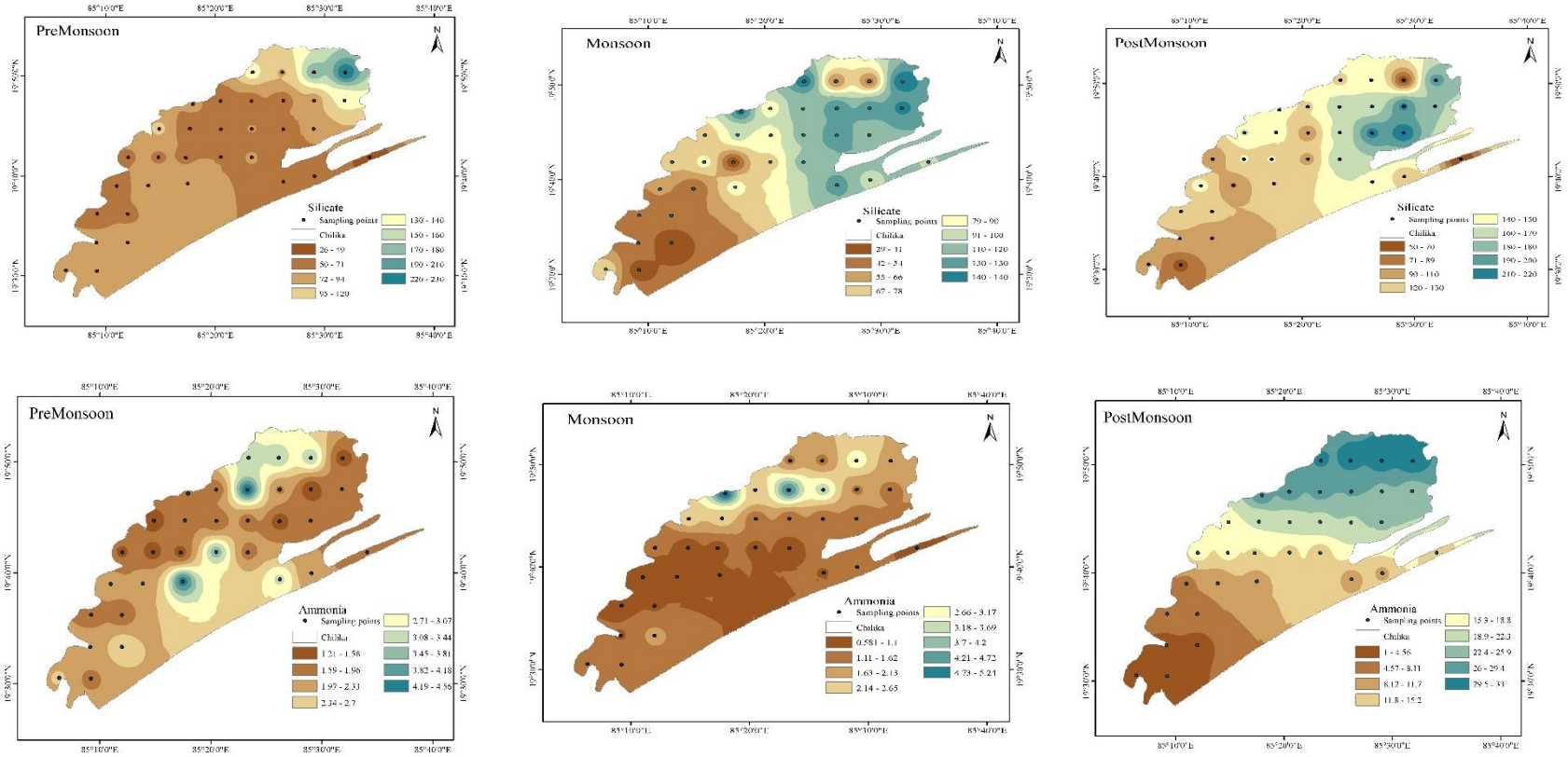

Fig. 4.1 Seasonal and spatial gradients of water quality variables in Chilika lake

Table 4.5 Pearsons's correlation matrix for water quality parameters of Chilaka lagoon (All sectors and seasons)

	WT	Transparency	Depth	Conductivity	Salinity	pH	Turbidity	Chl a	DO	BOD	Alkalinity	NO_2^-	NO_3^-	SiO_4^{4-}	PO_4^{3-}	NH_4^+
WT	1.00															
Trans	0.03	1.00														
Depth	-0.23*	0.47**	1.00													
Conductivity	0.51**	-0.10	-0.61**	1.00												
Salinity	0.50**	-0.09	-0.58**	0.99**	1.00											
pH	-0.59**	0.30**	0.06	-0.19	-0.19	1.00										
Turbidity	0.01	-0.83**	-0.33**	0.03	0.01	-0.36**	1.00									
Chl a	-0.10	-0.47**	0.02	-0.16	-0.15	-0.22*	0.53**	1.00								
DO	-0.62**	-0.04	0.21*	-0.43**	-0.42**	0.52**	0.02	0.21*	1.00							
BOD	0.75**	0.02	-0.12	0.43**	0.42**	-0.39**	-0.01	-0.04	-0.36**	1.00						
Alkalinity	-0.37**	0.40**	-0.03	0.11	0.12	0.48**	-0.46**	-0.41**	0.07	-0.31**	1.00					
NO_2^-	-0.32**	-0.23*	0.09	-0.17	-0.14	0.02	0.18	0.25*	0.29**	-0.19	-0.05	1.00				
NO_3^-	0.34**	-0.05	0.40**	-0.27**	-0.26**	-0.33**	0.06	0.06	-0.09	0.35**	-0.42**	0.17	1.00			
SiO_4^{4-}	-0.68**	-0.08	0.57**	-0.72**	-0.71**	0.30**	0.13	0.26**	0.55**	-0.41**	-0.05	0.30**	0.24*	1.00		
PO_4^{3-}	0.58**	0.22*	0.42**	-0.11	-0.10	-0.40**	-0.13	-0.01	-0.23*	0.49**	-0.38**	-0.23*	0.64**	-0.01	1.00	
NH_4^+	-0.27**	-0.36**	-0.37**	0.01	0.00	0.07	0.41**	0.10	0.20*	-0.26**	0.10	0.14	-0.30**	0.17	-0.31**	1.00

WT, water temperature; Trans, Transparency; Chl a, Chlorophyll a; DO, Dissolved oxygen; BOD; Biological oxygen demand; NO_2^-, Nitrite; NO_3^-, Nitrate; SiO_4^{4-} , Silicate; PO_4^{3-}, Phosphate; NH_4^+, Ammonia

*and ** represent significant difference at significance level of $p < 0.05$ and $p < 0.01$ respectively.

seasons. Different factors like, air temperature, solar radiation, wind speed and fresh water inflow influence the water temperature. Significant seasonal variation in WT was also recorded with highest during pre-monsoon (31.18±0.95°C) and lowest during post-monsoon (23.04±2.35°C). Lowest WT could be due to cooling effect of surface water during winter and highest WT could be due to heating of surface water due to receiving higher solar radiation during summer. A significant positive correlation of WT with nitrate ($r = 0.34$, $p < 0.01$) and phosphate ($r = 0.58$, $p < 0.01$) shows that higher nutrient solubility in warm water. A negative correlation between WT and DO ($r = -0.63$, $p < 0.01$) suggest higher solubility of oxygen in cold water (Weiss, 1970).

4.1.2 Depth

Depth is an important factor influencing the hydrodynamic process in the water column of the lagoon. Depth of the lagoon is controlled by the amount of water influx during MON and PSM and tidal flow during PRM. The one-way ANOVA revealed that depth of the lagoon varied significantly for both sectors ($p < 0.05$) and seasons ($p < 0.001$). Depth of the lagoon varied from 54 to 350 cm, 124 to 374 cm, and 56 to 257.4 cm with a mean value of 146.48, 207.12, 143.1 cm during PRM, MON, and PSM respectively. Sectoral variation of depth of the lagoon during PRM season follows the order; OC (220 cm)> SS (183 cm) > CS (134 cm) > NS (110 cm). Mean value of depth of the lagoon was 264. 14, 237.67, 191.33, and 175.38 during MON season. NS is the shallowest (130.96±39.52 cm) because of the loads of sediment deposition from the Mahanadi and its tributaries and OC is the deepest (212.44±64.62 cm) due to tidal influence. Tripathy (1995) observed highest depth of 3.5 m (CS) during 1995, which suggest that depth of the lagoon was decreasing with time due to sediment particle deposition. The lake receives silt particle from surface runoff from the catchment are nearly 3 million tonnes a year (Panigrahi *et al*., 2007). The lagoon was deepest during monsoon season

(207.12±62.82 cm) due to flow of large amount of water from river to sea through the lagoon. A significant positive correlation of depth with transparency (r= 0.47, $p< 0.01$), salinity (r= 0.58, $p< 0.01$) and DO (r= 0.21, $p< 0.01$) suggested that with increase in water depth, it reduces the photosynthesis.

4.1.3 Transparency

A sechi disk is lowered into water until it disappears from view to measure transparency. One-way ANOVA revealed that transparency of the lagoon varied significantly for both sector and seasons ($p < 0.001$). Transparency of the lake varied from 7 to 115 cm, 7 to 208 cm, and 6 to 133.12 cm during PRM, MON, and PSM season respectively. Sectoral mean value of transparency during PRM season was observed to be 58.29 cm, 15 cm, 55.07 cm, and 18.63 cm for SS, OC, CS, and NS respectively. This mean value was changed to 160 cm, 7 cm, 111.4 cm and 40 cm during MON season and 98.89cm, 40.67cm, 69.15cm, and 26. 38 cm during PSM season. NS showed lowest transparency (28.33±26.26 cm) owing to deposition of silt enriched runoff from the river and mixing of bottom sediment during all three seasons (Ganguly *et al*., 2015). Additionally, presence of suspended solid received from rivers and its tributaries makes penetration of light difficult. Significantly higher transparency was recorded in the SS (105.87±50.74 cm) as this sector was most undisturbed sector. Transparency of the lagoon was lowest during pre-monsoon season (43.27±28.6 cm) and highest during monsoon season (95.06±67.77 cm), as it receives fresh water inflow from the river during monsoon. Prevalence of wind force during summer makes the lagoon restless causing resuspension of bottom sediment causing lower transparency (Ramanadhan *et al.,* 1964). Negative and significant correlation between transparency and nitrite (r = -0.23, $p< 0.05$) and ammonia (r = -0.36, $p<0.01$) suggest their accumulation in water column due to suppression of nitrification in water with low transparency (Nixon, 1988).

4.1.4 Turbidity

Amount of suspended solid present in the lagoon controls the light penetration and turbidity of the lagoon. Thus, turbidity along with nutrient affect the growth of phytoplankton and its distribution. Along with suspended solid, tidal influx, wind force and freshwater influx controls the turbidity of the lagoon. Turbidity of the lake varied from 3.09-574, 0.66-183, and 2.06-329 NTU in the PRM, MON, and PSM season respectively. One-way ANOVA revealed significant variation of turbidity in the lake for sector ($p< 0.001$) and season ($p<0.05$). PRM season experienced highest turbidity with a mean value of 66 NTU followed by PSM (46.3NTU) and MON (27NTU). Resuspension of the bottom sediment and churning of water current due to strong southerly wind force makes the lake turbid during PRM season. Additionally, dredging and fishing boats also helps in resuspension of bottom sediment and increasing turbidity. NS experience highest turbidity during PRM (174NTU) and PSM (146.88NTU) season, whereas OC experience highest turbidity during MON (79.6NTU). NS receives silt particles and runoff from the rivers and its tributaries making this region of the lake turbid as compared to other sectors of the lake. Turbidity of the SS and CS are comparatively lower during all the season.

4.1.5 Salinity

Disparity of tributary discharge and sea water inundation from the sea mouth was the driving factor for spatiotemporal variation of salinity in the lagoon (Barik *et al*., 2017). Variation in salinity could act as proxy for studying the biodiversity of lagoon (Mrozińska *et al*., 2021). One-way ANOVA revealed that variation in salinity was significant for both the sectors and seasons ($p< 0.001$). Salinity of the lagoon varied from0.27- 35.2, 0.12- 6.55, and 0.062-24.32 PSU with a mean value of 13.48, 2.42, 5.5 PSU during PRM, MON, and PSM respectively. Sectoral variation of salinity was also observed, with highest salinity observed in

OC (28.61PSU) followed by CS (15.85PSU), SS (11.86PSU), and NS (4.76PSU) during PRM season. However, the salinity trend was somewhat reversed during MON season with highest salinity observed in SS (5.69PSU) followed by CS (2.47PSU), OC (0.52PSU) > NS (0.15PSU). During PSM season, highest salinity was observed in SS (15.5PSU) followed by OC (14.09PSU), CS (4.95PSU), and NS (0.38PSU). From the average value of three season, the lowest salinity was observed in NS (8.86±2.65PSU) and highest salinity was observed in OC (14.41±13.44PSU). Severe dilution, because of massive influx of fresh water from the Mahanadi River and its tributaries and western catchment (6,912 million cubic meters, nearly 78% of fresh water influx) (Srichandan *et al*., 2015) could be the reason for lowest salinity observed in NS and sea water intrusion and tidal influence could be the reason for highest salinity in the OC. Lagoon experiences highest salinity during pre-monsoon season (13.48±7.99PSU) and lowest salinity during monsoon season (2.42±2.37PSU). Inflow of freshwater to the lagoon is limited during summer season, which could be the reason behind highest salinity during PRM (Panigrahi, 2006). Earlier studies also recorded similar spatiotemporal variation in salinity in the lagoon (Panigrahi, 2007). Many other lakes from India and around the world exhibit similar fluctuation in salinity due to seasonal hydrology. Rochelle-Newall *et al*. (2011) reported heavy freshwater discharge during monsoon season decreased the salinity of Bach Dang estuary (Vietnam) to as low as 0.1 PSU. Negative correlation between salinity and nutrient contents (silicate, nitrate, phosphate) indicates that lower salinity regions of the lagoon like NS have higher nutrient concentration. Freshwater inflow from nearby catchment area could be the potential reason behind higher nutrient recorded in the NS region.

4.1.6 Dissolved Oxygen (DO)

Photosynthetic activities and respiratory activities of phytoplankton and macrophyte act as source and sink for DO respectively. Among the other physio-chemical variables, salinity

and water temperature control the level of DO in the lake. Therefore, there is significant variation in DO from season to season and place to place. DO of the lagoon varied from 4.14-9.53, 5.2-11.34, and 6.2-11.59 ppm for PRM, MON, and PSM respectively. Lagoon experience highest DO value for NS (11.62ppm) during PSM followed by CS (10.45ppm) whereas OC experience highest DO value during PRM (8.08ppm) and MON season (8.99ppm). Spatial variation in the DO was non-significant among the sectors. However, there was significant seasonal variation in DO ($p< 0.001$), with the lagoon recording highest DO during post-monsoon season (10.35±1.95ppm) and lowest during pre-monsoon season (7.18±1.45 ppm). Lowest DO during PRM may be due to consumption of oxygen for organic matter decomposition generated by macrophytes (Panigrahi *et al*., 2006). Highest DO during PSM could be due to influx of fresh water from tributary discharge and prevalence of higher photosynthetic activities by plankton communities (Nayak *et al*., 2004). DO values of the lagoon is primarily depended on extent of photosynthesis, respiration, and decomposition. Growth of macrophyte was maximum during PSM and started to decompose during summer with increasing salinity (Pal and Mohanty, 2002). According to Central Pollution Control Board, DO values of 4 to 6 mg/l indicates healthy ecosystem in the lagoon (CPCB, 2020). Higher DO value in our study suggests good aquatic life in the lagoon. Similar observation was made from the study of Shah and Joshi (2017) in Sabarmati River with mean DO values of lake 8 m/l. DO have a positive correlation with pH ($r = 0.52$, $p< 0.01$), silicate ($r = 0.55$, $p< 0.01$), ammonia ($r = 0.20$, $p< 0.05$) and a negative correlation with phosphate ($r= -0.23$, $p< 0.05$).

4.1.7 Biological oxygen demand (BOD)

Mean value of BOD was highest for PSM (2.99 ppm) followed by MON (2.64ppm), and PRM (2.56ppm). BOD of the lagoon varied from 0.23-5.11, 0.65-5.46, and 0.78-11.4 ppm for PRM, MON, and PSM season. NS experience highest mean BOD value during MON (2.78) and PSM (3.19) season followed by CS. One-way ANOVA revealed that the variation in BOD

was not significant between sectors, however there was significant seasonal variation in BOD ($p< 0.001$). As the influx from Mahanadi and its tributaries decreases and salinity increases BOD of the lagoon increased due to decomposition of macrophytes during PSM and PRM season (Panda *et al*., 2015). Positive correlation of BOD with nitrate (r= 0.35, $p< 0.01$) and phosphate (r = 49, $p< 0.01$) showed the non-point source of pollution. Major factor which contributes to non-point source of pollution were soil erosion, sewage from the nearby settlement and industries, agricultural runoff etc (Barik *et al*., 2019).

4.1.8 pH

pH controls the nutrient availability in the lake ecosystem. Generally, CO_2 assimilation by phytoplankton and macrophytes, mixing of sea water with freshwater, decomposition of organic matter controls the pH of the lagoon. Slight variation in the pH of the lagoon was observed with a range of 6.94-8.85 (7.99±0.36), 6.59-8.69 (7.97±0.49), and 8.04-9.66 (8.61±0.4) during PRM, MON, and PSM respectively. One-way ANOVA revealed seasonal variation of pH in the lagoon ($p< 0.001$). Higher photosynthesis and productivity during PSM may be the reason behind highest pH being observed during this period, whereas release of more CO_2 could be the reason behind lower pH observed during PRM and MON as compared to PSM. One-way ANOVA revealed that pH varied for sectors in the MON season with highest pH being recorded in CS (8.36±0.42) and lowest pH recorded in NS (7.91±0.68). Comparisons of the mean value of sectoral pH reveals that NS experience lowest pH (7.72) and SS experience highest pH value (8.14) with an intermediate pH observed in OC (7.91) and CS (8.08) during PRM season, however the difference was non-significant. The Central Pollution Control Board under Government of India mandates a pH value of 6.5-8.5 for coastal waterbodies. The pH value of the lagoon Chilika, falls in to the category. Alkaline environment of the lagoon makes it conducive for growth of aquatic organisms.

4.1.9 Alkalinity

Alkalinity is the acid neutralizing capacity or buffering capacity of the water. Bicarbonate, carbonate, and hydroxide impart to the alkalinity of water. pH of the natural water is between 6 to 8.5, a region where equilibrium between carbonate and bicarbonate is in the favour of bicarbonate. pH of the lake water in our study has a mean value of 8-8.5, suggesting, alkalinity in our lake water is approximately equal to bicarbonate concentration. Alkalinity of the lake water varied between 90-170 (125.27±20.4 meq L^{-1}), 75-158 (115.7±22.81meq L^{-1}), 95-194 (138.52±20.08meq L^{-1}) during PRM, MON, and PSM season respectively. One-way ANOVA revealed that mean alkalinity of SS (142.57±12.52meq L^{-1}) was highest followed by CS (131.93±21.59meq L^{-1}), OC (115±20.34meq L^{-1}), NS (106.54±17.55meq L^{-1}). High alkalinity in the lake water across the lake supported fact that there was less variation in seasonal and sectoral pH.

4.1.10 Nitrite

Nutrients are the important parameter influencing the productivity, metabolic activities of living organisms in the lagoon. The spatial and seasonal distribution of nutrients in the lagoon plays a major role in defining the ecosystem of the lagoon. Nutrient loading from the catchment basin threatens the lagoon health. Nutrient distribution was affected by the seasons, sea water influence, wind, fresh water inflow from river and runoff from the catchment. Nitrite is an intermediate product of nitrification, which can accumulate in the water column as a result of ammonia oxidation or nitrate reduction or released from the plankton communities as extracellular product (Santschi *et al*., 1990). Nitrite content varied from 0.01-2.37, 0.03-1.71, and 0.04-5.01µmol/l with a mean value of 0.42, 0.33, and 0.7 µmol/l for PRM, MON, and PSM respectively. One-way ANOVA revealed that nitrite concentration in the lagoon varied significantly for both, sector ($p< 0.05$), and seasons ($p< 0.01$). Highest nitrite content was

reported in the OC (0.84µmol/l) followed by the NS (0.81µmol/l), CS (0.28µmol/l), and SS (0.12µmol/l) for PRM season. Nitrite content of the sector followed similar trend during MON and PSM season also. Lowest concentration of nitrite was observed in SS (0.33±0.27µmol/l) as this sector is least influenced by mixing of lagoon water with riverine flow though it receives fresh water inflow from Rushikulya river through Palur canal. NS which receives high amount of fresh water inflow from rivers and agricultural drainage canals have higher nitrite concentration (0.69±1.08µm/l) as compared to SS and CS. Higher amount of nitrite concentration in OC could be due to exchange of lagoon water with sea through the mouth opening.

4.1.11 Nitrate

Nitrate content of the lake varied from 1.9-17.5, 0.17-17.21, and 0.71-21.9 µmol/l with a mean value of 5.12, 4.93, and 5.6µmol/l for PRM, MON, and PSM season. One-way ANOVA revealed that nitrate concentration varied significantly for both sector ($p< 0.001$) and season ($p< 0.001$). Nitrate concentration was highest for NS (11.34µmol/l) during PSM followed by CS (4.41µmol/l), whereas OC (12.36µmol/l) accounts for highest nitrate concentration during MON followed by NS (4.77µmol/l). Assimilation of nitrate by the plankton communities, runoff water from riverine inflow and dilution with sea water were major factor for spatiotemporal variation of nitrate in lagoon. SS, which has sea water influence has maintained lowest nitrate concentration (2.95±1.5µmol/l) in the lagoon. NS maintained the highest concentration (8.18±5.69µmol/l) in the lagoon as it received high nutrient from the riverine inflow carrying inland flow, and agricultural runoff carrying nutrients from the field. Fertilizer and domestic water were the main contributing source of nitrate in the runoff to lagoon (Craswell, 2021). Furthermore, significant negative correlation between salinity and nitrate concentration confirms freshwater influx as source of nitrate in the lagoon. Similar observation was reported by Baek et al. (2009). PRM and PSM have significantly higher nitrate

concentration due to high mineralization rate during this period as compared to monsoon season (Muduli *et al*., 2013; Gupta *et al*., 2008).

4.1.12 Ammonia

Ammonia content of the lagoon varied from 1.21-4.56, 0.58-5.24, and 1.48-7.81µmol/l with a mean value of 2.17, 1.65, and 2.5µmol/l for PRM, MON, and PSM seasons respectively. Highest ammonia content was recorded in CS (23.03µmol/l) during PSM followed by NS (3.73µmol/l). One-way ANOVA revealed significant variation in ammonia concentration among seasons ($p < 0.001$), while the variation among sector was significant only for PSM ($p < 0.001$). Highest ammonia concentration was observed during PSM and in the NS.

4.1.13 Phosphate

Phosphate is the most important nutrient for growth and metabolism of living organisms like algae, plankton communities and macrophyte in the lagoon. Phosphate content of the lagoon varied from 0.18-0.43, 0.03-0.13, and 0.02-0.74µmol/l with a mean value of 0.2, 0.1, 0.2 µmol/l for PRM, MON, PSM respectively. There is significant seasonal variation of phosphate content in the lagoon ($p<0.001$). There is little sectoral variation in phosphate content in all the three seasons. One-way ANOVA revealed that phosphate concentration varied among the sectors only during MON significantly ($p<0.001$). NS experienced highest concentration of phosphate due to high fresh water inflow from river which carries nutrient from the catchment area and agricultural field. In addition, desorption of phosphate from the sediment due to wind churning and redox reaction would enrich water with phosphate during monsoon season (Parsons *et al*., 2017). Lowest concentration of phosphate in SS and OC could be due to low discharge of fresh water into these sector and consumption of phosphate by plankton and macrophyte communities. A significant positive correlation of phosphate with BOD ($r= 0.49$, $p< 0.01$) and negative correlation with pH ($r = -0.40$, $p< 0.01$) suggest that

decomposition of organic compound which release phosphate to the ecosystem increases the oxygen demands and reduced pH of the lagoon (Panigrahi *et al*., 2006).

4.1.14 Silicate

Silicate content of the lagoon varied from 26.11-229.58, 29.09-139.60, and 50.31-222.94 µmol/l with a mean value of 81.24, 85.29, and 129.1µmol/l for PRM, MON, and PSM season. One-way revealed seasonal variation for silicate content ($p < 0.001$). NS has highest silicate content with a mean value of 168.24 µmol/l for PSM and 111.30 µmol/l for PRM, and 107.12µmol/l for MON. lowest silicate content was observed in SS with a mean value of 71.57µmol/l in PRM, which changed to 47.44 and 104.45 during MON and PSM respectively. One-way ANOVA revealed that silicate content varied significantly for sector ($p < 0.05$) with NS showing highest silicate content and SS having lowest silicate content. Highest silicate content could be due to runoff water received by the NS which carries loads of weathered silica material which discharge into the NS of the lagoon. Lowest silicate content in SS could be due to result of consumption by the diatoms for their biological activity and adsorption into sediment particles. In addition to this, coprecipitation of silicate with humic compounds and Fe also reduced its content (Rajasegar, 2003). PSM have higher silicate content than PRM and monsoon season. Significant negative correlation of silicate with salinity confirms the source of silicate as freshwater discharge from river.

4.1.15 Chlorophyll a (Chl a)

Chl-a content of the lagoon varied from 0.01-3.77, 0.07-1.73, and 0.04-6.78 µg/lfor PRM, MON, and PSM season. PRM (0.73µg/l) season experience highest chl-a content followed by PSM (0.7µg/l) and MON (0.42µg/l) season. However, the seasonal variation in Chl- a content was non-significant. NS recorded highest chl-a content for all the three seasons (PRM-1.55µg/l, MON- 0.94µg/l, PSM- 0.8µg/l 7) followed by OC, CS, and SS. Chl-a content

is an index of algal growth in the lagoon. One-way ANOVA revealed significant sectoral variation in Chl-a. The chl-a content of the lagoon followed the order; NS (1.12±0.97µg/l) > CS (0.57±1.1µg/l) > OC (0.5±0.32µg/l) > SS (0.17±0.13µg/l). Highest chl-a content in NS could be the reason behind high algae growth in this sector. As phytoplankton growth is governed by nutrient supply from the river and its tributaries, NS receiving high freshwater influx have higher nutrient concentration, which could be the possible explanation for higher Chl-a content. Significant negative correlation between chl-a and transparency ($r = -0.47$, $p < 0.01$) confirms the role of algae in the phytoplankton biomass of the lagoon. Though correlation between phosphate content and chl-a content was not significant, a significant correlation is established between (NO_2^-, NO_3^-, NH_4^+/ PO_4^{3-}) and chl-a suggesting role of nitrogen and phosphate in algal bloom in the lake.

4.2 Trophic state index (TSI)

The complex nature of Chilika lagoon ecosystem is partly due to strong influence of many sources of pollution (agricultural runoff, catchment area inflow, industrialization, domestic sewage etc.). The spatial and temporal changes of water quality parameters of lagoon were the result of seasonal changes in light, temperature, salinity, and nutrient load which discharge into the lagoon from the river. The variation in salinity and nutrient load explains the ecosystem health of the lagoon. In addition to this, evaluation of trophic state index (TSI) is fundamental to study the overall ecosystem health (Carlson, 1977). TN, TP, Chl-a and sechi depth was used in this study to evaluate TSI. It was found that the lake is still in oligotrophic and mesotrophic state (Fig. 4.2). However, the value of TSI, which is close to 50 indicates that the lake was on the verge of eutrophication.

Water quality index

Water quality index may be used to assess the overall quality of water in a single term. It assists in identifying potential risks to diverse water uses and developing mitigating strategies to deal with problematic issues. Water quality varied greatly during the pre-monsoon and post-monsoon seasons because to the distinct differences in salinity and fresh water intake from the rivers, rivulets, and drainage basins of the catchment region. WQI has been assessed for PRM,

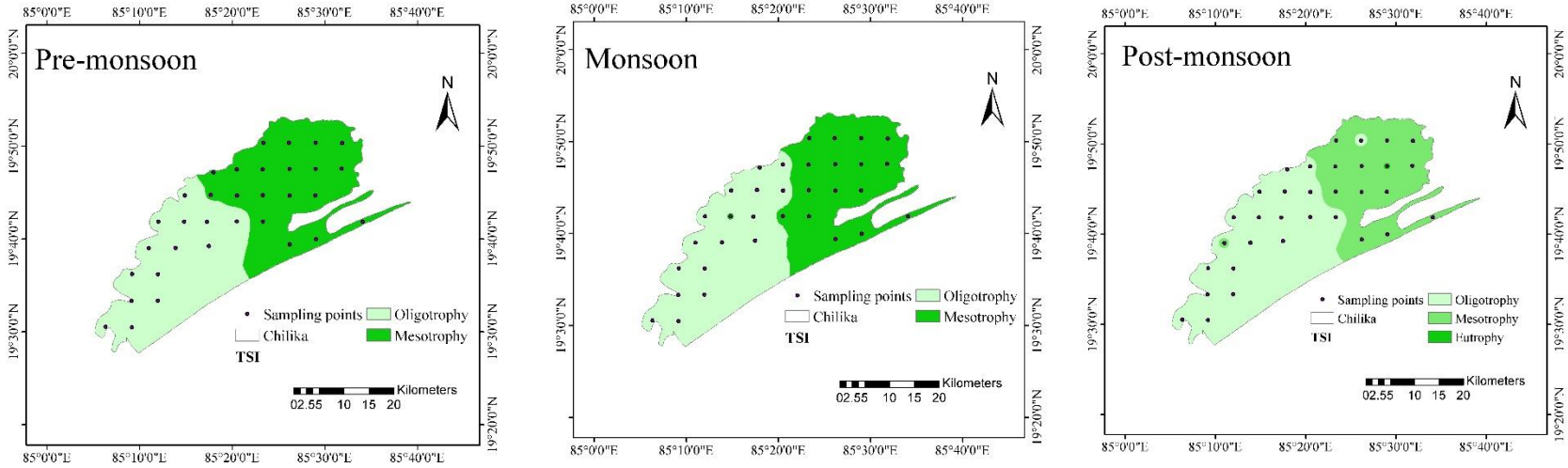

Fig.4.2 Seasonal variation in trophic state index (TSI) of Chilika lake

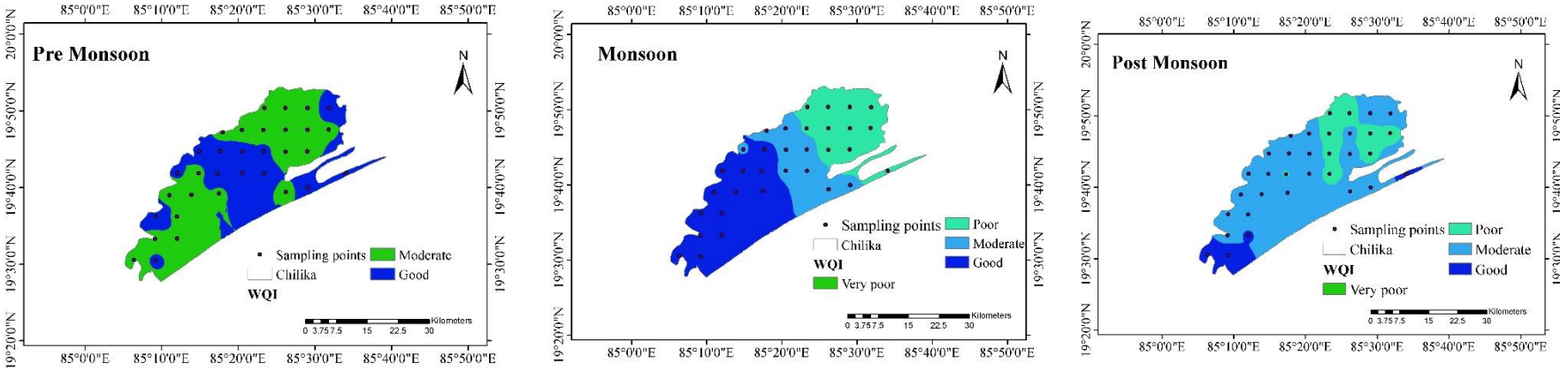

Fig.4.3 Seasonal variation in water quality index (WQI) of Chilika lake

MON, and PSM season and spatial variation in WQI is presented in Fig. 4.3. The WQI of the lake was classified into four categories based on value of WQI; very poor (<25), poor (25-50), moderate (50-75), and good (> 75). The Fig. 4.3 reveals that the water quality of lake was moderate to good during PRM season, which changes to poor-good during MON and PSM season. According to value of WQI, SS falls into good water quality category, while CS falls into moderate and NS falls into poor water quality category. Generally, dilution of lake water due to freshwater inflow carrying nutrient loads during MON season makes the water quality of lake poor. Low WQI value of NS could be due to low transparency, salinity and high Chl a content and high WQI value of SS could be due to better transparency and good salinity value and low a Chl-a content.

4.3 Principal component analysis

The water quality data set was used to run PCA for parameter reduction and differentiate source of variation. While retaining the maximum information in the data set, PCA reduces the dimensions of the dataset. Varimax rotation was used as it eliminates the variable with lower contribution to PCA variables and increase the more significant relationships. Three components with Eigen value more than 1 were extracted from PCA explaining 68.70% of the variability in the data set (Table 6). The variables were classified as strong, moderate, and weak based on their loading values of >0.75, 0.75-0.5 and < 0.5 respectively. PC1 accounted for 28.84% of the variability with strong negative loadings for salinity, and moderate negative loading for WT. This suggest that salinity was the major factor controlling variation in water quality of the lagoon. PC1 also have strong loading for silicate, moderate loading for depth and DO suggesting higher silicate content in the lower salinity area. PC 2 accounts for 20.51% variability with strong loadings for phosphate and nitrate, and moderate negative loadings for pH and positive loading for BOD. This suggest that phosphate and nitrate were the major nutrients controlling the growth of plankton communities and macrophyte in the lagoon.

Table 4.6 Principal component matrix of water quality variables of Chilika Lagoon

		Component	
Parameters	1	2	3
Water Temp	**-0.664**	0.685	-0.047
Transparency	0.109	0.053	**-0.904**
Depth	**0.715**	0.388	-0.377
Conductivity	**-0.917**	-0.093	0.004
Salinity	**-0.900**	-0.089	-0.007
pH	0.328	**-0.626**	-0.378
Turbidity	-0.046	0.030	**0.914**
Chl a	0.225	0.117	**0.670**
DO	**0.613**	-0.378	0.112
BOD	-0.492	**0.620**	-0.035
Alkalinity	-0.048	-0.619	-0.537
Nitrite	0.322	-0.133	0.351
Nitrate	0.290	**0.776**	0.060
Silicate	**0.880**	-0.074	0.166
Phosphate	0.059	**0.854**	-0.183
Ammonia	-0.008	-0.473	0.467
Eigen values	4.61	3.28	3.09
Total Variance	28.84	20.51	19.36
Cumulative Variance	28.84	49.35	68.70

DO, Dissolved oxygen; BOD, Biological oxygen demand; Chl a, Chlorophyll a.

Negative loading for BOD suggests high oxygen demand for decomposition of organic matter due to high macrophyte infestation in the lagoon. PC 3 accounts for 19.36% variability with strong positive loading for turbidity and strong negative loading for transparency and moderate loading for Chl-a. Chl-a is an important parameter which determines the water quality of lagoon influence the light penetration of water and growth of phytoplankton.

4.4 Cluster analysis

Cluster analysis was used to classify the lagoon and two major cluster (C1 and C2) based on similarity among the stations and dissimilarity with other station was found (Fig 4.4). C1 includes station number 22, 23, 24, 25, 26, 31, 32, 33 which falls geographically in the NS and station number 21, 27, 30 which falls in the CS. The station under C1 falls in the north west and north region of the lagoon geographically where all the major river and tributaries meet the lagoon. C1 indicated that most of the stations exhibiting impact of agricultural runoff from the catchment area with high loads of silt particle and nutrient through the tributaries. C2 includes rest of the stations which have characteristically different water quality from C1. Station number 15, 17, 18, 20, and 28 forms minor cluster under C2 which were situated close to a small populated town Balugaon. Along with human settlement, this region receives urban sewage, industrial waste and waste water from agro-based industries and prawn processing unit. This greatly affects the water quality of the station falling under this cluster. Station number 10,11, and 12 forms a minor cluster under C2 which falls in the outer channel and have influence of tidal flow and sea water exchange which governs the water quality of that region. Station number 1, 4, 5, 6, 7, 8, 13, 16, 19 forms another minor cluster under C2, wherein, majority of the stations lie under southern sector which receives little runoff from the Rushikulya river through Palur canal. The SS having some influence of tidal flow and no mixing of water with bottom sediment makes the water undisturbed and clear compared to other region of the lagoon. We observed a clear water quality gradient from east to west and

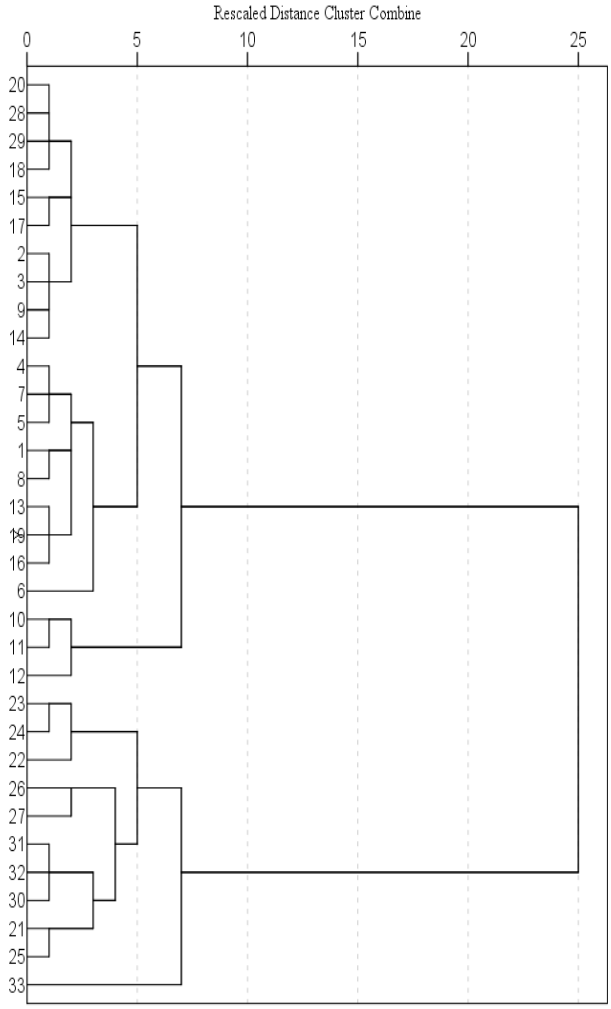

Fig. 4.4 Dendrogram of water quality variables showing cluster station wise.

north to south of the lagoon due to variation in supply of freshwater inflow, agricultural runoff, tidal exchange. Clustering of the stations reveal that nutrient input form the catchment area and fresh water inflow from the tributaries mainly governs the spatial difference in the water quality.

4.5 Catchment area delineation and land use and land cover map

The catchment area of lake Chilika was delineated using the method discussed in the material and method section. The land us land cover map of catchment area is presented in Fig. 4.5. The detailed land use type of catchment area is given in the Table 4.7. The catchment area of the lake was dominated by agricultural field accounting for approximately 57.49% of the total catchment area. the northern part of the catchment of the lake was especially dominated by agricultural land which comes under Mahanadi delta. Waterbodies was the second most dominant land use type in the catchment area constituting 24.95% of the catchment area. The waterbodies involve the lake Chilika and 14 major River around the lake. Daya, Bhargavi, Makara, and Luna are the major River draining the northern catchment of the lake. Forest land constitutes 13.82 % of the catchment area which is dominated in the western and southwestern part of the lake. wasteland and built-up land constitute 1.34 % and 2.68% of the catchment area.

4.6 External nutrient loading

The Chilika lake has a catchment area of approximately 4000 km^2, of which 68% of this is constituted bythe western catchment and 32% by the Mahanadi Delta inthe northeast. the north and north east watersheds, which drain to the Mahanadi and its tributaries Daya, Bhargavi, and Nuna, account for 55% of the water inflow. The south watershed is made up of the streams that enter Rushikulya. The Chilika lake receives 200 to 400 T (tonnes) of soil from Mahanadi riverbed (Mishra and Jena *et al*., 2015). Majority of sediment influx in the lake is from land

Table 4.7 Percentage coverage of different land use type in catchment area of lake Chilika

Land use type	Percentage coverage
Forest	13.82
Cropland	57.49
Built-up land	2.68
Wasteland	1.34
Waterbodies	24.95

Table 4.8 External nutrient loading (moles per day) of nutrient to lake through different river

	Silicate	Phosphate	Ammonia	Nitrate	Nitrite
Bhargavi	311635.1	741.7337	43060.65	43060.65	2733.055
Luna	94420.19	390.8376	20222.76	20222.76	3262.465
Daya	113594.4	556.0289	20436.02	20436.02	6919.036
Makara	602595.2	9166.878	46118.95	46118.95	31667.4
Mangalajodi	15792.97	56.5183	1773.992	1773.992	193.429
Tarimi	29462.87	55.48783	2162.857	2162.857	297.2979
Kantabania	152604.3	460.2305	8024.905	8024.905	1817.619
Kusumi	41626.09	81.37736	1183.884	1183.884	539.9075
Kansari	78281.82	1033.189	1249.152	1249.152	635.6195
Badanai	11678.66	27.68256	356.7974	356.7974	122.4184
Langaleswar	71981.56	391.1091	4457.144	4457.144	1170.828
Palur	72476.87	232.3279	4483.3	4483.3	808.4382
Janjira	94876.83	168.0169	3218.676	3218.676	965.2735
Malaguni	383459.7	720.4575	10255.02	10255.02	3311.039

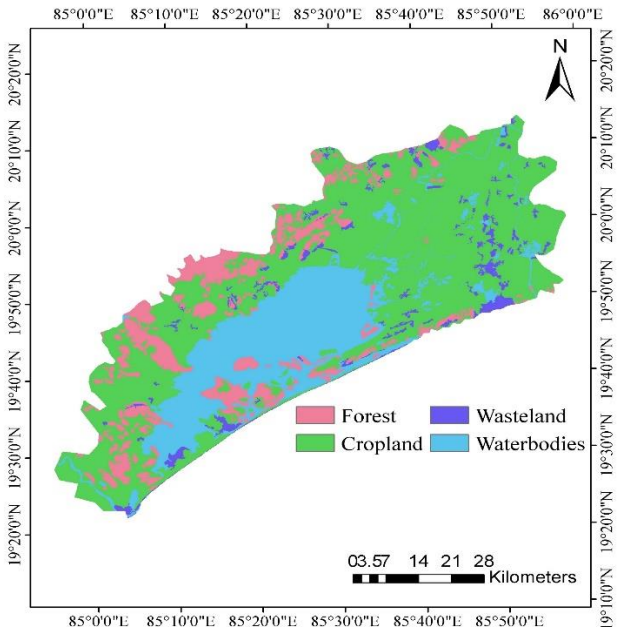

Fig. 4.5 Land use land cover map of catchment area of lake Chilika

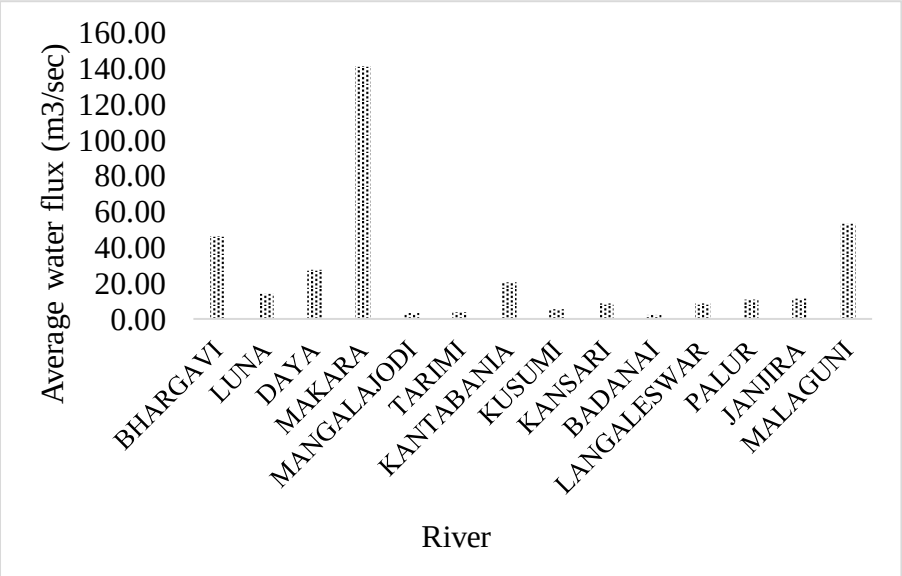

Fig 4.6 Average water flux to the Chilika lake through different river

degradation in the catchment area. Agricultural land and deforested land were major source of sediment deposition in the lake. Further, the distributaries of Mahanadi deposits 1.5 million tonnes of silt particle in the Lake (Sahu *et al*., 2014). The lake also receives 550 million tonnes of untreated sewage water from the nearby town of Bhubaneswar along with huge amount of domestic water from the 141 villages in and around the lagoon (Sahu *et al*., 2014). The Lake receives average 5090 million cubic meters total fresh water influx annually. The freshwater influx from the river carries loads of nutrient with it. Some of the major nutrient deposited in the lake and influencing its water quality are; silicate, ammonia, nitrite, nitrate, nitrate, and phosphate. Nitrogen and phosphorus are the limiting nutrient in the lake influencing trophic status of the lake. Therefore, estimation of nutrient loading especially nitrogen and phosphorus help to get a better insight into lake nutrient stoichiometry. Nutrient loading from the 14 major river streams were estimated and presented in the Table 4.8. Daily water flow rate and water depth were recorded and nutrient concentration in the water samples were analysed to calculate the water flux and nutrient flux in the lake. Average water flux of trough different River were presented in the Fig 4.6. Average water flux was highest for Makara River (141.15 m^3s^{-1}) followed by Malaguni River (53.23 m^3s^{-1}) and Bhargavi river (46.40 m^3s^{-1}). Nutrient concentration of water varied from river to river. The average nutrient concentration of the river water is presented in the Fig 4.7. Highest Silicate concentration was observed in the water samples of Kansari River (106.33μml^{-1}) followed by Langaleswar river (96.01μml^{-1}). External silicate loading to lake was highest through the Makara River (602595 moles day^{-1}) followed by Malaguni river (383460 moles day^{-1}). Total average loading of silicate is estimated to be 2074486 moles day^{-1}. Phosphate concentration was highest in the water samples of Kanasari River (1.40μml^{-1}) followed by Makara River (0.75μml^{-1}). External phosphate loading was highest through Makara River (9167moles day^{-1}). Water samples from Luna and Daya river

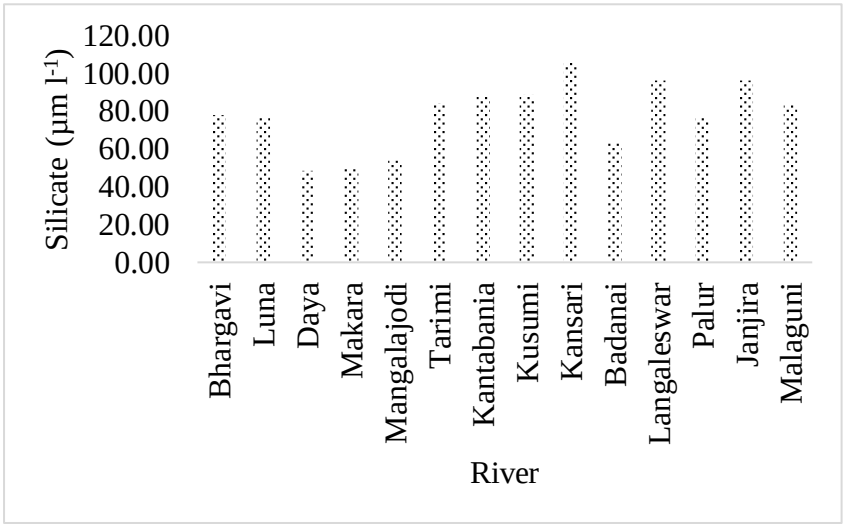

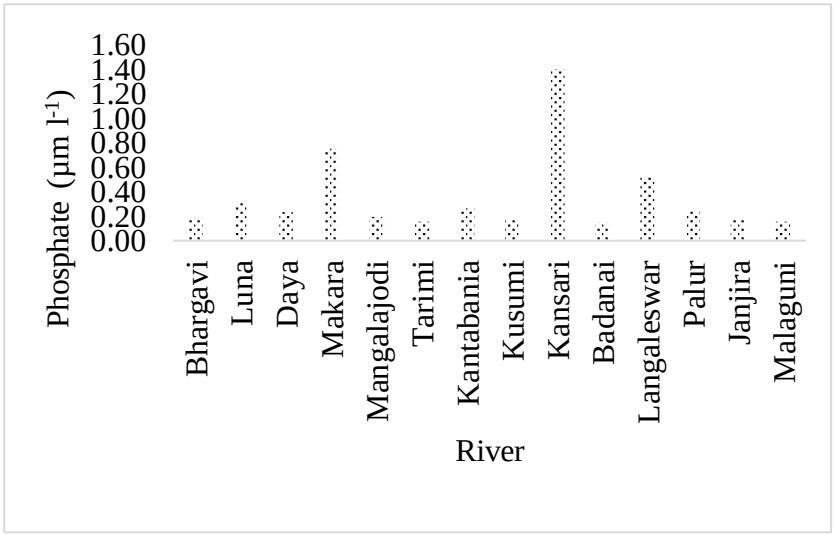

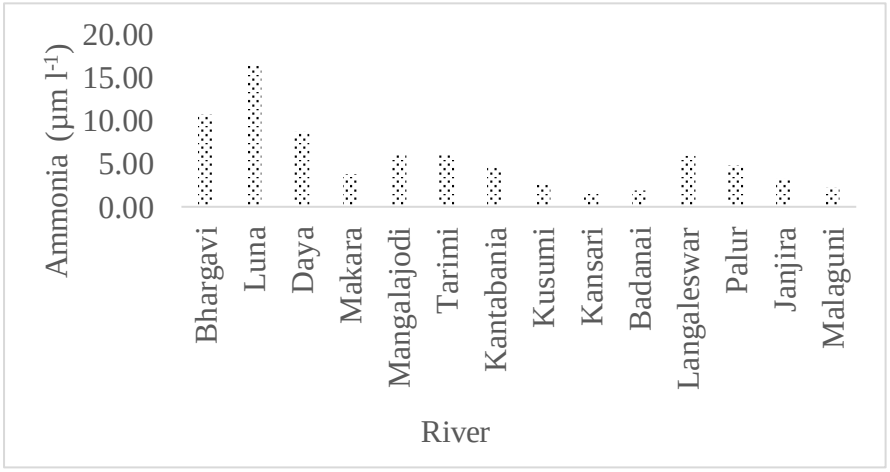

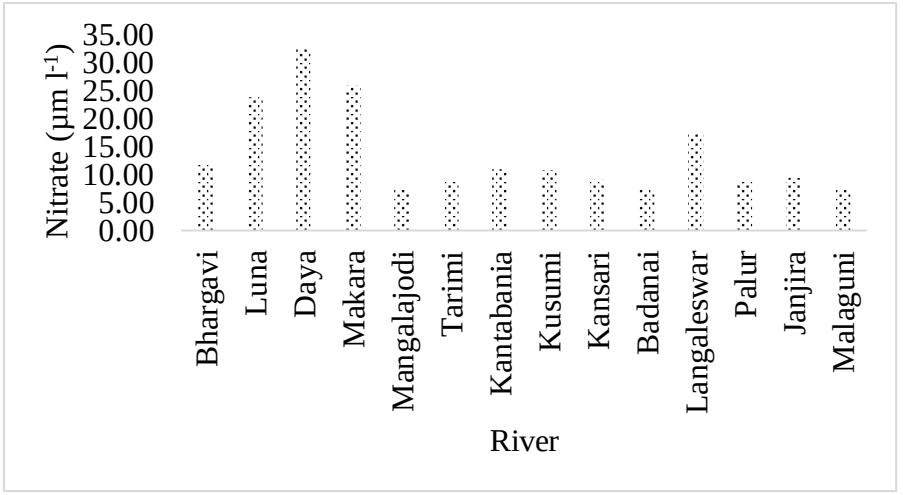

Fig 4.7 Average nutrient concentration in water samples of river

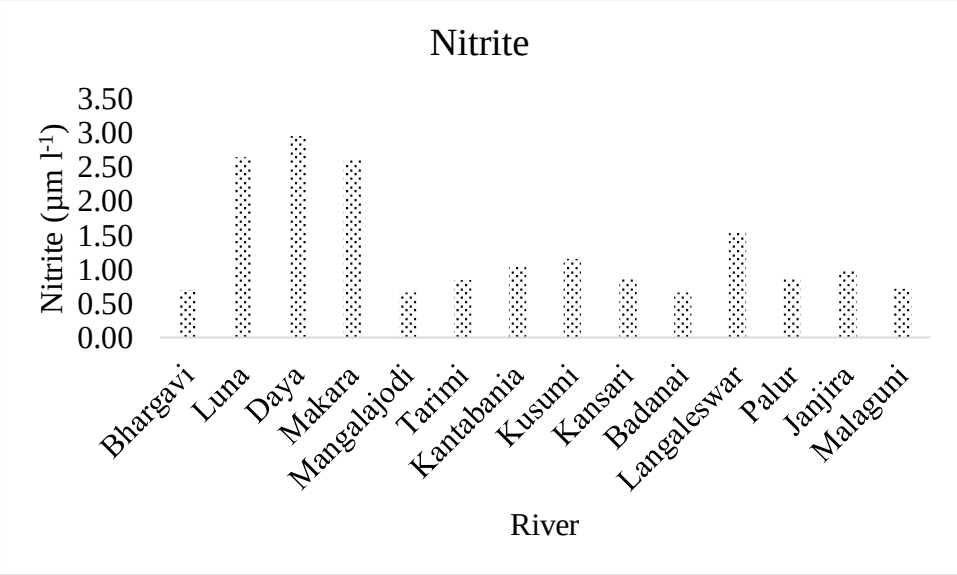
Nitrite
Nitrite (µm l-1)
3.50
3.00
2.50
2.00
1.50
1.00
0.50
0.00
Bhargavi
Luna
Daya
Makara
Mangalajodi
Tarimi
Kantabania
Kusumi
Kansari
Badanai
Langaleswar
Palur
Janjira
Malaguni
River

record highest nitrate and nitrite concentration, with Luna River depositing highest nitrate and nitrite loads in the lake.

4.7 Soil P fraction under different land use

Soil P fractions under soils of different land use types at the sampling sites are presented in the Table 4.9. The result of ANOVA analysis shows that that the site, land use type has significant effect on forms of P ($p < 0.05$). The concentration of L-P varied from 0.85 to 7.77 mg kg^{-1} in different land use types. The agriculture site at sampling point 8 had a significantly higher L-P than sampling point of other land use with an exception of sampling point 10. Mean value of L-P was highest for forest land soil followed by agricultural field soil. The concentration of Al & Fe-P varied from 9.85 to 408.97 mg kg^{-1}, with average of 109.32 mg kg^{-1}. The ANOVA results shows that there is significant spatial variation in content of Al & Fe-P among the sampling points. Out of different land use type, samples from agricultural sites have significantly ($p< 0.05$) higher Al & Fe-P (408.97 mg kg^{-1}). Agriculture site from sampling point 1 has highest Al & Fe-P content than other agricultural sites. The soil from forest site 1 has reported 227.89 mg kg^{-1} of Al & Fe-P. The mean concentration of Al & Fe-P follows the order agricultural site (101.32 mg kg^{-1}) > fallow site (91.86 mg kg^{-1}) > forest site (61.59 mg kg^{-1}). Mean Ca-P content of soil of different land use type follows the order settlement (670. 45 mg kg^{-1}) > agricultural site (31.92 mg kg^{-1}) > forest site (29.58 mg kg^{-1}) > fallow site (18.93 mg kg^{-1}). Mean R-P was highest for forest land soil (208.33 mg kg^{-1}) followed by forest soil, fallow soil, and agricultural soil (Table 4. 9). Application of organic fertilizer might be the explanation for higher R-P in the agricultural sites. Higher R-P in the forest sites could be attributed to high organic carbon content of forest soil.

The results shows that the land use type clearly influenced forms and distribution of P in the catchment area. This could be attributed to difference in anthropogenic activities around the sampling sites and the different biotic and abiotic processes affecting the forms of P. Soils of

Table 4.9 P fractions in the soils of lake catchment area and river sediment

Land use type		L-P ($mgkg^{-1}$)	Al & Fe-P($mgkg^{-1}$)	Ca-P($mgkg^{-1}$)	R-P($mgkg^{-1}$)	TP ($mgkg^{-1}$)
Agricultural soil (n=14)	Min	0.00	9.85	2.16	17.33	30.49
	Max	7.77	408.97	98.90	413.99	895.97
	Mean	0.96	101.32	31.92	201.68	319.06
Forest soil (n =2)	Min	0.00	87.46	13.56	236.39	404.46
	Max	5.44	97.31	75.18	388.61	499.49
	Mean	1.81	61.59	29.58	208.33	301.32
Fallow land soil (n =7)	Min	0.00	27.10	0.92	24.13	51.23
	Max	2.29	227.89	73.95	428.84	634.42
	Mean	0.45	91.86	22.08	199.08	310.32
River sediment	Min	0.54	40.29	12.71	135.32	192.12
	Max	1.20	316.14	134.52	434.60	838.69
	Mean	0.84	128.52	48.12	279.79	457.27

L-P, Loosely bound P; Al & Fe-P, Aluminum and iron bound P; Ca-P, Calcium bound P; R-P, Residual P; TP, Total P; n, Number of samples.

Table 4.10. Relative percentage (%) contribution of P fractions in catchment area sol and river sediment

Land use		L-P	Al & Fe-P	Ca-P	R-P
		% Contribution			
Catchment	Min	0.08	3.76	0.28	16.59
soil (n	Max	1.83	92.93	65.18	94.83
=23)	Mean	0.68	31.18	12.78	58.83
River	Min	0.54	40.29	12.71	135.32
sediment	Max	1.20	316.14	134.52	434.60
(n =12)	Mean	0.84	128.52	48.12	279.79

L-P, Loosely bound P; Al & Fe-P, Aluminum and iron bound P; Ca-P, Calcium bound P; R-P, Residual P; TP, Total P; n, Number of samples.

Table 4.11 The Physico-chemical properties and Total P content in the lake sediment.

Parameter	Minimum	Maximum	Mean	Std. Deviation
T-P (mg kg^{-1})	99.5	971.9	568.0	288.2
pH	6.20	9.35	7.88	0.61
EC (dSm^{-1})	0.35	28.50	5.46	5.21
OC (%)	0.23	2.11	0.97	0.54
$CaCO_3$ (%)	0.00	4.20	1.04	1.02
Sand (%)	3.43	91.30	52.65	25.22
Mud (%)	8.70	96.57	47.35	25.22

T-P, Total P; EC, Electrical conductivity; OC, organic carbon; CEC, cation exchange capacity; $CaCO_3$, Calcium carbonate.

the agricultural sites contained more labile inorganic P (L-P, Al & Fe-P). This might be due to application of large amount of synthetic fertilizer in the agricultural field (Cherubin *et al*., 2016). Higher labile P suggest that the agricultural site was vulnerable to P loss from the field to water bodies through erosion and leaching (Sharpley *et al*., 2003). Our result is in accordance with the finding of Rodrigues *et al*. (2016), where he attributed P fertilizer to increase content of labile P. It is noticeable that annual crop and perennial crop have different effect on soil P fractions. Crews and Brookes (2014) reported that crop species have a clear influence on soil P fractionation. Therefore, it is important to understand the effect of land use type on P fractions to evaluate the P loss potential from different land use.

1.7.1 P fractions along field soil / river stream / lake sediment continuum

Average contents of P fractions and their relative percentage contribution to sum of P fractions were presented in the Table 4.10. Total P content ranged from 30.49 to 1028.58 mg kg^{-1} (mean = 395.12 mg kg^{-1}) in soils of catchment area, 192 to 838.69 mg kg^{-1} (457.27mg kg^{-1}) in river sediment and 169.79 to 971.90 mg kg^{-1} (mean = 633.02 mg kg^{-1}) in the lake sediment. The results show the influence of P cycling that occurs during transport of sediment from field soil to lake sediment through river sediment. One-way ANOVA revealed a significant difference between TP of soils of catchment area, river sediment and lake sediment. Statistically significant increase in TP in the lake sediment area suggest external loading of nutrient due to deposition sediment in the lake as material is transported from field dominated by agriculture to lake sediment.

Spatial variation of individual P fractions was also observed from field to lake sediment. L-P was observed with lowest concentration from agricultural field to lake sediment, and the mean L-P in field, stream, and sediment was 0.87, 0.84, and 1.63 mg kg^{-1}. An increasing trend was observed for L-P from agricultural field to lake sediment. When compared as relative

percentage of L-P to TP, similar trend was observed, with greater percentage of L-P to TP in case of lake sediment than field soil or stream sediment.

Al & Fe-P is relatively stable under oxidizing condition encountered in shallow lake like Chilika, however high organic matter content of the lake may create reducing environment enabling dissolution of Fe oxyhydroxide, thereby releasing phosphate to aqueous phase. The average value of Al & Fe-P in the field soil (mean = 109.32 mg kg-1) and stream sediment (128.52 mg kg^{-1}) was comparable with lake sediment (mean = 105.13mg kg^{-1}). As a percentage of TP, the Al & Fe-P follows the order field soil (31.18%) > lake sediment (27.5%) > stream sediment (25.56%). Ca-P content of field soil/ stream sediment/ lake sediment continuum followed an increasing trend. However, as a percentage of TP, lake sediment (17.6%) observed highest Ca-P percent followed by field soil (12.25%), stream sediment (9.74%).

A decreasing trend was observed for field soil/ river sediment/ lake sediment continuum for R-P. R-P of field soil (mean = 225. 84 mg kg^{-1}) and stream sediment (mean = 279.79 mg kg^{-1}) was significantly higher as compared to lake sediment (mean = 210.23 mg kg^{-1}). However, as a percentage of TP, stream sediment has highest R-P percent (64.45%) with a lowest percent of R-P in case of field soil (56.38%). Highly variable content of R-P in our soils from catchment area could be due to variation in management and fertilization practice followed in the farm land. R-P content of forest soil is comparable with the R-P content of agricultural soil.

While increasing TP content is of great concern, individual P fraction content also plays an important role in determining the impact of P on aquatic bodies. Major changes occur with the composition of P fractions, along the field, stream sediment and lake sediment continuum. Percentage contribution of Al & Fe-P to sum of P fractions decreased from field soil to lake sediment while it was increased for Ca-P. Different physical and chemical process dominating in each environment with in the watershed determine the concentration of P in the sediment.

Considering the extent of synthetic and manure fertilizer applied in the agricultural field, dominance of R-P in the field soil is not surprising. Enrichment of lake sediment in organic matter due to deposition of eroded silt and clay particle and contribution of macrophyte bed explains the dominance of R-P in the lake sediment. Reactivity of Al with fine clay particle may be the reason behind highest Al & Fe-P in the field soil. Loss of fine silt and clay particle due to erosion could be the reason for low Al & Fe-P content in the lake sediment. Co-precipitation of Ca occur once the sediment enters the river stream or lake. This explains increased contribution of Ca-P to sum of P fractions in the lake sediment. As Ca-P is relatively stable and not available for biota, reduction in other P fractions could lead to lower in availability of P for planktons. Further, Makarewicz *et al*. (2009) reported decrease in macrophyte growth due to reduction in suspended sediment input to the lake. Overall, a significant amount of P is lost from field to lake sediment as sediment is transported and deposited in the bottom sediment of lake, which may be available to plankton communities or deposited in the deeper portion of lake. Further, impact of P on water bodies/ lake depends on the various mechanism that controls the P fractionation during transport of sediment from field to lake. In addition, different management practice and land use types have an influence on P fractionation pattern, with less P input in the agricultural field could help to reduce macrophyte growth in the lake.

4.8 Change in water geochemistry from PRM to PSM season

Change in water level from winter to summer can alter the chemical composition as well as mixing of lake water and pore water. The lake water depth varied from 1.43 to 1.46 m from PRM to PSM season. Maximum depth observed in the lake was as high as 3.5 m. Increase in lake water depth is attributed to rainfall and freshwater inflow from river. Raise in water level can cause a weaker contact between air and sediment, resulting in development of reducing environment in the water-sediment surface. An increase in hydraulic gradient between pore

water and lake water induces entry of lake water into sediment pore water (Wu *et al*., 2021). Rainfall in the catchment area and surface runoff brings the particulate matter into the lake and settled in the static region of lake i.e., the center region. This particulate matter will eventually deposit in the sediment pore and increase the content of Fe, Al, and organic matter, further leading to increase in Al & Fe-P, Organic P, and TP content. Usually, TOC content of sediment was high during summer due to decomposition of plants. Increase in Fe content leads to increase in ferrous mineral and subsequently adsorption of P and formation of ferrous phosphate mineral (Vivianite) (Wu *et al*., 2021).

4.9 Spatial variability of P fractions in the lake sediment

The physico-chemical properties of sediment of lake are presented in the Table 11. The Chilika lake receives tons of anthropogenic P from point and non-point source, much of which is deposited as sedimentary P. This deposited P may act as potential contributor to eutrophication of lake and negatively impact the water quality of the lake (Li *et al*., 2020). In terms of lake eutrophication, it is important to study the forms of P and its process in the sediment. Generally, the data were present as fraction percentage of total P to compare different locations as it is difficult to compare absolute values. However, we are presenting the data as absolute value as well as the proportion of different P forms with respect to TP to better elucidate the amount of P that might be available to plant biomass and biogeochemical cycle of P in the sediment. Seasonal variation in P fractions in sediments of lake Chilika is presented in the Table 4.12 and the sectoral variation in the P fractions is presented in the Table 4.13 and 4.14.

4.9.1 Total P

The northern sector receives its majority of total P loadings into the lake. The biogeochemical transfer within the lake allowed redistribution of nutrients across the entire lake (Yuan *et al*.,

2018). Total P concentration of the lake varied from 168.92 to 957.21, with an average value of 556.98 mg kg^{-1} during PRM, and varied between 169.79 to 971.90 with an average value of

Table 4.12 Seasonal variation of P fractions (mg kg^{-1}) in sediments of Chilika Lake

Season	Range	WSP	L-P	Al & Fe-P	Ca-P	R-P	Total P
Post monsoon (n =25)	Min.	0.08	0.29	39.08	22.55	38.72	169.79
	Max.	7.03	4.75	198.60	150.79	356.12	971.90
	Avg.	2.12[a]	1.63[a]	105.13[a]	64.36[a]	210.23[a]	633.02[a]
	Std.	1.79	1.19	43.50	29.77	86.91	234.35
Pre-monsoon (n =25)	Min.	ND	0.17	22.03	34.94	47.94	168.92
	Max.	ND	2.65	173.22	265.94	302.17	957.21
	Avg.	ND	0.78[b]	79.54[b]	94.61[b]	169.97[b]	556.98[b]
	Std.	ND	0.71	39.47	57.82	70.54	204.73

L-P, Loosely bound P; Al & Fe-P, Aluminum and iron bound P; Ca-P, Calcium bound P; R-P, Residual P; n, number of samples; ND, Not detected. Means followed by different lower-case letters are significantly different.

Table 4.13 Sectoral variation of P fractions (mg kg^{-1}) in Chilika Lake (Pre-monsoon season)

Sector	Range	L-P	Al & Fe-P	Ca-P	R-P	Total P
SS	Min.	0.27	22.03	34.94	47.94	168.92
	Max.	2.65	84.83	265.94	153.00	489.86
	Avg.	1.40[a]	60.79[a]	111.47	92.14[a]	333.15[a]
	Std.	1.05	22.47	104.63	42.28	127.13
CS	Min.	0.17	29.48	56.85	79.56	365.99
	Max.	1.74	130.11	167.11	302.17	810.81
	Avg.	0.68[ab]	77.35[a]	95.45	195.35[b]	589.05[b]
	Std.	0.50	31.68	37.54	71.18	169.83
NS	Min.	0.22	30.47	44.52	159.12	472.97
	Max.	0.62	173.22	130.59	214.20	957.21
	Avg.	0.37[b]	103.03[b]	75.94	192.82[b]	711.34[b]
	Std.	0.15	58.90	30.88	19.22	156.27
Lake	Min	0.17	22.03	34.94	47.94	168.92
	Max	2.65	173.22	265.94	302.17	957.21
	Avg.	0.78	79.54	94.61	169.97	556.98
	Std	0.71	39.47	57.82	70.54	204.73

SS, Southern sector; CS, Central sector; NS, Northern sector; L-P, Loosely bound P; Al & Fe-P, Aluminum and iron bound P; Ca-P, Calcium bound P; R-P, Residual P. Means followed by different lower case letter in a column are significantly different.

Table 4.14. Sectoral variation of P fractions (mg kg^{-1}) in Chilika lake (post-monsoon season)

Sector	Range	WSP	L-P	Al& Fe-P	Ca-P	R-P	Total P
SS	Min.	2.56	0.50	39.08	22.55	38.72	169.79
	Max.	7.03	0.86	108.75	150.79	261.48	480.09
	Avg.	4.60[a]	0.67[a]	74.13	68.93	157.29	342.51[a]
	Std.	1.56	0.12	26.71	60.14	86.27	123.41
CS	Min.	0.08	0.29	61.77	43.10	62.54	415.69
	Max.	3.16	4.75	198.60	91.24	330.56	925.06
	Avg.	1.28[b]	2.23[b]	109.73	65.71	210.70	693.57[b]
	Std.	0.83	1.32	46.43	12.18	77.91	199.53
NS	Min.	0.26	0.60	84.06	32.86	122.84	649.88
	Max.	3.89	2.23	183.13	71.19	356.12	971.90
	Avg.	1.44[b]	1.32[ab]	126.18	56.87	262.17	792.35[b]
	Std.	1.26	0.72	38.15	13.58	87.42	107.49
Lake	Min.	0.08	0.29	39.08	22.55	38.72	169.79
	Max.	7.03	4.75	198.60	150.79	356.12	971.90
	Avg.	2.12	1.63	105.13	64.36	210.23	633.02
	Std.	1.79	1.19	43.50	29.77	86.91	234.35

SS, Southern sector; CS, Central sector; NS, Northern sector; L-P, Loosely bound P; Al & Fe-P, Aluminum and iron bound P; Ca-P, Calcium bound P; R-P, Residual P; Means followed by different lower case letter in a column are significantly different.

Table 4.15. Sectoral fraction percent (%) of sum of P fractions of WSP, L-P, Al & Fe-P, Ca-P and R-P

Season	Sector	Fraction % of sum of P fractions				
		WSP	L-P	Al & Fe-P	Ca-P	R-P
PSM	SS	1.69	0.27	27.43	21.41	49.19
	CS	0.33	0.60	28.35	17.98	52.74
	NS	0.32	0.34	26.59	13.30	59.45
	Average	0.8	0.4	27.5	17.6	53.8
PRM	SS	ND	0.53	22.87	41.94	34.67
	CS	ND	0.18	25.88	52.96	25.88
	NS	ND	0.10	27.69	20.40	51.81
	Average	ND	0.27	23.84	29.41	46.48

PRM, Pre-monsoon; PSM, Post-monsoon, SS, Southern sector; CS, Central sector; NS, Northern sector; WSP, Water soluble P; L-P, Loosely bound P; Al & Fe-P, Aluminum and iron bound P; Ca-P, Calcium bound P; R-P, Residual P; ND, Not detected

Table 4.16. Correlation matrix of sediment properties and P fractions of the lake.

Parameter	WSP	L-P	Fe & Al-P	Ca-P	R-P	Total P	pH	EC	OC	CaCO3	Silt+Clay
WSP	1										
L-P	0.099	1									
Fe & Al-P	-0.204	0.294*	1								
Ca-P	0.140	0.043	0.020	1							
R-P	0.023	0.051	0.321*	0.088	1						
Total P	-0.176	0.238	0.321*	0.121	0.731**	1					
pH	-0.016	0.182	-0.336*	-0.135	-0.127	-0.108	1				
EC	0.585**	-0.051	-0.308*	0.016	-0.265	-0.438**	0.120	1			
OC	0.169	-0.001	0.222	0.068	0.456**	0.397**	-0.345*	-0.253	1		
CaCO3	0.175	0.084	-0.002	0.401**	0.417**	0.385**	0.179	0.143	0.445**	1	
Silt+Clay	0.422*	-0.056	-0.049	0.047	0.299*	0.241	-0.307*	0.168	0.456**	0.408**	1

WSP, Water soluble P; L-P, Loosely bound P; Al & Fe-P, Aluminum and iron bound P; Ca-P, Calcium bound P; R-P, Residual P; EC, Electrical conductivity; OC, Organic carbon; CaCO3,Calcium carbonate

*and ** represents significance at $p < 0.05$ and $p < 0.01$ respectively.

633.02 mg kg^{-1} during PSM season (Table 4.12). High total P content in the lake suggested the intensification of anthropogenic activities in the catchment area. One-way ANOAV revealed spatial variation of total P across the lake ($p < 0.001$). Higher total P observed in the PSM could be due to the riverine flow received during monsoon season which carries loads of silt enriched with P from the catchment area. The spatial variation of total P in the lake might be due to difference in anthropogenic activity and landscape causing varying degree of nutrient enrichment through river. The lake received its majority of riverine flow by the river Daya, Bhargavi, and Luna from the north and northwest regions of the lake, which might be the explanation for high total P observed in the station falls under NS and CS. The higher total P concentration in the NS and CS were attributed to deposition of fine sediment brought by the freshwater flow from river. There is net outflow of P from the lake to sea through the outer channel causing lower total P of the sediment in the station falls under cluster SS. In addition to this, sandy texture of sediment found in the SS holds less P. The central sector receives P from both point and non-point source. The waste water from industries, prawn processing unit contribute to the point source of P pollution while domestic wastewater, agricultural run-off carrying P contribute to the non-point source of P pollution.

In shallow lake like Chilika, seasonal or transient hypoxic condition can develop during pre-monsoon season which can disturb the oxic surface sediment layer and facilitate release of P from sediment to water column (Giles *et al*., 2016). Although increase in total P concentration in the lake is of great concern, concentration of different P fraction also plays an important part in determining negative impact of P enrichment in the lake ecosystem. However, all the P fraction are not bioavailable and subsequently contribute to eutrophication of lake. Type of sediment, redox state of sediment, mineralization rate is some of the factors which controls the distribution of the P fractions across the lake. Both external loading and internal loading

contribute to saturation of P in the lake sediment. P release from the sediment to lake water contribute to internal loading while riverine flow from catchment area contribute to external loading. Shallow water like Chilika is more susceptible to internal loading due to frequent mixing of lake water and bottom sediment.

4.9.2 Water soluble P (WSP)

The soluble reactive P in the pore water is referred as water-soluble P also deliberated as directly available P. As this fraction of P is extracted after filtering through 0.45µ membrane filter and measured using Murphey & Riley reagent, this fraction is also called as soluble reactive P. Concentration of WSP is primarily depend upon solubility product and adsorption-desorption equilibria between pore water and lake water. Also release of P from sediment-water interface is govern by the concentration gradient between pore water and lake water. WSP concentration of the lake varied from 0.08 to 7.03, with an average value of 2.12 mg kg^{-1}. One-way ANOVA revealed that spatial variation of WSP exist across the lake. Table 4.13 & 4.14 represent the spatial variation of different P fractions during PRM and PSM season. Significantly lower WSP content in the NS is attributed to abundance of algal bloom and consumption of WSP by it. WSP can also use as P saturation of the lake.

4.9.3 Loosely bound P (L-P)

The loosely bound P (L-P) refers to the dissolved P in the pore water, also signifies readily desorbable P or algal P (Zhou *et al*., 2001). L-P is the most important fraction to determine the bioavailability of P in the sediment, which is present in the form of orthophosphate in the pore water. Algae can uptake L-P directly and promote eutrophication of lake (Yalcin *et al*., 2012). This P can be released from pore water to water column through dissolution of $CaCO_3$ associated P and release from decaying cells of bacterial biomass (Barik *et al*., 2019). This pool is also called as seasonally variable pool. The concentration of L-P varied between 0.17 to

2.65with an average value of 0.78mg kg^{-1}during PRM and varied between 0.29 to 4.75with a mean value of 1.63 mg kg^{-1} during PSM (Table 4.12). One-way ANOVA revealed significant seasonal variation ($p < 0.05$) of L-P for studied stations. Significantly higher value of L-P during PSM as compared to PRM could be attributed to higher TP in the lake during PSM due to massive influx of fresh water carrying nutrient rich silt particle. Stations falling under northern and central sector reported higher value of L-P as compared to SS. Significantly lower value of L-P in the SS associated with high salinity could be due to competition between dissolved anions like Cl^-, SO_4^{2-}, OH^- and phosphate for adsorption into same sites on the sediments. This finding is further confirmed by negative correlation of L-P with salinity and pH though the correlation was non-significant ($r = -0.051$) (Table 4.16). The mean concentration of L-P was the second least among the fractions of P. L-P represented less than 1 % of IP in the sediments (Table 4.15). Barik *et al*. (2016) also reported contribution of L-P to TP as less than 1% in the surface sediment of Chilika lake. However, contribution of L-P to TP was observed to be as high as 25 % in the Lake Kolleru, India (Njenga, 2005). The observation was in agreement with the previous findings, where contribution of L-P to TP was between 1% to 25% in the sediments, and also contribute more in the calcareous lake because of high degree of $CaCO_3$ saturation. This suggest that the present studied lake has low degree of $CaCO_3$ saturation.

4.9.4 Aluminum bound and Iron bound P (Al-P& Fe-P)

This fraction of sediment denotes P combined with metal oxide or hydroxide, mostly Al, and Fe and referred as potentially mobile pool of P. Al-P & Fe-P is the most important inorganic P fraction in the lake ecosystem contributing 23.84-27.5 % of sum of P fractions (Table 4.15). The inorganic P fraction associated with aluminosilicate clay mineral is referred as Al-P. This form of P is not readily available for plant biomass as it is strongly bonded with discrete aluminum phosphate phase. Al-P is relatively stable under both oxidized and reduced condition

(Cai et al., 2020). Fe-P is both pH and redox sensitive, and most bioavailable P fraction in lake. Usually, Fe-P is not bioavailable under oxidizing condition. However, under reducing condition, dissolution of Fe oxyhydroxide occurs, releasing P to the aqueous phase (Liu *et al*., 2016). Though release of P from Fe-P is prevalent in anoxic condition, there are evidence of mobilization of Fe-P under both oxidizing and reducing condition (Rydin *et al*., 2000).

Mean concentration of Al & Fe-P varied between 22.03 to 173.22, with an average value of 79.54 mg kg^{-1} during PRM and varied from 39.08 to 198.60with an average value of 105.13 mg kg^{-1} during PSM (Table 4.12). One ANOVA revealed significant seasonal variation of Al & Fe-P in the studied lake ecosystem. Significantly lower Al & Fe-P observed during PRM season could be due to higher pH accelerating conversion of detrital inorganic P into authigenic (Wu *et al*., 2021). This is further confirmed by a significant negative correlation between pH and Al & Fe-P($r = -0.336$, $p < 0.05$) (Table 4.16).High pH during summer and winter favours mobilization of P from Fe (hydro) oxides, as phosphate is substituted by hydroxide ion. In addition to this, bacterial activity also enhances P release form Fe bound P (Perkins and Underwood, 2001). Zhang *et al*. (2016) observed a negative correlation between pH and Al & Fe-P and concluded that higher pH decreases the sorption capacity of Al & Fe. Increase in pH leads to replacement of orthophosphate ion by hydroxide ion through ligand exchange (Hupfer and Lewandowski, 2008). One way ANOVA revealed spatial variation of Al & Fe-P among the different stations of the lake. NS have significantly higher value of Al & Fe-P as compared to other sectors. Spatial variation in Al & Fe-P could be attributed to variation in salinity and pH across the lake, where low salinity and higher pH accelerates the mobilization of phosphate from Fe-P and replaced by hydroxide ion in alkaline condition (Barik *et al*., 2019). Higher value of Al & Fe-P in the northern and western part of the lake suggests that pollution as source of this fraction in the lake sediment and anthropogenic impact. Previous research also suggest that positive correlation exist between Al & Fe-P and phosphate concentration of overlaying

water (Long *et al.*, 2023). Influx of industrial and domestic wastewater from northern and western catchment of lake through river and its tributaries polluted the lake and major driving factor behind majority of Al & Fe-P in the lake. Ni *et al*. (2020) also attributed domestic and wastewater as source of Al & Fe-P in a lake in China.

4.9.5 Calcium bound P (Ca-P)

Ca-P is usually the most important P fraction in the alkaline coastal ecosystem of lakes. Ca-P is the most stable inorganic fraction in the lake ecosystem. Ca-P is associated with calcium carbonate and discrete phase of Ca. Origin of Ca-P could be attributed to (i) detrital fluorapatite of igneous and metamorphic rock, (ii) biogenic skeletal debris and carbonate fluorapatite precipitations. The Ca-P belonging to first group is non-bioavailable as it is stable under both oxic and anoxic environment and considered as permanent burial; and the Ca-P associated to later group is a sink for reactive P (Ruttenberg, 1992). One-way ANOVA revealed seasonal variation of Ca-P in the lake sediment. Ca-P content was varied between 34.94 to 265.94, with a mean concentration of 94.61 mg kg^{-1} during PRM and varied between 22.55 to 150.79, with an average value of 64.36 mg kg^{-1} during PSM season (Table 4.12). Significantly higher Ca-P observed during PRM could be due to higher salinity of the lake during summer season facilitating precipitation of phosphate with $CaCO_3$ (Anshumali and Ramanathan, 2007; Hou *et al*., 2009). In addition, higher pH during PRM also facilitate adsorption and co-precipitation of P into sediment of the lake. Salinity is the major factor controlling spatial variability of Ca-P in the lake ecosystem, as high salinity observed in the southern and outer channel favoured the precipitation of calcite. This might be the reason behind dominance of Ca-P in the region with higher salinity. A positive correlation between $CaCO_3$ content and Ca-P ($r= 0.401$, $P< 0.01$) suggest calcareous nature of the Lake.

4.9.6Residual P (R-P)

Residual P consist of some of inorganic P (which were not extracted with the sequential extraction) and organic P. R-P content of the lake varied between 47.94 to 302.17, with an average value of 169.97 mg kg^{-1} during PRM, and varied between 38.72 to 356.12with an average value of 210.23 mg kg^{-1} during PSM season (Table 4.12). One-way ANOVA revealed spatial variation of R-P in the lake sediment. R-P is the most dominant P fraction in our studied lake contributing 43.48-53.8 % to the sum of P fractions (Table 4.15). Dominance of R-P in the lake could be attributed to intensive agriculture practice, aquaculture pollution in the catchment area of the Lake. Ni *et al.* (2020) reported R-P as dominating fraction in the lake and attributed agriculture as the source of R-P. Application of large amount of fertilizer could be the reason behind drastic value of R-P in the studied lake ecosystem. Generally, only 15 to 20% applied P was taken by plant, rest of the P losses to river and reached lake through different stream flow and as agricultural runoff. This could be the explanation for addition of large amount of phytate P contributing to organic P in the lake.

Aquaculture and domestic pollution in the villages in the catchment area could be reason for spatial variation of R-P. Long *et al*. (2023) attributed domestic sewage, livestock breeding discharge produced by the resident as primary factor leading to variability of organic P in the lake of China. Higher value of R-P in the northern stations might be due to presence of vegetation which are capable of adsorbing P from water column and store as organic P. Besides, mineralization rate controls the seasonal variation in R-P. Organic P is subject to mineralization and regeneration in the sediment. This regenerated P further sequestered by ferric hydroxide or included in the freshly formed mineral (Katsev, 2016; Li *et al*., 2018). This Fe-oxide subsequently release phosphate to pore water as it undergoes reductive dissolution (Xiong *et al*., 2019; Markovic *et al*., 2019). In general, Organic P may release bioavailable P which may be directly or indirectly utilized by planktons in the overlaying water (Liu *et al*., 2012; Feng *et al*., 2016; Li *et al*.,2019). This bioavailable P may convert to active P by chemical or biological

process and negatively impact water quality of lake (Bridgman *et al*., 2012). Some of the soluble P may migrate upward and release into water column. Rydin (2000) reported that 50-60% organic P may be hydrolysed to bioavailable P. Though release of phosphate from R-P as compared to Al & Fe-P may take longer time, its potential contribution to long-term release cannot be ignored. Spatial distribution of R-P in the lake suggest that it may contribute to potential release of phosphate in the northern and central sector.

4.10 Cluster analysis

Sediments play an important role in nutrient dynamics in the lake (Yuan *et al*., 2020). Because of varied sediment characteristics, physical, chemical, and biological properties of the water column, the mechanism controlling the P release from sediment also vary with in the lake spatially and seasonally. Clustering of the different stations across the lake based on different sediment characteristics and P fractions can help to understand the different mechanism controlling the P release. Cluster analysis helps to differentiate the lake into two groups based on the dissimilarity among the cluster with respect to sediment characteristics and distribution of P fractions (Fig 4.8). The C1 includes the stations falling under southern sector and some station of central sector experiencing tidal influence and receiving little freshwater inflow as compared to other sectors of the lake. C2 included the stations which mostly falls under central and northern sector which experiences influence of anthropogenic activities and receives massive fresh water inflow through river draining the catchment area.

4.11 Principal component analysis

Principal component analysis is a strong tool of multi-variate statistical analysis which helps to reduce the number of original variable and extract important principal component to assess the relationship between variable. In the present study, the P fractions and the physico-chemical parameter of sediment were processed for principal component analysis. Principal components

Table 4.17. Principal component matrix of P fractions and sediment properties

Parameter	Components			
	1	2	3	4
WSP	-0.040	0.044	**0.886**	0.155
L-P	0.115	**0.976**	0.082	0.075
Fe-P	0.286	0.123	-0.177	**0.634**
Ca-P	0.115	**0.976**	0.082	0.075
R-P	**0.823**	0.081	-0.162	0.225
TP	**0.741**	0.177	-0.474	0.100
pH	0.112	0.024	0.128	**0.904**
EC	0.017	0.198	**0.813**	-0.221
OC	0.763	0.092	0.021	0.275
CaCO3	0.754	0.402	0.283	-0.303
Silt + Clay	0.662	-0.148	0.424	0.222
Eigen value	3.61	2.42	1.63	1.24
Total variance	32.74	20.38	14.81	11.40
Cumulative variance	32.74	53.12	67.92	79.38

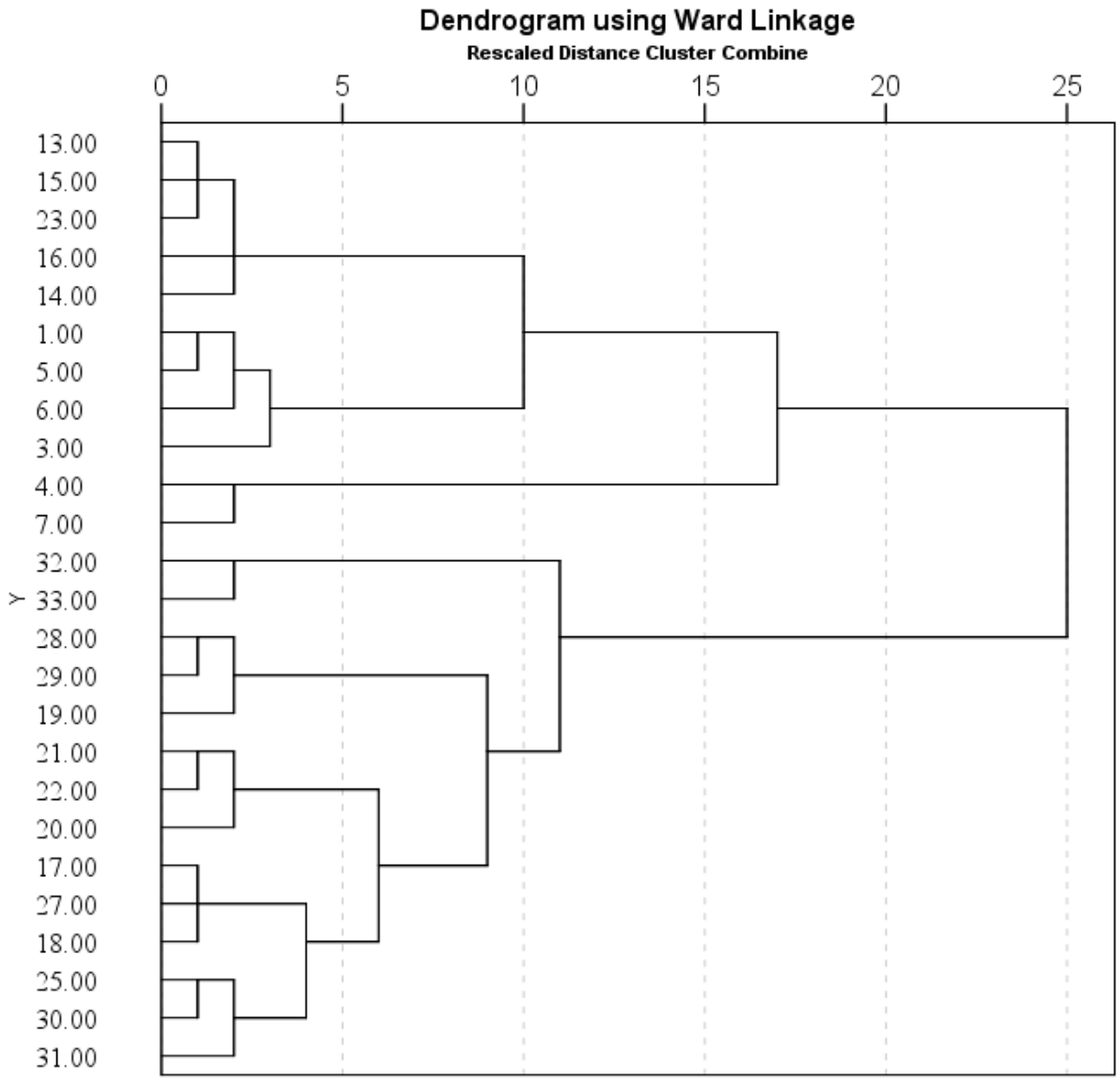

Fig. 4.8 Dendrogram of P fraction and sediment physico-chemical properties showing clusters.

with eigen value > 1 are further considered for discussion. The variables under each PC were classified as strong, moderate, and weak based on their factor loading values of >0.75, 0.75-0.5 and < 0.5 respectively. Four principal components were extracted which explains 79.38 % of total variation in the data set (Table 4.17). PC 1 explains32.74 % of variation with strong loading for R-P and Total P and moderate loading for Organic carbon, $CaCO_3$, and Silt+ Clay. It indicates that total P availability of the lake remained mostly as residual P and positively correlated with organic carbon content of the sediment. PC2 explains 20.38 % variability with strong loading for L-P and Ca-P and moderate loading for CaCO3 indicating Ca-P content of the lake is governed by the $CaCO_3$ content of the lake. Strong loading for L-P suggest that phosphate availability to algal bloom is controlled by its content. PC3 explains 14.81% variability with strong loading for WSP and EC. Strong loadings for WSP and moderate loading for mud content suggests that it might be the factor controlling the WSP content of the lake. Strong loading for EC indicates that P fraction content of the lake is governed by the salinity of the lake. PC4 explains 11.40 % of the variability with strong loading for pH and moderate loading for Al & Fe-P suggesting pH of the lake controls the content of al & Fe-P.

4.12 Adsorption study

The phosphorus adsorption behaviour of the sediment samples was illustrated by the adsorption isotherm and the data pertaining to it were given in the Appendix. Varied concentration of phosphate solution (1, 2, 4, 6, 10,20, 40 mg L^{-1}) were added to 0.5 g sediment and equilibrated for 24 hrs. Phosphate concentration in the equilibrium solution was measured and adsorption isotherm was constructed. Nature of adsorption isotherm was studied by plotting Ce (equilibrium P concentration) vs x/m (amount of P adsorbed) (Appendix). The amount of adsorbed P showed a non-linear relationship with the equilibrium P concentration when the concentration of added P was low, whereas at higher concentration of added P, it was roughly linear to steady state value. According to classification of Giles (1960), the adsorption

isotherms were of L shaped, indicating high adsorption at lower concentration of added P, with decrease in the adsorption at higher value of added P. Considerably, more P was adsorbed by the sediments of NS and CS than by SS sediments at higher concentration of added P (10-40 mg kg^{-1}).

4.12.1 P sorption and fractions of P adsorbed with increasing initial P levels

As shown in Appendix, P sorption on the sediments of all the sector was maximum at lower concentration of added P and thereafter decreases at higher concentration of added P, and the decrement was more in southern sector. At low concentration of added P (1 mg kg^{-1}), the amount of adsorbed P was 19.78 mg kg^{-1} (~99% of added P) for sediments of station number 25(NS) and 19.56 mg kg^{-1} for sediments of station number 33 (NS) (~98% of added P). However, at higher concentration of added P (40 mg kg^{-1}), the amount of P adsorbed was 634.4 mg kg^{-1} (79% of added P) for station number 25 and 429.1 mg kg^{-1} for station number 33 (53% of added P). Similarly, amount of adsorbed P at lower concentration of added P was 98 and 99% of added P for central sector and southern sector respectively. At higher concentration of added P, amount of adsorbed P was 66% for central sector, however it was 53% and 32% for southern sector. The percentage adsorbed P decreased as the P concentration increased. This was probably due to buffering capacity of solid phase and residence time (Bhadha et al., 2012). The adsorption of P by soil or sediment is regarded as multistage kinetics process started with fast adsorption stage followed by slower adsorption stage (Wang and Liang, 2014). P adsorption process can be divided into chemical and physical adsorption. At low concentration of added P, a rapid chemical adsorption process dominates. Ion exchange and ligand exchange contribute to chemical adsorption of P by soil or sediment (Yang et al., 2019). As the adsorption sites were saturated ate higher P concentration, the chemical adsorption slows down and the P was adsorbed to sediment at a slower rate physically. This slow process is called physical adsorption.

Comparatively, P sorption was highest for sediments of NS and lowest for SS at similar initial level of added P ($p< 0.05$). Higher organic matter content and lower salinity could be reason behind higher P adsorption observed in NS. Addition of P with increasing concentration greatly affect the adsorption behaviour of P by the sediment, which might be due to changing bonding energy of the sorption sites. At low concentration of added P, there were a lot of accessible adsorption sites available on the sediment leading to high phosphate adsorption upon addition of P. P adsorption into the soil/ sediment can be explained by initial adsorption into surface and then precipitation of phosphate molecule (Huang *et al*., 2012).

4.12.2 Adsorption isotherm model

Generally, both Langmuir and Freundlich models are used to describe the sorption properties of P. Langmuir isotherm model (R^2 =0.91 to 0.99) was superior to Freundlich model (R^2 = 0.58 to 0.82) for describing P sorption properties of sediment in the present study (Table 4.18). This result suggests monolayer adsorption of P in sediments (Hu *et al.,* 2018). Most of the studies also found Langmuir isotherm to better fit the adsorption data despite the assumption that it only describes monolayer adsorption with uniform bonding energy on homogenous surface (Cucarella and Renman, 2009; Fang *et al*., 2013). Adsorption constant related to Langmuir model was calculated from the straight line obtained from the plot of Ce/x/m Vs Ce. Adsorption maxima (Q_{max}, µg/g) was calculated from reciprocal of slope and bonding energy (mL/g) was calculated by dividing slope with intercept. Maximum P sorption capacity evaluates number of adsorption sites per unit weight of sediment. Maximum P sorption (Q_{max}) and bonding energy calculated from the Langmuir isotherm model and presented in the Table 4.18. Maximum P sorption (Q_{max}) of NS, CS, and SS varied from 418- 644 mg kg^{-1}, 505-532 mg kg^{-1}, 257 mg kg^{-1} respectively. Q_{max} of the lake sediment follows the order of NS > CS > SS. Phosphorus sorption index (PSI) is also used to determine P adsorption capacity of sediment and an effective alternative tool to evaluating maximum P adsorption capacity. PSI values of lake

Table 4.18. Sorption parameter and desorption index of lake sediment

Sector	Station No.	Langmuir equation			Freundlich equation			DI	WSP (mg kg^{-1})	Al & Fe-P (mg kg^{-1})
		Adsorption maxima (mg kg^{-1})	Bonding energy (L mg^{-1})	R^2	K_f (µg mL^{-1} g^{-1})	n	R^2			
NS	33	428.73	1.02	0.96	183.91	3.52	0.58	24.77	1.20	105.14
	25	654.93	1.96	0.97	315.43	2.59	0.76	5.88	1.10	114.16
CS	18	541.96	1.18	0.97	215.13	2.48	0.75	3.98	1.88	92.48
	28	518.52	1.04	0.96	207.78	2.52	0.82	12.15	1.32	84.45
SS	1	409.11	0.91	0.96	174.98	2.98	0.78	1.06	2.56	108.75
	5	260.04	4.96	0.99	145.81	3.63	0.68	1.07	3.46	39.08

DI; Desorption Index; WSP, Water soluble P; AL& Fe-P, Aluminum and iron bound P

Table 4.19 Correlation matrix of Sediment properties with adsorbed desorbed P

	Adsorbed P	pH	EC	OC	CEC	CaCO3	Silt+ Clay	Amount of P desorbed
Amount of adsorbed P	1							
pH	-0.050	1						
EC	-0.240	0.043	1					
OC	0.103	-0.340	-0.091	1				
CEC	-0.138	-0.265	0.236	0.701**	1			
CaCO3	0.099	0.132	0.137	0.623**	0.537**	1		
Silt + Clay	-0.142	-0.261	0.185	0.501**	0.747**	0.357	1	
Amount of P desorbed	-0.694**	0.231	0.198	-0.201	0.109	-0.058	0.038	1

EC, Electrical conductivity; OC, Organic carbon; CEC, Cation exchange capacity;

*and ** represent significant difference at significance level $p < 0.05$ and $p < 0.01$ respectively.

sediment varied from 101.10 to 622.72 with an average value of 307.99 (Table 4.20). Mean value of PSI was highest for sediments of CS (346.80) followed by NS (311.82). this value further confirms high sorption capacities of sediments of CS and NS. Sorption capacities of river sediment was evaluated using PSI, and the value varied from 15.03 to 327.80, with an average value of 192.88. Significant correlation between PSI and Q_{max} ($r = 0.99$, $p < 0.001$) suggest that PSI can be used to characterize adsorption capacity of sediment for a quick assessment.

Bonding energy reflects the affinity of sediment for P. Higher value for bonding energy suggests stronger adsorption and adsorption of P is a spontaneous process (Wang and Liang, 2014). However, bonding energy of the lake sediment follows the order of SS > NS > CS. Bonding energy decreased with increase in organic matter content. Similar observation was made by Yang *et al*. (2019).

Freundlich isotherm constant were calculated form the straight line obtained by plotting log Ce vs log x/m. Freundlich constant (K_f) was calculated by taking antilog of intercept of the straight line. The constant K_f indicates the relative adsorption capacity of the adsorbate. K_f value of Freundlich equation is comparable with adsorption maxima of Langmuir equation as it indicates extent of P removal from solution. The "n" value was calculated from the reciprocal of the slope. The value "n" provides idea about intensity of adsorption. It also provides the degree of nonlinearity between solution concentration and adsorption. When the value of n is equal to 1 it indicates linearity of adsorption process, n value > 1 indicates physical adsorption process and n value < 1 indicates adsorption process is chemical. Value of "n" was higher than 1 in our study suggesting physical adsorption in the adsorption process of phosphate by sediments (Xie *et al*., 2019).

4.12.3 Effect of hydrological condition on adsorption-desorption of phosphate in Lake:

Table 4.20 Phosphorus sorption index (PSI) and kinetics desorption parameter of lake sediment and different land use.

Sector		PSI (mg kg^{-1})	β (mg P kg^{-1})	α (mg P kg^{-1} hr^{-1})	R (mg P $kg^{-1}hr^{-0.5}$)	b (mg P kg^{-1})	P desorption (%)
SS (n =6)	Min	144.15	0.36	0.21	0.64	1.18	19.7
	Max	293.14	0.74	9.09	1.29	2.19	55.1
	Mean	229.47	0.51	4.15	0.97	1.66	41.2
CS (n =13)	Min	119.46	0.50	2.41	0.08	1.24	15.7
	Max	568.67	5.52	68.53	0.94	3.98	53.2
	Mean	346.80	1.19	30.61	0.57	2.85	27.1
NS (n =6)	Min	173.85	0.38	1.46	0.31	0.54	13.7
	Max	547.28	1.52	86.66	1.17	4.89	74.5
	Mean	311.82	0.78	32.51	0.73	2.21	43.0
Agricultural soil (n=14)	Min	87.67	1.22	0.01	0.12	0.01	4.00
	Max	424.41	3.86	1.71	0.39	0.92	20.78
	Mean	231.60	1.96	0.28	0.23	0.33	12.11
Forest soil (n=2)	Min	145.49	0.85	0.05	0.14	0.20	4.49
	Max	398.73	3.33	0.48	0.55	0.37	35.32
	Mean	272.11	2.09	0.27	0.35	0.28	19.91
Fallow field (n=7)	Min	212.14	0.78	0.01	0.10	0.01	2.29
	Max	499.96	4.59	0.93	0.60	0.67	9.80
	Mean	332.72	2.43	0.19	0.20	0.26	5.55
River (n=12)	Min	15.03	0.39	1.90	0.30	0.73	
	Max	327.80	1.49	27.07	1.17	3.23	
	Mean	192.88	0.70	8.30	0.79	1.60	

PSI, Phosphorus sorption index; β, rate of P desorption; α, desorption constant; R, diffusion rate constant (desorption rate factor); b, desorption intensity parameter;

Hydrological condition of lagoon can influence the adsorption-desorption process of phosphate in the water column. Freshwater influx from the catchment area, oceanic exchange, and seasonal cyclone characterized by drying and wetting cycle can influence the hydrological condition of the lagoon by virtue of its changing electron availability. For example, oxidation or reduction state of water column can influence solubility of ferrous ion leading to desorption or adsorption of P. In the present study, the sampling station falling under central and northern sector which were close to the lake boundary proximity showed higher P adsorption compared to the all-other sampling station. Change in sediment properties (e.g., SOM, silt, pH, salinity, Al, and Fe) in the sampling station nearer to the lake boundary due to large influx of fresh water from catchment area could be the possible explanation for its higher P adsorption. Flower et al. (2017) reported decreased P sorption efficiency of limestone bedrock of coastal aquifer due to increase in salinity. Salinity of lake sediment is an important factor influencing the adsorption of P. Overall, the P adsorption decreased with increase in salinity which is indicated by a negative correlation between adsorbed amount of P and EC (r = -0.240) (Table 4.19). However, the correlation is non-significant, which can be explained by increase in adsorbed P with increase in salinity at low value of EC. The sediments from NS and CS have relatively low salinity compared to SS of the lake. The amount of P adsorbed increased with salinity at NS while it is decreased with salinity at SS. Jun *et al*. (2013) observed adsorption of P increased with increase in salinity at low range of salinity of overlaying water, whereas P adsorption decreased above a threshold value of salinity. This might be due to adsorption of P occur through particle aggregation at low salinity and at higher salinity competition from other anions (Cl^-, SO_4^{2-}, and OH^-) compete for adsorption site decrease the P adsorption (Bai *et al*., 2017).

Effect of pH on P adsorption and competition with other anion for P adsorption site has been well documented in the literature (Gustafsson *et al*., 2012). In our study, pH has a negative correlation (r= -0.050) with amount of P adsorbed, however the correlation was non-significant.

Gustafsson *et al*. (2012) observed maximum P adsorption at a pH range of 5.0 -7.0, as P was in the form HPO_4^{2-} and H_2PO^{4-}, which can be easily adsorbed by the soil. As the pH of the soil decreases below 5.0, dissolution of P occurs, and at above 7.0, there is increasing competition for accessible site for P adsorption with OH^- (Jalali and Matin, 2015).

Freshwater input in the northern sector carrying a large proportion of finer soil particle (preferably silt) which could effectively improve the buffering capacity of phosphorus release to the water column (Wang *et al*., 2007; Bai *et al*., 2015). Additionally, higher TOC content in the sediment of NS could increase the P sorption sites owing to its reaction with Fe/Al oxides. Meanwhile, higher P adsorption in the sampling station near the lake boundary proximity coupled with higher contribution of Al & Fe-P to the freshly precipitated P indicates that freshwater inclusion into the lake could improve the P sorption efficiency of lake sediment. Bai *et al*. (2017) reported that flooding can encourage redox condition in the lake sediment which could inhibit crystallization of Al & Fe, increasing sorption of phosphate through formation of complex between Al, Fe & phosphate. However, under anaerobic condition more P could release to the water column owing to bonding of more Fe^{2+} to the sulfide forms resulting in decrease in P sorption (Dijk *et al*., 2015; Li *et al*., 2016).

With eutrophication of lake Chilika, organic matter content of the lake increasing which could promote physical adsorption of P by sediments. When the phosphate content of overlaying content decreases due to algal bloom, these loosely sorbed phosphate by sediments could be internal load for bioavailable P (Zhu *et al*., 2016). This results in release of P from sediment to support algal blooming (Zhu *et al*., 2013). Thus, organic matter content of the sediments is also an important factor to maintain P concentration in the lake. It suggests that P input into the lake need to be reduced to safer level to control eutrophication of lake.

4.13 P desorption isotherm and percentage desorption after P sorption

P desorption from sediment was reverse of P adsorption process and the environmental consequences due to release of P from sediment makes P desorption more important than P adsorption (Wang and Liang, 2014). Amount of P desorbed was less than amount of P adsorbed for every station, indicating sediment could desorb P to some extent and P adsorption is not entirely a reversible process. Data pertaining to P desorption were fitted to Freundlich equation. Coefficient of correlation varied from 0.46 to 0.99 (Appendix). Poor correlation in station number 33 could be due to fast desorption during 1st step and slow desorption during successive step of desorption. Percent desorption to the adsorbed P was calculated and presented in the Table 4.20. Percent desorption was highest for NS followed by SS and CS. Highest percent desorption was observed for station number 22 (74%) and some stations of SS and NS shows percentage desorption of more than 50% indicating desorption capacity of lake sediment under favourable conditions. Percentage desorption of sampling station was less than 100% suggesting the sediments of lake are still acting as sink for P. However, sediment could also act as source for P to overlaying water if anoxic condition develops in the lake, which is a common phenomenon in shallow lake like Chilika.

The value of desorption index (DI) varied from 1.06 to 24.77 across the experimental sediment (Table 4.18). Both reversible (DI value close to 1) and hysteric (DI value more than 1) type of desorption were obtained. DI value closer to 1 in the SS sector suggest that sediments of SS are not acting as sink for P. Higher labile P in the SS, especially higher WSP in the SS indicates that sediment could act as potential source for phosphate in the overlaying water column and could enhance algal bloom in the SS.

4.14 Kinetics of P desorption

Desorption process was evaluated after single point adsorption of sediment. The amount of cumulative desorption was higher during first 6hr of equilibration than the successive

equilibration phase. The cumulative desorption of P from the lake sediment gradually increases and the desorption curve flattens after 42 hr of desorption (Appendix). The desorption curve also showed two reactions, first one is faster desorption during initial 6 hr and second one is slow desorption afterwards. The initial rapid reaction is attributed to more labile P pools whereas slow desorption is attributed to less labile pool. P desorption was higher for sediment of NS and CS during initial 6 hr indicating presence of more desorbable P in the sediment of Cs and NS. The desorption data were fitted to Elovich equation and Parabolic diffusion for better understanding of desorption process. In Elovich model, cumulative P desorption was plotted against natural log of time. The Elovich equation is,

$$Q = (1/\beta) \ln \alpha\beta + (1/\beta) \ln t$$

Where, q is concentration of P in the sediment at time t ($\mu g\ g^{-1}$), time (h), and α, β are the desorption constant. β is the rate of P desorption while α is desorption constant.

Rate of desorption (β) varied across the lake from 0.36 to 5.52 mg P kg^{-1}, with sediments of CS showing the highest rate of desorption (5.52 mg P kg^{-1}) (Table 4.20). Average rate of P desorption was highest for CS (mean = 1.19 mg P kg^{-1}) followed by NS (mean = 0.78 mg P kg^{-1}) and SS (mean = 0.51 mg P kg^{-1}). Rate of P desorption of soils from different land use varied from 0.50 to 4.59 mg P kg^{-1}, with the mean value of α increased in the order of agricultural soil (1.96 mg P kg^{-1}) > forest soil (2.09 mg P kg^{-1}) > fallow field (2.43 mg P kg^{-1}). Whereas, value of desorption constant varied from 0.01 to 2.42 mg P kg^{-1} hr^{-1}. Greater β value in agricultural soil than lake sediment suggest that agricultural soil is more susceptible to P loss due to desorption. The value of desorption rate varied from 0.39 to 1.49 mg P kg^{-1} for sediments of the river draining to lake whereas value of α varied from 1.90 to 27.07 mg P kg^{-1} hr^{-1}.

The kinetics data were also fitted to Parabolic diffusion equation to test its suitability explaining the desorption process. The parabolic diffusion equation is,

$P = Rt^{1/2} + b$, where P is quantity of P desorbed in time t, R is diffusion rate constant (desorption rate factor), b is related to intensity parameter. The linear relationship between $t^{1/2}$ and cumulative P desorbed indicates that P desorption is a diffusion-controlled process. The value of R was higher for SS (0.97 mg P kg^{-1} $hr^{-0.5}$) followed by NS (0.73 mg P kg^{-1} $hr^{-0.5}$) and CS (0.57 mg P kg^{-1} $hr^{-0.5}$) however the value of b was higher for CS and CS, and similar to desorption constant of Elovich equation (Table 4.20). R value of soils from different land use varied from 0.10 to 0.91 mg P kg^{-1} $hr^{-0.5}$ with highest mean value observed in soils of forest (0.35 mg P kg^{-1} $hr^{-0.5}$) followed by agricultural soil (0.23 mg P kg^{-1} $hr^{-0.5}$) and fallow soil (0.20 mg P kg^{-1} $hr^{-0.5}$). The value of intensity factor (b) was highest for agricultural soil followed by forest soil and fallow soil. The value of diffusion rate constant varied from 0.30 to 1.17 mg P kg^{-1} and value of intensity factor varied from 0.73 to 3.23 mg P kg^{-1}.

In this study, magnetic adsorbent was synthesized using chemical co-precipitation method. La was doped into magnetite to synthesise lanthanum based magnetic adsorbent at 5%, 25%, 50%, and 75% mass ratio of La $(OH)_3$/$(LaOH)_3$ + Fe_3O_4).

4.15 Characterization of magnetite and M-La $(OH)_3$

4.15.1 XRD

The method of synthesis and concentration of the chemical reagent used determine their physical and chemical properties influencing its crystallinity. The XRD pattern of pure La $(OH)_3$, Fe_3O_4, and M-La $(OH)_3$ with different La $(OH)_3$/ (La $(OH)_3$ + Fe_3O_4) ratios are shown in Fig 4.9. Characteristic diffraction peak at 2θ = 15.5°, 27.1°,27.9° 31.4°, 39.1°, 42.1°, 48.4°, 55° are well indexed as hexagonal phase of lanthanum hydroxide, which is found to be in good agreement with the Joint Committee on Powder Diffraction Standards (JCPDS No. 36-1481) (Lin *et al*., 2019). Well defined cubic structure of magnetite was evidenced by characteristics diffraction peak at 2θ = 30.1°, 35.4°, 43.1°, 57°, and 62.6° (JCPDS No. 019-0629) (Fang et al.,

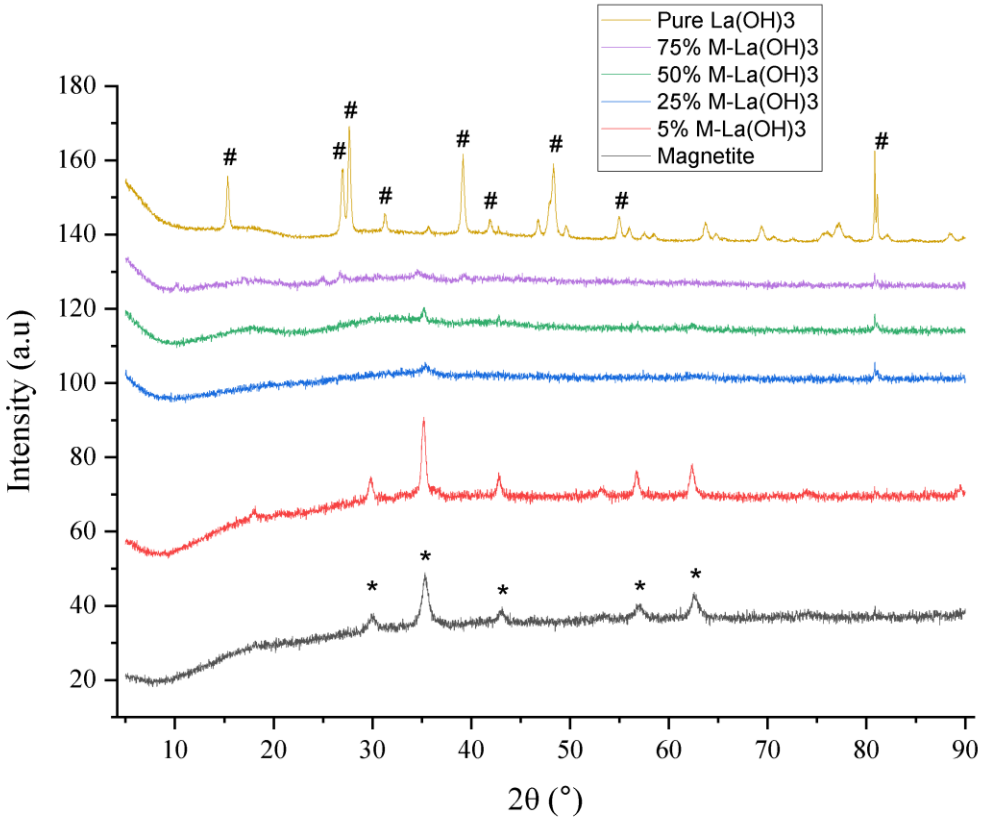

Fig.4.9 XRD diffraction pattern of pure La $(OH)_3$ and M-La $(OH)_3$ with different content of La $(OH)_3$.

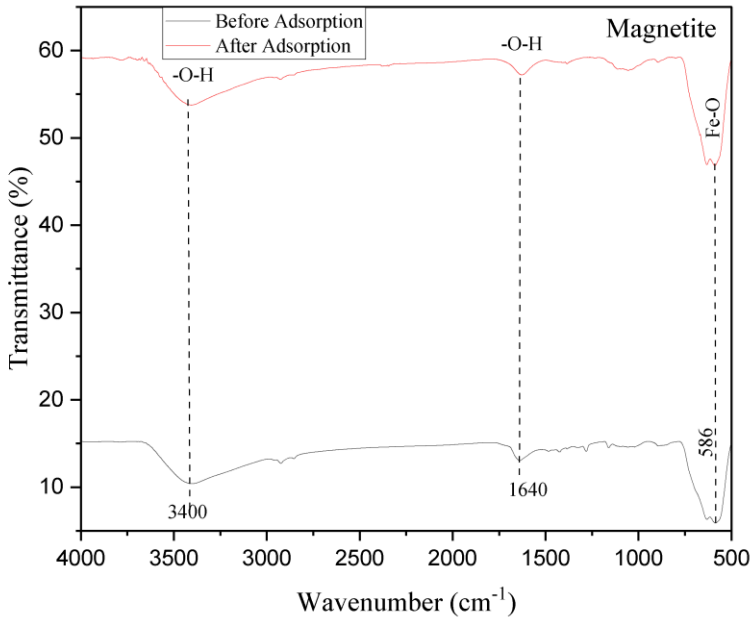

Fig 4.10. (a). FTIR spectra of magnetite before and after phosphate adsorptio

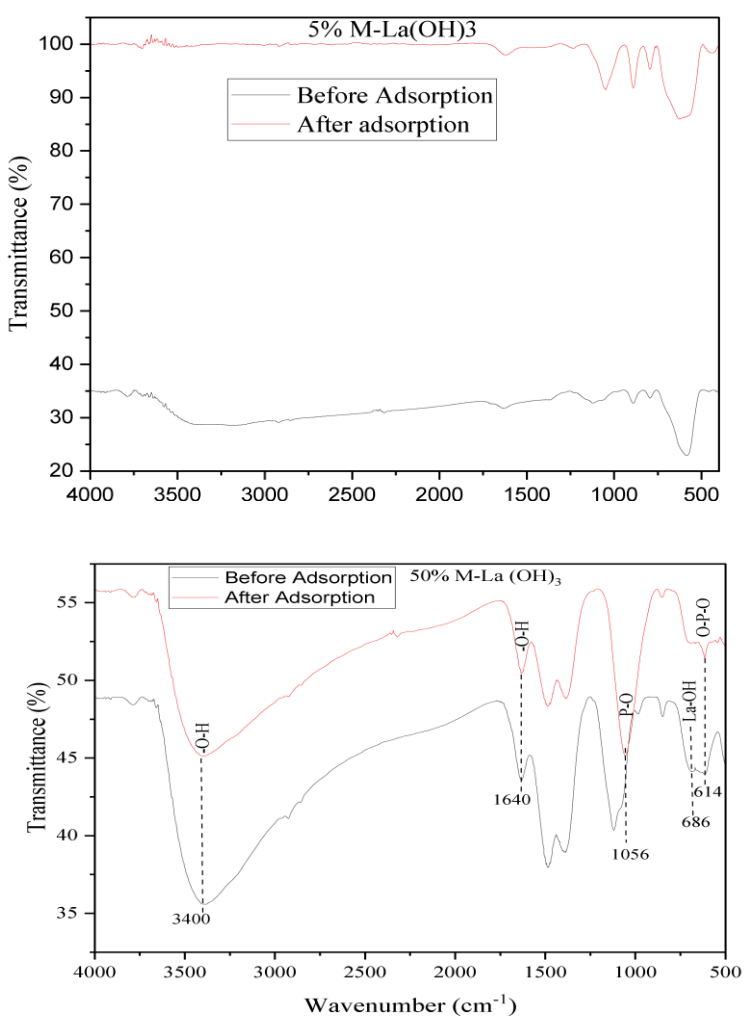

Fig 4.10. FTIR spectra of (b) 5% M-La $(OH)_3$ (c) 25% M-La (OH)3 (d) 50% M-La (OH), (e) 75% M-La $(OH)_3$before and after phosphate adsorption.

2017). In the XRD pattern of synthesized M-La $(OH)_3$, not only the characteristics peak of La $(OH)_3$ (27.1°, 39.1°, 80.8°) but also the characteristics peak of magnetite was observed. The characteristics peak of La and magnetite was identical with the peaks observed by Xing et al. (2014). The observation demonstrates that synthesized M-La $(OH)_3$ have intact crystal structure of both magnetite and La $(OH)_3$. Intensities of characteristic peaks of La $(OH)_3$decrease with decreasing content of La $(OH)_3$ in M-La $(OH)_3$hybrid. Intensities of the characteristics peak of magnetite decrease with increase in La $(OH)_3$ content in the M-La $(OH)_3$hybrid. The mean crystallite size of the M-La $(OH)_3$ was calculated based on FWHM (Full Width at Half Maximum) using Debye-Scherrer equation, as: $D = \frac{0.89\lambda}{\beta cos\theta}$

Where, λ is the X-ray wavelength used (1.5406 A°), θ is diffraction angle, and β is the full width at half maximum (FWHM, in radians) of diffraction peak. The calculated crystallite size was calculated to be 4 nm. Thus, indicating the nano size of synthesized magnetite.

4.15.2 FTIR analysis

FTIR was carried out to identify different functional groups present on the synthesized material. FTIR spectra of samples before and after P adsorption was carried out to investigate the mechanism of phosphate removal by M-La $(OH)_3$ composite. FTIR peaks in the range of 400-4000 cm^{-1} are shown in the Fig 4.10 (a-e). The FTIR spectrum of synthesized magnetite exhibited vibration at 586, and 631 cm^{-1} characteristics of magnetite (Zheng *et al*., 2011). The narrow and intense band at 586 cm^{-1} could be due to vibration of Fe^{2+} -O^{2+} functional group. The splitting peak at 631 cm^{-1} could be attributed to symmetry degeneration on octahedral B sites (Zheng *et al*., 2011). There is a wide transmittance around 3400 cm^{-1} and small peak at 1640 cm^{-1}, which could be due to stretching vibration of O-H group and bending vibration of surface adsorbed H-O-H molecule on surface of magnetite (Kumari *et al*., 2015; Liu *et al*., 2019). As show in Fig 2, synthesized 50% M-La $(OH)_3$ adsorbent before P adsorption exhibit

two distinct band at 614 and 686 cm^{-1} which can be assigned to bending vibration of La-OH bonds (Li *et al*., 2012).

4.15.3 SEM

Scanning electron microscope (SEM) is a powerful tool for material characterization. SEM is used for morphological studies (texture, pore size) of the material as it uses electron for imaging of material under investigation. Fig 4.11. shows the surface morphology of magnetite and M-La $(OH)_3$. SEM image of pure magnetite revealed its diameter from 969nm- 6.5 µm, which is more than the size of Fe_3O_4obtained by co-precipitation method. Further coating of La on magnetite formed a smooth surface (Fig. 4.1). During the loading of La $(OH)_3$, the Fe_3O_4 particles were entrapped in the matrix. Morphology of Fe_3O_4 remains intact after loading of La $(OH)_3$. Formation of new structure with precipitation of La $(OH)_3$ causes increase in size of the nanocomposite. The particle size of M-La $(OH)_3$ increased to 198 nm-8.41µm. EDX further confirms the successful formation of M-La $(OH)_3$, as it has peaks of La, Fe, O in the EDS spectrum. Different areas were focused during EDX measurement and the corresponding peaks were recorded. Both Fe_3O_4 and La $(OH)_3$ can be seen in the synthesized composite nanostructure in the EDX spectrum. Details of the EDX spectra of the composite measured in atomic and weight % are presented in Fig 4.11. The quantity of La, Fe, and O for 5% M-La $(OH)_3$ were 3.13, 62.51, and 34.36 respectively and 17.42, 29.30, and 45.97 for 50% M-La $(OH)_3$.

4.15.4 BET

A large portion of the atom in a nanomaterial is present at its surface area which determine properties of the particle. Therefore, determination of specific surface area (SSA) is essential to understanding the behaviour of the nanomaterials. Brunauer-Emmett-Teller(BET) method was used to determine specific surface area of the pure magnetite and M-La $(OH)_3$ based on

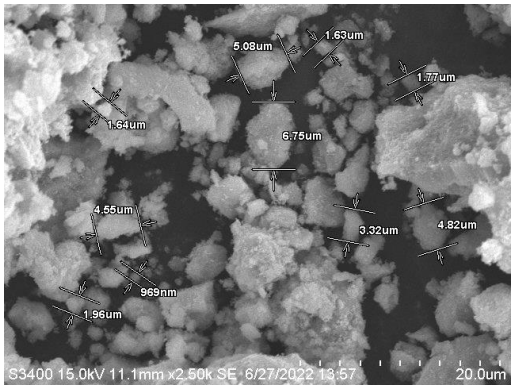

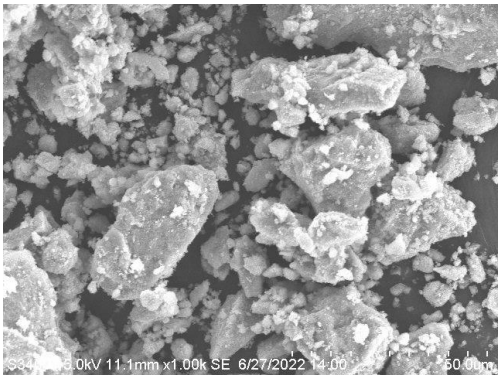

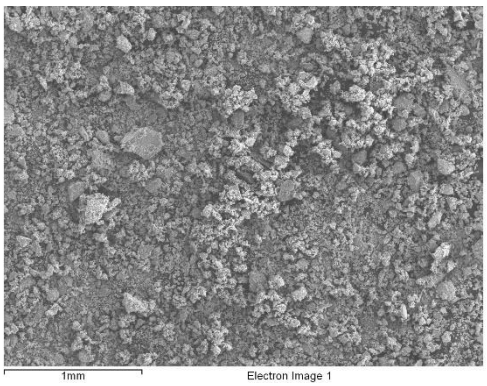

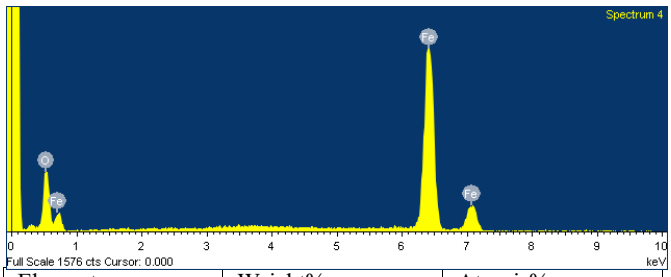

Element	Weight%	Atomic%
O K	34.09	64.35
Fe K	65.91	35.65
Total	100	

(a) SEM images and EDX spectra for Magnetite

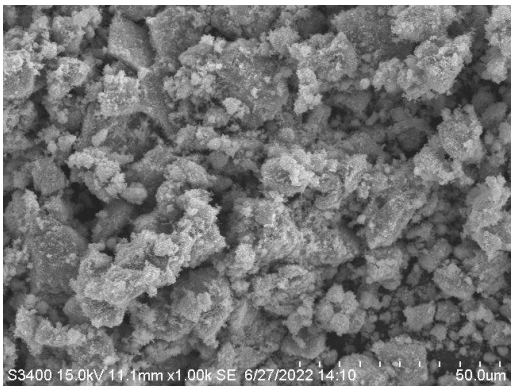

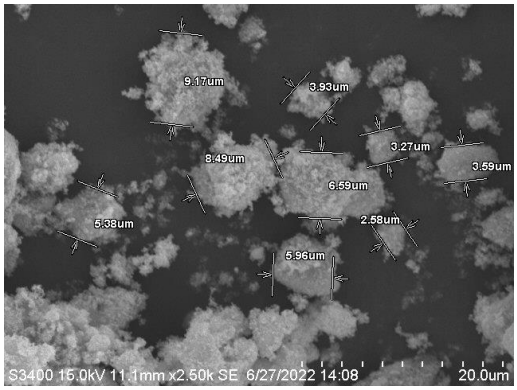

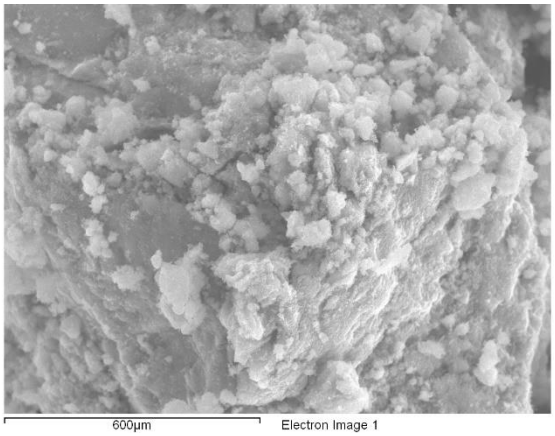

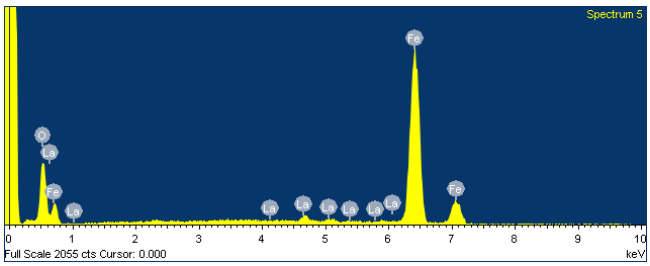

Element	Weight%	Atomic%
O K	O K	34.36
Fe K	Fe K	62.51
La L	La L	3.13
Total	100	

(b) SEM images and EDX spectra for 25% M-La $(OH)_3$.

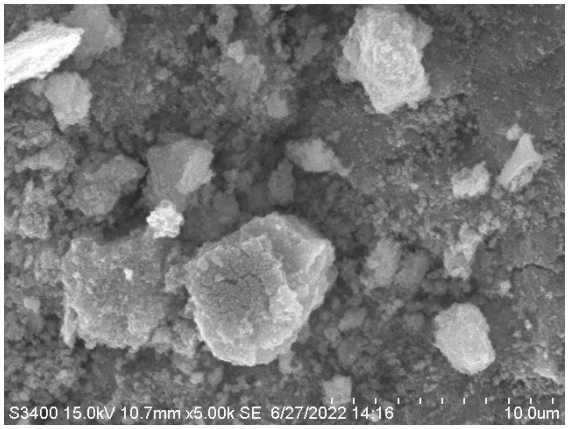

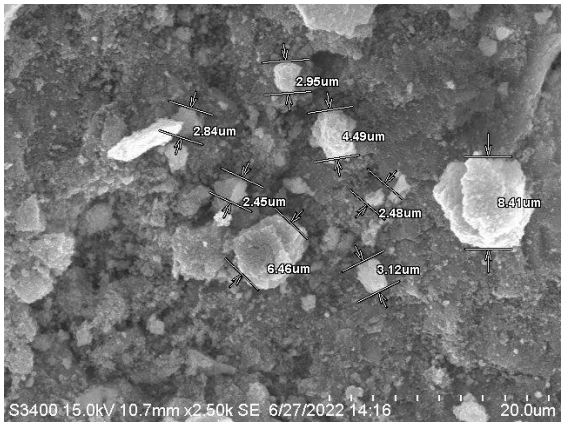

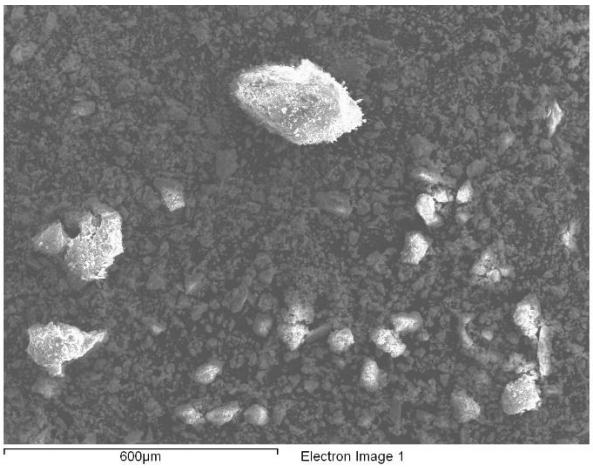

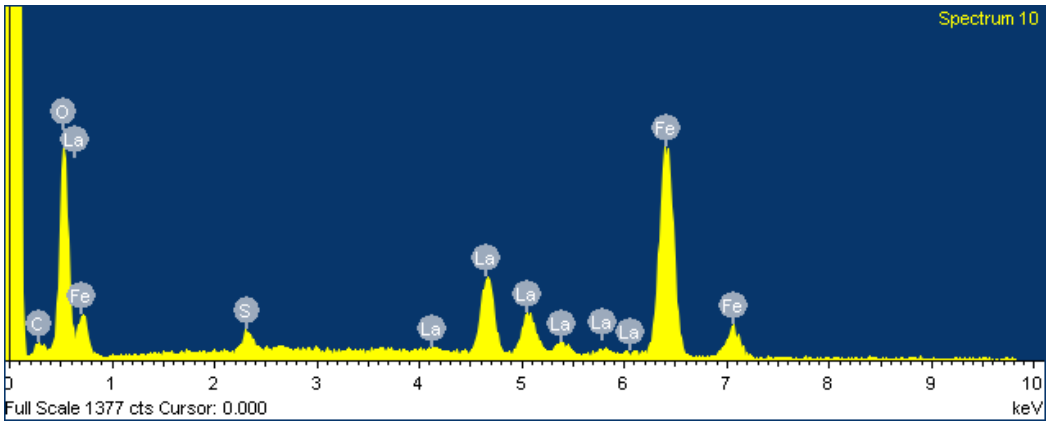

Element	Weight%	Atomic%
C K	5.89	12.08
O K	45.97	70.80
S K	1.43	1.10
Fe K	29.30	12.93
La L	17.42	3.09
Totals	100.00	

Fig 4.11. (c) SEM images and EDX spectra for 50% M-La $(OH)_3$.

Table 4.21 Specific surface area and pore size distribution of magnetite and M-La $(OH)_3$.

Material	Parameters	Adsorption	Desorption	BET
Magnetite	Surface area (m^2/g)	85.331	105.98	93.066
	Pore volume (cc/g)	0.875	0.88	
	Pore radius Dv (r) (A)	86.863	61.884	
5% M-La $(OH)_3$	Surface area (m^2/g)	60.79	76.642	64.193
	Pore volume (cc/g)	1.551	1.557	
	Pore radius Dv (r) (A)	925.37	87.447	
25% M-La $(OH)_3$	Surface area (m^2/g)	109.976	151.073	182.182
	Pore volume (cc/g)	0.437	0.455	
	Pore radius Dv (r) (A)	17.083	17.006	
50% M-La $(OH)_3$	Surface area (m^2/g)	99.709	114.275	163.632
	Pore volume (cc/g)	0.445	0.448	
	Pore radius Dv (r) (A)	15.302	17.019	
75% M-La $(OH)_3$	Surface area (m^2/g)	110.936	136.578	156.237
	Pore volume (cc/g)	0.367	0.379	
	Pore radius Dv (r) (A)	15.294	17.031	

nitrogen adsorption isotherm measurement at 77K. Adsorption isotherm between amount of gas adsorbed and equilibrium pressure was used to derive SSA of the nanomaterial. Degassing is carried out on the dried sample to remove the dissolved gases, water and other impurities which could affect the N_2 adsorption. Specific surface area, pore assize and pore diameter of magnetite and M-La (OH)3 are presented in the Table 4.21.

The SSA of pure magnetite is found to be 93.07 m^2 g^{-1}, which is higher than 5% M-La $(OH)_3$. Decrease in SSA of M-La $(OH)_3$ could be due to increase in size of particle and aggregation of particle during synthesis (Wu *et al*., 2017). However, the SSA of other M-La $(OH)_3$ is greater than pure magnetite. The SSA of synthesized M-La (OH)3 follows the order 25% M-La $(OH)_3$> 50% M-La $(OH)_3$> 75% M-La $(OH)_3$> 5% M-La $(OH)_3$. The N_2 adsorption-desorption isotherm of M-La $(OH)_3$ exhibited characteristics of type IV adsorption isotherm suggesting existence of mesopore. Pore size was measured using Barret-Joyner-Halenda (BJH) adsorption and desorption isotherm methods. The average pore radius of synthesized magnetite was 7.4 nm, and pore radius of 5% M-La $(OH)_3$, 25% M-La $(OH)_3$,50% M-La $(OH)_3$, 75% M-La (OH)3 were 5.06, 1.7, 1.6, and 1.56 nm respectively, which falls in mesopore range according to IUPAC classification. Average pore volume of synthesized M-La $(OH)_3$ was 0.70 cc g^{-1}.

4.15.5XPS

Generally surface properties of adsorbents are analysed using X-ray photoelectron spectroscopy. To measure the chemical composition and probe further in to mechanism behind complexation between phosphate and M-La $(OH)_3$ XPS of 50% M-La $(OH)_3$ before and after adsorption was performed. The wide scan XPS spectra indicates presence of Fe, O, and La elements suggesting successful adsorption of phosphate on to the adsorbent (Fig 4.12.a). The high-resolution spectra of La 3d before and after adsorption were illustrated in the Fig 4.12.b. The characteristics peak of La 3d1/2 are located at binding energy of 849.45 eV and 853.4 eV and peaks of La 3d5/2 are centred at binding energy of 832.8 eV and 836.65 eV. Shifting in

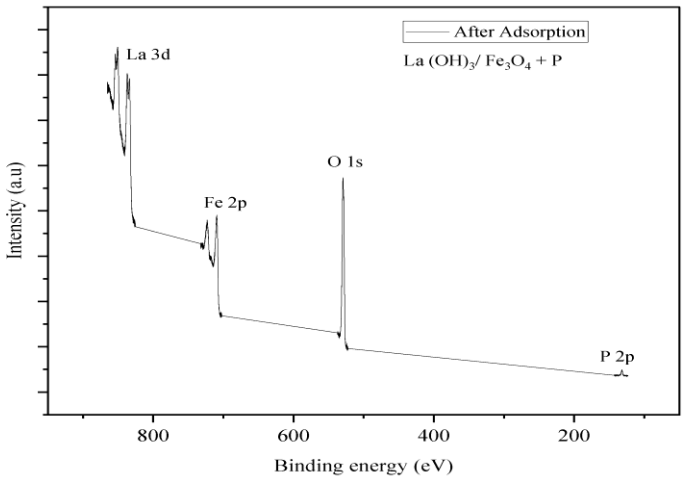
After Adsorption
La (OH)3/ Fe3O4 + P
La 3d
Fe 2p
O 1s
P 2p
Intensity (a.u)
800
600
400
200
Binding energy (eV)

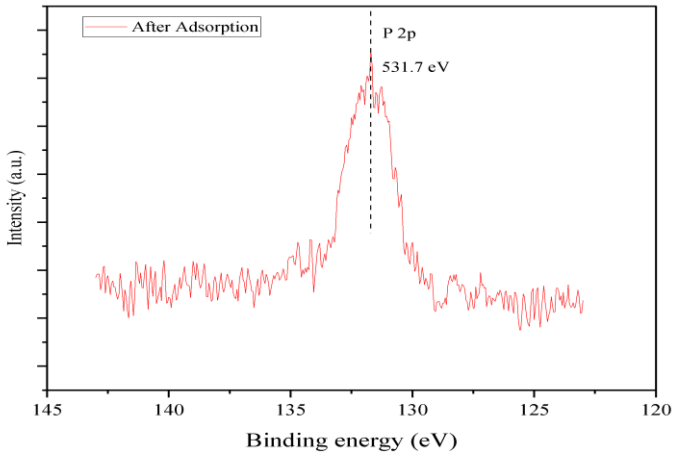
After Adsorption
P 2p
531.7 eV
Intensity (a.u.)
145
140
135
130
125
120
Binding energy (eV)

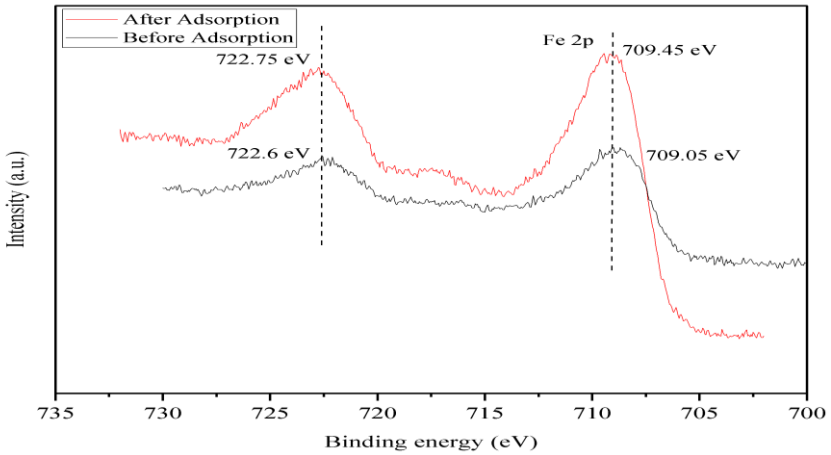
After Adsorption
Before Adsorption
722.75 eV
722.6 eV
Fe 2p
709.45 eV
709.05 eV
Intensity (a.u.)
735
730
725
720
715
710
705
700
Binding energy (eV)

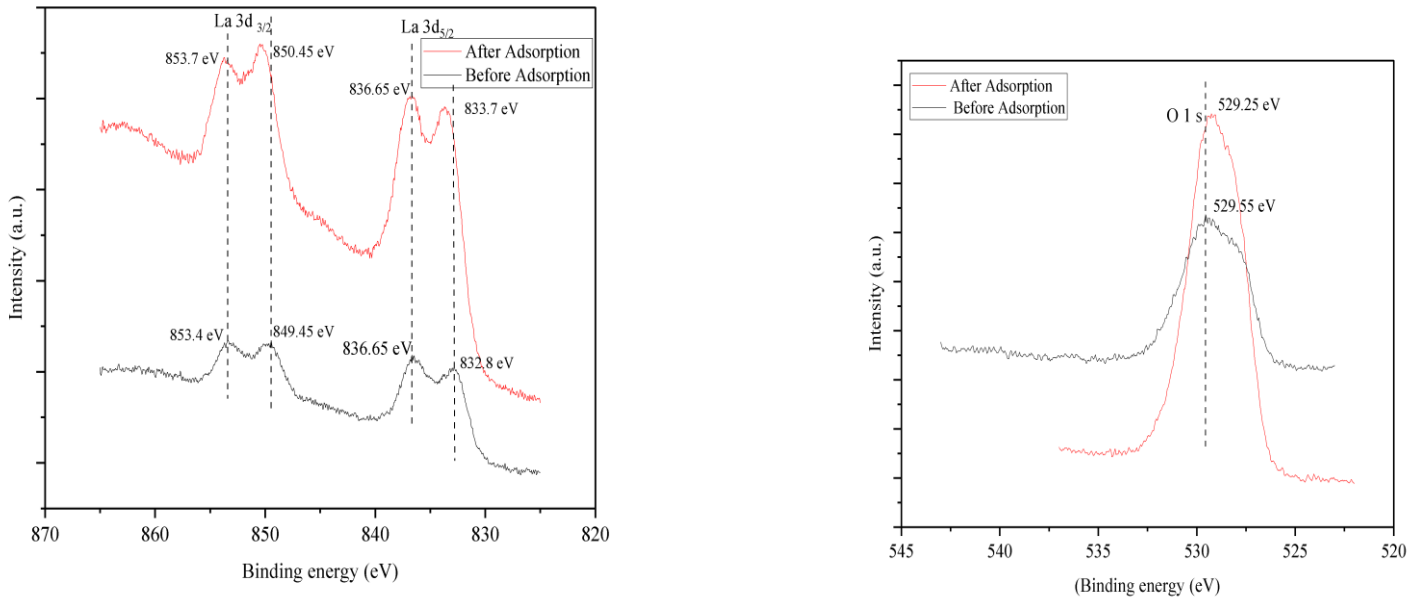

Fig 4.12. XPS spectra of (a) wide scan, (b) P 2p, (c) Fe 2p, (d) La 3d (e) O 1s of 50% M-La $(OH)_3$ before and adsorption of P

binding energy of La 3d1/2 and La3d5/2 to a higher value after phosphate could be due to possible transfer of electron from valance bond of La 3d to 4f orbital of La atom, suggesting formation of La-O-P inner sphere complex. These observations were in line with the finding reported in other literature describing possible mechanism behind phosphate adsorption onto La based adsorbent (). The Fe 2p spectra showed that the peak at 709.05 eV shifted to higher value of 709.45 eV after P adsorption suggesting formation of Fe-P bond (4.12.c). Appearance of characteristics peak of P 2p at binding energy of 131.7 eV after adsorption suggest formation of complex between phosphate and La $(OH)_3$(Fig 4.12.d). The high-resolution spectra of O 1s can be divided into three overlapping peaks at 530.4, 531.4, and 533.3 eV corresponding to O^{2-}, OH^-/ O-P, and H_2O respectively (Fig. 4.12.e). Relatively decreased intensity at 529.55 for M-La $(OH)_3$ after adsorption could be due to binding of P with O-La or O-Fe, subsequently forming La-O-P and Fe-O-P bond.

4.15. 6 Magnetic properties:

Magnetic properties of the synthesized adsorbents were analysed at room temperature by using the magnetic hysteresis curve. Saturation magnetization values magnetite is 43.7 emu g^{-1} and for 5% M-La (OH)3 its was 41.1 emu g^{-1}. Lower values of saturation magnetization observed in M-La $(OH)_3$ could be attributed to increase in lanthanum content, thereby diluting the magnetic property. However, the saturation magnetization value was sufficient for separation from aqueous solution. Presence of magnetic property in the adsorbents helps for its easy separation from aqueous solution suing external magnetic field.

4.16 Sorption isotherm of phosphate in water

Maximum phosphate sorption capacity of the synthesized M-La $(OH)_3$ with different ratio of La $(OH)_3$ was investigated by conducting sorption isotherm as a function of phosphate concentration (0, 10, 20, 30, 40, 50, 75, and 100 mg P L^{-1}). The phosphate adsorption data were

fitted to both Langmuir and Freundlich model. The sorption constant of the experiment is presented in the Table 4.22. The adsorption data fitted well to the Langmuir equation over the entire range of P concentration studied, suggesting monolayer P sorption onto the homogenous sites of the M-La $(OH)_3$. This may be attributed to selective adsorption between phosphate and lanthanum (Dithmer et al., 2015). According to the classification of Giles (1960), the isotherm was L shaped (Fig. 4.13) indicating high affinity of adsorbate at low concentration, with the affinity diminishing as the initial concentration of phosphate increases. The adsorption data were fitted to Langmuir equation by plotting Ce versus Ce/x/m (Fig. 4.14). The results show that the regression values of phosphate sorption isotherm using Langmuir equation varied from 0.80 to 0.99 (Table 4.22). A graph of log Ce versus log x/m was plotted and the data pertaining to the graph was fitted to Freundlich equation (Fig. 4.15). The result shows that the regression coefficient varied from 0.93 to 0.99. A comparatively higher value of coefficient of regression in Langmuir equation as compared to Freundlich equation indicates that monolayer adsorption of phosphate on surface of M-La $(OH)_3$.

The q_{max} value obtained from the Langmuir equation indicates maximum adsorption capacity of the material. Maximum P adsorption capacities of M-La $(OH)_3$increased from 18.8 to 50.6 mg P/g of adsorbate as La content increase from 5%M-La $(OH)_3$ to M-La $(OH)_3$75% (Table 4.22). Maximum P adsorption capacities of 50% M-La $(OH)_3$(47.7 mg P g^{-1})) and 75% M-La $(OH)_3$(50.6 mg P g^{-1}) are comparable which are higher than MPAC of lower contents of M-La $(OH)_3$. Maximum P adsorption capacities observed in our study is comparable to MPAC of other magnetic or La based adsorbent reported in other literature (Wu *et al*., 2017, Fang *et al*., 2017). P removal capacities of M-La $(OH)_3$ is higher than that of pure magnetite and pure La

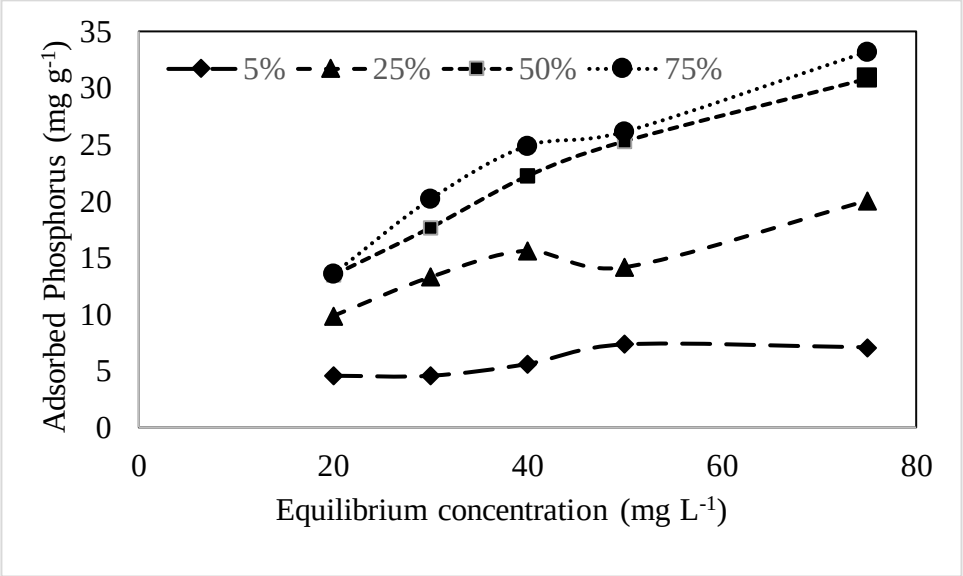

Fig 4. 13 Langmuir isotherm for phosphate sorption by M-La $(OH)_3$ by prepared with 5, 25, 50, and 75 % substitution of La.

Table 4.23 Fitted parameters for pseudo first order and pseudo second order kinetics for 50% M-La $(OH)_3$.

Pseudo first order			Pseudo second order		
qe (mg P g^{-1})	K_2 (1/min)	R^2	qe (mg P g^{-1})	K_2 (g/ mg-min)	R^2
33.14	0.15	0.72	35.88	0.0064	0.93

q_t and q_e are the sorption capacities (mg/g) at time t and at equilibrium, respectively; k_2 is the rate constants of pseudo-second-order sorption (mg/g/min); t is the contact time (min).

Table 4.22 fitted parameter for Langmuir and Freundlich isotherm of phosphate adsorption on M-La $(OH)_3$

Sorbents	Langmuir isotherm			Freundlich isotherm		
	q_{max} (mg-P/g)	K_L(L/mg)	R^2	n	K_f ($\mu gmLg^{-1}$)	R^2
M-5% La $(OH)_3$	18.8^a	0.016^a	0.80	1.69^a	0.83^a	0.94
M-25% La $(OH)_3$	35.9^b	0.026^b	0.99	1.81^b	2.37^b	0.99
M-50% La $(OH)_3$	47.7^c	0.032^c	0.97	1.85^b	3.66^c	0.98
M-75% La $(OH)_3$	50.6^c	0.034^c	0.99	1.82^b	3.91^c	0.93

Qmax, Maximum P adsorption capacity, K_L, Bonding energy

Means followed by different lower-case letters are significantly different ($p < 0.05$)

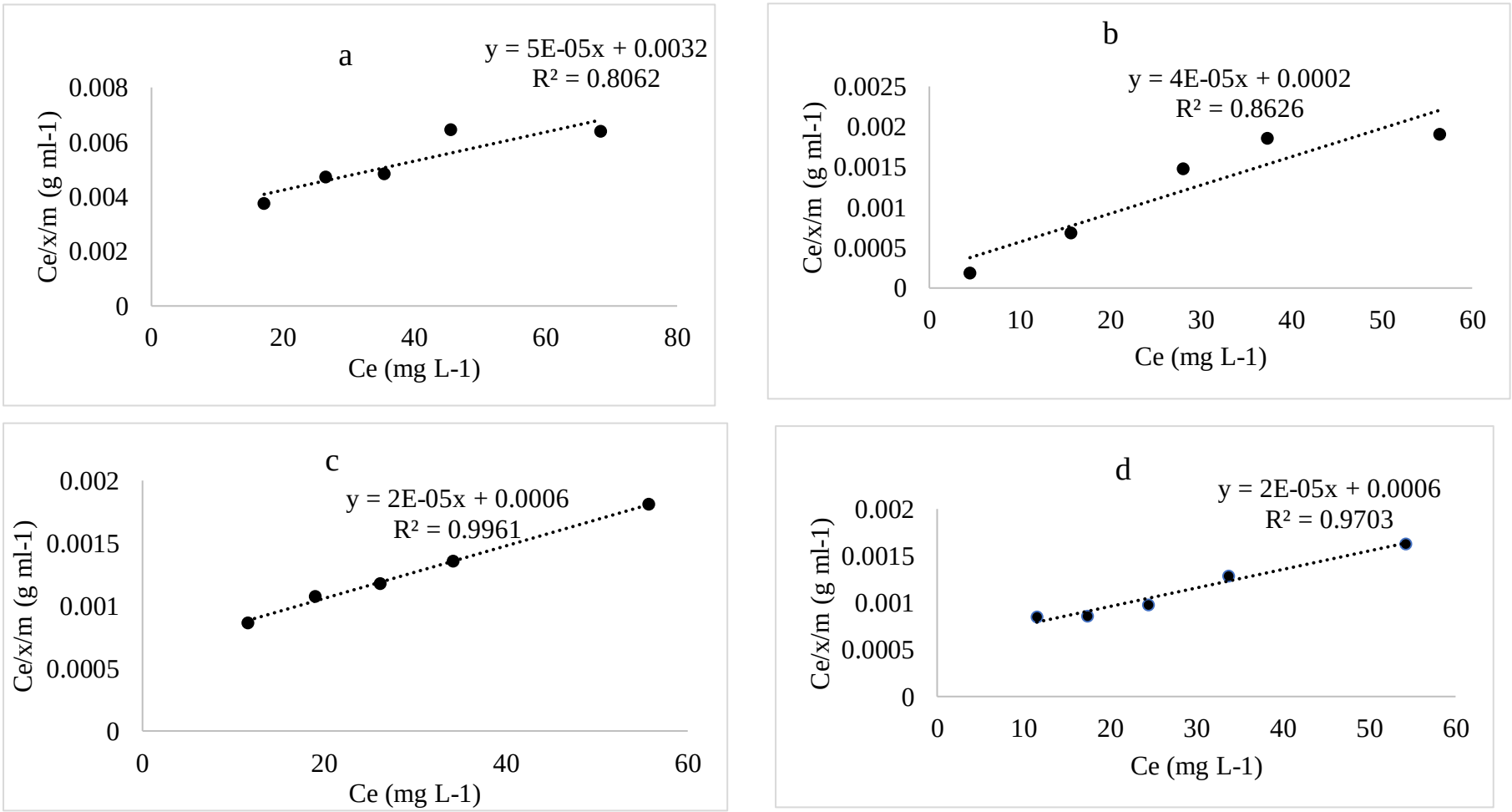

Fig 4.14. Langmuir isotherm for M-La $(OH)_3$ with different La $(OH)_3$ content. (a) 5% M-La $(OH)_3$, (b) 25% M-La $(OH)_3$, (c) 50% M-La $(OH)_3$, (d) 75% M-La (OH)

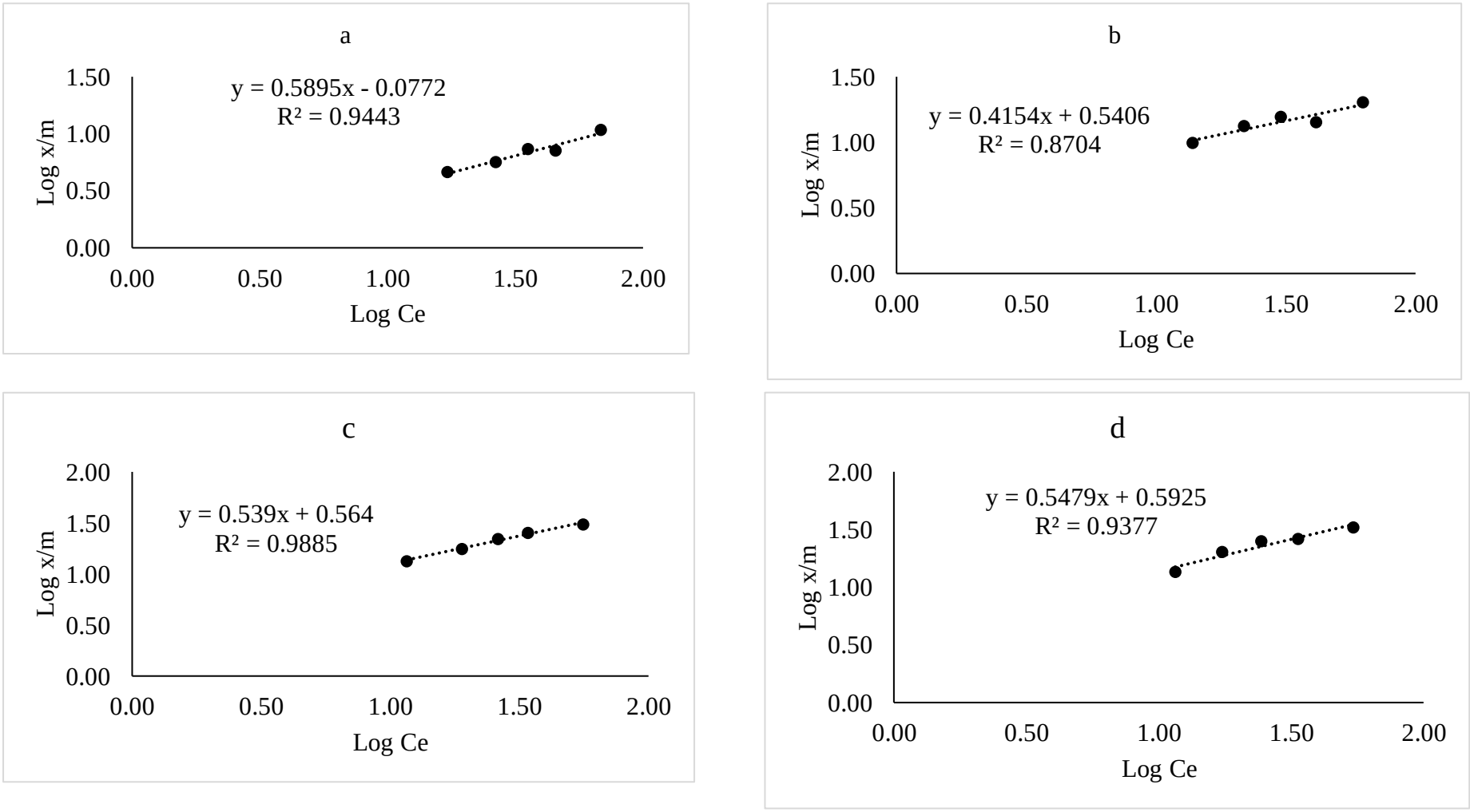

Fig 4.15. Freundlich isotherm for M-La $(OH)_3$ with different La $(OH)_3$ content. (a) 5% M-La $(OH)_3$, (b) 25% M-La $(OH)_3$, (c) 50% M-La $(OH)_3$, (d) 75% M-La $(OH)_3$.

$(OH)_3$. Higher phosphate sorption capacity in our study was due to difference in the number of active sites (i.e., La) that are responsible for P sorption, the density of surface hydroxyl group on the active sites, and surface charge on surface of sorbents. In addition, lanthanum hydroxide provides more adsorption sites (hydroxyl sites) than lanthanum oxides (Zhang *et al*., 2012). Wu et al. (2017) attributed P sorption to the electrostatic attraction between positive surface of La $(OH)_3$ and negatively charged phosphate species.

The formation of lanthanum-phosphate inner sphere complex via ligand exchange plays a significant role in removal of P by pure lanthanum hydroxide (Xie *et al*., 2014; Lin *et al*., 2019). High P removal by other La or magnetite-based adsorbent was documented in the literature (Chen *et al*., 2018; Fu *et al*., 2018; Kong *et al*., 2018). Fu *et al*. (2018) attributed phosphate removal by magnetite to the ligand exchange between PO_4^{3-} and OH^- group. Therefore, we can conclude that formation of inner sphere complex and ligand exchange are two primary driving factors for phosphate removal by La based magnetic sorbents.

Magnetic properties of M-La $(OH)_3$helps to efficiently recover the La element after treatment. Considering the increment of La content from 50% M-La $(OH)_3$to 75% M-La $(OH)_3$, increment in P adsorption capacity is negligible. Therefore, 50% M-La $(OH)_3$is suggested as best magnetic sorbent for effective removal of P.

4.17 Sorption kinetics of phosphate in water

The kinetics experiment was conducted to compare the rate constant of the sorption kinetics of different ration of M-La $(OH)_3$ composite for removal of phosphate from water. The P removal efficiency as a function of time is depicted in the Fig 4.16. It was observed that sorption of 30 mg P L^{-1} phosphate to M-La $(OH)_3$ was rapid and reached equilibrium within 120 minutes. The strong affinity of La for P makes the sorption kinetics a rapid reaction (Fang *et al*., 2017). To

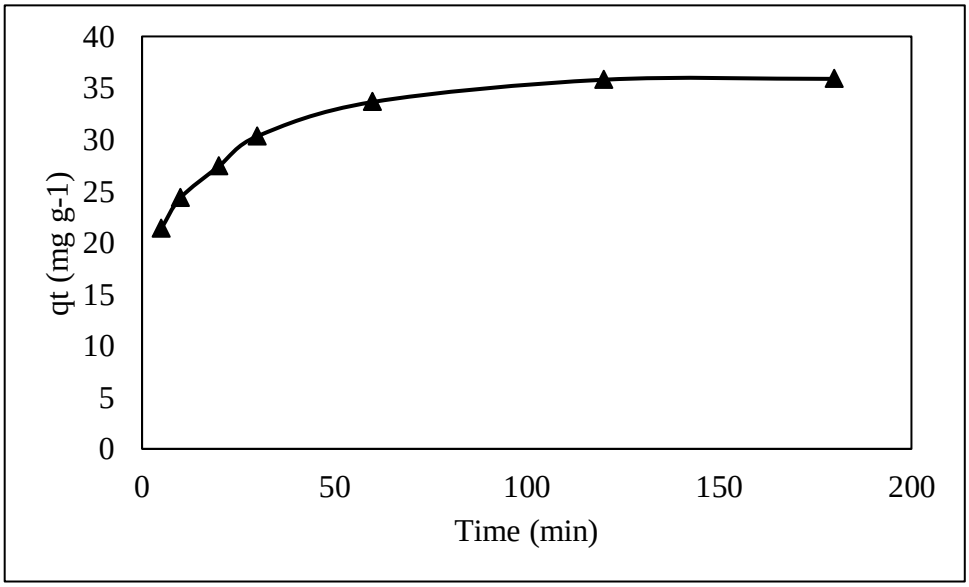

Fig 4.16. Amount of P adsorbed by 50% M-La $(OH)_3$ as a function of time

further understand the sorption kinetics, the data was fitted to pseudo-second-order model using following equation;

$$qt = \frac{q_e^2 k_2 t}{1+q_e^2 k_2 t}$$

where q_t and q_e are the sorption capacities (mg/g) at time t and at equilibrium, respectively; k_2 is the rate constants of pseudo-second-order sorption (mg/g/min); t is the contact time (min).

The kinetics rate constant and other fitted parameter were presented in the Table 4.23 and Fig. 4.19. Perusal of Table 4.23 shows that data fitted to both the kinetic models i.e., pseudo-first order and pseudo-second order model with a high R^2 value. Correlation coefficient of adsorption kinetics was 0.72for pseudo first order and 0.93for pseudo second order reaction. Similar results were observed for other phosphate sorption by magnetite or La based adsorbents such as, Lanthanum hydroxide (Xie *et al*., 2014), Magnetite lanthanum hydroxide (Lin *et al*., 2019; Fang *et al*., 2017), Lanthanum modified SBA-15 (Yang *et al*., 2011), and lanthanum modified polyacrylonitrile fibres (He *et al*., 2015).

Relatively higher correlation coefficient for pseudo second order kinetics indicates that P adsorption to M-La $(OH)_3$ was a chemisorption process. Our findings agree with the findings of phosphate sorption to other magnetite and lanthanum hybrids reported in the literature (Chen *et al*., 2016, Fang *et al*., 2017).

4.18 Effect of pH on phosphate sorption

pH of the natural water varies widely, especially in the eutrophicated lakes with high photosynthetic activity, where the pH can raise up to 10.5. Furthermore, pH of the solution influence speciation of P in solution, as it may change the surface properties of adsorbents. At pH lower than 2.1, neutral H_3PO_4 dominates, between pH 2.2 to 7.2, monovalent species

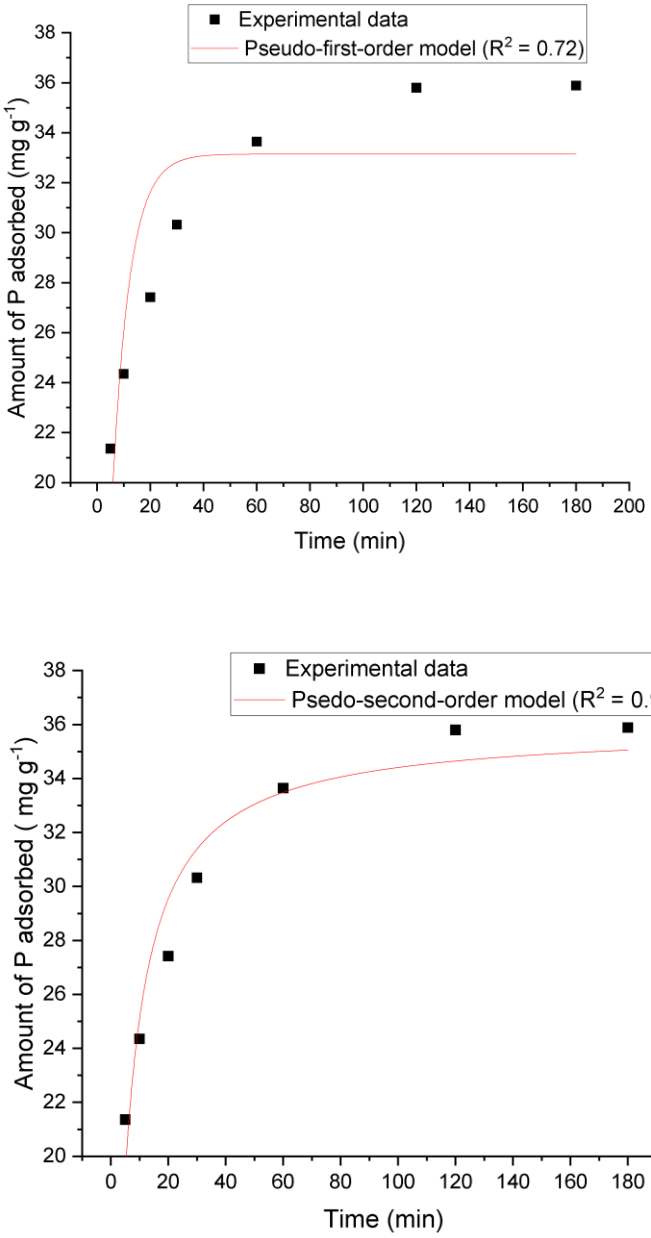

Fig 4.17 Pseudo first order and pseudo second order kinetics for phosphate sorption by 50% M-La $(OH)_3$.

$H_2PO_4^-$ dominates, and at pH more than 7.2, bivalent species HPO_4^{2-} dominates. Therefore, phosphate sorption by M-La $(OH)_3$ is strongly governed by the pH of the solution.

The effect of pH, from 3.5 to 11, on phosphate sorption by different ratio of M-La $(OH)_3$ were investigated and the results are presented in the Fig. 4.20. Phosphate removal was highest at pH 3.5 (86%) and rapidly diminished at higher pH (50% at pH 7.5). Then P removal extent gradually decreases to a minimum value of 30% at pH 10 and slightly increases up to 37% at pH 11. At lower pH, bivalent $H_2PO_4^{2-}$ predominates in water which results in electrostatic attraction between positive surface charge of M-La $(OH)_3$and negatively charged phosphate species giving maximum sorption capacity. However, with increase in pH, there is decrease in affinity of the surface of the M-La $(OH)_3$for divalent$H_2PO_4^{2-}$compared to monovalent $H_2PO_4^-$ resulting in drastic decrease in sorption capacity. A possible explanation is that at higher pH, there is an increase in hydroxyl ion which compete with phosphate ion for same adsorption site (Fu *et al*., 2018). Previous studies also suggest greater sorption capacity of M-La $(OH)_3$formonovalent $H_2PO_4^-$athigher pH due to hydroxylation of lanthanum ions (Zhang *et al*., 2011). At higher pH, the surface of M-La $(OH)_3$becomes less positively charged which is not favourable for strong electrostatic attraction, consequently decreasing sorption capacity (Xu *et al*., 2017). However, there was still Phosphorus sorption over pH 8, where other interaction process dominates other than electrostatic attraction, which were discussed in the next section. This result shows that adsorption process of M-La $(OH)_3$ was pH dependent, but still exhibit good phosphate removal capacity over a wide range of pH (between 3.5 to 11). The average pH of our studied lake was 8.5, and the P removal extent at that pH is 47%. Therefore, we could use M-La $(OH)_3$to sequester phosphate from lake water. As phosphate removal extent of M-La $(OH)_3$gradually decreases with increase in pH, it is necessary to apply the M-La $(OH)_3$forremediation of sediment prior to further increase in pH due to high photosynthetic activity of the Lagoon.

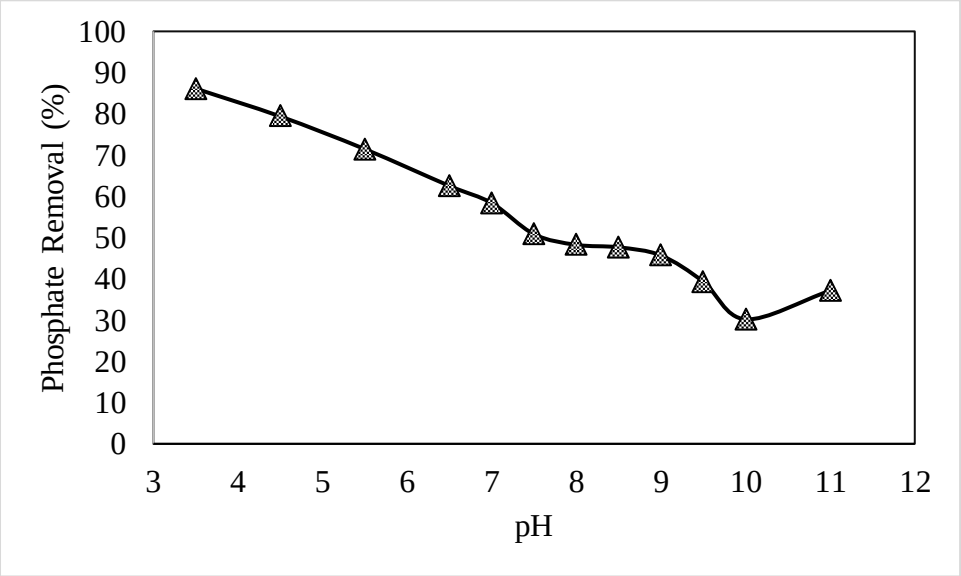

Fig 4.18. Effect of pH on P adsorption by 50% M-La $(OH)_3$

4.19 Removal mechanism of phosphate by M-La $(OH)_3$

To gain insight into P adsorption by M-La $(OH)_3$, FTIR analysis of sample after adsorption process was performed. As shown in Fig 4.10, after adsorption, there is slight shift in the band at 586 cm^{-1} to 591 cm^{-1}which corresponds to Fe-O bond, indicating the formation of Fe-O-P on the magnetic surface. In addition to this, there is a new peak observed at 1056 cm^{-1} corresponding to the asymmetric stretch *v*3 vibration of HPO_4^{2-} or $H_2PO_4^-$ for the lanthanum hydroxide upon P adsorption (Zhang *et al*., 2021). Zhang *et al*. (2021) attributed the band at 1051 cm^{-1} after P adsorption to stretching vibration of non-surface complexed P-O bonds of the adsorbed phosphate species. The new peak appearing at 614 cm^{-1} after P adsorption is attributed to bending vibration of O-P-O bonds. All these peaks described above are characteristic vibration bands of lanthanum phosphate (Huittinen *et al*., 2018). The characteristic bands for vibration of La-OH at around 686 cm-3 disappeared after P adsorption Fu *et al*. (2018) observed similar characteristic peak for La-OH bond. After P adsorption (Fig X a-e), characteristics peak at 478 cm^{-1}, 543 cm^{-1}, 614 cm^{-1}, and 1056 cm^{-1}coresoponding to vibration band of $LaPO_4$ indicating formation of inner-sphere complex between the phosphate and synthesized lanthanum hydroxide adsorbent (Zhang *et al*., 2016; Fang *et al*., 2017). Such ligand exchange can be described to the following equations;

$La\text{-}OH + H_2PO_4^- \leftrightarrow La\text{-}H_2PO_4 + OH^-$

$La{=}OH + H_2PO_4^- \leftrightarrow La = HPO4 + 2OH^-$

$La \equiv OH + PO_4^{3-} \leftrightarrow La \equiv PO4 + 3OH^-$

Change in pH of the solution after adsorption of phosphate by M-La $(OH)_3$ also suggest the involvement of ligand exchange process. Initial pH of the 30 mg P/L phosphate solution was

3.0, which gradually increased to 6.1 after adding the M-La $(OH)_3$after 2 hr. increase in pH of the solution was attributed to release of OH- during ligand exchange between phosphate and hydroxyl group as described above.

This finding agrees with the previous studies where a new peak was observed at 1038 cm-1 after P adsorption by magnetite forming P-O-Fe complex (Lu *et al*., 2013, Yoon *et al*., 2014). Adly *et al*. (2022) reported presence of sharp band at 3412 cm^{-1} and attributed it to presence of molecular water after adsorption of P.

Based on the characterization of M-La $(OH)_3$, 50% M-La $(OH)_3$was suggest as best adsorbent for removal of phosphate from aqueous solution of P. Adsorption of P to La $(OH)_3$was considered as a quick chemical reaction which reaches equilibrium within 2 hrs of shaking, so 2hr is recommended as equilibration time. Further significant P removal efficiency was observed between pH 7.5-9 which suggest that M-La $(OH)_3$ can be used as an effective adsorbent for phosphate removal from lake water till the lake water pH attains 9.5.

Chapter V

Summary and Conclusion

The present investigation to study the variation in water quality of Chilika lake (Odisha) with special reference to phosphorus and its sequestration using novel adsorbents was conducted at Department of Soil science and Agricultural chemistry, Institute of agricultural science, BHU during the year 2017-2022. The water samples of Chilika lake were analysed for determination of water quality index, trophic state index, and water quality variables in three seasons (Pre monsoon, Monsoon, and Post monsoon). Sediment samples of the Chilika lake, river and catchment area covering different land use system were collected during pre-monsoon and post-monsoon season and analysed for P speciation and its adsorption-desorption behaviour. A La based novel adsorbent was synthesized and used to evaluate the P removal efficiency. The results of the experiment were summarized here under;

(1) The depth of lagoon varied significantly for both season and sector, and was observed to deepest during monsoon season with a depth of 202 cm. Transparency of the lake was observed to be highest during monsoon season (95.06±67.77 cm) and lowest during pre-monsoon season (43.27±28.6 cm). spatial variation of transparency in the lagoon is evident with highest transparency observe in SS (105.87±50.74 cm) and lowest in NS (28.33±26.26 cm). The lagoon experiences highest salinity during PRM season (13.48±7.99 PSU) and lowest during monsoon season (2.42±2.37 PSU), whereas OC (14.41±13.44 PSU) experiences highest salinity and NS (8.86±2.65 PSU) experiences lowest salinity.

(2) There was significant seasonal variation in DO ($p < 0.001$), with the lagoon recording highest DO during post-monsoon season (10.35±1.95ppm) and lowest during pre-monsoon season (7.18±1.45 ppm). Seasonal variation of BOD was significant with highest BOD observed during PSM (2.9 ppm) followed by MON (2.64 ppm), and PRM (2.56 ppm) season. Significant seasonal variation of pH of the lake was observed with highest pH observed during PSM (8.6) followed by PRM (7.99), and MON (7.97).

(3) One-way ANOVA revealed significant seasonal and spatial variability in nitrate concentration with highest value recorded during PSM (5.6 µmol/l), followed by PRM (5.12 µmol/l), and MON (4.93 µmol/l). SS, which has sea water influence has maintained lowest nitrate concentration (2.95±1.5 µmol/l) in the lagoon and NS maintained the highest concentration (8.18±5.69 µmol/l) in the lagoon. Similar trend was observed for other nutrient concentration such as nitrite, ammonia, silicate, and phosphate in the lake. Chl-a which is index of algal growth in the lagoon varied significantly for sectors, with highest value observed in NS (1.12±0.97 µg/l) followed by OC (0.57±1.1 µg/l), CS (0.5±0.32 µg/l)), and SS (0.17±0.13 µg/l).

(4) Evaluation of TSI of lagoon revealed that SS, CS, and OC falls in mesotrophic state while NS falls in eutrophic state. WQI classifies the lagoon into four classes with, water quality of lagoon varied from moderate-good during PRM and poor- good during MON and PSM. Spatial variability of lagoon was evident with SS falls into good water quality, while CS falls into moderate and NS falls into poor water quality.

(5) PCA was used to extract three principal components explaining 68.70% variation of water quality in the lagoon. Strong loading for salinity in PC1, phosphate and nitrate in PC2, turbidity in PC3 suggest that these water quality variables control the overall water quality of the lagoon. Cluster analysis classifies the lagoon into two cluster (C1 and C2) based on similarity among the water quality variables, with C1 repressing stations

falling under north west and northern region of the lagoon where effect of agricultural runoff from the catchment area due to freshwater flow from the river influence its water quality. Water quality of the station falling under C2 is influenced by the urban sewage, industrial effluent and tidal flow and sea water exchange.

(6) Land use type significantly influence the forms of P in the soil, with agricultural site having highest value of L-P. Al & Fe-P of different land use type follows the order; agricultural site (101.32 mg kg^{-1}) > Fallow site (91.86 mg kg^{-1}) > Forest site (61.59 mg kg^{-1}). In case of Ca-P, the order is; settlement (670. 45 mg kg^{-1}) > agricultural site (31.92 mg kg^{-1}) > Forest site (29.58 mg kg^{-1}) > Fallow site (18.93 mg kg^{-1}). Soils from human settlement exhibit highest value of R-P followed by forest soil, fallow soil, and agricultural soil.

(7) Transport of soil from catchment area to lake significantly affect the distribution of form of P with increasing trend of total P observed from catchment area (395.12 mg kg^{-1}) to lake sediment (633.02 mg kg^{-1}) through river system (457.27 mg kg^{-1}). Similar trend was observed for L-P (field soil = 0.87, river = 0.84, lake = 1.63 mg kg^{-1}). As a percentage of total P, Al & Fe-P follows the order field soil (31.18%) > lake sediment (27.5%) > stream sediment (25.56%). Percentage contribution for Ca-P was highest for lake sediment (17.6%) followed by field soil (12.25%) and river sediment (9.74%). R-P was highest for river sediment (279.79 mg kg^{-1}) followed by field soil (225. 84 mg kg^{-1}), lake sediment (210.23 mg kg^{-1}).

(8) The lagoon exhibits spatial-temporal variation in total P with a mean value of 556.98 mg kg^{-1} during PRM and 633.02 mg kg^{-1} during PSM season. NS and CS recorded higher total P compared to SS and OC. Spatial-temporal variation of WSP was evident with highest concentration observed in SS and lowest concentration in NS. Significantly higher value of L-P was recorded during PSM (1.63 mg kg^{-1}) compared

to PRM (0.78 mg kg^{-1}). Stations falling under NS and CS recorded higher L-P compared to SS. L-P contribute less than 1% to total P in the sediment.

(9) Al & Fe-P is the 2nd dominant fraction of P contributing 23.84-27.5% of sum of P fractions. Significantly higher mean value of Al & Fe-P was observed for PSM (105.13 mg kg^{-1}) compared to PRM (79.54 mg kg^{-1}). One-way ANOVA revealed significant sectoral variation in Al & Fe-P with NS exhibiting highest mean value compared to other sectors. However, mean concentration of Ca-P was significantly higher for PRM (94.61 mg kg^{-1}) compared to PSM (64.36 mg kg^{-1}). A positive correlation was observed between Ca-P and $CaCO_3$. R-P exhibit spatial-temporal variation in the lagoon, with highest average value for PSM (210.23 mg kg^{-1}) as compared to PRM (169.97 mg kg^{-1}). R-P is the dominant fraction contributing 43.48-53.8% to the sum of fractions.

(10) Cluster analysis helps to differentiate the lagoon into two groups/cluster according to dissimilarity among the cluster based on P distribution and sediment characteristics. C1 includes stations experiencing tidal influence and receive little fresh water influx whereas C2 includes stations falling under centra and northern sector which receives freshwater influx from the river and its tributaries. PCA was used to extract four principal components explaining 79.38% of variability in the P distribution in the lagoon. Strong loading for R-P and Total P suggest that most of the total P remain as R-P and positively correlated with organic carbon. PC2 have strong loading for L-P and C-P, whereas PC3 have strong loadings for WSP and EC. Strong loading for pH in PC4 explains its role in controlling distribution of P in the lagoon.

(11) Characterization of synthesized M-Lanthanum adsorbent through SEM, XRD, FTIR revealed successful doping of lanthanum hydroxide on magnetite. BET was performed to determine the specific surface area (SSA) of synthesised M-La $(OH)_3$. SSA was highest for 25% M-La $(OH)_3$ followed by 50% M-La $(OH)_3$.

(12) FTIR analysis after P adsorption revealed different functional group responsible for phosphate removal by M-La $(OH)_3$. XPS was used to further probe mechanism of phosphate removal, and the results indicates successful removal of phosphate by M-La $(OH)_3$. Shifting of bonding energy peak indicates formation of La-O-P inner sphere complex as mechanism for P removal.

(13) High correlation coefficient for pseudo second order equation suggests that phosphate adsorption to M-La $(OH)_3$ was chemisorption process. Adsorption isotherm was used to determine sorption maxima of different M-La $(OH)_3$. $_{50\%}$ M-La $(OH)_3$ was suggest as best sorbent for phosphate removal as it has highest sorption maxima value.

(14) pH of the solution greatly affect the phosphate removing capacity, with higher phosphate removal capacity observed at low pH, and an decrease in phosphate capacity is recorded due to competition form hydroxide ion with increase in pH.

- Evaluation of different water quality parameter, TSI, and WQI suggest that the lake falls in oligotrophic to mesotrophic state. However, the TSI value are closer to values of eutrophic state suggesting the lake was in the verge of eutrophication with further enrichment of lake with nutrient. As the lake receives loads of nutrient through river draining into lake Chilika, the lake sediment is enriched with nutrient due to flow of freshwater carrying nutrient enriched silt particle. Seasonal variation in TP is observed with PSM season recording highest TP. Sectoral variation of TP was observed with NS and CS experiencing highest TP load. P fractionation of river and lake sediment revealed that R-P was the dominant P fractions followed by Al & Fe-P. most redox sensitive Al & Fe-P contributes 27.5% of sum of P fractions suggesting high P release potential from sediment to overlaying water in anoxic/hypoxic conditions. Phosphate removal using M-La $(OH)_3$ suggest that P removal was chemisorption process with

50% M-La $(OH)_3$ recording highest sorption maxima. Characterization of M-La $(OH)_3$ before and after P adsorption revealed that formation of inner sphere complex and ligand exchange are the process responsible for high P removal efficiency of M-La $(OH)_3$. As phosphate removal extent of M-La $(OH)_3$ gradually decreases with increase in pH, it is necessary to apply the M-La $(OH)_3$ for remediation of sediment prior to further increase in pH due to high photosynthetic activity of the lake.

References

Adly, A., Mostafa, N. G., & Elawwad, A. (2022). Adsorption of phosphorus onto nanoscale zero-valent iron/activated carbon: removal mechanisms, thermodynamics, and interferences. *Water Reuse*, 12(1), 111-130.

Kocer, M. A. T., & Sevgili, H. (2014). Parameters selection for water quality index in the assessment of the environmental impacts of land-based trout farms. *Ecological Indicators*, 36, 672-681.

Amirbahman, A., Lake, B. A., & Norton, S. A. (2013). Seasonal phosphorus dynamics in the surficial sediment of two shallow temperate lakes: a solid-phase and pore-water study. *Hydrobiologia*, 701(1), 65-77.

An, B., Lee, S., Kim, H. G., Zhao, D., Park, J. A., & Choi, J. W. (2019). Organic/inorganic hybrid adsorbent for efficient phosphate removal from a reservoir affected by algae bloom. *Journal of industrial and engineering chemistry*, 69, 211-216.

Annon (2003) Chilika (Newsletter). *Wetlands International South Asia*,4, 24–26.

Bai, J., Ye, X., Jia, J., Zhang, G., Zhao, Q., Cui, B., & Liu, X. (2017). Phosphorus sorption-desorption and effects of temperature, pH and salinity on phosphorus sorption in marsh soils from coastal wetlands with different flooding conditions. *Chemosphere*, 188, 677-688.

Bai, J., Zhao, Q., Lu, Q., Wang, J., & Reddy, K. R. (2015). Effects of freshwater input on trace element pollution in salt marsh soils of a typical coastal estuary, China. *Journal of Hydrology*, 520, 186-192.

Banerjee, T., & Srivastava, R. K. (2009). Application of water quality index for assessment of surface water quality surrounding integrated industrial estate-Pantnagar. *Water Science and Technology*, 60(8), 2041-2053.

Barakat, A., El Baghdadi, M., Rais, J., Aghezzaf, B., & Slassi, M. (2016). Assessment of spatial and seasonal water quality variation of Oum Er Rbia River (Morocco) using multivariate statistical techniques. *International soil and water conservation research*, 4(4), 284-292.

Barik, S. K., Bramha, S., Bastia, T. K., Behera, D., Mohanty, P. K., & Rath, P. (2019). Distribution of geochemical fractions of phosphorus and its ecological risk in sediment cores of a largest brackish water lake, South Asia. *International Journal of Sediment Research*, 34(3), 251-261.

Barik, S. K., Bramha, S. N., Mohanty, A. K., Bastia, T. K., Behera, D., & Rath, P. (2016). Sequential extraction of different forms of phosphorus in the surface sediments of Chilika Lake. *Arabian Journal of Geosciences*, 9(2), 1-12.

Barik, S. K., Muduli, P. R., Mohanty, B., Behera, A. T., Mallick, S., Das, A., ... & Pattnaik, A. K. (2017). Spatio-temporal variability and the impact of Phailin on water quality of Chilika lagoon. *Continental Shelf Research*, 136, 39-56.

Basatnia, N., Hossein, S. A., Rodrigo-Comino, J., Khaledian, Y., Brevik, E. C., Aitkenhead-Peterson, J., & Natesan, U. (2018). Assessment of temporal and spatial water quality in international Gomishan Lagoon, Iran, using multivariate analysis. *Environmental Monitoring and Assessment*, 190(5), 1-17.

Bastami, K. D., Neyestani, M. R., Raeisi, H., Shafeian, E., Baniamam, M., Shirzadi, A., & Shahrokhi, B. (2018). Bioavailability and geochemical speciation of phosphorus in surface sediments of the Southern Caspian Sea. *Marine Pollution Bulletin*, 126, 51-57.

Bhadha, J. H., Daroub, S. H., & Lang, T. A. (2012). Effect of kinetic control, soil: solution ratio, electrolyte cation, and others, on equilibrium phosphorus concentration. *Geoderma*, 173, 209-214.

Bhatnagar, A., & Sillanpää, M. (2011). A review of emerging adsorbents for nitrate removal from water. *Chemical Engineering Journal*, 168(2), 493-504.

Bouyoucos, G. J. (1927). The hydrometer as a new method for the mechanical analysis of soils. *Soil science*, 23(5), 343-354.

Bowers, K. E., & Westerman, P. W. (2005). Performance of cone-shaped fluidized bed struvite crystallizers in removing phosphorus from wastewater. *Transactions of the American Society of Agricultural Engineers*, 48(3), 1227-1234.

Boyacioglu, H. (2007). Development of a water quality index based on a European classification scheme. *Water SA*, 33(1).

Bridgeman, T. B., Chaffin, J. D., Kane, D. D., Conroy, J. D., Panek, S. E., & Armenio, P. M. (2012). From River to Lake: Phosphorus partitioning and algal community compositional changes in Western Lake Erie. *Journal of Great Lakes Research*, 38(1), 90-97.

Cao, J., Hou, Z., Li, Z., Chu, Z., Yang, P., & Zheng, B. (2018). Succession of phytoplankton functional groups and their driving factors in a subtropical plateau lake. *Science of the Total Environment*, 631, 1127-1137.

Carey, C. C., & Rydin, E. (2011). Lake trophic status can be determined by the depth distribution of sediment phosphorus. *Limnology and oceanography*, 56(6), 2051-2063.

Carlson, R. E. (1977). A trophic state index for lakes 1. *Limnology and oceanography*, 22(2), 361-369.

Celen, I., & Turker, M. (2001). Recovery of ammonia as struvite from anaerobic digester effluents. *Environmental technology*, 22(11), 1263-1272.

Central Pollution Control Board. (2020). National Ambient Air quality and Trends. National Ambient Air Quality Monitoring Series, 45.

Chao, J. Y., Zhang, Y. M., Kong, M., Zhuang, W., Wang, L. M., Shao, K. Q., & Gao, G. (2017). Long-term moderate wind induced sediment resuspension meeting phosphorus demand of phytoplankton in the large shallow eutrophic Lake Taihu. *PloS one*, 12(3).

Chen, H., Lu, C., & Yang, H. (2020). Lanthanum compounds-modified rectorite composites for highly efficient phosphate removal from wastewater. *Applied Clay Science*, 199, 105875.

Chen, L., Li, Y., Sun, Y., Chen, Y., & Qian, J. (2019). La (OH) $_3$ loaded magnetic mesoporous nanospheres with highly efficient phosphate removal properties and superior pH stability. *Chemical Engineering Journal*, 360, 342-348.

Chen, M., Huo, C., Li, Y., & Wang, J. (2016). Selective adsorption and efficient removal of phosphate from aqueous medium with graphene–lanthanum composite. *ACS Sustainable Chemistry & Engineering*, 4(3), 1296-1302.

Cherubin, M. R., Franco, A. L., Cerri, C. E., Karlen, D. L., Pavinato, P. S., Rodrigues, M., & Cerri, C. C. (2016). Phosphorus pools responses to land-use change for sugarcane expansion in weathered Brazilian soils. *Geoderma*, 265, 27-38.

Copetti, D., Finsterle, K., Marziali, L., Stefani, F., Tartari, G., Douglas, G., Reitzel, K., Spears, B.M., Winfield, I.J., Crosa, G., D'Haese, P., Yasseri, S., & Lurling, M. (2016). Eutrophication management in surface waters using lanthanum modified bentonite: a review. *Water Research*, 97, 162–174.

Craswell, E. (2021). Fertilizers and nitrate pollution of surface and ground water: an increasingly pervasive global problem. *SN Applied Sciences*, 3(4), 1-24.

Crews, T. E., & Brookes, P. C. (2014). Changes in soil phosphorus forms through time in perennial versus annual agroecosystems. *Agriculture, ecosystems & environment*, 184, 168-181.

Cucarella, V., & Renman, G. (2009). Phosphorus sorption capacity of filter materials used for on-site wastewater treatment determined in batch experiments–a comparative study. *Journal of environmental quality*, 38(2), 381-392.

David, V., Tortajada, S., Savoye, N., Breret, M., Lachaussée, N., Philippine, O., Robin, F.X., Dupuy, C. (2020). Impact of human activities on the spatio-seasonal dynamics of plankton diversity in drained marshes and consequences on eutrophication, *Water Research*, 170, 115287, 0043-1354.

Ding, S., Sun, Q., Chen, X., Liu, Q., Wang, D., Lin, J., & Tsang, D. C. (2018). Synergistic adsorption of phosphorus by iron in lanthanum modified bentonite (Phoslock®): new insight into sediment phosphorus immobilization. *Water research*, 134, 32-43.

Ding, Y., Sun, L., Qin, B., Wu, T., Shen, X., & Wang, Y. (2018). Characteristics of sediment resuspension in Lake Taihu, China: A wave flume study. *Journal of Hydrology*, 561, 702-710.

Dithmer, L., Lipton, A. S., Reitzel, K., Warner, T. E., Lundberg, D., & Nielsen, U. G. (2015). Characterization of phosphate sequestration by a lanthanum modified bentonite clay: a solid-state NMR, EXAFS, and PXRD study. *Environmental Science & Technology*, 49(7), 4559-4566.

Dong, S., Wang, Y., Zhao, Y., Zhou, X., & Zheng, H. (2017). La^{3+}/La (OH) $_3$ loaded magnetic cationic hydrogel composites for phosphate removal: effect of lanthanum species and mechanistic study. *Water Research*, 126, 433-441.

Douglas, G. B., Adeney, J. A., & Robb, M. S. (1999, May). A novel technique for reducing bioavailable phosphorus in water and sediments. *In International Association Water Quality Conference on Diffuse Pollution*, 517523.

Douglas, G. B., Hamilton, D. P., Robb, M. S., Pan, G., Spears, B. M., & Lurling, M. (2016). Guiding principles for the development and application of solid-phase phosphorus adsorbents for freshwater ecosystems. *Aquatic ecology*, 50(3), 385-405.

Du, C., Ren, X., Zhang, L., Xu, M., Wang, X., Zhuang, Y., & Du, Y. (2016). Adsorption characteristics of phosphorus onto soils from water level fluctuation zones of the Danjiangkou Reservoir. *CLEAN–Soil, Air, Water*, 44(8), 975-983.

Dutta, S., Dwivedi, A., & Suresh Kumar, M. (2018). Use of water quality index and multivariate statistical techniques for the assessment of spatial variations in water quality of a small river. *Environmental monitoring and assessment*, 190(12), 1-17.

Egemose, S., Wauer, G., & Kleeberg, A. (2009). Resuspension behaviour of aluminium treated lake sediments: effects of ageing and pH. *Hydrobiologia*, 636(1), 203-217.

Fan, C., Zhong, J., Zhang, L., Liu, C., & Shen, Q. (2020). Research progress and prospect of environmental dredging decision-making of lake sediment. *Journal of Lake Sciences*, 32, 1254-1277.

Fang, H. W., Chen, M. H., Chen, Z. H., Zhao, H. M., & He, G. J. (2013). Effects of sediment particle morphology on adsorption of phosphorus elements. *International Journal of Sediment Research*, 28(2), 246-253.

Fang, L., Shi, Q., Nguyen, J., Wu, B., Wang, Z., & Lo, I. M. (2017). Removal mechanisms of phosphate by lanthanum hydroxide nanorods: investigations using EXAFS, ATR-FTIR, DFT, and surface complexation modeling approaches. *Environmental Science & Technology*, 51(21), 12377-12384.

Fang, L., Liu, R., Li, J., Xu, C., Huang, L. Z., & Wang, D. (2018). Magnetite/Lanthanum hydroxide for phosphate sequestration and recovery from lake and the attenuation effects of sediment particles. *Water Research*, 130, 243-254.

Fang, L., Shi, Q., Nguyen, J., Wu, B., Wang, Z., & Lo, I. M. (2017). Removal mechanisms of phosphate by lanthanum hydroxide nanorods: investigations using EXAFS, ATR-FTIR, DFT, and surface complexation modeling approaches. *Environmental Science & Technology*, 51(21), 12377-12384.

Feng, W., Zhu, Y., Wu, F., Meng, W., Giesy, J. P., He, Z., & Fan, M. (2016). Characterization of phosphorus forms in lake macrophytes and algae by solution 31P nuclear magnetic resonance spectroscopy. *Environmental Science and Pollution Research*, 23(8), 7288-7297.

Fink, G., Alcamo, J., Florke, M., & Reder, K. (2018). Phosphorus loadings to the world's largest lakes: sources and trends. *Global Biogeochemical Cycles*, 32(4), 617-634.

Fink, J. R., Inda, A. V., Bavaresco, J., Barrón, V., Torrent, J., & Bayer, C. (2016a). Adsorption and desorption of phosphorus in subtropical soils as affected by management system and mineralogy. *Soil and Tillage Research*, 155, 62-68.

Fink, J. R., Inda, A. V., Tiecher, T., & Barrón, V. (2016b). Iron oxides and organic matter on soil phosphorus availability. *Ciencia e agrotecnologia*, 40, 369-379.

Flower, H., Rains, M., Lewis, D., Zhang, J. Z., & Price, R. (2017). Saltwater intrusion as potential driver of phosphorus release from limestone bedrock in a coastal aquifer. *Estuarine, Coastal and Shelf Science*, 184, 166-176.

Fu, H., Yang, Y., Zhu, R., Liu, J., Usman, M., Chen, Q., & He, H. (2018). Superior adsorption of phosphate by ferrihydrite-coated and lanthanum-decorated magnetite. *Journal of Colloid and Interface Science*, 530, 704-713.

Fu, J., Zhang, Z., & Li, G. (2019). Progress on the development of DNA-mediated metal nanomaterials for environmental and biological analysis. *Chinese Chemical Letters*, 30(2), 285-291.

Funes, A., De Vicente, J., Cruz-Pizarro, L., Álvarez-Manzaneda, I., & de Vicente, I. (2016). Magnetic microparticles as a new tool for lake restoration: a microcosm experiment for evaluating the impact on phosphorus fluxes and sedimentary phosphorus pools. *Water research*, 89, 366-374.

Ganguly, D., Patra, S., Muduli, P. R., Vardhan, K. V., Robin, R. S., & Subramanian, B. R. (2015). Influence of nutrient input on the trophic state of a tropical brackish water lagoon. *Journal of Earth System Science*, 124(5), 1005-1017.

Gilbert, J. D., Guerrero, F., & de Vicente, I. (2014). Sediment desiccation as a driver of phosphate availability in the water column of Mediterranean wetlands. *Science of the total environment*, 466, 965-975.

Giles, C. H., MacEwan, T. H., Nakhwa, S. N. & Smith, D. (1960). 786. Studies in adsorption. Part XI. A system of classification of solution adsorption isotherms, and its use in diagnosis of adsorption mechanisms and in measurement of specific surface areas of solids. *Journal of the Chemical Society* (Resumed), 3973-3993.

Giles, C. D., Isles, P. D., Manley, T., Xu, Y., Druschel, G. K., & Schroth, A. W. (2016). The mobility of phosphorus, iron, and manganese through the sediment–water continuum of a shallow eutrophic freshwater lake under stratified and mixed water-column conditions. *Biogeochemistry*, 127(1), 15-34.

Gong, J.J., Ni, Z.K., Xiao, J.B., Zhao, H.C., Xi, Y., & Wang, S.R. (2019). Effects and difference of dissolved organic and inorganic phosphorus release in different sediments covered by different materials of Erhai Lake. *Environmental Science*. 04, 1-12.

Grantz, E. M., Haggard, B. E., & Scott, J. T. (2014). Stoichiometric imbalance in rates of nitrogen and phosphorus retention, storage, and recycling can perpetuate nitrogen deficiency in highly-productive reservoirs. *Limnology and Oceanography*. 59, 2203- 2216,

Gupta, G. V. M., Sarma, V. V. S. S., Robin, R. S., Raman, A. V., Jai Kumar, M., Rakesh, M., & Subramanian, B. R. (2008). Influence of net ecosystem metabolism in transferring riverine organic carbon to atmospheric CO2 in a tropical coastal lagoon (Chilka Lake, India). *Biogeochemistry*, 87(3), 265-285.

Gustafsson, J. P., Mwamila, L. B., & Kergoat, K. (2012). The pH dependence of phosphate sorption and desorption in Swedish agricultural soils. *Geoderma*, 189, 304-311.

Han, H. J., Los, F. J., Burger, D. F., & Lu, X. X. (2016). A modelling approach to determine systematic nitrogen transformations in a tropical reservoir. *Ecological Engineering*, 94, 37-49.

He, J., Wang, W., Shi, W., & Cui, F. (2016). La 2 O 3 nanoparticle/polyacrylonitrile nanofibers for bacterial inactivation based on phosphate control. *RSC advances*, 6(101), 99353-99360.

He, J., Wang, W., Sun, F., Shi, W., Qi, D., Wang, K., & Chen, X. (2015). Highly efficient phosphate scavenger based on well-dispersed La $(OH)_3$ nanorods in polyacrylonitrile nanofibers for nutrient-starvation antibacteria. *ACS nano*, 9(9), 9292-9302.

He, Y., Lin, H., Dong, Y., & Wang, L. (2017). Preferable adsorption of phosphate using lanthanum-incorporated porous zeolite: characteristics and mechanism. *Applied Surface Science*, 426, 995-1004.

He, Z. J., Cai, J. J., Ni, Z. K., Huang, Y., Zhao, J. D., & Wang, S. R. (2018). Seasonal characteristics of nitrogen sources from different ways and its contribution to water nitrogen in Lake Erhai. *Acta Scientiae Circumstantiae*, 38(5), 1939-1948.

Hesse, P. R., & Hesse, P. R. (1971). A textbook of soil chemical analysis.

Horton, R. K. (1965). An index number system for rating water quality. *Journal (Water Pollution Control Federation*), 37(3), 300-306.

Hou, L. J., Liu, M., Yang, Y., Ou, D. N., Lin, X., Chen, H., & Xu, S. Y. (2009). Phosphorus speciation and availability in intertidal sediments of the Yangtze Estuary, China. *Applied Geochemistry*, 24(1), 120-128.

Hu, F., Wang, M., Peng, X., Qiu, F., Zhang, T., Dai, H., & Cao, Z. (2018). High-efficient adsorption of phosphates from water by hierarchical CuAl/biomass carbon fiber layered double hydroxide. *Colloids and Surfaces A: Physicochemical and Engineering Aspects*, 555, 314-323.

Huang, J., Xu, S., Lu, S., Zhao, B., & Chen, F. X. (2017). Effect of nitrogen removal by ecological permeable belts treating domestic wastewater of Erhai Lake basin. *Chinese Journal of Environmental Engineering*, 11(10), 5409-5416.

Huittinen, N., Scheinost, A. C., Ji, Y., Kowalski, P. M., Arinicheva, Y., Wilden, A., & Stumpf, T. (2018). A spectroscopic and computational study of Cm3+ incorporation in lanthanide phosphate rhabdophane ($LnPO_4 \cdot 0.67\ H_2O$) and monazite ($LnPO_4$). *Inorganic chemistry*, 57(11), 6252-6265.

Huo, S., Ma, C., Xi, B., Zhang, Y., Wu, F., & Liu, H. (2018). Development of methods for establishing nutrient criteria in lakes and reservoirs: a review. *Journal of Environmental Sciences*, 67, 54-66.

Hupfer, M., & Lewandowski, J. (2008). Oxygen controls the phosphorus release from Lake Sediments–a long-lasting paradigm in limnology. *International Review of Hydrobiology*, 93(4-5), 415-432.

Jalali, M., & Hemati Matin, N. (2015). Sorption of phosphorus in calcareous paddy soils of Iran: effects of soil/solution ratio and pH. *Environmental Earth Sciences*, 73(5), 2047-2059.

Ji, B., Zhao, Y., Vymazal, J., Qiao, S., Wei, T., Li, J., & Mander, Ü. (2020). Can subsurface flow constructed wetlands be applied in cold climate regions? A review of the current knowledge. *Ecological Engineering*, 157, 105992.

Ji, N.N., Wang, S.R., Li Zhang, L. (2017). Characteristics of dissolved organic phosphorus inputs to freshwater lakes: A case study of Lake Erhai, southwest China, *Science of The Total Environment*, 601–602, 1544-1555.

Jing, X., Wang, Y., Chen, L., Wang, Y., Yang, X., Jiang, Y., & Yan, Y. (2019). Free-standing large-mesoporous silica films decorated with lanthanum as new adsorbents for efficient removal of phosphate. *Journal of Molecular Liquids*, 296, 111815.

Jun, M., Altor, A. E., & Craft, C. B. (2013). Effects of increased salinity and inundation on inorganic nitrogen exchange and phosphorus sorption by tidal freshwater floodplain forest soils, Georgia (USA). *Estuaries and Coasts*, 36(3), 508-518.

Kadekodi, G. K., & Nayampalli, A. (2005). Reversing biodiversity Degradation: A case of Chilika Lake. Dimensions of Environmental and Ecological Economics, University Press, Hyderabad, 527-545.

Grasshoff, K., Kremling, K., & Ehrhardt, M. (Eds.). (1999). Methods of seawater analysis. *John Wiley & Sons. erabad*, 527-545.

Kangur, K., Kangur, P., Ginter, K., Orru, K., Haldna, M., Möls, T., & Kangur, A. (2013). Long-term effects of extreme weather events and eutrophication on the fish community of shallow Lake Peipsi (Estonia/Russia). *Journal of Limnology*, 72(2).

Kar, D. (2013) Wetlands and lakes of the world. Springer, London

Katsev, S. (2016). Phosphorus effluxes from lake sediments. *Soil Phosphorus*, 115-132.

Khan, R., & Jhariya, D. C. (2017). Groundwater quality assessment for drinking purpose in Raipur city, Chhattisgarh using water quality index and geographic information system. *Journal of the geological society of India*, 90(1), 69-76.

Kim, D.K., Javed, A., Yang, C., George B. Arhonditsis, G.B. (2018). Development of a mechanistic eutrophication model for wetland management: Sensitivity analysis of the interplay among phytoplankton, macrophytes, and sediment nutrient release. *Ecological Informatics*, 48, 198-214, 1574-9541.

Kong, L., Tian, Y., Li, N., Liu, Y., Zhang, J., Zhang, J., & Zuo, W. (2018). Highly-effective phosphate removal from aqueous solutions by calcined nano-porous palygorskite matrix with embedded lanthanum hydroxide. *Applied Clay Science*, 162, 507-517.

Kroes, H.W. (1980). Replacement of phosphates in detergents. *Hydrobiological Bulletin*, 14(1), 90-93.

Kumari, M., Pittman Jr, C. U., & Mohan, D. (2015). Heavy metals [chromium (VI) and lead (II)] removal from water using mesoporous magnetite (Fe3O4) nanospheres. *Journal of colloid and interface science*, 442, 120-132.

Kuzawa, K., Jung, Y. J., Kiso, Y., Yamada, T., Nagai, M., & Lee, T. G. (2006). Phosphate removal and recovery with a synthetic hydrotalcite as an adsorbent. *Chemosphere*, 62(1), 45-52.

Lai, L., Xie, Q., Chi, L., Gu, W., & Wu, D. (2016). Adsorption of phosphate from water by easily separable Fe_3O_4@ SiO_2 core/shell magnetic nanoparticles functionalized with hydrous lanthanum oxide. *Journal of Colloid and Interface Science*, 465, 76-82.

Lei, P., Zhang, H., Wang, C., & Pan, K. (2018). Migration and diffusion for pollutants across the sediment-water interface in lakes: A review. *Journal of Lake Sciences*, 30(06), 1489-1508.

Li, G.S., & Lei, L.R. (2018). Remediation of Black-odorous River with aeration reoxygenation combined with microbial agent process. *Environment Engineering*. 36(3).

Li, H., Li, Y., Xu, Y., & Lu, X. (2020). Biochar phosphorus fertilizer effects on soil phosphorus availability. *Chemosphere*, 244, 125471.

Li, J., Li, B., Huang, H., Zhao, N., Zhang, M., & Cao, L. (2020). Investigation into lanthanum-coated biochar obtained from urban dewatered sewage sludge for enhanced phosphate adsorption. *Science of the Total Environment*, 714, 136839.

Li, J., Zhang, Y., & Katsev, S. (2018). Phosphorus recycling in deeply oxygenated sediments in Lake Superior controlled by organic matter mineralization. *Limnology and Oceanography*, 63(3), 1372-1385.

Li, R., Li, Q., Gao, S., & Shang, J. K. (2012). Exceptional arsenic adsorption performance of hydrous cerium oxide nanoparticles: Part A. Adsorption capacity and mechanism. *Chemical Engineering Journal*, 185, 127-135.

Li, S., Peng, C., Cheng, T., Wang, C., Guo, L., & Li, D. (2019). Nitrogen-cycling microbial community functional potential and enzyme activities in cultured biofilms with response to inorganic nitrogen availability. *Journal of Environmental Sciences*, 76, 89-99.

Li, X., Guo, M., Duan, X., Zhao, J., Hua, Y., Zhou, Y., & Dionysiou, D. D. (2019). Distribution of organic phosphorus species in sediment profiles of shallow lakes and its effect on photo-release of phosphate during sediment resuspension. *Environment international*, 130, 104916.

Li, Y.P., Wang, S.R., Zhang, L., Zhao, H.C., Jiao, L.X., Zhao, Y.L., & He, X.S. (2014). Composition and spectroscopic characteristics of dissolved organic matter extracted from the sediment of Erhai Lake in China. *Journal of Soils and Sediments*. 14: 1599-1611.

Li, Z., Sheng, Y., Yang, J., & Burton, E. D. (2016). Phosphorus release from coastal sediments: Impacts of the oxidation-reduction potential and sulfide. *Marine pollution bulletin*, 113(1-2), 176-181.

Li-kun, Y., Sen, P., Xin-hua, Z., & Xia, L. (2017). Development of a two-dimensional eutrophication model in an urban lake (China) and the application of uncertainty analysis. *Ecological Modelling*, 345, 63-74.

Lin, J., Zhao, Y., Zhang, Z., Zhan, Y., Zhang, Z., Wang, Y., Yu, Y. & Wu, X. (2019). Immobilization of mobile and bioavailable phosphorus in sediments using lanthanum hydroxide and magnetite/lanthanum hydroxide composite as amendments. *Science of the total environment*, 687,232-243.

Lin, S.S., Shen, S.L., Zhou, A.N., & Lyu, H.M. (2020). Sustainable development and environmental restoration in Lake Erhai, China. *Journal of Cleaner Production*, 258(2020), 120758.

Liu, B., Yu, Y., Han, Q., Lou, S., Zhang, L., & Zhang, W. (2020). Fast and efficient phosphate removal on lanthanum-chitosan composite synthesized by controlling the amount of cross-linking agent. *International journal of biological macromolecules*, 157, 247-258.

Liu, G.H., Zong, Z.M., Liu, F.J., Ma, Z.H., Wei, X.Y., Bai, H.C., Guo, Q.J. & Zhao, T.S. (2019). Clean and effective catalytic hydrolysis of bagasse waste to small-molecular compounds over a hydrothermally stable Ru/La(OH)$_3$. *Journal of Cleaner Production,* 23, 117909.

Liu, L., Zhang, Y., Efting, A., Barrow, T., Qian, B., & Fang, Z. (2012). Modeling bioavailable phosphorus via other phosphorus fractions in sediment cores from Jiulongkou Lake, China. *Environmental Earth Sciences,* 65(3), 945-956.

Liu, W., Wang, S., Zhang, L., Ni, Z., Zhao, H., & Jiao, L. (2015). Phosphorus release characteristics of sediments in Erhai Lake and their impact on water quality. *Environmental Earth Sciences,* 74(5), 3753-3766.

Liu, X., Sheng, H., Jiang, S., Yuan, Z., Zhang, C., & Elser, J. J. (2016). Intensification of phosphorus cycling in China since the 1600s. *Proceedings of the National Academy of Sciences,* 113(10), 2609-2614.

Loganathan, P., Vigneswaran, S., Kandasamy, J., & Bolan, N. S. (2014). Removal and recovery of phosphate from water using sorption. *Critical Reviews in Environmental Science and Technology,* 44(8), 847-907.

Long, Z., Ji, Z., & Pei, Y. (2023). Characteristics and distribution of phosphorus in surface sediments of a shallow lake. *Journal of Environmental Sciences,* 124, 50-60.

Lǔ, J., Liu, H., Liu, R., Zhao, X., Sun, L., & Qu, J. (2013). Adsorptive removal of phosphate by a nanostructured Fe–Al–Mn trimetal oxide adsorbent. *Powder Technology,* 233, 146-154.

Luo, F., Feng, X., Jiang, X., Zhou, A., Xie, P., Wang, Z., Tao, T. & Wan, J. (2021). Lanthanum molybdate/magnetite for selective phosphate removal from wastewater: Characterization,

performance, and sorption mechanisms. *Environmental Science and Pollution Research*, 28(4), 4342-4351.

Ma, L., He, F., Huang, T., Zhou, Q., Zhang, Y., & Wu, Z. (2016). Nitrogen and phosphorus transformations and balance in a pond-ditch circulation system for rural polluted water treatment. *Ecological Engineering*, 94, 117-126.

Maghsoodi, M. R., Ghodszad, L., & Lajayer, B. A. (2020). Dilemma of hydroxyapatite nanoparticles as phosphorus fertilizer: Potentials, challenges and effects on plants. *Environmental Technology & Innovation*, 19, 100869.

Mahananda, M. R., Mohanty, B. P., & Behera, N. R. (2010). Physico-chemical analysis of surface and ground water of Bargarh District, Orissa, India. *International journal of research and reviews in applied sciences*, 2(3), 284-295.

Makarewicz, J.C., Lewis, T.W., Bosch, I., Noll, M.R., Herendeen, N., Simon, R.D., Zollweg, J. & Vodacek, A. (2009). The impact of agricultural best management practices on downstream systems: Soil loss and nutrient chemistry and flux to Conesus Lake, New York, USA. *Journal of Great Lakes Research*, 35, 23-36.

Makita, Y., Sonoda, A., Sugiura, Y., Ogata, A., Suh, C., Lee, J.H. & Ooi, K. (2020). Phosphorus removal from model wastewater using lanthanum hydroxide microcapsules with poly (vinyl chloride) shells. *Separation and Purification Technology*, 241, 116707.

Malagó, A., Bouraoui, F., Grizzetti, B., & De Roo, A. (2019). Modelling nutrient fluxes into the Mediterranean Sea. *Journal of Hydrology: Regional Studies*, 22, 100592.

Manjare, S. A., Vhanalakar, S. A., & Muley, D. V. (2010). Analysis of water quality using physicochemical parameters Tamdalge tank in Kolhapur district, Maharashtra. *International journal of advanced biotechnology and research*, 1(2), 115-119.

Markovic, S., Liang, A., Watson, S.B., Guo, J., Mugalingam, S., Arhonditsis, G., Morley, A., & Dittrich, M. (2019). Biogeochemical mechanisms controlling phosphorus diagenesis and internal loading in a remediated hard water eutrophic embayment. *Chemical Geology*, 514, 122–137.

Mehlich, A. (1984). Mehlich 3 soil test extractant: A modification of Mehlich 2 extractant. *Communications in soil science and plant analysis*, 15(12), 1409-1416.

Mockler, E. M., Deakin, J., Archbold, M., Gill, L., Daly, D., & Bruen, M. (2017). Sources of nitrogen and phosphorus emissions to Irish rivers and coastal waters: Estimates from a nutrient load apportionment framework. *Science of the Total Environment*, 601, 326-339.

Moore Jr, A., & Reddy, K. R. (1994). Role of Eh and pH on phosphorus geochemistry in sediments of Lake Okeechobee, Florida (Vol. 23, No. 5, pp. 955-964). *American Society of Agronomy, Crop Science Society of America, and Soil Science Society of America*.

Mrozińska, N., Glińska-Lewczuk, K., & Obolewski, K. (2021). Salinity as a Key Factor on the Benthic Fauna Diversity in the Coastal Lakes. *Animals*, 11(11), 3039.

Muduli, P.R., Kanuri, V.V., Robin, R.S., Kumar, B.C., Patra, S., Raman, A.V., Rao, G.N. & Subramanian, B.R. (2013). Distribution of dissolved inorganic carbon and net ecosystem production in a tropical brackish water lagoon, India. *Continental Shelf Research*, 64, 75-87.

Mukherjee, R., Muduli, P. R., Barik, S. K., & Kumar, S. (2019). Sources and transformations of organic matter in sediments of Asia's largest brackish water lagoon (Chilika, India) and nearby mangrove ecosystem. *Environmental Earth Sciences*, 78(11), 1-15.

Murphy, J. A. M. E. S., & Riley, J. P. (1962). A modified single solution method for the determination of phosphate in natural waters. *Analytica chimica acta*, 27, 31-36.

Nalley, J.O., ODonnell, D.R., & Litchman, E. (2018). Temperature effects on growth rates and fatty acid content in freshwater algae and cyanobacteria. *Algae Research*. 35, 500-507.

Nelson, D. W., & Sommers, L. E. (1996). Total carbon, organic carbon, and organic matter. *Methods of soil analysis: Part 3 Chemical methods*, 5, 961-1010.

Ni, Z., Wang, S., Wu, Y. & Pu, J. (2020). Response of phosphorus fractionation in lake sediments to anthropogenic activities in China. *Science of the Total Environment*, 699, 134242.

Nixon, S. W. (1988). Physical energy inputs and the comparative ecology of lake and marine ecosystems. *Limnology and Oceanography*, 33(4 part 2), 1005-1025.

Njenga, N.J. (2005). Comparative studies on geochemistry of Lake Nakuru and Lake Naivasa (Kenya) and Lake Kolleru (India). PhD thesis, Jawaharlal Nehru University New Delhi, India.

Nurnberg, G. K. (2020). Internal phosphorus loading models: a critical review. Internal Phosphorus Loading: Causes, Case Studies, and Management. *J. Ross Publishing, Plantation*, Florida, 45-62.

Nyenje, P. M., Foppen, J. W., Uhlenbrook, S., Kulabako, R., & Muwanga, A. (2010). Eutrophication and nutrient release in urban areas of sub-Saharan Africa—a review. *Science of the total environment*, 408(3), 447-455.

Olsen, S. R. (1954). Estimation of available phosphorus in soils by extraction with sodium bicarbonate (No. 939). US Department of Agriculture.

Ortiz-Reyes, E., & Anex, R.P. (2018). A life cycle impact assessment method for freshwater eutrophication due to the transport of phosphorus from agricultural production. *Journal of Cleaner Production*, 177, 474-482.

Pal, S. R., & Mohanty, P. K. (2002). Use of IRS-1B data for change detection in water quality and vegetation of Chilika lagoon, east coast of India. *International Journal of Remote Sensing*, 23(6), 1027-1042.

Panda, U.C, Rath, P., Brahma, S.N., & Sahu K.C. (2010). Application of factor analysis in geochemical speciation of heavy metals in the sediment of a lake system—Chilika (India): A case study. *Journal of Coastal Research*, 26(5), 860–868.

Panigrahi, S. N. (2006). Seasonal variability of phytoplankton productivity and related physico-chemical parameters in the Chilika lake and its adjoining sea. Ph.D. Thesis, Berhampur University, India, 1–286

Panigrahi, S., Acharya, B. C., Panigrahy, R. C., Nayak, B. K., Banarjee, K., & Sarkar, S. K. (2007). Anthropogenic impact on water quality of Chilika lagoon RAMSAR site: a statistical approach. *Wetlands Ecology and Management*, 15(2), 113-126.

Parsons, C.T., Rezanezhad, F., O'Connell, D.W. & Van Cappellen, P. (2017). Sediment phosphorus speciation and mobility under dynamic redox conditions. *Biogeosciences*, 14(14), 3585-3602.

Paytan, A., & McLaughlin, K. (2007). The oceanic phosphorus cycle. *Chemical reviews*, 107(2), 563-576.

Perkins, R. G., & Underwood, G. J. C. (2001). The potential for phosphorus release across the sediment–water interface in an eutrophic reservoir dosed with ferric sulphate. *Water Research*, 35(6), 1399-1406.

Qin, B., Zhou, J., Elser, J. J., Gardner, W. S., Deng, J., & Brookes, J. D. (2020). Water depth underpins the relative roles and fates of nitrogen and phosphorus in lakes. *Environmental science & technology*, 54(6), 3191-3198.

Qiu, H., Liang, C., Yu, J., Zhang, Q., Song, M., & Chen, F. (2017). Preferable phosphate sequestration by nano-La (III) hydro- oxides modified wheat straw with excellent properties in regeneration. *Chemical Engineering Journal*, 315, 345-354.

Rajasegar, M. (2003). Physico-chemical characteristics of the Vellar estuary in relation to shrimp farming. *Journal of environmental biology*, 24(1), 95-101.

Rajasulochana, P., & Preethy, V. (2016). Comparison on efficiency of various techniques in treatment of waste and sewage water- A comprehensive review. *Resources- Efficient Technologie*s. 2, 175-184.

Ramanadham, R., Reddy, M. P. M., & Murty, A. V. S. (1964). Limnology of the Chilka lake. *Journal of the Marine Biological Association of India*, 6(2), 183-201.

Ramanathan, A.L. (2007). Phosphorus fractionation in surficial sediments of Pandoh lake, lesser Himalaya, Himachal Pradesh, India. *Applied Geochemistry*, 22(9), 1860-1871.

Rittmann, B. E., Mayer, B., Westerhoff, P., & Edwards, M. (2011). Capturing the lost phosphorus. *Chemosphere*, 84(6), 846-853.

Rochelle-Newall, E. J., Chu, V. T., Pringault, O., Amouroux, D., Arfi, R., Bettare, I. Y., Bouvier, T., Bouvier, C., Got, P., Nguyen, T. M. H., Mari, X., Navarro, P., Duong, T. N., Cao, T. T. T., Pham, T. T., Ouillon, S., & Torréton, J.-P. (2011). Phytoplankton diversity and productivity in a highly turbid, tropical coastal system (Bach Dang Estuary, Vietnam). *Marine Pollution Bulletin*, 62, 2317–2329.

Rodrigues, M., Pavinato, P.S., Withers, P.J.A., Teles, A.P.B. and Herrera, W.F.B. (2016). Legacy phosphorus and no tillage agriculture in tropical oxisols of the Brazilian savanna. *Science of the Total Environment*, 542, 1050-1061.

Rosemarin, A. (2004). The precarious geopolitics of phosphorus. *Down to Earth Science Environment Fortn*, 27–31.

Ruttenberg, K.C. (1992). Development of a sequential extraction method for different forms of phosphorus in marine sediments. *Limnology and oceanography*, 37(7), 1460-1482.

Rydin, E. (2000). Potentially mobile phosphorus in Lake Erken sediment. *Water Research*, 34(7), 2037-2042.

Santschi, P., Höhener, P., Benoit, G. & Buchholtz-ten Brink, M. (1990). Chemical processes at the sediment-water interface. *Marine chemistry*, 30, 269-315.

Scalenghe, R., Edwards, A. C., Barberis, E., & Ajmone-Marsan, F. (2014). Release of phosphorus under reducing and simulated open drainage conditions from over fertilised soils. *Chemosphere*, 95, 289-294.

Shah, K.A. & Joshi, G.S. (2017). Evaluation of water quality index for River Sabarmati, Gujarat, India. *Applied Water Science*, 7(3), 1349-1358.

Sharpley, A. N. (1981). The contribution of phosphorus leached from crop canopy to losses in surface runoff (Vol. 10, No. 2, pp. 160-165). American Society of Agronomy, Crop Science Society of America, and Soil Science Society of America.

Sharpley, A.N., Weld, J.L., Beegle, D.B., Kleinman, P.J., Gburek, W.J., Moore, P.A. & Mullins, G. (2003). Development of phosphorus indices for nutrient management planning strategies in the United States. *Journal of Soil and Water Conservation*, 58(3), 137-152.

Siddiqui, S. Z. (1995). Limnology of Chilika lake. Fauna of Chilika lake.

Song, Q., Huang, S., Xu, L., Wang, N., Hu, Z., Luo, X. & Zheng, Z. (2020). Synthesis of magnetite/lanthanum hydroxide composite and magnetite/aluminum hydroxide composite for removal of phosphate. *Science of the Total Environment*, 723, 137838.

Srichandan, S., Kim, J.Y., Bhadury, P., Barik, S.K., Muduli, P.R., Samal, R.N., Pattnaik, A.K., & Rastogi, G. (2015). Spatiotemporal distribution and composition of phytoplankton assemblages in a coastal tropical lagoon: Chilika, India. *Environmental Monitoring and Assessment*, 187(2), 1-17.

Steffen, W., Richardson, K., Rockström, J., Cornell, S. E., Fetzer, I., Bennett, E. M., & Sorlin, S. (2015). Planetary boundaries: Guiding human development on a changing planet. *Science*, 347(6223), 1259855.

Sun, W., Xia, C., Xu, M., Guo, J., & Sun, G. (2016). Application of modified water quality indices as indicators to assess the spatial and temporal trends of water quality in the Dongjiang River. *Ecological Indicators*, 66, 306-312.

Tammeorg, O., Nurnberg, G., Horppila, J., Haldna, M. & Niemisto, J. (2020). Redox-related release of phosphorus from sediments in large and shallow Lake Peipsi: Evidence from sediment studies and long-term monitoring data. *Journal of Great Lakes Research*, 46(6), 1595-1603.

Tripathi, M. & Singal, S.K. (2019). Use of principal component analysis for parameter selection for development of a novel water quality index: a case study of river Ganga India. *Ecological Indicators*, 96, 430-436.

Tripathy, S. K. (1995). Studies on the Chemical properties of the Chilika lagoon, east caost of India (Doctoral dissertation, Ph. D. Thesis, Berhampur University, Odisha, India, PP-1-193).

United Nation World Water Day (2010) http://unwater-archive.stage. gsdh.org/WWD-2010//www.unwater.org/wwd10/faqs.html. Accessed 26 Jan 2015

van Dijk, G., Smolders, A. J., Loeb, R., Bout, A., Roelofs, J. G., & Lamers, L. P. (2015). Salinization of coastal freshwater wetlands; effects of constant versus fluctuating salinity on sediment biogeochemistry. *Biogeochemistry*, 126(1), 71-84.

Vymazal, J. (2002). The use of sub-surface constructed wetlands for wastewater treatment in the Czech Republic: 10 years' experience. *Ecological Engineering*, 18(5), 633-646.

Wang, C., Wu, Y., Wang, Y., Bai, L., Jiang, H., & Yu, J. (2018). Lanthanum-modified drinking water treatment residue for initial rapid and long-term equilibrium phosphorus immobilization to control eutrophication. *Water research*, 137, 173-183.

Wang, J., Wang, W., Xiong, J., Li, L., Zhao, B., Sohail, I., & He, Z. (2021). A constructed wetland system with aquatic macrophytes for cleaning contaminated runoff/storm water from urban area in Florida. *Journal of Environmental Management*, 280, 111794.

Wang, L., & Liang, T. (2014). Effects of exogenous rare earth elements on phosphorus adsorption and desorption in different types of soils. *Chemosphere*, 103, 148-155.

Wang, L., Kumeria, T., Santos, A., Forward, P., Lambert, M. F., & Losic, D. (2016). Iron oxide nanowires from bacteria biofilm as an efficient visible-light magnetic photocatalyst. *ACS Applied Materials & Interfaces*, 8(31), 20110-20119.

Wang, S., Jin, X., Zhao, H., Zhou, X., & Wu, F. (2007). Effects of Hydrilla verticillata on phosphorus retention and release in sediments. *Water, Air, and Soil Pollution*, 181(1), 329-339.

Wang, S.R., Zhao, H.C., Li, Y.P., Zhang, L., Jiao, L.X., Li, L.X., & Gu, Y.T. (2017). Transportation of dissolved carbon, nitrogen and phosphorus in Lake Erhai. *The Science Publishing Company*.

Wang, Y., Yang, X., Jing, X., Dai, J., Dong, M., & Yan, Y. (2020). Adsorption of phosphorus on lanthanum doped carbon films guided by self-assembly of cellulose nanocrystalline. *Journal of Molecular Liquids*, 319, 114148.

Wang, Z., Lu, S., Wu, D., & Chen, F. (2017). Control of internal phosphorus loading in eutrophic lakes using lanthanum-modified zeolite. *Chemical Engineering Journal*, 327, 505-513.

Weiss, R. F. (1970). The solubility of nitrogen, oxygen and argon in water and seawater. In Deep sea research and oceanographic abstracts ,17 (4), 721-735, Elsevier.

Wu, B., Fang, L., Fortner, J. D., Guan, X., & Lo, I. M. (2017). Highly efficient and selective phosphate removal from wastewater by magnetically recoverable La $(OH)_3$/Fe_3O_4 nanocomposites. *Water research*, 126, 179-188.

Wu, X., Ma, T., Du, Y., Jiang, Q., Shen, S. & Liu, W. (2021). Phosphorus cycling in freshwater lake sediments: Influence of seasonal water level fluctuations. *Science of the Total Environment*, 792, 148383.

Xia, X.H., Zhang, S., Li, S.L., Zhang, L.W., Wang, G.Q., Zhang, L., Wang, J.F., & Li, Z.H., (2018). The cycle of nitrogen in river system: sources, transformation, and flux. *Environmental Science Processes & Impacts*, 20(6), 863-891.

Xia, Y., Tang, Y., Shih, K., & Li, B. (2020). Enhanced phosphorus availability and heavy metal removal by chlorination during sewage sludge pyrolysis. *Journal of hazardous materials*, 382, 121110.

Xie, F., Dai, Z., Zhu, Y., Li, G., Li, H., He, Z., Geng, S. & Wu, F. (2019). Adsorption of phosphate by sediments in a eutrophic lake: Isotherms, kinetics, thermodynamics and the

influence of dissolved organic matter. *Colloids and Surfaces A: Physicochemical and Engineering Aspects*, 562, 16-25.

Xie, F.Z., Li, L., Song, K., Li, G.L., Wu, F.C., & Giesy, J.P. (2019). Characterization of phosphorus forms in a Eutrophic Lake, China. *Science of The Total Environment*, 659, 1437-1447.

Xie, J., Lai, L., Lin, L., Wu, D., Zhang, Z., & Kong, H. (2015). Phosphate removal from water by a novel zeolite/lanthanum hydroxide hybrid material prepared from coal fly ash. *Journal of Environmental Science and Health, Part A*, 50(12), 1298-1305.

Xie, J., Lin, Y., Li, C., Wu, D. & Kong, H. (2015). Removal and recovery of phosphate from water by activated aluminum oxide and lanthanum oxide. *Powder Technology*, 269, 351-357.

Xie, J., Wang, Z., Lu, S., Wu, D., Zhang, Z., & Kong, H. (2014). Removal and recovery of phosphate from water by lanthanum hydroxide materials. *Chemical Engineering Journal*, 254, 163-170.

Xing, Z. H., Wang, S. S., & Xu, A. W. (2014). Dipole-directed assembly of Fe_3O_4 nanoparticles into nanorings via oriented attachment. *CrystEngComm*, 16(8), 1482-1487.

Xiong, Y., Guilbaud, R., Peacock, C. L., Cox, R. P., Canfield, D. E., Krom, M. D., & Poulton, S. W. (2019). Phosphorus cycling in Lake Cadagno, Switzerland: a low sulfate euxinic ocean analogue. *Geochimica et Cosmochimica Acta*, 251, 116-135.

Xu, D., Yan, P., Liu, Z., Zhang, M., Yan, W., Liu, Y., Wu, Z. & Zhang, Y. (2021). Spatial distribution of phosphorus forms and the release risk of sediments phosphorus in West Lake, Hangzhou, China. *Ecological Engineering*, 173, 106421.

Xu, R., Zhang, M., Mortimer, R. J., & Pan, G. (2017). Enhanced phosphorus locking by novel lanthanum/aluminum–hydroxide composite: implications for eutrophication control. *Environmental Science & Technology*, 51(6), 3418-3425.

Xue, P., Pang, Y., Xiang, S., Hu, X., & Wang, X. (2017). Nitrogen loss characteristics of farmland runoff under simulated precipitation conditions. *Journal of Agro-Environment Science*, 36(7), 1362-1368.

Yalçın¸ S., Demirak, A., & Keskin, F. (2012). Phosphorus fractions and its potential release in the sediment of Koycegiz Lake, Turkey. *Lakes Reservoirs and Ponds*, 6,139–153.

Yan, F., Qiao, D., Qian, B., Ma, L., Xing, X., Zhang, Y., & Wang, X. (2016). Improvement of CCME WQI using grey relational method. *Journal of Hydrology*, 543, 316-323.

Yan, X. C., Zhang, C. Q., Ji, M., Wang, M., Ran, S., Xu, X., & Wang, G. (2018). Concentration of dissolved greenhouse gas and its influence factors in the summer surface water of eutrophic lake. *Journal of Lake sciences*, 30(5), 1420-1428.

Yang, J., Zeng, Q., Peng, L., Lei, M., Song, H., Tie, B., & Gu, J. (2013). La-EDTA coated Fe3O4 nanomaterial: preparation and application in removal of phosphate from water. *Journal of Environmental Sciences*, 25(2), 413-418.

Yang, J., Zhou, L., Zhao, L., Zhang, H., Yin, J., Wei, G., & Yu, C. (2011). A designed nanoporous material for phosphate removal with high efficiency. *Journal of Materials Chemistry*, 21(8), 2489-2494.

Yang, L.K., Zhao, X.H., Peng, S., & Li, X. (2016). Water quality assessment analysis by using combination of Bayesian and genetic algorithm approach in an urban lake, China. *Ecological Modelling*, 339, 77-88.

Yang, X., Chen, X. & Yang, X. (2019). Effect of organic matter on phosphorus adsorption and desorption in a black soil from Northeast China. *Soil and Tillage Research*, 187, 85-91.

Yang, Y., Koh, K. Y., Li, R., Zhang, H., Yan, Y., & Chen, J. P. (2020). An innovative lanthanum carbonate grafted micro-fibrous composite for phosphate adsorption in wastewater. *Journal of hazardous materials*, 392, 121952.

Yang, M., Lin, J., Zhan, Y., & Zhang, H. (2014). Adsorption of phosphate from water on lake sediments amended with zirconium-modified zeolites in batch mode. *Ecological engineering*, 71, 223-233.

Yin, H., Han, M., & Tang, W. (2016). Phosphorus sorption and supply from eutrophic lake sediment amended with thermally-treated calcium-rich attapulgite and a safety evaluation. *Chemical Engineering Journal*, 285, 671-678.

Yoon, S. Y., Lee, C. G., Park, J. A., Kim, J. H., Kim, S. B., Lee, S. H., & Choi, J. W. (2014). Kinetic, equilibrium and thermodynamic studies for phosphate adsorption to magnetic iron oxide nanoparticles. *Chemical engineering journal*, 236, 341-347.

Young, J. C. (1973). Chemical methods for nitrification control. *Journal (Water Pollution Control Federation*), 637-646.

Yu, J., Xiang, C., Zhang, G., Wang, H., Ji, Q., & Qu, J. (2019). Activation of lattice oxygen in LaFe (oxy) hydroxides for efficient phosphorus removal. *Environmental Science & Technology*, 53(15), 9073-9080.

Yuan, F., Chaffin, J. D., Xue, B., Wattrus, N., Zhu, Y., & Sun, Y. (2018). Contrasting sources and mobility of trace metals in recent sediments of western Lake Erie. *Journal of Great Lakes Researc*h, 44(5), 1026-1034.

Yuan, F., Li, H., Kakarla, R., Kasden, C., Yao, S., Xue, B. & Sun, Y. (2020). Variability of sedimentary phosphorus fractions in the western and Sandusky basins of Lake Erie. *Journal of Great Lakes Research*, 46(4), 976-988.

Zach-Maor, A., Semiat, R., & Shemer, H. (2011). Synthesis, performance, and modeling of immobilized nano-sized magnetite layer for phosphate removal. *Journal of colloid and interface science*, 357(2), 440-446.

Zhang, J., Buyang, S., Yi, Q., Deng, P., Huang, W., Chen, C. & Shi, W. (2023). Connecting sources, fractions and algal availability of sediment phosphorus in shallow lakes: An approach to the criteria for sediment phosphorus concentrations. *Journal of Environmental Sciences*, 125, 798-810.

Zhang, J., Shen, Z., Shan, W., Mei, Z., & Wang, W. (2011). Adsorption behavior of phosphate on lanthanum (III)-coordinated diamino-functionalized 3D hybrid mesoporous silicates material. *Journal of Hazardous Materials*, 186(1), 76-83.

Zhang, L., Liu, Y., Wang, Y., Li, X. & Wang, Y. (2021). Investigation of phosphate removal mechanisms by a lanthanum hydroxide adsorbent using p-XRD, FTIR and XPS. *Applied Surface Science*, 557, 149838.

Zhang, L., Zhou, Q., Liu, J., Chang, N., Wan, L., & Chen, J. (2012). Phosphate adsorption on lanthanum hydroxide-doped activated carbon fiber. *Chemical Engineering Journal*, 185, 160-167.

Zhang, Q., Teng, J., Zou, G., Peng, Q., Du, Q., Jiao, T., & Xiang, J. (2016). Efficient phosphate sequestration for water purification by unique sandwich-like MXene/magnetic iron oxide nanocomposites. *Nanoscale*, 8(13), 7085-7093.

Zhang, S., Yi, Q., Buyang, S., Cui, H., & Zhang, S. (2020). Enrichment of bioavailable phosphorus in fine particles when sediment resuspension hinders the ecological restoration of shallow eutrophic lakes. *Science of the Total Environment*, 710, 135672.

Zhang, T., Bowers, K. E., Harrison, J. H., & Chen, S. (2010). Releasing phosphorus from calcium for struvite fertilizer production from anaerobically digested dairy effluent. *Water Environment Research*, 82(1), 34-42.

Zhang, W.S., Li, H.P., & Li, Y.L. (2019a). Spatio-temporal dynamics of nitrogen and phosphorus input budgets in a global hotspot of anthropogenic inputs. *Science of The Total Environment*, 656, 1108-1120.

Zhang, W., Pueppke, S. G., Li, H., Geng, J., Diao, Y., & Hyndman, D. W. (2019). Modeling phosphorus sources and transport in a headwater catchment with rapid agricultural expansion. *Environmental Pollution*, 255, 113273.

Zhang, Y., Gao, X., Wang, C., Chen, C.T.A., Zhou, F. & Yang, Y. (2016). Geochemistry of phosphorus in sediment cores from Sishili Bay, China. *Marine pollution bulletin*, 113(1-2), 552-558.

Zhang, Y.F., Liang, J., Zeng, G.M., Tang, W.W., Lu, Y., Luo, Y., Xing, W.L., Tang, N., Ye, S.J., Li, X., & Huang, W. (2020). How climate change and eutrophication interact with microplastic pollution and sediment resuspension in shallow lakes: A review. *Science of The Total Environment*, 705, 135979.

Zhang, Y.X., Zhang, Y.C., Zhou, W., Zhang, M., & Ma, R.H. (2018). Inherent optical properties of typical cyanobacteria in eutrophic lakes. *Journal of lake sciences*. 30(6), 1681-1692.

Zheng, L., Su, W., Qi, Z., Xu, Y., Zhou, M., & Xie, Y. (2011). First-order metal–insulator transition and infrared identification of shape-controlled magnetite nanocrystals. *Nanotechnology*, 22(48), 485706.

Zhong, Z., Lu, X., Yan, R., Lin, S., Wu, X., Huang, M., Liu, Z., Zhang, F., Zhang, B., Zhu, H. & Guo, X. (2020). Phosphate sequestration by magnetic La-impregnated bentonite granules: A combined experimental and DFT study. *Science of The Total Environment*, 738, 139636.

Zhou, J., Li, D., Zhao, Z., Song, X., Huang, Y., & Yang, J. (2020). Phosphorus immobilization by the surface sediments under the capping with new calcium peroxide material. *Journal of Cleaner Production*, 247, 119135.

Zhou, Q., Gibson, C.E. & Zhu, Y. (2001). Evaluation of phosphorus bioavailability in sediments of three contrasting lakes in China and the UK. *Chemosphere*, 42(2), 221-225.

Zhu, Y., Wu, F., Feng, W., Liu, S., & Giesy, J. P. (2016). Interaction of alkaline phosphatase with minerals and sediments: activities, kinetics and hydrolysis of organic phosphorus. *Colloids and Surfaces A: Physicochemical and Engineering Aspects*, 495, 46-53.

Zhu, Y., Zhang, R., Wu, F., Qu, X., Xie, F. & Fu, Z. (2013). Phosphorus fractions and bioavailability in relation to particle size characteristics in sediments from Lake Hongfeng, Southwest China. *Environmental earth sciences*, 68(4), 1041-1052.

Zhuang, W., Gao, X., Zhang, Y., Xing, Q., Tosi, L., & Qin, S. (2014). Geochemical characteristics of phosphorus in surface sediments of two major Chinese mariculture areas: the Laizhou Bay and the coastal waters of the Zhangzi Island. *Marine pollution bulletin*, 83(1), 343-351..

Zou, W., Zhu, G.W., Cai, Y.J., Vilmi, A., Xu, H., Zhu, M.Y., Gong, Z.J., Zhang, Y.L., & Qin, B.Q. (2020). Relationships between nutrient, chlorophyll a and Secchi depth in lakes of the

Chinese Eastern Plains ecoregion: Implications for eutrophication management. *Journal of Environmental Management*, 260, 109923.

Ouriginal by Turnitin

Document Information

Analyzed document	Satya_Department of Soil Science & Ag. Chemistry.docx (D143522938)
Submitted	9/2/2022 11:56:00 AM
Submitted by	
Submitter email	satyanarayanapradhan22@gmail.com
Similarity	0%
Analysis address	cenlib2014.bhuni@analysis.urkund.com

Sources included in the report

W URL: https://www.sciencedirect.com/science/article/pii/S0167198721002877
Fetched: 10/29/2021 6:59:59 AM — 1

SA **The University of Burdwan, Bardhaman / Geetanjali Dutta.pdf**
Document Geetanjali Dutta.pdf (D41407936)
Submitted by: bikash_mukherjee@yahoo.com
Receiver: bikash_mukherjee.unibur@analysis.urkund.com — 1

Entire Document

Ecology, Environment and Conservation

PEER-REVIEWED JOURNAL

INDEXED IN GOOGLE SCHOLAR

UGC-CARE JOURNAL

(List II- Globally recognized databases)

Please check by ISSN -0971-765X

Brief About Ecology, Environment and Conservation

Published Quarterly Since 1995. Ecology, Environment and Conservation is published in March, June, September and December every year.

ECOLOGY, ENVIRONMENT AND CONSERVATION is one of the leading International environmental journals. It is widely subscribed in India and abroad by Institutions and Individuals in education and research as well as by Industries, Govt. Departments and Research Institutes.

Ecology, Environment and Conservation is in the Master Journal List of ISI (Thomson Reuters, U.S.A.).

Ecology, Environment and Conservation is abstracted/covered in:

- SCOPUS (1997-2021)
- Cambridge Science Abstracts
- Ecology Abstracts
- Pollution Abstracts
- Eco-Disc CD Rom
- Geological Abstracts
- International Development Abstracts
- Oceanographic Literature Review
- Indian Science Abstracts, Niscair, India

Archived Issues

Download Sample Paper

Download Sample Issue

Subscription Rates

Submit Article

Editorial Board

Aims, Objectives & Scope

Eco. Env. & Cons. 28 (2) : 2022; pp. (1051-1054)
Copyright@ EM International
ISSN 0971–765X

Synthesis and Characterization of Magnetite for Pollutant Remediation

S.N. Pradhan[1], R. Maurya[2], A.K. Ghosh*[3], D. Panda[4], S.K. Bhadani[5] and Baburam[6]

[1, 2, 3,4,5,6]Department of Soil Science & Agricultural Chemistry, Institute of Agricultural Sciences, BHU, Varanasi 221 005, UP, India

(Received 3 March, 2022; Accepted 10 April, 2022)

ABSTRACT

Phosphorus is one of the limiting nutrients for crop production, especially in developing countries where soil available P is low. To counter P deficiency, P has been applied at a rate above crop uptake which makes management of P fertilizer a challenge for the scientific community, as high input P can have environmental consequences like eutrophication of water bodies. Physico-chemical and biological methods are widely used for the removal of soluble P from wastewater. Adsorption of P onto a paramagnetic substance like magnetite holds a great promise for its removal and subsequent recovery of adsorbed P. The present study was carried out with the objective of synthesis of magnetite in different molar ratios and its characterization to select the best magnetite material for removal of P. Magnetite was synthesized using the co-precipitation method using ferrous and ferric ions at different molar ratios (1:1, 1:2, 2:1, 5:1) and characterized for Xray diffraction, Fourier transforms infrared spectroscopy, and Brunauer-Emmett-Tellermethod surface area. All the synthesized material resembled the Joint Committee on Powder Diffraction Standards XRD patterns of reference magnetite and showed strong peaks at 220, 311, 400, 511, and 440 cm^{-1}. FTIR analysis showed the presence of Fe-O bond at 580 cm^{-1} and characteristic peaks at 1633 and 3400 cm^{-1} suggesting the presence of a hydroxyl group. Highest surface area (93.001 (m^2/g) was observed for magnetite synthesized with a molar ratio of 1:2 (Fe^{2+}/ Fe^{3+}), whereas the surface area of the rest of the synthesized magnetite was close to 50 m^2/g. The smallest pore radius was also found in magnetite synthesized with a molar ratio of 1:2 (Fe^{2+}/ Fe^{3+}) which contributed to the highest pore volume

Key words: *Adsorption, Magnetite, XRD, BET, Phosphorus*

Introduction

Water quality is important in every aspect of the ecosystem and the well-being of humans. The river and lake and other aquatic body ecosystems directly or indirectly influence human health and aquatic life (Kar, 2013). Meeting the water quality of aquatic bodies was also a major issue as these are the source for supplying water for various domestic, industrial, and agricultural use. The importance of P originating from agricultural sources to the nonpoint source of environmental pollution has been a challenging issue of the 21st century. To increase food production multi-fold to cope with the rising food security fertilizer are applied at a rate greater than crop uptake (Pradhan *et al.,* 2021). Continued application of P fertilizer and its subsequent movement to different water bodies triggers eutrophication (Zafar *et al.,* 2016). Therefore, removal of P from the contaminated water is a must for the safe use of water. Removal technologies of P are divided into three types, (i) physical-chemical (precipitation: primary, simultaneous, or final) (ii) biological (enhanced biological removal), or (iii) membrane purification techniques.

Corresponding author's email: amlankumar@yahoo.com

Out of these physico-chemical techniques, adsorption and ion exchange, and magnetic separation are known to be more useful and economical. Adsorption is a surface phenomenon in which electrostatic attractionoccurs between positively charged surfaces of iron oxides and negatively charged phosphate ions, forming an outer-sphere complex. The main principle behind the use of magnetite for the separation of P is the use of a magnetic field to separate particles. To separate P from the wastewater P must be converted into insoluble form and the adsorbent must possess the magnetic property for its separation. Magnetite (Fe_3O_4) is a substance having paramagnetic properties. The present study was carried out with the objective of (i) synthesis of magnetite in different molar ratios (ii) Characterization of magnetite and evaluation of the best molar ratio for magnetite synthesis.

Materials and Methods

Magnetite was synthesized using the chemical co-precipitation method using ferrous sulphate ($FeSO_4.6H_2O$) and ferric chloride ($FeCl_3$) in a different ratio (Table 1). Fe (II) and Fe (III) salts were taken in four different ratios and dissolved separately in a beaker. Then, the $FeSO_4.7H_2O$ solution was poured into the $FeCl_3$ solution and the resulting mixture was placed on a magnetic stirrer and stirred at 60-700 C for 5 Min at 200 rpm. Nitrogen gas was supplied to eliminate oxygen from the working environment. The pH of the solution was then adjusted to pH 10-11 by adding 20% NaOH dropwise using a burette. The colour of the mixture changes from orange to brown at pH 6 and dark black at pH 10-11 indicating the formation of magnetite. The resultant suspension was kept for settling and washed with distilled water to attain neutrality. The precipitate was placed on a porcelain dish and dried at 50° C in a hot air oven and finally ground to pass through a 100-mesh sieve.

Characterization of magnetite

The synthesized magnetite was characterized using X-ray diffraction technology for the identification of the crystal structure of the mineral and (FTIR) was used for the determination of the functional group. Before the FTIR analysis, the samples were prepared by mixing with KBr at a ratio of 1:100(w/w) Fourier transform infrared spectroscopy and pressed into a film. The specific surface area was measured from the adsorption branch of the isotherm using the Brunauer-Emmett-Teller (BET) method.

Result and Discussion

X-ray diffraction (XRD)

The crystal structure of the magnetite was determined using X-ray diffraction technology (Fig. 1). The XRD peak of synthesized magnetite matched well with the Joint Committee on Powder Diffraction Standards (JCPDS) reference pattern of magnetite (JCPDS N0. 89-4319). Characteristics peak at 2ε = 35.44 and 62.90 due to reflections from planes of (311) and (440) were observed for magnetite. The very broad peak of the magnetite in the XRD pattern suggests the ultra-fine nature and small crystalline

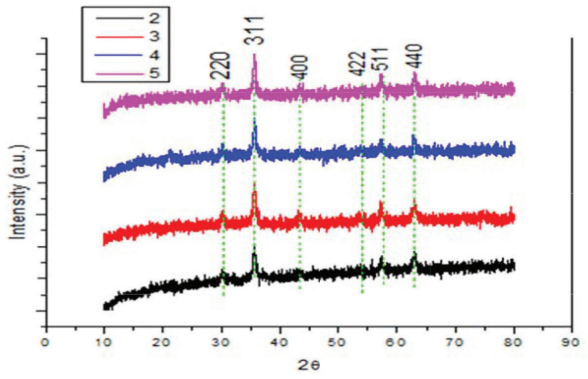

Fig. 1. XRD peak of synthesized magnetite of different molar ratio of Fe^{2+}/ Fe^{3+}. (2)- 1:1, (3)- 1:2, (4)- 2:1 and (5)- 5:1.

Table 1. BET and Barrett-Joyner-Halendra adsorption summary

Fe^{2+} / Fe^{3+}	Fe^{2+}(g)	Fe^{3+}(g)	Correlation coefficient	Surface Area (m^2g^{-1})	Pore Volume (cc g^{-1})	Pore Radius (A°)
1:1	1	1	0.99	51.56	0.13	17.01
1:2	0.5	0.66	0.99	93.00	0.19	15.29
2:1	2	1.33	0.99	50.40	0.11	17.03
5:1	5	1.83	0.99	49.76	0.14	17.12

structure of the magnetite. Kim *et al.* (2012) found a similar peak for synthesized magnetite. The size of the crystallite is determined using Debye Scherrer's formula, $D = k\lambda / \beta \cos\theta$, where k = 0.89, λ is the X-ray wavelength of Cu Kα radiation, β is the full width at half maximum (FWHM) of the peaks and θ is the glancing angle and the average crystallite size is 10 nm.

Fourier transform infrared spectroscopy (FTIR)

The functional group of the magnetite was determined using FTIR (MAKE: JASCO, Model 4700) analysis at 4000-400 cm^{-1} wave number and recording the corresponding Transmittance (%). The plot of wave number and percentage transmittance was presented in Fig. 2. The wave number associated with the different functional groupsis revealed by their characteristics peak. The vibration of the Fe-O bond was indicated by a band at 580 cm^{-1}. The vibration of the hydroxyl group on the surface of the magnetite was indicated by characteristics peaks at 1633 and 3400 cm^{-1}. Choi (2016) reported characteristics peak after phosphorus adsorption and observed major peaks at 1632, 1070, 619, and 469 cm^{-1}, which corresponded to the bending vibration of H_2O molecules and the stretching vibration of Fe–OH groups. In addition to this, four new bands appear at 1404, 1530, 2852, and 2923 cm^{-1} which suggest the presence of coating agents that are bonded to the surface of magnetite as esterification occurs between carboxyl and hydroxyl group. The bands at 1404 and 1530 cm^{-1} are assigned to the asymmetric and symmetric stretching vibrations of the carboxyl group (COO^-), respectively (Saranya *et al.*, 2015).

Brunauer-Emmett-Teller Method (BET)

The surface area of the synthesized magnetite was presented in Table 1. A perusal of Table 1 suggests that magnetite synthesized at a molar ratio of 1:2 (Fe^{2+} / Fe^{3+}) has the highest surface area with a value of 93.001 m^2g^{-1} followed by magnetite synthesized at a molar ratio of 1:1 (Fe^{2+} / Fe^{3+}). The smallest surface area observed in magnetite synthesized at a molar ratio of 1:1, 2:1, and 5:1 ((Fe^{2+} / Fe^{3+}) could be attributed to a large amount of aggregation during synthesis. Nitrogen adsorption and desorption isotherm and the pore radius and pore volume were also shown in Table 1. Barrett–Joyner–Halenda (BJH) analysis confirmed the contribution of mesopore to the increased surface area of the magnetite. Adsorption isotherm of nitrogen gas suggests that magnetite (1:2) ratio has the highest specific surface area of

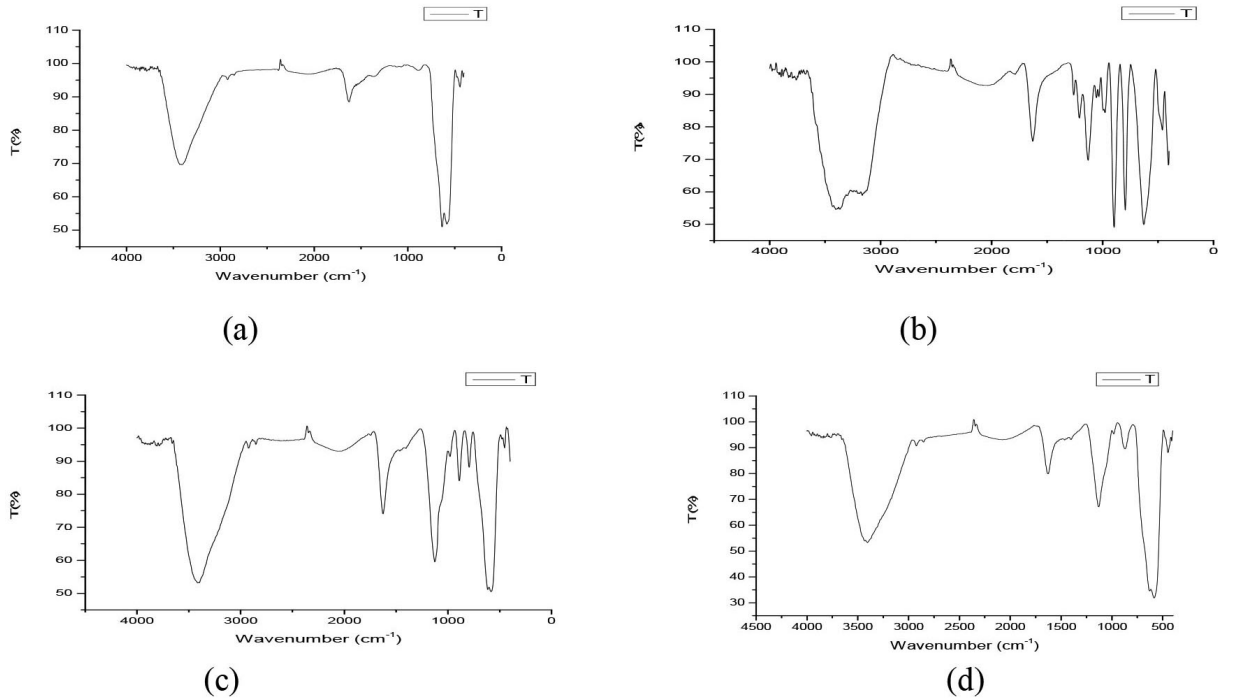

Fig. 2. FTIR analysis showing characteristics peak corresponds to different functional group. (a) 1:1, (b) 1:2, (c) 2:1, (d) 5:1

62.484 m^2/g, pore volume of 0.19 cc g^{-1}, and pore radius of 15.293 A^o. The surface area of magnetite synthesized at other molar ratios (1:1, 2:1, and 5:1) was lower as compared to 1:2 molar ratio magnetite.

Acknowledgments

The authors are grateful to Department of Soil Science and Agricultural Chemistry, Banaras Hindu University, for providing the necessary facilities and infrastructure to carry out the investigation.

Conflict of Interest

There is no potential conflict of interest.

References

Choi, J., Chung, J., Lee, W. and Kim, J. O. 2016. Phosphorous adsorption on synthesized magnetite in wastewater. *Journal of Industrial and Engineering Chemistry*. 34: 198-203.

Kar, D. 2013. Wetlands and lakes of the world. Springer, London

Kim, W., Suh, C. Y., Cho, S. W., Roh, K. M., Kwon, H., Song, K. and Shon, I. J. 2012. A new method for the identification and quantification of magnetite–maghemite mixture using conventional X-ray diffraction technique. *Talanta.* 94 : 348-352.

Pradhan, S.N., Ghosh, A.K., Ram, S., Pal, Y. and Pradhan, C. 2021. Changes in degree of phosphorus saturation and risk of P loss upon twelve years of manuring and reduced tillage. *Geoderma*. 404 : 115277.

Saranya, T., Parasuraman, K., Anbarasu, M. and Balamurugan, K. 2015. XRD, FT-IR and SEM study of magnetite (Fe 3 O 4) nanoparticles prepared by hydrothermal method. *Nano Vision.* 5 : 149-154.

Zafar, M., Tiecher, T., de Castro Lima, J.A.M., Schaefer, G.L., Santanna, M.A. and Dos Santos, D.R. 2016. Phosphorus seasonal sorption-desorption kinetics in suspended sediment inresponse to land use and management in the Guaporé catchment, Southern Brazil. *Environmental Monitoring and Assessment*. 188(11) : 1-20.

ScienceDirect

Marine Pollution Bulletin

Supports *open access*

9.2	7.001
CiteScore	Impact Factor

Submit your article | Guide for authors

Menu | Search in this journal

Latest issue

Volume 183

In progress • October 2022

About the journal

The International Journal for Marine Environmental Scientists, Engineers, Administrators, Politicians and Lawyers

Marine Pollution Bulletin is concerned with the rational use of maritime and m**arine resources** in estuaries, the seas and oceans, as well as with documenting **marine pollution** and introducing new forms of measurement and analysis. A wide range of topics are discussed as news, comment, reviews and ...

View full aims & scope

2.2 weeks
Publication Time

View all insights

Editors-in-Chief | View full Editorial Board

FEEDBACK

Marine Pollution Bulletin

Spatial variation in sedimentary phosphorus fractions and its ecological risk assessment of Asia's largest brackish water lake (Chilika, India)

--Manuscript Draft--

Manuscript Number:	
Article Type:	Research Paper
Keywords:	Lake sediment; Phosphorus fractions; Eutrophication. Ecological risk assessment
Corresponding Author:	Amlan Kumar Ghosh, Ph.D. Banaras Hindu University Institute of Agricultural Sciences Varanasi, Uttar Pradesh INDIA
First Author:	Satya Narayana Pradhan
Order of Authors:	Satya Narayana Pradhan
	Amlan Kumar Ghosh
	Prasannajit Acharya
	Pradipta R. Muduli
	Ishan Biswajit Sahoo
	Preeti Singh
	Dibyajyoti Panda
Abstract:	Investigating the patterns of phosphorus (P) distribution in sediments and carrying out ecological risk assessments are crucial for effective eutrophication control and ecosystem restoration. Studying the sediment P availability is essential to achieving the restoration goal. The largest brackish water lake, Chilika, was used in this study to examine the regional variation in distribution of P fractions and its bioavailability. The most redox sensitive iron and aluminum bound P comprised 27.5% of sum of P fractions, suggesting high P release potential from the sediment to overlaying water in anoxic sediment. Principal component analysis revealed that R-P, organic carbon, and texture as important parameter in determining distribution of P fractions in the lake. The ecological risk of sediment phosphorus was evaluated using biological effective parameter. According to single pollution index and biological effective index, 57 to 60% of the samples studied falls under slightly to moderately polluted.
Suggested Reviewers:	Sivaji Patra, Ph.D. Scientist, National Centre for Coastal Research sivajipatra@nccr.gov.in He is an experienced scientist doing research in the field of coastal ecosystem like lake.
	Vishnu Vardhan Kanuri, Ph.D. Eastern Regional Directorate, National Ganga River Basin Authority, Central Pollution Control Board, India vishnuchemistry@gmail.com He has good knowledge about ecological risk assessment of water bodies and doing research in the field of health status of Ganga river basin, India
	Rajani Kanta Mishra, Ph.D. Scientist, National Centre for Polar and Ocean Research rajanimishra@ncpor.res.in He is experienced scientist in the field of polar and ocean research

Spatial variation in sedimentary phosphorus fractions and its ecological risk assessment of Asia's largest brackish water lake (Chilika, India)

Satya Narayana Pradhan[1], A. K. Ghosh[1*], Prasannajit Acharya[2], Pradipta R. Muduli[3], Ishan Biswajit Sahoo[3], Preeti Singh [1,4], Dibyajyoti Panda[1]

[1] Soil Technology and Carbon Sequestration Laboratory, Department of Soil Science and Agricultural Chemistry, Institute of Agricultural Sciences, Banaras Hindu University, Varanasi 221005, India

[2]Institute of Technical Education and Research, Department of Chemistry, Siksha 'O' Anusandhan (Deemed to be University), Bhubaneswar, 751030, India

[3]Wetland Research and Training Centre, Chilika Development authority, Balugaon, 752030, India

[4]ICAR-IARI, Gauria Karma, Hazaribag 825405, Jharkhand, India

*Corresponding author: A. K. Ghosh (Email: amlankumar@yahoo.com; Mobile: 9451363054; Fax: +91-542-2368993)

Abstract

Investigating the patterns of phosphorus (P) distribution in sediments and carrying out ecological risk assessments are crucial for effective eutrophication control and ecosystem restoration. Studying the sediment P availability is essential to achieving the restoration goal. The largest brackish water lake, Chilika, was used in this study to examine the regional variation in distribution of P fractions and its bioavailability. The content of loosely bound phosphorus (L-P), aluminium and iron-bound phosphorus (Al & Fe-P), residual phosphorus (R-P), and total phosphorus (P) significantly differed across the lake, based to one-way ANOVA. Residual P was the dominating P fraction in the lake suggesting effect of P load from

agricultural activities in the catchment area on lake ecosystem. The most redox sensitive iron and aluminum bound P comprised 27.5% of sum of P fractions, suggesting high P release potential from the sediment to overlaying water in anoxic sediment. Principal component analysis revealed that R-P, organic carbon, and texture as important parameter in determining distribution of P fractions in the lake. The lake is divided into two cluster based on sediment properties and contents of P fractions, one showing effect of tidal influence and another exhibiting effect of anthropogenic activity in the catchment area and freshwater inflow from the river and its tributaries. The ecological risk of sediment phosphorus was evaluated using biological effective parameter. According to single pollution index and biological effective index, 57 to 60% of the samples studied falls under slightly to moderately polluted.

Keywords: Lake sediment, Phosphorus fractions, Eutrophication. Ecological risk assessment

Introduction

Transfer or loss of P from agricultural field and other land use system in the watershed have been main contributing factor for enrichment of P in waterbodies, streams, and lakes. P has been identified as the most limiting nutrient for primary productivity in the lake (Worsfold et al., 2016; Tu et al., 2019), which in excess can cause eutrophication of water bodies (Immers et al., 2015; Zhang et al., 2016). Eutrophication has been global concern for decades especially lake receiving freshwater inflow. Eutrophication significantly alters the ecological equilibrium and endangers human health.

Numerous strategies and technologies are developed to control eutrophication which includes external nutrient loading control (waste water treatment plant, controlling non-point source pollution), internal loading control (dredging, oxidation, biotechnology etc.), freshwater restoration in lake, integrated watershed management (Guo et al., 2017; Wang et al., 2019; Ni et al., 2020). Out of these control mechanism, external P loading control is the basic mechanism

to control P eutrophication. A lot of studies focused on to quantify the external P loading and its effect on eutrophication of lake. After control of external input of P loading from catchment area, internal P loading has become global concern due to its potential contribution to P cycling in the overlaying water thereby enhancing primary productivity in and lake trophic status (Hartzell et al., 2017; Gasparatos et al., 2019; Upreti et al., 2019; Wang et al., 2005).

Estimation of total P in sediment provides details about its enrichment in lake, however, quantification of total P alone is not enough to have a precise understanding of P mobilization in lake (Soliman et al., 2017; Barik et al., 2019). Therefore, P speciation is necessary to have a good understanding of potential risk of eutrophication due to elevated concentration of P and evaluate P release risk from sediment. Some specific fraction of P can be an effective indicator for which activities have altered the P cycle and availability of P in water bodies. Analysis of sequential P fractionation have allowed us to determine the different inorganic and organic fractions widely used. The extractable inorganic fractions include loosely bound P (mobile), potential mobile P (Fe and Al bound P, reductant soluble P), non-mobile (Ca-P, occluded P).

Within the lake system, various process and mechanism controls the P fractionation. House (2003) discussed the importance of different process like adsorption, coprecipitation, reduction, and oxidation reaction involved in the P transformation within its fractions. Two types of zones were usually identified in the lake sediment; one is oxidized zone at the sediment-water interface and other is a reduced zone below it. These sediments may act both as source of sink for P depending on the equilibrium between P in the overlaying water and the sediment. Though P mobilization is generally thought to be prevalent in the hypolimnion of stratified lake, P mobilization in oxic condition has also been reported widely (Bostrom et al., 1989; Rydin 2000; Noll et al., 2009). Exchangeable P, Fe bound P and organic P are thought to be mobile in both oxic and anoxic condition as compared to Ca-P which is associated with immobile or permanently bound P.

Lake sediment plays an important role in dynamics of P in shallow waterbodies (Orihel et al., 2015; Yuan et al., 2020). As sediment characteristics and other physical, chemical condition varies across the overlaying water of lake, P release pattern may also vary from place to palace and season to season in a lake (Amirbahman et al., 2013; Yuan et al., 2020). Different biochemical changes occurring in the lake sediment may alter the fractionation of P and finally determine the bioavailability of P and its environmental fate. Release of P from the sediment to overlaying water is the most important factor controlling the water quality and P concentration in the overlaying water. However, not all the fractions can be released from the sediment and render to lake eutrophication. Therefore, knowledge about P release from sediment under the different factors and environmental conditions could reveal the contribution of P fractions to its eutrophication.

Weather is an important parameter that can significantly influence the P recycling in the lake. In a large shallow lake like Chilika, P recycling has great implication on the water quality. Understanding the interaction between sediment and water quality is still unclear. Estuarine tidal marsh represents a transitional ecosystem where land, ocean and fresh wate converge and tidal fluctuation significantly influence the reduction state in the sediment from oxic to anoxic. Since the reporting of first phenomena of P release from sediment (Mortimer, 1941), the evidences draw the conclusion that redox release from Fe-oxy hydroxide is the major primary phenomena that governs the P mobilization from sediment. P is strongly adsorbed to Ferric oxyhydroxide however, under anoxic condition its reduction causes release of P from the Fe-bound compound (Smolders et al., 2017). This mobilized P can well be release to overlaying water when there is an anoxic condition prevail especially due to high temperature during summer season. Besides, high temperature can mobilize P through stimulating desorption of P, mineralization of organic matter, reducing redox potential and promoting diffusion of P from deeper layers.

P deposited as part of organic matter may mineralize with time and the regenerated P may adsorbed to ferric oxyhydroxide or became part of freshly prepared mineral (Katsev, 2016). Under certain environmental condition, soluble P is vulnerable to migrate into overlaying water column, though the oxic layer formed at the water-sediment interface probably limit its migration (Matisoff et al., 2016). However, a weak circulation during prolonged summer season may lead to thermal stratification, followed by development of anoxic layer at sediment-water interface which may migrate the soluble P (Giles et al., 2016). Also, lake shallow lake like Chilika subject to resuspension during some extreme events like cyclone which are more and more common during recent years. This led to increase in the total P concentration and increase in turbidity of the lake and encourage P migration across the water-sediment interface by disrupting the oxic layer.

Chilika lake is habitant to several endangered species listed in International Union for Conservation of Nature (IUCN) Red List of threatened species. Chilika lake receives more than a million bird in winter and has global importance as waterfowl habitat (Balachandran et al., 2003). The lake is also habitat to rare Irrawadi dolphin (world Bank, 2005). Given the ecological importance of Chilika lake, a lot of international and national body has been conducting research about various theme. Several researchers have been studied related to water quality, phytoplankton population, hydrodynamics, and many other themes. However, studies related to P speciation and its related environmental risk assessment is limited (Barik et al., 2017;).

Although P fraction in the lake sediment of Chilika has been studied previously by some researcher, little is known about the release or remobilization of P. To have a better understanding of the processes that controls the P release from sediment, characterization of sediment P fractions is a prerequisite. Analysis of P fractionation will give important insight into P release risk from sediment. Such work will reveal role of internal loading and shed light

on futuristics water management in large shallow lake. Considering the importance of P in enrichment of lake and its associated risk of environmental pollution due to catchment area and intense agricultural activity, a study was undertaken with the aim of revisiting following objective; (1) to determine P fractions of sediment, (2) to investigate spatial changes of P fraction across the lake. The results of the studies would help the model developer and policy maker to take appropriate management strategies to tackle eutrophication.

2. Material and Method

2.1. Study area

The largest brackish water lagoon in Asia, Chilika, which is situated on India's east coast (190 28'-19054' N; 850 60'-850 35' E), was the site of the current study. The semi-enclosed, shallow lacustrine water body, with a mean depth of 2 m, exhibits a rare combination of marine, brackish, and freshwater habitats with estuary characteristics (Mukherjee, Muduli, Barik, & Kumar, 2019). The lagoon was divided into four parts based on topography: the southern sector, which is connected to the sea through the Palur Canal; the central sector; the outer channel; and the northern sector (Fig.1). During the monsoon, the lagoon's surface area is 1165 km^2, while in the summer, it drops to 950 km^2 (Acharya et al., 2022). An artificial opening made in September 2000 connects the lagoon with the Bay of Bengal close to Satapara (Sipakuda). Due to oceanic exchange, a significant inflow of freshwater, and nutrient loading from rivers and rivulets draining the catchment region, the lagoon experiences substantial spatial variability in physical, chemical, and biological characteristics.

Approximately 4406 km^2 make up the lagoon's catchment area, with the western catchment making up 68% of it and the Mahanadi Delta in the northeast accounting for 32%. The lagoon receives freshwater and sediment intake from the river and streams; of these, the north and northeast watershed contribute 78% of the freshwater inflow, followed by the northwest

watershed (12%), centre watershed (6%), and south watershed (4%). (Muduli et al., 2013). There are 54 percent of agricultural lands, 12.2 percent forests, 4.4 percent perennial plants, 1.6 percent swamps and wetland areas, and 2 percent grassy mudflats in the drainage basin (Kadekodi et al 2005). The lagoon is heavily overrun with weeds, such as Azolla, Eichhornia, Nymphea, Pistia, and Ipomea, which are growing at a rate of 15 km^2 per year (Panigrahi et al., 2009). Physico-chemical characteristics of the water column in the lagoon are influenced by the diversity of macrophytes and microalgae.

2.2. Sample collection and analysis

The sediment samples were taken in the winter of 2018 from 25 locations chosen by CDA, covering four ecological sections of the lagoon. The top 10 cm of lagoon sediment was sampled with a Van-Veen grab sampler (KC Denmark). The sediment samples were held in a wide-mouth bottle with lake water in the headspace to keep them anaerobic. To slow biological activity, sand samples were stored at 40 ºC and sent to the lab for analysis.

Phosphat was analyzed using a nutrient autoanalyzer (SKALAR SANplus). Sediment was air-dried, sieved through 0.5mm, and tested for pH, EC, organic carbon, cation exchange capacity, $CaCO_3$, and texture. pH was measured in 1:2.5 sediment-water suspensions and texture with a hydrometer (Bouyoucous, 1927). The potassium dichromate sulfuric acid oxidation technique measured organic carbon (Nelson and Sommers, 1982). $CaCO_3$ of sediment was measured using the fast titration method of Puri (1930). CEC was measured by Hesse's (1971).

2.3. P fractionation scheme

The P fractionation was carried out using wet sediment by using the method described by van Eck (1982) as modified by Moore and Reddy (1994). Wet sediment was transferred to a centrifuge tube of known weight and centrifuged to extract the pore water. The pore water is immediately filtered using a 0.45µ membrane filter and acidified to avoid precipitation of

soluble iron as soluble P. The acidified, filtered sample is analysed by the Murphy-Riley method (Murphy and Riley, 1962) and referred to as water-soluble or soluble reactive P. Then the remaining sample was shaken with 1 *M* KCl, 0.1 *M* NaOH, and 0.5 *M* HCl for 2hr, 17 hr, and 24 hr to extract loosely sorbed P (L-P), Aluminum and iron-bound P (Al & Fe-P) and calcium-bound P (Ca-P) respectively. The extract after shaking was filtered using a 0.45µ membrane filter and then centrifuged for determination of phosphate concentration of respective fractions using the Murphy-Riley method (Murphy and Riley, 1962). The remaining sample was analysed for residual P (R-P) following digestion Hydrofluoric acid (HF) perchloric acid and nitric acid. Total P of the dry sediment was analysed following digestion with Hydrofluoric acid (HF), perchloric acid, and nitric acid.

2.4. Data analysis

Using SPSS, sediment properties and P fractions were analysed using principal component analysis. Kaiser-Meyer-Olkin (KMO) and Bartlett's tests were used to analyse PCA variable data. KMO test was 0.67 and Bartlett's significance level was 0.0 (<0.05), demonstrating PCA may explain variance in the P distribution produced by variables. PCA was used to minimise the number of variables and extract relevant variables that influence the spatial variation of P in lake sediments. Varimax rotation reduced the significance of minor variables. Classifying the sector based on sediment characteristics and P fractions used hierarchical cluster analysis. Arc GIS was used to create single pollution index and biological effective index maps. Sediment-correlation Physico-chemical properties and P forms, and discriminant analysis were analysed using SPSS.

Risk assessment method

Ecological risk assessment of sediment of the lake was evaluated using a single pollution index and biological effectiveness indices for phosphorus. A widely used risk assessment approach

employed a single pollutant index based on Ontario, Canada's Environmental Quality Assessment Guidelines (1992).

$$Pi = \frac{Ci}{Cs}$$

Pi is the single assessment index, Ci is TP's observed concentration, and Cs is TP's standard concentration. Sediment Quality Guidelines (SQGs) regulate safe nutrient concentration limits in aquatic life (Alvarez-Guerra et al., 2010), the standard concentrations TP should be 600 mg kg^{-1}. According to value of Pi index, the risk can be divided in to four levels; $P_{TP} < 0.5$- clean (I), $0.5 < P_{TP} < 1$- slightly polluted (II), $1 < P_{TP} < 1.5$ – moderately polluted (III) and $1.5 < P_{TP}$ – severely polluted (IV).

In terms of the bioavailability of P, a single pollution method was modified. The ratio of bioavailable P (WSP + L-P + Fe & Al-P) to non-bioavailable P (Ca-P) was called the bioavailable coefficient of P. Bioavailable index evaluation method of P was described as follows;

$$PKi = Ki.\ Pi$$

$$K_P = C_{BAP} / (C_{TP} - C_{BAP})$$

Where PKi is the biological effective index for P, K_P is the biological efficiency coefficient of P. Ci and Cs are the defined same as above. C_{TP} and C_{BAP} are the standard concentration of TP and BAP. According to the value of the biological effective index for P, the risk can be divided in to 4 levels; < 0.25 (I), 0.25-0.5 (II), 0.5 – 0.75 (III) and > 0.75 (IV).

Result & Discussion

Sediment characteristics

The general properties of the sediment at various stations were presented in Table 1. The textural analysis showed great variation among the sampling stations. The Silt + Clay fraction was the major fraction and varied between 10.7 to 96.6 % with an average value of 51.6%. Relatively higher content of sand in the outer channel could be due to inflow and outflow of seawater which prevents settlement of finer particles near the seashore. Higher Silt + Clay content in rest of the parts of the lake especially in the northern sector (NS) and southern sector (SS) could be due to the inflow of freshwater enriched with fine particles and the absence of any influence due to seawater intrusion. The pH of the sediment was neutral to alkaline and varied between 6.2 to 8.75. Extreme pH observed in some stations of the lake was due to the addition of pollutants and deposition of organic matter in the sediment. The pH of the sediment was a great factor in controlling the release of P from the lake sediment as it controls the sorption-desorption, precipitation-solubilization, and oxidation-reduction reaction through varying the concentration of Al, Fe, and Ca (Zhang et al., 2016). EC of the sediment varied greatly between 0.35 to 10.76 dSm^{-1}. EC was found to be higher SS and lower in the northern sector. Higher EC in the SS could be attributed to the exchange of water with sea whereas lower EC in the northern sector could be attributed to dilution of water due to massive inflow of water from tributaries of Mahanadi. The organic carbon content of the lake sediment varied from 0.27 to 2.11 % with an average of 1.04%. Organic carbon content was lowest for sediments of the southern sector and highest for the northern sector. Higher sand content in the sediments of the Southern sector than other parts of the lake lead to the lower organic carbon content, however comparatively higher silt + clay content in the northern sector results in higher organic carbon content as finer particles can hold more organic carbon. Clean water in the southern sector allows the growth of phytoplankton which when die adds to the organic carbon content in the sector. Anthropogenic activity contributed to higher organic carbon in

the sediment sampled near the lake boundary compared to inner parts of the lake. The calcium carbonate ($CaCO_3$) content of the lake sediment varied from 0 to 4.2% with an average of 1.19.

Cluster analysis

Cluster analysis was performed to classify the sampling stations based on the similarity among the sampling stations and projected on the factorial axes (Figure 2). Cluster analysis helps to differentiate the lake into two different groups with stations under each cluster having similarity among the sediment characteristics and distribution of forms of P. The cluster 1 (C1) includes sampling stations falling under the southern sector (Station No. 1,2,3,4,5,6,) and central sector (Station No. 7,8,9,10,11,12) having tidal influence and have little effect on freshwater inflow from the catchment area. It further confirms the influence of higher salinity and alkalinity on sediment properties and distribution of P forms in these sectors. The cluster 2 (C2) includes the sampling station located nearer to the sea where mixing of seawater and freshwater occurs. C2 includes most of the station falling under central sector (Station No. 13,14,15,16,19,20,21,22) and northern sector (Station no. 17,18,23,24,25), which receives the huge freshwater influx loaded with anthropogenic inputs from the river and rivulets.

Total P

Total P content ranged from 169.8 to 971.9 mg kg^{-1} with an average value of 610.19 mg kg^{-1} (Table 1). One-way ANOVA revealed significant spatial variation of total P across the lake ($p < 0.001$, n = 25). The total P content was highest for the cluster 2 (Avg. 800.43 mg kg^{-1}) and lowest for the cluster 1 (420.08 mg kg^{-1}). Spatial variation in the total P content across the lake/sector could be due to a difference in nutrient load in the riverine inflow owing to the difference in landscape and anthropogenic activity in the lake catchment area. The lake receives its major portion of riverine inflow from the north and northwest part by the river Daya, Bhargavi, and Luna carrying anthropogenic inputs which might be the reason behind the

highest total P observed in the northern sector. There was a net outflow of lake water to sea during the monsoon season which was probably the reason behind the low total P content in cluster 1. Additionally, the sandy texture of the sediment found in the outer channel holds less P. The river and rivulet draining the catchment area of the central sector receive P load from both point and non-point sources. The municipal waste and effluent contribute to the point source of P in the river while the run-off from the catchment area receiving detergent containing domestic wastewater, flush pesticide, and fertilizer from the agricultural field contributes to the non-point source of P load in the lake. Total P content was positively correlated with OC content ($r = 0.63$, $p < 0.01$), CaCO3 ($r = 0.47$, $p < 0.05$), and CEC ($r = 0.45$, $p < 0.05$) (Table 4).

Spatial variability of P fractions in the lake sediment

While the higher concentration of total P raises environmental concerns, the proportion of the various P fractions also has a significant impact on how P affects the lake water system since some fractions are biologically accessible while others sequester P in a very immobile phase. Phosphorus distribution is typically correlated with the chemical properties of sediment, including sediment type, organic content, redox state, rate of mineralization, etc. P is added to lake water both internally and externally, through loading. Internal loadings describe the release of P into the water column from various P fractions. However, the entire P fraction does not contribute to the release of P into the water column. While sediment contributes to the internal loading of lake water P by the release of P from various P fractions into bioavailable P, freshwater input from the riverine adds to the external loading. Particularly, shallow water lakes are more susceptible to internal P loading because they frequently mix the overlying water with the sediment and bedrock, which releases P and stimulates primary production (Welch and Cooke, 2005; Kiani et al., 2020).

Results of P fractions were presented as their absolute value and the percentage of the P in that fraction relative to the sum of the P fractions in that sample (Table 2). Presenting the P fractions as a fractional percentage of the sum of P instead of actual concentration gives a clearer view of the transform of P from one fraction to another especially when comparing different locations. Spatial variability map for different fractions of lake sediment is presented in the figure 3.

Calcium bound P (Ca-P)

With a contribution of 15.68 % to the total P fractions, Ca-P was the third most prevalent inorganic P fraction. After residual P, Al & Fe-P, and residual P, Ca-P was the most significant factor affecting the lake's P %. Ca-P for cluster 1 varied from 22.55 to 150.79 mg kg-1 with a mean value of 64.89 mg kg-1, whereas for cluster 2, it varied from 51.44 to 91.24 mg kg-1 with a mean value of 65.95 mg kg-1. Other alkaline coastal habitats have also seen a Ca-P dominance in their lake sediment (Andrieux-Loyer and Aminot, 2001). Since calcite acts as an adsorption surface for dissolved phosphorus, the lake's high salinity encourages its synthesis by precipitation reaction. The fact that Ca-P is linked to calcium carbonate content, the distinct calcium phase, and the most stable form of P in sediment was further substantiated by the positive correlation between $CaCO_3$ and Ca-P ($r = 0.45$, $p < 0.05$) (Table 4). (Adhikari et al., 2015). Ca-P is not bioavailable and is the hardest compound to release (Cavalcante et al., 2018). No significant difference in Ca-P across the lake was found by one-way ANOVA. Ca-P contributions to the total P percentages are in the following order: Cluster 1 (16.56%) > Cluster 2 (14.80 percent). Given that the salinity of these sectors is similar to that of normal seawater, the preponderance of Ca-P in cluster 1 is corroborated by this observation. Additionally, the high alkalinity found in these areas encourages the precipitation of calcite.

Water soluble P (WSP)

The most biologically available fraction (WSP) was observed with the lowest concentration (0.08 to 7.03 mg kg^{-1}). Water-soluble P represents the concentration of soluble reactive P in pore water (soluble since the pore water is filtered through 0.45µ membrane filter and reactive as the P concentration is analysed using Murphey & Riley reagent) (Murphey & Riley, 1962). One-way ANOVA revealed that here is no significant difference in WSP content across the lake. Average value of WSP was higher for cluster 1 (2.78 mg kg^{-1}) than cluster 2 (1.51 mg kg^{-1}). Phosphorus transmission from pore water to lake water is significantly influenced by the concentration of P that is water soluble. The solubility product and adsorption/desorption equilibria between pore water and lake water have a significant impact on the concentration of pore water P, which can be utilised as a marker for P saturation of lake sediment. According to Boström, Andersen, Fleischer, and Jansson (1988), the concentration gradient between pore water and lake water P determines the release of P from across the sediment-water interface. A rise in the lagoon's total P content is associated with an increased probability of an algal bloom, according to a negative correlation between WSP and chlorophyll a ($r = -0.41$, $p < 0.05$). For the cluster 2, WSP's contribution to the sum of P fractions was the smallest. An abundance of algal bloom in this cluster lowers WSP levels because algal bloom consumes WSP, which explains the inverse relationship between WSP and Total P.

Loosely sorbed P (L-P)

Loosely sorbed P represents the fraction of sediment P which was readily bioavailable and varied from 0.29 to 4.75 mg kg^{-1}. Mean value of L-P for cluster 1 was 1.19 mg kg^{-1} where as it was 2.25 mg kg^{-1} for cluster 2. Percentage contribution of L-P was 0.38% and 0.51 % of sum of P fractions for cluster 1 and 2 respectively. This fraction remains in dynamic equilibrium with overlaying water and immediately available for plant growth. One-way ANOVA revealed significant variation in L-P content across the lake ($p < 0.01$, $n = 25$). The relatively lower content of L-P in the sediment of cluster 1could be due to competition of phosphate with other

anions owing to higher salinity observed in these sectors compared to the rest of the lake (Liu et al., 2002). L-P content was significantly correlated to the total P content ($r = 0.46$, $p < 0.05$).

Aluminum and Iron bound P (Al & Fe-P)

Al & Fe-P was the most important inorganic fractions contributing 27.24 % of the sum of P fractions (Table 3). Mean value of Al & Fe-P for cluster 1 and 2 are 85.34 mg kg^{-1} and 121.24 mg kg^{-1} respectively. One-way ANOVA revealed significant variation in AL & Fe-P content across the lake ($p < 0.05$, $n = 25$). Al-P is generally associated with P bound to aluminosilicate clay mineral or discrete aluminum phosphate phase. This fraction is not readily bioavailable as P tends to form a strong bond with Al. Fe-P is also relatively stable under oxidizing conditions, however under reducing conditions usually encountered in a lake with high organic matter content, Fe oxyhydroxide will become soluble releasing associated P to the aqueous phase. Though cycling of P was prevalent in an anoxic environment, there was evidence of Fe-P mobilization in both oxic and anoxic conditions (Rydin et al., 2000).

Untreated industrial and domestic wastewater was the major source of the Al & Fe-P in the lake sediment (Ruban, 2001). An increase in population, urbanization, and industrial activity in the catchment area of the lake resulted in the enrichment of lake sediment with Al & Fe-P. Northern and southern sector which falls in cluster 2 receives a major portion of industrial and domestic wastewater inflow to the lake which further confirms the dominance of Al & Fe-P fractions in these sectors. A similar observation was reported in the lake of China receiving domestic and industrial wastewater (Ni, Wang, Wu, & Pu, 2020). In comparison, the Al & Fe-P was lowest for the outer channel and southern sector which falls in cluster, as these sectors were less influenced by domestic and industrial effluent. In addition to this, high salinity and pH observed in the cluster 1 could also result in the release of phosphate from the sediment in competition with hydroxide ion. An increase in sediment pH led to a decrease in sorption

capacity of Al & Fe and hence a negative correlation of Al & Fe-P with pH (r =- 0.363) (Table 4) (Zhang et al., 2016). Overly the concentration of Al & Fe-P of the lake was controlled by the inflow of domestic and industrial effluent and thus, the content of Al & Fe-P can also be used as an indicator of the extent of environmental pollution (Zhang et al., 2005). Our finding is consistent with the other studies reporting that Fe-P is the primary contributor to internal P loading and most important fraction available to algal population in shallow lake (Petticrew and Arocena, 2001; Zhu et al., 2013; Kiani et al., 2020).

Residual P (R-P)

Residual P includes some Al & Fe-P (which was not previously removed with alkali extract) and organic P. one-way ANOVA revealed significant variation in R-P across the lake ($p < 0.01$, n = 25). R-P content varied from 38.72 to 261.48 mg kg^{-1} with a mean value of 158.88 mg kg^{-1} for cluster 1, whereas it was varied from 153.78 to 356.12 mg kg^{-1}, with a mean value of 254.42 mg kg^{-1} for cluster 2. Residual P was the dominant P fraction contributing 53.84 % of the sum of P fractions. Ni et al. (2020) reported that agricultural activities increase the proportion of organic P dramatically. This suggests that the dominance of organic P in our lake could be attributed to intense agricultural activities in the catchment area. With an increase in population and food demand P fertilizer and manure application has been increased drastically. P fertilizer applied to the agricultural field over a long period exist as monoester P (phytate P) (Copetti et al., 2019). Only 15-20 % of the applied P is absorbed by soil & plant and the rest is loosed to river and lake environment through runoff and subsurface flow. This explains the enrichment of lake sediment with organic P as a large amount of phytate P was added to the lake ecosystem. P associated with organic is 60% mobile and organic P will become slowly bioavailable as the organic matter undergoes decomposition. P loss from fertilizer, manure, and livestock breeding was the driving factor controlling the accumulation of organic P in the lake sediment.

Path analysis:

To elucidate the relationship further between WSP (i.e., the immediately available pool of P) with other P fractions, path analysis was carried out. Path analysis divides the correlation between WSP and other fractions into direct and indirect effects. The coefficient of regression analysis was presented by a matrix of direct and indirect effects (Table 5). Significant value of coefficient of determination of the regression analysis implies that path analysis explains the dependence of WSP on P fractions. Although all the P fractions are correlated with each other, path analysis helps to determine the transformation of P fractions to the water-soluble form. L-P ($r = 0.48$, $p < 0.05$) and Fe & Al-P ($r = 0.46$, $p < 0.05$) has significant direct effect on WSP. Highest and significant direct effect of these two fractions indicates domination of these two fractions in controlling the bioavailability of P in the water column as they can become source of WSP. Although the absolute amount of L-P was very low as compared to other inorganic fractions of P, it was the most readily available form of P which can be available to the algal bloom. The indirect effect of L-P and Fe & Al-P through R-P was negative which indicates R-P act as sink for WSP. Positive but insignificant direct effect of Ca-P on WSP indicates that Ca-P was not available in near term.

Principal component analysis

Principal component analysis was used to quantify the relationship between P fractions and sediment properties. Results of the PCA were presented in Table 6. and four components were extracted with Eigenvalue more than 1 explaining 77.28 % variability in the distribution of P fractions. The components were classified as strong, moderate, and weak based on their factor loading values of > 0.75, 0.75-0.5, and < 0.5 respectively. PC1 explained 31.43% variability with strong loading values for R-P, OC, silt + clay and moderate loading for TP and $CaCO_3$. Positive loading for OC and silt + clay content suggests that OC content is positively related to

the fineness of particles and the sediment properties influencing the distribution of forms of P in the lagoon. PC2 explains 21.32% variability with strong loading for WSP, Ca-P and EC. PC3 explains 14.81 % variability with strong positive loadings for L-P explaining the P fractions which controls its availability in the lake. PC4 explains 9.69% variability with strong loading for Al & Fe-P. Negative loading for WSP in PC3 and PC4 suggests that L-P and Fe-P could act as a source for WSP. This component emphasizes the fact that Fe-P was the dominant P fraction in lake especially in cluster 3 controlling bioavailability of P in the lake. By plotting PC 1 and PC 2, the sampling stations were separated according to difference in various sediment characteristics and forms of P (Fig x). Direction and length of arrow shows the degree of corelation between variables and principal components. Arrow corresponds to different variable with low angles are were highly correlated. Sampling stations of southern sector which falls in cluster 1 are separated from cluster 2 with high values of EC, WSP. The sampling stations of central sector and northern sector which falls under cluster 2 were characterized with high values of TP, R-P, Al & Fe-P, and OC.

Discriminant Analysis (DA)

Stepwise discriminant analysis was carried out using Wilk's method by giving entering sampling stations (sector wise) as grouping variable and entering P fractions and basic physico-chemical properties of lake sediment as independent variables. The summary of discriminant analysis was presented in the Table 7. Very low value of wilk's Lamba shows high significance and high ability to discriminant power of the model. Eigen values of two discriminant function were 9.078 and 0.718 showing discriminating ability of the function. High canonical correlation (F1 = 0.949, F2 = 0.646) for both the discriminant function suggest the predictor are successful in grouping the sampling stations into different sectors. Further F-value of < 0.05 shows that the discriminant between the variable is highly significant. The first canonical discriminant function accounts for 92.7% of and second discriminant functions accounts for

7.3% discriminating ability of the variables. The standardized canonical coefficient showed that WSP (0.626), pH (-0.684), and TP (0.748) attributed to first discriminant score and while EC (0.955) attributed to second discriminant score.

Ecological risk assessment of P in sediment

Single pollution index

The single pollution index of the lake sediment ranged from 0.05 to 1.62 and the risk level ranging from clean to severely polluted (Table 8) (Figure 4). Sampling stations under the southern station and outer channel fall under risk level I (Clean) and the sampling station under the central sector falls under slightly polluted (level II) to moderately polluted (level III). Most of the sampling stations falling under the northern sector were categorized as moderately polluted (level III) to severely polluted (level IV). The percentage of the sampling station falls under risk level I and II were 30.3% and 27.3 %, whereas 30.3% and 12.1% sampling station falls risk level III and IV. Therefore, it was concluded that risk of TP was more prominent in the central and northern sector.

Biological effectiveness

The bioavailability indices for P in the lake's sediments ranged from 0.04 to 0.82, and the risk ranges from level I to level IV (Table 8). (Figure 5). For the total number of sediment sampling stations, the percentage of samples with risk levels I, II, III, and IV was 33.3 %, 39.4 %, 21.2 %, and 6.1 %, respectively. As a result, there is a risk of phosphorus release into the aqueous phase as well as ecological concern associated with phosphorus in some sediments of the lake, particularly in the northern sector. This outcome was in line with the evaluation findings based on the single factor index of phosphorus in the Chilia lake sediment mentioned in the previous sentence. The total and bioavailable phosphorus in the sediment were taken into account in the

phosphorus assessment approach based on bioavailability index. Consequently, the suggested assessment approach can account for the ecological danger provided by the lake's phosphorus.

Conclusion

The study presents result of five phosphorus fractions and TP in the surface sediment of Chilika lake. The relative abundance of the five P fractions is in the order of R-P, Al & Fe-P, Ca-P, WSP, and L-P. R-P was the dominant fraction in the studied lake which could be due to intense agricultural activities in the catchment area contributing organic P to the sediment. Al & Fe-P is the second most dominant P fractions which can be attributed to domestic waste water and industrial effluents as its source. This fraction is algal available and can release water to overlaying water in case of reduced condition. A positive relation between Ca-P and $CaCO_3$ suggest that salinity of the lake favours precipitation of calcite in the lake and thereby governing Ca-P content. Though WSP and L-P content were observed to be least among the fractions, these two fractions are most bioavailable to algae and aquatic plant species and could enhance eutrophication. Strong loading for OC and silt + clay suggest their role in controlling concentration of P fractions. Further, cluster analysis classifies the lake into two cluster with one including the sampling stations falling under southern sector and some station of central sector which have tidal influence. While the second cluster includes the station falling under northern sector and central sector which receives majority of freshwater inflow enriched with nutrient content from the river and its tributaries. In the future, the results of the study will be useful for the assessment of P release potential of sediment and selecting control measures for preventing eutrophication of lake.

Acknowledgement

The authors express their gratitude to the Indian Council of Agricultural Research, New Delhi, The Director, Institute of Agricultural Sciences and Head, Department of Soil Science and

Agricultural Chemistry, Banaras Hindu University, for providing the necessary facilities and infrastructure to carry out the investigation. The author also expresses their gratitude to researcher and supporting staff of Wetland Research and Training Centre, Chilika Development authority for their assistance during water and sediment sampling and analysis.

Declarations

The authors declare that there is no conflict of interest.

Author contributions

Satya Narayana Pradhan: Sample collection, instrumental analysis, laboratory analysis, original draft writing

A.K. Ghosh: Conceptualization, Data analysis, Editing, Overall supervision

Prasannajit Acharya: Sample Collection and instrumental analysis, Editing

Pradipta R. Muduli: Conceptualization, Editing, Reviewing

Ishan Biswajit Sahoo: Sample collection, Lab work

Preeti Singh: Data analysis, Editing, Reviewing

Dibyajyoti Panda: Lab work, reviewing

References

Acharya, P., Muduli, P.R., Mishra, D.R., Kumar, A., Kanuri, V.V. and Das, M., 2022. Imprints of COVID-19 lockdowns on total petroleum hydrocarbon levels in Asia's largest brackish water lagoon. Mar. Pollut. Bull. 174, p.113137.

Adhikari, P.L., White, J.R., Maiti, K., Nguyen, N., 2015. Phosphorus speciation and sedimentary phosphorus release from the Gulf of Mexico sediments: implication for hypoxia. Estuar. Coast. Shelf Sci. 164, 77–85.

Alvarez-Guerra, M., Viguri, J.R., Casado-Martínez, M.C., DelValls, T.A., 2010. Sediment quality assessment and dredged material management in Spain: Part I, application of sediment quality guidelines in the Bay of Santander. Integr. Environ. Assess. Manag. 3, 529–538.

Amirbahman, A., Lake, B.A., Norton, S.A., 2013. Seasonal phosphorus dynamics in the surficial sediment of two shallow temperate lakes: a solid-phase and porewater study. Hydrobiologia 701, 65–77.

Andrieux-Loyer, F., Aminot, A., 2001. Phosphorus forms related to sediment grain size and geochemical characteristics in French coastal areas. Estuari Coast Shelf Sci. 52, 617–629.

Balachandran, S., Rahmani, A.R., Sathiyaselvam, P., 2003. Habitat evaluation of Chilika Lake with special reference to birds as bio-indicators. Chilika Newsletter, 4 (December), 17–19.

Barik, S.K., Bramha, S., Bastia, T.K., Behera, D., Mohanty, P.K. and Rath, P., 2019. Distribution of geochemical fractions of phosphorus and its ecological risk in sediment cores of a largest brackish water lake, South Asia. Int. J. Sediment Res, 34(3), pp.251-261.

Barik, S.K., Muduli, P.R., Mohanty, B., Behera, A.T., Mallick, S., Das, A., Samal, R.N., Rastogi, G. and Pattnaik, A.K., 2017. Spatio-temporal variability and the impact of Phailin on water quality of Chilika lagoon. Cont. Shelf Res., 136, pp.39-56.

Boström, B., Andersen, J.M., Fleischer, S. and Jansson, M., 1988. Exchange of phosphorus across the sediment-water interface. In Phosphorus in freshwater ecosystems (pp. 229-244). Springer, Dordrecht.

Bostrom, B., Pettersson, A.K., Ahlgren, I., 1989. Seasonal dynamics of a cyanobacterial dominated microbial community in surface sediments of a shallow eutrophic lake. Aquat. Sci. 51, 153–178.

Bouyoucos, G.J., 1927. The hydrometer as a new method for the mechanical analysis of soils. Soil sci. 23(5), pp.343-354.

Cavalcante, H., Araujo, F., Noyma, N.P., Becker, V., 2018. Phosphorus fractionation in sediments of tropical semiarid reservoirs. Sci. Total Environ. 619-620, 1022–1029.

Central Inland Fishery Research Institute (CIFRI), Barrakpur Kolkata, 2015. Annual Report on the 'Post Restoration assessment of the ecology and fisheries diversity of Chilika Lake' (Submitted to Chilika Development Authority).

Copetti, D., Tartari, G., Valsecchi, L., Salerno, F., 2019. Phosphorus content in a deep river sediment core as a tracer of long-term (1962–2011) anthropogenic impacts: A lesson from the Milan metropolitan area. Sci. Total. Environ. 646, 37–48.

Gasparatos, D., Massas, I., Godelitsas, A., 2019. Fe-Mn concretions and nodules formation in redoximorphic soils and their role on soil phosphorus dynamics: Current knowledge and gaps. Catena 182.

Giles, C.D., Isles, P.D.F., Manley, T., Xu, Y., Druschel, G.K., Schroth, A.W., 2016. The mobility of phosphorus, iron, and manganese through the sediment–water continuum of a shallow eutrophic freshwater lake under stratified and mixed water-column conditions. Biogeochemistry 127, 15–34.

Guo, H.C., He, B., Song, L.R., Duan, C.Q., Xu, X.M., Luo, Y., Liu, Y., 2017. Control techniques of water pollution and eutrophication in Dianchi watershd. Beijing: China Environmental Science Press (in Chinese).

Hartzell, J.L., Jordan, T.E., Cornwell, J.C., 2017. Phosphorus sequestration in sediments along the salinity gradients of Chesapeake Bay subestuaries. Estuar. Coast. 40, 1607–1625.

Hesse, P.R. 1971. A Textbook for Soil Chemical Analysis, pp. 335-361. J. Murray, London, England.

House, W.A., 2003. Geochemical cycling of phosphorus in rivers. Appl. Geochem. 18, 739–748.

Immers, A.K., Bakker, E.S., Van Donk, E., Ter Heerdt, G.N.J., Geurts, J.J.M., Declerck,S.A.J., 2015. Fighting internal phosphorus loading: an evaluation of the largescale application of gradual Fe-addition to a shallow peat lake. Ecol. Eng. 83,78–89.

Kadekodi, G.K., 2005. Environmental economics in practice: case studies from India. Resources, Energy, and Development, 2(2), pp.155-156.

Katsev, S., 2016. Phosphorus Effluxes from Lake Sediments, Soil Phosphorus. Taylor Francis.

Kiani, M., Tammeorg, P., Niemistö, J., Simojoki, A. and Tammeorg, O., 2020. Internal phosphorus loading in a small shallow lake: response after sediment removal. Sci. Total. Environ. 725, p.138279.

Liu, M., Hou, L.J., Xu, S.Y., Ou, D.N., Zhang, B.L., Liu, Q.M., Yang, Y., 2002. The characteristics of phosphate adsorption on tidal surface sediments of the Yangtze Estuary. Acta Geograph. Sin. 57, 397–406.

Matisoff, G., Kaltenberg, E.M., Steely, R.L., Hummel, S.K., Seo, J., Gibbons, K.J., Bridgeman, T.B., Seo, Y., Behbahani, M., James, W.F., Johnson, L.T., Doan, P., Dittrich, M., Evans, M.A., Chaffin, J.D., 2016. Internal loading of phosphorus in western Lake Erie. J. Great Lakes Res. 42, 775–788.

Moore Jr, A., and Reddy, K.R., 1994. Role of Eh and pH on phosphorus geochemistry in sediments of Lake Okeechobee, Florida (Vol. 23, No. 5, pp. 955-964). American Society of Agronomy, Crop Science Society of America, and Soil Science Society of America.

Mortimer, C.H., 1941. The exchange of dissolved substances between mud and water in lakes. J. Ecol. 29, 280–329.

Muduli, P.R., Kanuri, V.V., Robin, R.S., Kumar, B.C., Patra, S., Raman, A.V., Rao, G.N. and Subramanian, B.R., 2013. Distribution of dissolved inorganic carbon and net ecosystem production in a tropical brackish water lagoon, India. Cont. Shelf Res. 64, pp.75-87.

Mukherjee, R., Muduli, P.R., Barik, S.K. and Kumar, S., 2019. Sources and transformations of organic matter in sediments of Asia's largest brackish water lagoon (Chilika, India) and nearby mangrove ecosystem. Environ. Earth Sci. 78(11), pp.1-15.

Murphy, J. and J.P. Riley. 1962. A modified single solution method for the determination of phosphate in natural waters. Analytica Chimica Acta 27:31-36.

Nelson, D. W., L. E. Sommers. 1982. Total carbon, organic carbon and organic matter.In A. L. Page, R. H. Miller, and D. R. Keeney (eds.). Methods of Soil Analysis, Part 2.Agronomy 9:539–579.

Ni, Z., Wang, S., Wu, Y. and Pu, J., 2020. Response of phosphorus fractionation in lake sediments to anthropogenic activities in China. Sci. Total Environ. 699, p.134242.

Noll, M.R., Szatkowski, A.E. and Magee, E.A., 2009. Phosphorus fractionation in soil and sediments along a continuum from agricultural fields to nearshore lake sediments: Potential ecological impacts J. Great Lakes Res., 35, pp.56-63.

Orihel, D.M., Schindler, D.W., Ballard, N.C., Graham, M.D., O'Connell, D.W., Wilson, L. R., Vinebrooke, R.D., 2015. The ''nutrient pump:" Iron-poor sediments fuel low nitrogen-to-phosphorus ratios and cyanobacterial blooms in polymictic lakes. 60, 856–871.

Panigrahi, S., Wikner, J., Panigrahy, R., Satapathy, K., Acharya, B., 2009. Variability of nutrients and phytoplankton biomass in a shallow brackish water ecosystem (Chilika Lagoon, India). Limnology 10, 73e85.

Petticrew, E.L. and Arocena, J.M., 2001. Evaluation of iron-phosphate as a source of internal lake phosphorus loadings. Sci. Total Environ. 266(1-3), pp.87-93.

Puri, A.N., 1930. A new method of estimating total carbonates in soils. J. Agric. Res. Pusa Bulletin 206, 7.

Ruban, V., Lo´ pez-Sa´ nchez, J.F., Pardo, P., Rauret, G., Muntau, H., Quevau-viller, P., 2001. Harmonized protocol and certified reference material for the determination of extractable contents of phosphorus in fresh-water sediments—a synthesis of recent works. Fresenius J. Anal. Chem. 370, 224.

Rydin, E., 2000. Potentially mobile phosphorus in Lake Erken sediments. Water Res. 34, 2037–2042.

Smolders, E., Baetens, E., Verbeeck, M., Nawara, S., Diels, J., Verdievel, M., Peeters, B., De Cooman, W., Baken, S., 2017. Internal loading and redox cycling of sediment iron explain reactive phosphorus concentrations in lowland rivers. Environ. Sci. Technol. 51, 2584–2592.

Soliman, N. F., El Zokm, G. M., & Okbah, M. A. (2017). Evaluation of phosphorus bioavailability in El Mex Bay and Lake Mariut sediment. Int. J. Sediment Res. 32(3), 432-441.

Tu, L., Jarosch, K.A., Schneider, T. and Grosjean, M., 2019. Phosphorus fractions in sediments and their relevance for historical lake eutrophication in the Ponte Tresa basin (Lake Lugano, Switzerland) since 1959. Sci. Total Environ. 685, pp.806-817.

Upreti, K., Maiti, K., Rivera-Monroy, V.H., 2019. Microbial mediated sedimentary phosphorus mobilization in emerging and eroding wetlands of coastal Louisiana. Sci. Total Environ. 651, 122–133.

Van Eck, G.T.M., 1982. Forms of phosphorus in particulate matter from the Hollands Diep/Haringvliet, The Netherlands. In Sediment/Freshwater Interaction (pp. 665-681). Springer, Dordrecht.

Wang, S., Jin, X., Pang, Y., Zhao, H., Zhou, X. and Wu, F., 2005. Phosphorus fractions and phosphate sorption characteristics in relation to the sediment compositions of shallow lakes in the middle and lower reaches of Yangtze River region, China. J. Colloid Interface Sci. 289(2), pp.339-346.

Wang, Z.C., Huang, S., Li, D.H., 2019. Decomposition of cyanobacterial bloom contributes to the formation and distribution of iron-bound phosphorus (Fe-P): Insight for cycling mechanism of internal phosphorus loading. Sci Total Environ. 652, 696-708.

Welch, E.B. and Cooke, G.D., 2005. Internal phosphorus loading in shallow lakes: importance and control. Lake Reserv. Manag. 21(2), pp.209-217.

Worsfold, P., McKelvie, I., Monbet, P., 2016. Determination of phosphorus in natural waters: a historical review. Anal. Chim. Acta 918, 8–20. https://doi.org/10.1016/j. aca.2016.02.047.

Yuan, F., Li, H., Kakarla, R., Kasden, C., Yao, S., Xue, B. and Sun, Y., 2020. Variability of sedimentary phosphorus fractions in the western and Sandusky basins of Lake Erie. J. Great Lakes Res. 46(4), pp.976-988.

Zhang, C., Tian, H., Liu, J., Wang, S., Liu, M., Pan, S. and Shi, X., 2005. Pools and distributions of soil phosphorus in China. Global biogeochemical cycles, 19(1).

Zhang, Y., He, F., Liu, Z., Liu, B., Zhou, Q. and Wu, Z., 2016. Release characteristics of sediment phosphorus in all fractions of West Lake, Hang Zhou, China. Ecol. Eng. 95, pp.645-651.

Zhu, M., Zhu, G., Li, W., Zhang, Y., Zhao, L. and Gu, Z., 2013. Estimation of the algal-available phosphorus pool in sediments of a large, shallow eutrophic lake (Taihu, China) using profiled SMT fractional analysis. Environ. Pollut. 173, pp.216-223.

Table 1. The Physico-chemical properties and Total P content in the lake sediment.

Parameter	Minimum	Maximum	Mean	Std. Deviation
T-P (mg kg^{-1})	169.8	971.90	645.4	238.8
pH	6.20	8.75	7.92	0.56
EC (dSm^{-1})	0.35	10.76	3.82	3.01
OC (%)	0.27	2.11	1.04	0.57
CEC (cmol (p+) kg^{-1})	8.10	22.96	17.41	4.65
$CaCO_3$ (%)	0.00	4.20	1.19	1.07
Silt + Clay (%)	10.70	96.6	51.6	25.9

T-P, Total P; EC, Electrical conductivity; OC, organic carbon; CEC, cation exchange capacity; $CaCO_3$, Calcium carbonate.

Table 2. Contents of P (mg kg^{-1}) fractions of Lake Chilika in Post-Monsoon season

		WSP	L-P	Fe-P	Ca-P	R-P	Total P
Cluster 1 (n =12)	Min	0.08	0.29	39.08	22.55	38.72	169.79
	Max	7.03	3.55	176.15	150.79	261.48	591.33
	Mean	2.78	1.19	85.34	64.89	158.88	420.08
	Std	2.25	1.09	34.42	41.63	72.95	125.13
Cluster 2 (n =13)	Min	0.26	0.60	61.77	51.44	153.78	562.06
	Max	3.89	4.75	198.60	91.24	356.12	971.90
	Mean	1.51	2.25	121.24	65.95	254.42	800.43
	Std	0.97	1.29	52.02	19.38	92.79	239.69
Lake	Mean	2.14	1.72	103.29	65.42	206.65	610.26

Table 3. Sector wise fraction percent (%) of the sum total of inorganic P fractions of WSP, L-P, Fe & Al-P and Ca-P for lake sediments.

Sectors	WSP	L-P	Fe & Al-P	Ca-P	R-P
Cluster 1 (n= 12)	0.89	0.38	27.26	16.56	50.75
Cluster 2 (n= 13)	0.34	0.51	27.21	14.80	57.10
Lake	0.61	0.44	27.24	15.68	53.93

WSP, water soluble P; L-P, loosely sorbed P; Al & Fe-P, aluminum, and iron bound P; Ca-P, calcium bound P.

Table 4. Correlation matrix of sediment properties and P fractions of the lake.

Parameter	WSP	L-P	Al-P	Ca-P	R-P	TP	pH	EC	OC	CaCO3	Mud	CEC
WSP	1											
L-P	-0.124	1										
Al-P	-0.219	0.210	1									
Ca-P	0.399*	0.062	-0.086	1								
R-P	-0.201	-0.012	0.231	0.111	1							
TP	-0.456*	0.459*	0.384	0.026	0.673**	1						
pH	-0.054	0.304	-0.363	-0.168	-0.273	-0.049	1					
EC	0.731**	-0.274	-0.299	0.276	-0.325	-0.57**	0.061	1				
OC	-.0117	0.161	0.249	0.094	0.633**	0.505*	-0.318	-0.352	1			
CaCO3	0.091	0.225	-0.071	0.471*	0.395	0.406*	0.225	0.056	0.574**	1		
Mud	0.163	-0.013	-0.052	0.123	0.515**	0.300	-0.305	0.202	0.474*	0.316	1	
CEC	0.263	0.244	0.169	0.208	0.510**	0.455*	-0.286	0.193	0.687**	0.498*	0.713**	1

* $p < 0.05$, ** $p < 0.01$

Table 5. Path analysis of causal relationships, both direct (represented by bold diagonals) and indirect (off diagonals) effects between water soluble P and different P forms.

P fractions	L-P	Fe-P	Ca-P	R-P	R^2
L-P	0.48*	0.11	0.06	-0.02	0.56
Fe-P	0.12	0.46*	-0.06	-0.09	
Ca-P	0.15	-0.15	0.18	-0.04	
R-P	0.04	0.20	0.03	-0.20	

Table 6. Principal component matrix of P fractions and sediment properties

Parameter	**Components**			
	1	**2**	**3**	**4**
WSP	-0.082	**0.866**	-0.143	-0.052
L-P	0.000	-0.078	**0.850**	0.030
Al-P	0.037	-0.182	0.275	**0.820**
Ca-P	0.215	**0.724**	0.300	0.117
R-P	**0.851**	-0.193	0.011	0.171
TP	0.614	-0.400	0.508	0.196
pH	-0.276	-0.121	0.436	-0.771
EC	-0.173	**0.792**	-0.299	-0.236
OC	**0.812**	-0.083	0.158	0.200
CaCO3	0.643	0.301	0.480	-0.297
Mud	**0.761**	0.211	-0.238	-0.022
Eigen value	3.46	2.34	1.63	1.06
Total variance	31.46	21.32	14.81	9.69
Cumulative variance	31.46	52.78	67.59	77.28

Table 7. Discriminant analysis of phosphorus fractions and physico-chemical properties of lake sediment.

	Discriminant functions	
	F1	F2
Eigen values	9.078	0.718
% Variance	92.7	7.3
Cumulative Variance	92.7	100
Canonical correlation	0.949	0.646
Wilk' Lambda	0.058	0.582
Degree of freedom	8	3
Significance	0.00	0.01
Variables	Standardized canonical coefficient	
WSP	0.626	-0.179
pH	-0.684	0.185
EC	0.327	0.955
TP	0.748	0.126

Table 8. classification of single point index and biological effective index in lake sediment (%)

Risk level	single point index	biological effective index
I	30.3	33.3
II	27.3	39.4
III	30.3	21.2
IV	12.1	6.1

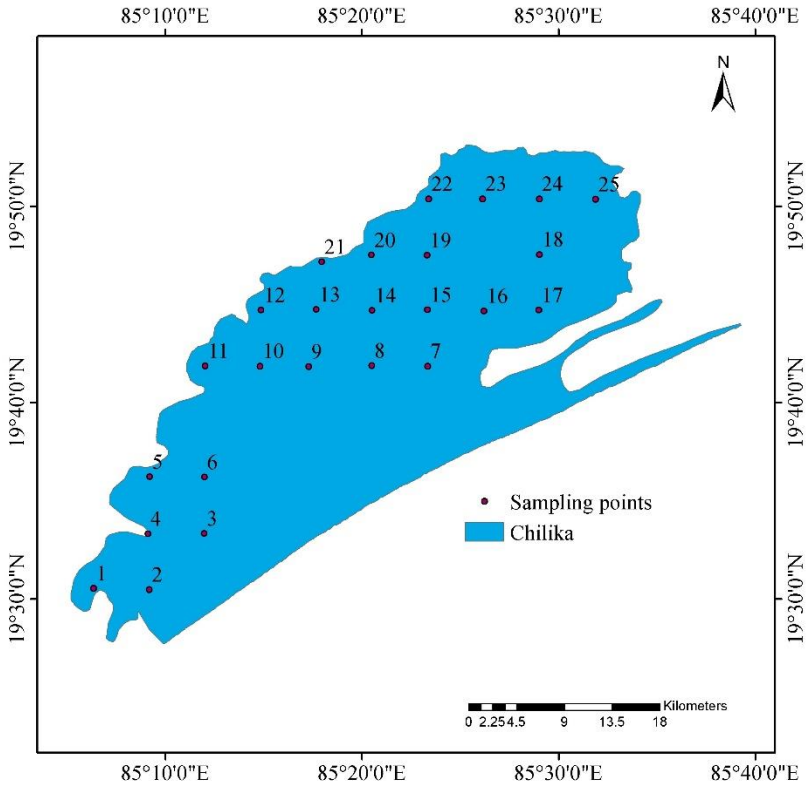

Figure 1. Map of Chilika lake showing sampling stations.

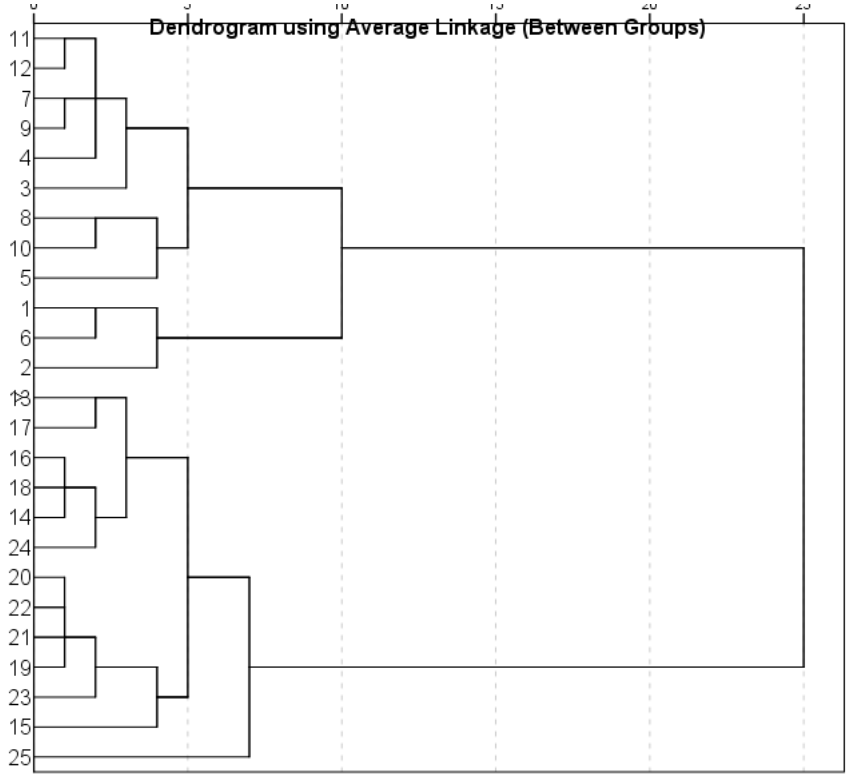

Figure 2. Dendrogram of sediment characteristics and P fractions showing cluster in the lake Chilika.

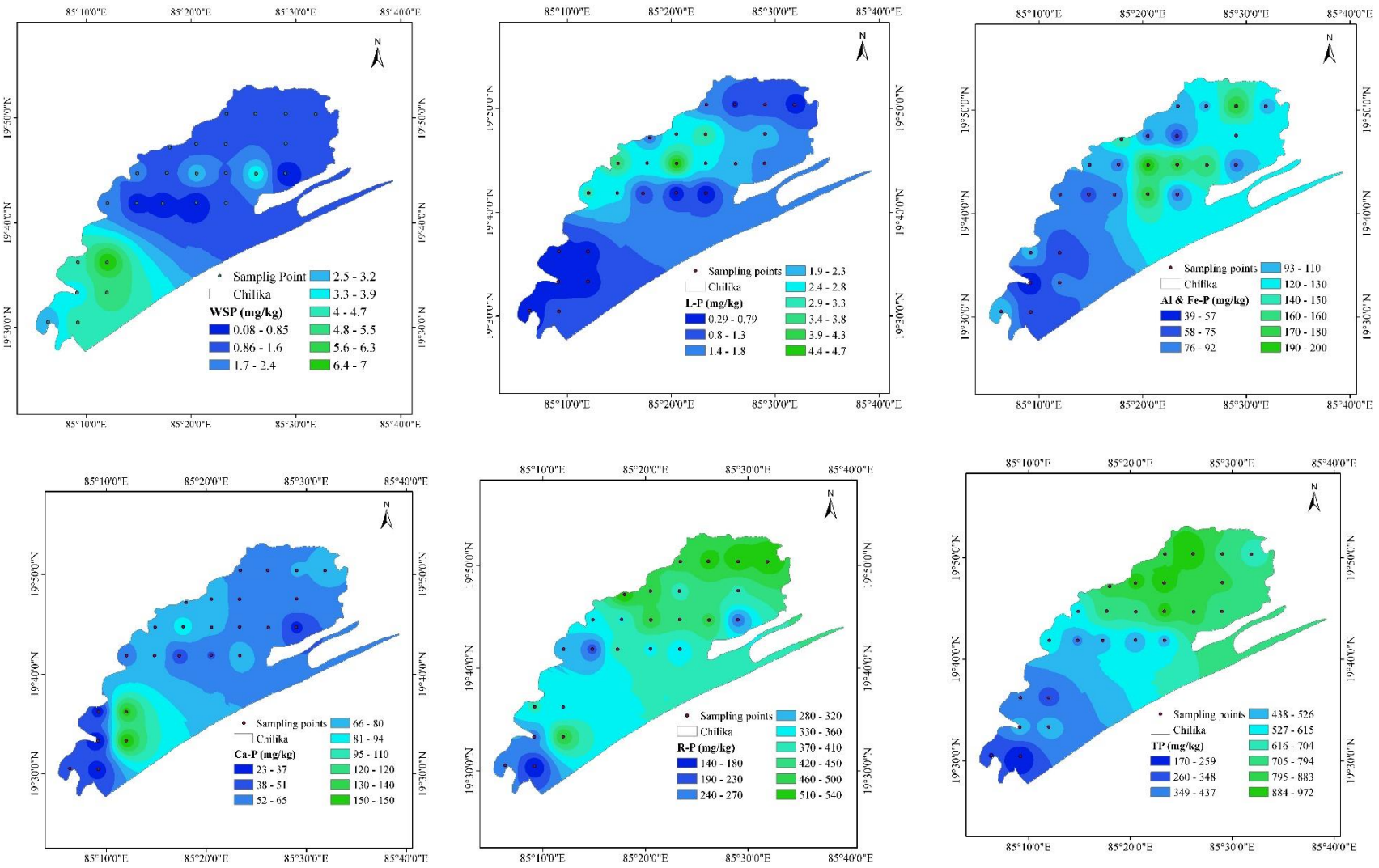

Figure 3. Spatial distribution of P fractions in sediments of lake Chilika

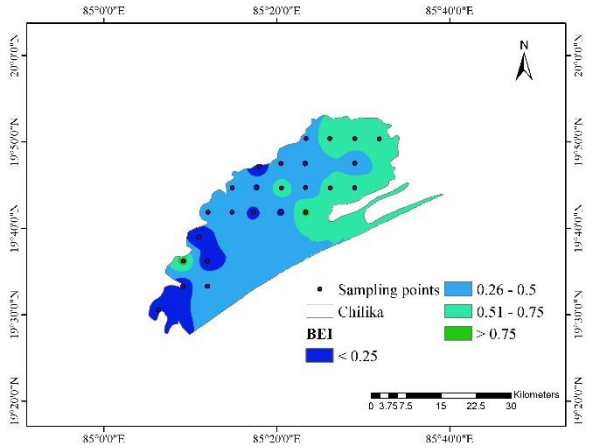

Figure 4. Map of Chilika showing Pollution Index

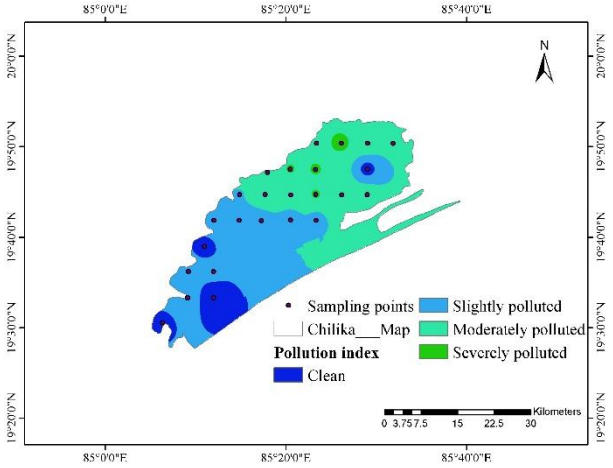

Figure 5. Map of Chilika showing biological effective index.

Declaration of interests

☒The authors declare that they have no known competing financial interests or personal relationships that could have appeared to influence the work reported in this paper.

☐The authors declare the following financial interests/personal relationships which may be considered as potential competing interests:

RESUME

SATYA NARAYANA PRADHAN
(Ph. D. (Soil Science & Ag. Chemistry),
Department of Soil Science & Ag. Chemistry,
Institute of Agricultural Sciences
BHU, Varanasi)
MOBILE: 7205208485, 7839187262
EMAIL ID: satyanarayanapradhan22@gmail.com

EDUCATIONAL QUALIFICATIONS:

ACADEMIC QUALIFICATION	BOARD/UNIVERSITY	YEAR OF PASSING	SUBJECT/STREAM	%/OGPA	REMARKS
Ph.D.	BHU, Varanasi	2022	Soil Science & Ag. Chemistry	8.40	1st division
M.Sc.(Ag)	BHU, Varanasi	2017	Soil Science & Ag. Chemistry	8.56	1st division
B.Sc. (Ag)	OUAT, Bhubaneswar	2015	Agriculture	8.39	1st division **with Hons**.
Higher secondary	OMBBS residential college (CHSE, Odisha)	2011	Physics, Chemistry, Maths, Biology, English, Hindi	72.00	1st division
High school	Kukudakhandi high school (BSE, Odisha)	2009	Odia, English, Hindi, Maths, Science, Social science	88.50	1st division

RESEARCH WORK

M.Sc. Thesis work

Title- phosphorus dynamics in a long-term rice-lentil cropping sequence as influenced by tillage and organic manure addition

Ph.D. Thesis work

Title- Variation in water quality of Chilika lake (Odisha) with special reference to phosphorus and its sequestration using novel adsorbents

Extra Skill

NET (ICAR) Soil Science & Agricultural Chemistry

Member of Indian Society of Soil Science, New Delhi

Software: Microsoft Office Word, PowerPoint and Excel, SPSS software for statistical analysis.

Personal Detail

Father's name	Bijaya Pradhan
Mother's name	Sumita Pradhan
Date of birth	25/03/1994
Permanent address	At- Srikrushna nagar 4th lane, po- Lanjipalli, Dist-Ganjam, Odisha, PIN-760008
Nationality	Indian
Languages known	Odia, English, Hindi

DECLARATION:

I hereby declare that all the above information stated above is true to the best of my knowledge.

PLACE: Varanasi (SATYA NARAYANA PRADHAN)